DESIGN AND MODELLING OF PASSIVE UHF RFID TAGS FOR ENERGY EFFICIENT LIQUID LEVEL DETECTION APPLICATIONS

A. A. ATOJOKO

Ph.D

UNIVERSITY OF BRADFORD

2016

DESIGN AND MODELLING OF PASSIVE UHF RFID TAGS FOR ENERGY EFFICIENT LIQUID LEVEL DETECTION APPLICATIONS

A study of various techniques in the design, modelling, optimisation and deployment of RFID reader and passive UHF RFID tags to achieve effective performance for liquid sensing applications.

Achimugu Alpha ATOJOKO
B.Eng., M.Sc.

Submitted for the degree of

Doctor of Philosophy

Faculty of Computing and Informatics

University of Bradford

2016

ABSTRACT

DESIGN AND MODELLING OF PASSIVE UHF RFID TAGS FOR ENERGY EFFICIENT LIQUID LEVEL DETECTION APPLICATIONS

A study of various techniques in the design, modelling, optimisation and deployment of RFID reader and passive UHF RFID tags to achieve effective performance for liquid sensing applications

KEYWORDS

Radio Frequency Identification (RFID), Passive UHF RFID tags, RFID Reader, Energy efficient, Genetic Algorithms, Quadrifilar Helical Antenna (QHA), Antennas, Antenna Polarisation, Radiation pattern, Sensor Monitoring.

Sewer and oil pipeline spillage issues have become major causes of pollution in urban and rural areas usually caused by blockages in the water storage and drainage system, and oil spillage of underground oil pipelines. An effective way of avoiding this problem will be by deploying some mechanism to monitor these installations at each point in time and reporting unusual liquid activity to the relevant authorities for prompt action to avoid a flooding or spillage occurrence.

This research work presents a low cost energy efficient liquid level monitoring technique using Radio Frequency Identification Technology. Passive UHF RFID tags have been designed, modelled and optimized. A simple rectangular tag, the P-shaped tag and S-shaped tag with UHF band frequency of operation (850-950 MHz) has been designed and modelled. Detailed parametric analysis of the rectangular tag is made and the optimised design results analysed and presented in HFSS and Matlab. The optimised rectangular tag designs are then deployed as level sensors in a gully pot. Identical tags were deployed to detect 4 distinct levels in alternate positions and a few inches in seperation distance within the gully pot height (Low, Mid, High and Ultra high). The radiation characteristic of tag sensors in deployment as modelled on HFSS is observed to show consistent performance with application requirements.

An in-manhole chamber antenna for an underground communication system is analysed, designed, deployed and measured. The antenna covers dual-band impedance bandwidths (i.e. 824 to 960 MHz, and 1710 to 2170 MHz). The results show that the antenna prototype exhibits sufficient impedance bandwidth, suitable radiation characteristics, and adequate gains for the required underground wireless sensor applications.

Finally, a Linearly Shifted Quadrifilar Helical Antenna (LSQHA) designed using Genetic Algorithm optimisation technique for adoption as an RFID reader antenna is proposed and investigated. The new antenna confirms coverage of the RFID bandwidth 860-960 MHz with acceptable power gain of 13.1 dBi.

ACKNOWLEDGEMENT

I would like to start by giving thanks to God Almighty for His awesome grace and favor that has seen me through all levels of my academic pursuit.

Special thanks to my family that has been my backbone of support, my wife and little angels (Igo, Eneojo and Ojochogu mi). To my parents, Mr. and Mrs. U.S. Atojoko, thank you for giving me the impetus for introspection, you have been the major catalyst for positive change in my life without which I will be grossly malnourished in my masculine soul. I have been blessed with incredible support from amazing siblings, thanks for your constant encouragement, couldn't have made it this far without your love and support.

I am greatly indebted to my supervisors, Professor Raed Abd-Alhameed, Dr C. H. See and Professor McEwan who have motivated and taken time to push me beyond my limits to attain the results presented in this report, thanks a mega billion!

This research work has been supported by Petroleum Technology Development Fund (PTDF) and National Space Research and Development Agency (NASRDA); I am highly appreciative of your support and encouragement that has always come in time of need.

To my colleagues and the entire staff of the Centre for Technology Development (CSTD), thanks for your contribution, they came in handy. Special thanks to Professor. Saidu Mohammed and Dr Spencer Onuh for believing in me and giving me the opportunity to pursue my dream. You have added colour to my life in so many ways, God bless you.

This acknowledgement would be incomplete without mentioning my Godfathers, Dr Amadu Ali and Engineer Suleiman Akowe Achimugu, thanks for the motivation at every beck and call.

To my academic father, late Professor J.N. Egila,thanks for providing the first spark that has kept my research zeal burning; thanks for your constant motivation, you inspire me in so many ways you may never know; you are highly appreciated.Continue to rest in the bossom of our dear lord.

To my reseach colleagues and friends in academia, thanks for your invaluable contributions which gave my research findings a whole new perspective. Wish I could pull down the rainbow and write your names on it and put it back to the sky so everyone can see how beautiful life has been with people like you. Thanks for making all my efforts meaningful. God bless you all.

This piece of work is dedicated to the Atojoko's : it is a priviledge to kick start our success story in the academia and it is my wish that this spark of excellence grow into greater heights for that generation of Nigeria who will never fail to strive, learn and work hard to open new creative grounds for the development of our dear nation and the renewal of our culture for the emancipation of our people...

TABLE OF CONTENTS

LIST OF TABLES

LIST OF FIGURES

ABBREVIATIONS

AC	Alternating Current
AIDC	Automated Identification and Data Capture
AUT	Antenna Under Test
BT	Bow Tie Antenna
CCTV	Closed Circuit Television
CP	Circular Polarization
CRLH	Composite Right-Left Handed
CST	Computer Simulation Technology
COF	Centre Operating Frequency
DARPA	Defense Advanced Research Projects Agency in USA
DRMPSO	Divided Range Multi objective Particle Swarm Optimisation
EAS	Electronic Article Surveillance
EEPROM	Electronic Programmable Read Only Memory
EIRP	Effective Isotropic Radiation Power
EM	Electromagnetic
EMC	Electromagnetic Compatibility
EMR	Electromagnetic Radiation
EPC	Electronic Product Code
FDTD	Finite Difference Time Domain
FDX	Full Duplex
FEM	Finite Element Method
FIS	Fuzzy Interference System
FORTRAN	Formula Translator
GA	Genetic Algorithm
HDX	Half Duplex
HF	High Frequency
HFSS	High Frequency Structure Simulator
IC	Integrated Circuit
ID	Identification
IEEE	Institute of Electrical and Electronics Engineers
ISO	International Standard Organization
ITU	International Telecommunications Union

LCP	Left Circular Polarization
LF	Low Frequency
LP	Left Polarization
LSQHA	Linearly Shifted Quadrifilar Helix Antenna
MIMO	Multiple Input Multiple Output
MOGA	Multi Objective Genetic Algorithm
NLOS	Non-line of Sight
MoM	Method of Moments
MOSA	Multi Objective Simulated Annealing
PLC	Programmable Logic Controller
PML	Perfectly Matched Layer
QHA	Quadrifilar Helical Antenna
RBT	Reverse Bow Tie Antenna
RCGA	Real Coded Genetic Algorithm
RFID	Radio Frequency Identification
RCP	Right Circular Polarization
RSSI	Received Signal Strength Indicator
SARS	Severe Acute Respiratory Syndrome
SRAM	Static Random Access Memory
STB	Sensor To Basestation
STS	Sensor to Sensor
UHF	Ultra High Frequency
UPC	Universal Product Code
UWB	Ultra-Wide Band
UWSN	Underground Wireless Sensor Network
VSWR	Voltage Standing Wave Ratio
WORM	Write-Once-Read-Many
WUSN	Wireless Underground Sensor Networks
WSN	Wireless Sensor Network

CHAPTER 1

INTRODUCTION

1.1 BACKGROUND AND RESEARCH MOTIVATION

The increasing demand for smart, energy efficient wireless communications technology in every field of endeavour has resulted in multifaceted research leading to dynamic advances in wireless communications systems and networks. Radio Frequency Identification (RFID) tags have been of particular interest in wireless communication technology because of their low cost, simplicity, and most importantly; their energy saving capabilities. RFID technology finds applications in such as: secure access control, distribution logistics, documents and parcel tracking, livestock or pet tracking , automotive systems [1] etc. They were initially used for identification purposes; however further researches into deployment techniques for various applications has revealed their versatility and importance particularly in the area of monitoring, indication and control of engineering installations in order to provide early warning signals.

RFID tags are classified into three major types which are active, passive and semi-active tags. Passive tags are made of a small patch antenna designed on a substrate using the etching process, these substrates come in various forms; these type of tags are not powered but rely on the power generated from the reader antenna to retransmit the unique identification information stored on the chip. An RFID transponder stores and transmits data to the reader in a seamless fashion using the

all-important radio waves. Active tags on the other hand are battery powered, they are most suited for longer range detection purposes, and, as a result, require more complex compositional connections as compared to passive tags. RFID serves as a perfect replacement for other similar identification systems, like barcodes and magnetic strip cards. The tags can be contactless and carry unique and a higher density of information over a longer range as compared to previously deployed identification systems.

This research focuses on the design, modelling and efficient deployment of passive UHF (Ultra High Frequency) RFID tags for energy efficient liquid level detection applications. A RFID tag consists of a printed antenna on a substrate and a chip IC (Integrated Circuit) which is usually placed at the fixed feed input source of the tag. The information stored on this chip is relayed back into space when queried by the reader antenna. The frequency of operation of the tag antenna for the intended application needs to be specified from the onset of the design; this is very important because it dictates the size and geometry of the tag antenna for effective performance within the specified operating frequency. The geometry is then optimised for this frequency of operation to match the reader antenna frequency for maximum link coupling [2, 3]. Various devices for monitoring and control can be integrated within the RFID system. The unique information on the chip of a tag can be transmitted via a wireless interface to a database for referencing or to trigger a range of other control activities via a PLC (Programmable Logic Controller) [2, 3].

The current design adopts and implements the passive tag approach because of its low cost, ease of deployment and energy saving capabilities compared to other

wireless sensors. This is why emphasis is laid on UHF passive tag sensors for liquid level detection applications in this research work. The challenges faced when tags are placed near metallic surfaces and liquids are a matter of serious concern, which have been considered for the tag sensors proposed in this research work. Environmental factors and the nature of material used for printing the tags, including the substrate, are factors which significantly affect the performance of the tags. The RFID reader must not be selective to certain dielectric mixtures, since tags based on various substrates with different electrical conducting properties will be designed.

The detection range of the tags is, to a large extent, influenced by the power intensity received from the reader antenna. A successful and balanced passive antenna tag design should not only focus on size, memory capacity and high data read/write rate capabilities but also consider the signal security and integrity issue [4]. The chip on the tag stores the unique identification numbers which have been coded into it and represent a particular product or item; in this research work, liquid level identification information has been coded into the chips mounted on the designed tag antenna. This information carried by the tag can be static or dynamic; data can be read/write enabled running into a few kilobytes with constant response to changes in the environment in which they are deployed to sense, for example, liquid level, pressure, temperature profiles.

RFID tags have various data writing and storage capacities based on the type of chip IC mounted at the input source of the tag antenna. Some are read-only and others are read-write enabled. The read-only types of chip IC are not rewritable, and only store a unique ID, while the read-write enabled chip ICs are reprogrammable and can have

other important capabilities like password coding, kill, lock and unlock coding features. The software which also keeps records on a database can be deployed for monitoring purposes. This software can be run on a mobile device or laptop with distant wireless communication capabilities via a terrestrial network, making the entire system set up automated [5, 6]. The tag is printed with a thin conducting material on a substrate of a specified thickness [7, 8]. Most tag designs come with the basic features of read/write range, orientation sensitivity and a range of other important features such as the amount and size of information carriage capability, number of reads achieved per second and the geometrical dimensions of the antenna.

The fundamental physical constraint is addressed by an appropriate antenna selection and construction which is one of the focus areas of this thesis. A simple selection of tags, readers and a database or application interface makes up a complete RFID system. A tag attached to a product passing through a region of electromagnetic field typically generated by the reader antenna simply responds by identifying itself and passing other range of information both numeric and pictorial as pre-programmed by the application requirement. The passive tag approach in a wireless sensor network environment is an emerging perspective to the deployment of RFID tags for various applications; this has become the dominant contactless identification method deployed for next generation networks [9].

The common challenge with designing chipped tags operating in the UHF band is the impedance matching, which affects the radiation characteristics of the antenna if not properly matched. The tag sensitivity and detection range also become very important issues to consider which often make the antenna design complex [10].

For every antenna design, certain geometry properties must be sacrificed for the other in order to obtain an optimum design performance. The tag size must be commensurate with the frequency of operation; the omnidirectional property of the antenna also plays an important role in avoiding polarization mismatch between the tag and the reader. Polarisation and gain of the antenna are the two most important factors that affect the signal coupling of any antenna [11]. The tuning or optimisation procedure for effective matching of an antenna varies for different antenna types. The antenna's performance is usually degraded when placed on metallic objects or near water; the return loss of the antenna is degraded by nearby objects of different electrical conducting properties, especially when the antenna radiates Omni-directionally. The effect is also observed on the antenna resonance frequency particularly when the nearby object is a dielectric. Antennas with high directivity do not suffer from this problem, so an inventive way of overcoming this problem, is by designing an antenna with improved directivity [11, 12]. Signal attenuation by the environment and objects in proximity of the tag antenna must also be taken into consideration when assessing the operational efficiency of the design.

Computational numerical methods are employed to analyse and evaluate some of these antenna problems. These numerical methods are embedded in optimisation algorithms which are a part of the major simulation packages (HFSS, CST, GA and MATLAB). Some of these techniques are: Method of Moments (MoM), Finite Element Method (FEM), and Finite-Difference-Time-Domain (FDTD) [13]. Differential equations are adopted to obtain fast convergence of results in the FDTD technique. These equations are invoked into discrete time and space counterparts in order to evaluate and fully analyse a model. This approach usually forms an initial

stage of executing a reasonable geometry for numerical evaluation and modelling on computers [14, 15].

In MoM, integral equations appropriate for analysing electromagnetic radiation characteristics of transmitting models are created. MoM is usually applied in a homogenous setting, where a set of arranged metallic bodies forming a specific geometry have been embedded. A combination of FDTD and MoM can be explored to form a hybrid numerical method to analyse various antenna problems. [16-17].

In this work, the High Frequency Structure Simulator (HFSS) software was used to design and model the various tag geometries and the deployment scenarios. The design realisations were fully modelled with a comprehensive parametric analysis for the rectangular tag presented. Their physical deployment into a wireless network and their responses in terms of signal coupling were also analysed and effectively simulated. The sensor tags realised in this thesis were deployed for use as liquid level sensors. Details of the practical work and measurements are also explored.

1.2 RESEARCH MOTIVATION

The ever increasing demand for reliable and more efficient automated processing systems, the need for more efficient and effective process monitoring and control techniques, and an increasingly tough and unforgiving government and private regulator schemes have made it imperative for process engineers to seek for more robust, accurate and dependable level measurement techniques. Energy efficiency and increased precision in liquid level measurement have led to a tremendous

reduction in complicated chemical-process monitoring and control. This has resulted to improved product quality, cost savings, and avoidance of wastage in the process, which directly implies increased profit and lower cost of production across these industries [18].

In the oil and gas industry, particularly in the author's country of Nigeria, there has been much vandalism of oil pipelines resulting in massive spillage and wastage of crude oil with resulting damage to the ecosystem and the means of livelihood for the local settlements whose major occupations are farming and fishing.

Nigeria has lost about $14B within the last ten years as a result of spillage of crude oil due to pipeline rupture. Within this period, a total of 16,083 pipeline leakages were recorded; 398 of these incidences were due to rupture while 15,685 breaks were due to vandalism [19]. The country loses about 800,000 barrels of crude oil daily as a result of pipeline rupture and criminal vandalism, which accounts for 97% of these occurrences, leading to over $55.23B in product losses and repairs of pipelines within the last ten years. The damage done to the ecosystem, the impact on the socio-economic life of the local community and the cost of cleaning up the environment is unquantifiable. This has had a boomerang effect on the economy of the nation as the country has been brought into crisis as a result of these wastages, which have been worsened with the activities of the vandals. Several attempts have been made to combat this problem, but these have not yielded a lasting solution. Military force has been deployed to guard the areas of concern against vandalism, but extensive sabotage has made this ineffective. Drones have been proposed for deployment to

monitor pipelines, but these have been estimated to be very expensive and not the best solution as they can be shot down by vandals.

It therefore becomes imperative to develop appropriate measures to mitigate this problem. This challenge has motivated the present search for an energy efficient, reliable and cost effective monitoring system for liquid level detection in order to escalate unusual fluid level for an early response to curtail wastage attributed to pipeline spillage issues. Newer level measurement technologies have helped in fulfilling laid down specifications for the performance metrics of operations with an increased capacity for electronically reporting control processes.

This thesis demonstrates the deployment of passive UHF RFID tags, and reader including novel in-manhole antenna design for energy efficient liquid level detection applications.

1.3 AIMS AND OBJECTIVES

Emphasis is laid on the design and development of passive UHF RFID tags to achieve novel geometries with improved radiation characteristics backed by theoretical and physical measurements. The theoretical simulation results are compared with the physical measurements to confirm the performance results obtained. The RFID reader frequency of operation, lies in the UHF band between 865-868MHz. The design frequency for the tags in this research has therefore been centred on this frequency band which is the standard frequency range for RFID

European UHF band 865-868 MHz. The Alien RFID reader used for physical detection of the printed tags in this work operates in this frequency band.

This research presents the design and modelling of various tag geometries and reader antenna for deployment as liquid level sensors. This involves the design and development of passive tags and reader antennas, printed on different substrates with various dielectric properties. The sensor tag is simulated in HFSS and the performance of the entire sensor and reader set up is characterised with different environments and with various angle and height positioning of the RFID reader.

The main aims of this research study is as enumerated below:

- To design, model and deploy passive UHF RFID tags for energy efficient liquid level sensing applications.
- To demonstrate that liquid level information can be effectively and efficiently communicated using novel characterisation and deployment of RFID technology.

The Objectives of this research work are as stated below:

- Using HFSS to design and model simple passive tag geometries and analyzing their radiation characteristics (gain, reflection coefficient, Read/Write range, and orientation sensitivity).
- Performing a detailed optimisation and parametric analysis on the realized tag.
- Improving on the radiation performance of the tag especially when placed on surfaces with different electrical conducting properties.

- Characterising the realised tags as liquid level sensors on HFSS and observing their radiation behavior when changes are introduced to their sensing environment.
- Programming the chip IC and subjecting the designed tag to practical measurements and comparing these results to the theoretical results obtained.
- Design and modeling of a novel RFID reader antenna using Genetic Algorithm.
- Proposing and investigating new antenna sensor design concepts for ground level operation in manhole communications, these being modelled, implemented and measured to operate over the GSM frequency spectrum.

1.4 RESEARCH CONTRIBUTION

The major areas of this research contribution is as enumerated below:

- Comparative analysis of previous approaches to liquid level monitoring in terms of their simplicity, energy efficiency and cost implication is presented
- Novell characterisation of passive UHF RFID tags as liquid level sensors is achieved and explored for energy efficient gully pot monitoring and automatic liquid level indication and control.
- HFSS has been used to design, simulate, and model the behaviour of achieved tag designs when deployed for liquid sensing applications.
- Passive UHF tags with two different types of substrates has been achieved for mounting on multiple surfaces with different electrical conducting properties.

- This work clearly demonstrates that liquid level information can be communicated wirelessly in real time using simpler, energy efficient and cost effective solution.
- A novel Linearly Shifted Quadrifilar Helix Antenna (LSQHA) has been achieved using Genetic Algorithm (GA)
- A novel dual band In-manhole chamber antenna has been designed and deployed as a reader antenna.

A study of the radiation characteristics of tags when mounted on different materials is taken into account with the aim of maximizing the link coupling of the system. Tag geometries with optimum geometrical dimensions have been extensively explored in order to achieve a longer detection range within the acceptable frequency range. A full parametric analysis of a rectangular tag and the optimised design is presented, the S-shaped and the mirrored P-shaped tag designs also presented. The rectangular tag design is then deployed for use as liquid level sensors for gully pot monitoring. The simulation on HFSS combines the effects of the surface on which these tags are mounted, and the separation gaps between the tags (level sensors) to analyse the overall performance and efficiency of the tags as liquid level sensors.

This thesis is particularly focused on the improvement of the size, quality, polarisation, detection range, and deployment of passive RFID tags for liquid level monitoring. It takes into consideration the adopted methods of establishing statistical measurements on tag reader positioning at different angles and distances in space and time. The maximum detection range of prototype tags mounted on different

material is also considered for evaluation purpose. The reader antenna realised shows good performance in terms of directivity and read range.

RFID deployment for use as liquid level sensors is a novel application area where considerable success has been achieved. Various tag geometries are designed and deployed; their perfomances have been analysed and tested. The factors affecting the performance of passive UHF tags is taken into consideration for improvement of the design realisations presented. Passive UHF RFID tags are modelled, simulated, optimised and printed on different substrates with various electrical conducting properties.

1.5 ORGANISATION OF THE REPORT

The rest of this thesis is structured as enumerated below:

Chapter 2: Presents an extensive literature review of RFID technology and applications; it then presents an analysis of the various RFID based fluid monitoring and measurement techniques and challenges faced. RFID system history, feature variations and tag types, operating frequency of the selected design and the environmental effects on the signals of tag antenna, chip types and their associated memory size differences have been fully discussed and presented. A background of dual band antennas is discussed with a critical analysis of previous antenna designs using GA is presented.

Chapter 3: Showcases an energy efficient gully pot monitoring system using passive RFID tags. The design of the adopted s-shaped and meander tag is presented with practical deployment results analysed.

Chapter 4: Presents the design and analysis of a passive tag to be deployed as a liquid sensor. The tag is modelled and the prototype is printed on different substrates, one with metallic ground and the other without the ground plane. The tag design is modelled and simulated in HFSS. A parametric analysis of the tag is extensively explored to obtain the optimised design presented. The deployment of the designed tag for liquid level monitoring application is presented. This is modelled and simulated on HFSS with practical and simulation results presented. The tags were mounted within a gully pot with same tag used as the reader antenna and the reflections observed in order to extend the modelling perspective further to see what effects this will have on the overall performance of the system set up. HFSS platform was used to simulate the tag antenna's performance in an operating environment. The characterisation of a P-mirrored shaped tag for automatic liquid level indication and control is presented.

Chapter 5: The design and modelling of an in-manhole chamber antenna for underground communication systems is presented with detailed practical measurements. A detailed analysis of the U-shaped antenna is presented operating over the GSM frequency spectrum.

Chapter 6: Discusses the reader antenna design using Genetic Algorithm. A review of previous approaches to the antenna design problem using GA is fully discussed and analysed. The spiral and helical antenna with their associated advantages, differences and suitability for adoption as reader antenna for the proposed design is fully discussed. Presents the LSQHA design using GA. The optimisation results are presented and discussed.

Chapter 7: Presents the conclusion and recommendations for future work.

CHAPTER 2

LITERATURE REVIEW

2.1 HISTORY AND REVIEW OF RFID SYSTEMS

Radio Frequency Identification (RFID) is a means of identifying a unique object or person using radio frequency transmission. RFID technology is expected to become a core technology of ubiquitous infrastructure as it identifies objects and users, and automatically takes advantage of contextual information. RFID technology has gained popularity in commercial and industrial processes and systems. This has resulted in multiple rapid deployment of this technology as part of an overall wireless network for monitoring and control of simple or complex systems.

Recent trends in applications have also seen tremendous deployment of the technology in homecare, and healthcare systems; other interesting application areas are in high- security and high- integrity settings such as national defence. RFID in logistics or commercial applications is an empowering technology as it simplifies application and service processes. For instance, a customer's details can be extracted from a tag attached to products purchased by the customer and inputted into a database as a part of a network of information set.

The tags unique identification, reader identification, the product code or symbol and other associated information form a string of data set transmitted to a database for monitoring and in some cases, control purposes [20]. This obviously brings increasing efficiency to supply chain management operations and introduces a higher

level of security by improved asset visibility and remote independent monitoring. Some of these applications are also deployed in military operations and medical sciences for increased security, asset tracking and management [21]. The versatile nature of technology in the wireless communication world has not allowed for total dominance of RFID systems in wireless networks. However, RFID deployment to existing networks has increasingly gained popularity, especially among the major players in the industry. Real-time asset tracking and identification has been made more effective with the deployment of RFID technology in these industries [22]. This has led to a continuous research demand into the application areas of this technology, especially in a bid to conserve space and energy and improve overall efficiency and effectiveness of operations of major manufacturing supply chain management systems.

The concept of radio frequency engineering is related to the electromagnetic theory of waves by James C. Maxwell in 1864. His discovery of ether, made transmission of light, heat and radio waves possible; this paved the way to numerous innovations in the electronic communications world. Heinrich Hertz, who discovered radio waves, made his findings based on Maxwell's extension of the electromagnetic theory of light which has opened doors of advancement particularly in this area of science and technology [23]. The previous laws that existed before Maxwell did not effectively predict waves as they were only laws of electrostatic, which only correctly described the near field; these were Ampère's law of magnetostatics, Faradays law of induction, and Gauss flux theorem. The near field can be illustratively described as, the electrostatic field of an electric charge and the magnetostatics field of a current loop. The impacts of the interplay between electric

charges and magnetic fields in close proximity to a source is described by these laws; however, the impacts of these forces in the far field region is not addressed. The laws described that a conductor fed with alternating current produces a magnetic field where the E – and – h fields co-exist with varying magnitude and are relatively static with no propagation.

Maxwell showed that the electric and magnetic fields at a certain distance beyond the quasi-static near field separate themselves from the conducting surface and propagate as a combined wave into space at the speed of light. This significant transformation happens at a point called the far-field. The interaction between the electric and magnetic fields in their inter-woven nature is expressed in Maxwell's mathematical equations; he derived the speed of light from his computations and concluded that the phenomenon of light is an electromagnetic phenomenon. The complete set of the electrodynamics laws were corrected and assembled by Maxwell for the first time. The laws, which clearly established the relationship between the electric field quantities and the magnetic field quantities, was published in his text in 1873 [4]. Maxwell's equations provide the basis for the modern electromagnetism theory.

The first major deployment of RFID was during the Second World War for the friend or foe identification system. Transponders were mounted on planes which revealed their unique identity when queried. This helped air and land fighters to distinguish between enemy and friendly artillery. In the 1960's, RFID applications relating to the electromagnetic theory were developed and this led to a commercialisation of the technology, one of such gave rise to the development of the

Electronic Article Surveillance (EAS) application. These systems were largely dedicated for short range communication in retail stores to complement other anti-theft systems in place such as the Closed Circuit Television (CCTV). Auto-ID RFID technology is a massive improvement over the Automated Identification and Data Capture (AIDC) barcode standards for products identification. The AIDC barcode used in line with the Universal Product Code (UPC) has been largely deployed in retail consumer shops basically for item identification and tracking, for inventory and retail chain management [24].

RFID systems and tags have gained increased popularity and have now been widely deployed for non-contact item identification and tracking which is a major step ahead of the predominant methods of item identification. In the 1970s, many educational and corporate organisations embraced the RFID technology and more attention was given to the practical aspects of this technology by various company and government laboratories. This then culminated in the mass deployment of the technology for multiple application in the 1980s.

The evolution of RFID technology can be attributed to WWII where the early foundation for this identification technique was laid. The activities of the Auto Identification and Media labs at MIT served as a major centre for innovation and a meeting point for key players in the technology development industry. This paved a way for massive improvement in the major application areas of this technology. There were also simultaneous developments in USA involving projects executed through DARPA, [24, 25]. During the Severe Acute Respiratory Syndrome (SARS), which broke out in Singapore in 2003, RFID was deployed to track and monitor the

syndrome outbreak among in house patients at the Alexandra Hospital (Singapore). The unique ID on the tags formed a statistical network of data used as a reference point, or as a sort of an infection map on a network to predict rate of occurrences and study the pattern of the syndrome outbreak in order to effectively curtail and combat the outbreak [24, 25]. RFID tags has been deployed and implanted on bank notes to track note circulation and also to track criminal activities; this was adopted an enforcement application by the European Central Bank in 2005 [26]. Early adoption and deployment of the RFID technique in retail chain management is found in both trade and academic journal publications [24, 26].

The increased interest in RFID as a tracking and identification technology has triggered other wide range of applications for which they are now deployed. Some of these applications are: pet and animal tracking, industrial process automation, inventory and access control, automatic parking, moisture and crack detection, liquid level indication, monitoring and control [26]. This has led to associated advances in micro-electronics, embedded systems software, and nanotechnology. Bar codes, and magnetic stripes cards have been used for a long period of time for identification of products majorly in the retail sector; this technology could only identify a product one at a time as they pass through a region for onward processing.

The deployment of these smart tags has seen increased efficiency in retail chain management as identification and tracking has been made faster and much easier with capabilities of identifying multiple products at once as they pass through each stage of the retail process. An RFID system is made up of the RFID tag, reader, RFID software, and a database. The reader scans the tags simultaneously and

transmits the information to a database where it is stored for referencing. Figure 2.1 gives an illustration of the various types of auto-ID systems of which RFID has become most popular and dominant. The other forms of auto identification system are mostly contact based and employ line of sight mode for identification and consequently, can only track or identify one tagged item at a time. A RFID system on the other hand does not require line of sight communications, and can identify and, at the same time, track multiple tagged items wirelessly.

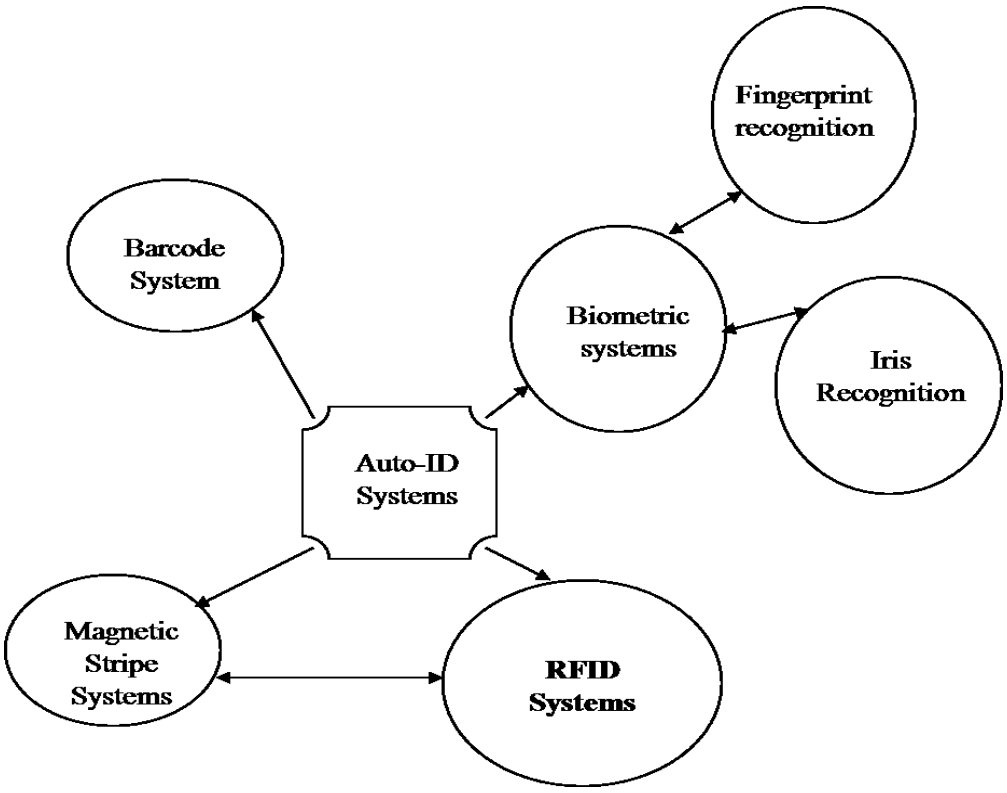

Figure 2.1: Types of Auto-ID systems

The recognition of objects is made possible with the use of radio waves in RFID systems [24], as opposed to barcode systems which use line-of-sight technology. This makes the barcode systems contact and close proximity hungry because of the nature of the signals which must be physically aligned with the code for efficient and successful reading. The barcodes are easily degraded by minor damages or blockage

to line-of-sight signals and cannot easily be updated [27]. They often require manual handling and this makes them susceptible to human error and lack independent operation which also makes their use in automation less suitable. The RFID system, on the other hand, can cope with different environmental variants without causing a major disruption to the application for which they have been deployed. They use radio waves for communication, and do not need the line-of-sight rays as deployed in barcodes.

This gives RFID systems increased effectiveness in multiple tracking, although with some associated problems in regards to tag jamming, but in general are more compact, robust, rugged, and more efficient means for identification. They are cheap to develop and maintain; their portability also makes then suitable for deployment to existing networks with space constraints [24, 27]. Some of the benefits of RFID systems and general applications over other identification systems are as enumerated below:

- Omni directional radiation pattern for easy and fast detection.
- They are cheap and easy to manufacture and do not require a complicated manufacture process.
- They carry a chip where the unique identification is stored for referencing.
- They are easily read with reading rates up to 1000 tags/sec.
- The chip on the tags can be read/write enabled.
- The detection range is better than those of other identification systems.

In spite of the numerous benefits of RFID systems, which actually outweigh its limitations, it is important to look into and analyse these limitations, as some of these limitations are challenges for consideration during this research work. Some of these are as outlined below:

- Tags have no adequate security and can be read easily by any reader.
- Degradation in tags radiation characteristics when mounted on surfaces with different electrical properties.
- RFID reader and associated middleware are expensive.
- Tag jamming when multiple tags are in close proximity.

RFID standards often specify tag-reader communication protocols. The item information obtained can then be made available to higher level applications for monitoring and control, or other purposes. Some of the advantages of deploying RFID technology particularly for liquid detection applications are:

- Real time autonomous identification and tracking,
- Passive RFID is cheaper to buy, install and maintain
- Low power consumption making them a better energy efficient and cost effective solution.
- Non-pollutant, better durability compared to other liquid sensors.
- Simple and easy to deploy to existing infrastructure.
- Wireless communication capability with on-board rewritable chip memory for unique coding and identification.

- It easily fit into any existing wireless network accessing information any day, at any time, and relaying this back to a remote installation for monitoring and control proposes.

This research brings a new perspective to the application of the RFID tags in liquid level sensing, indication and control applications. The advantages of the passive tag is fully explored to justify its preference for the work presented in this thesis. They are energy efficient, durable, light in weight and size, cost effective, user friendly, readily deployable to existing systems, and simple in design and complexity.

RFID technology poses privacy and security concerns because tags can be read contactless and without evidence. A tag uniquely identifies the object's product description, unique identity, manufacturer and any other information the manufacturer intends to input especially for programmable tags. RFID system is prone to multiple types of attacks because of the system's components open nature and high mobility.

Survivability of passive tags is a strong characteristic, which makes the passive tags very useful to deploy especially for energy efficient systems. Survivability is a system's ability to withstand malicious external attack without having a detrimental effect on the systems operational efficiency even when a part of the system has been damaged. This as a system property relates the amount of service provided to the overall level of damage done to the system, and the impacts of the operating environment; the timeliness in processing results irrespective of harmful attacks with the risk of system failure; and the ability of the system to offer non optimum but accepted services to various subscribers even when the component parts has been

damaged. This clearly shows the recovery capabilities of the system with improved environmental factors. The major challenge for survivability in RFID systems is the constrained memory resources that can be dedicated to security functions for the tag and the power requirements of the security algorithms [2]. With the increasing application of RFID technology in various fields, the requirement for a more reliable and resilient system for RFID applications has been on the constant increase.

A tag can be designed to transmit and receive signals at different frequency bands like Low Frequency band (LF, e.g., 124-135 KHz), High Frequency (HF, e.g., 13.5 MHz), Ultrahigh Frequency band (UHF, e.g., 860-960 MHz), and the microwave bands. Several antenna design realisation are classified into two main types based on the nature of their polarization.

- Omni-directional Antennas: These type of antenna radiate equally in all directions and are often of low input impedance (50-80) Ω. Some typical examples are the monopole or dipole antennas, other omnidirectional antennas comes with high input impedance (100-300) Ω, typically in closed loop, and (10-200) Ω for the open loop counterpart geometries (folded dipole). This type of antenna is generally characterised with low gains [28].

- Directional or beam antennas: These are antennas with high directivity which are most suited for long range communications; the power radiated is greater in one particular direction. They have increased efficiency in performance in both transmit and receive operations with minimal interference from external or environmental sources. The Yagi-uda is a typical example of this. However, same performance is now being achieved with patch antennas

adopted for RFID systems. The printed board antenna with impedances of (50-100) Ω and the micro-strip counterpart (30-100) Ω are increasingly being deployed for RFID antenna systems.

Generally, most tag designs aim for the omni-directional radiation property for the tag antenna; this is in order to make the tag less orientation sensitive. The reader design is made to be highly directive in order to achieve greater read/write ranges for the entire system. Fixed frequencies are usually assigned to RFID application to mitigate the impacts of signal attenuation by external factors. The amount of data a tag's signal is able to carry increases with operating frequency. RFID systems that are designed to operate at longer range typically use UHF and microwave frequencies. Data is obtained from a tag when a reader in proximity queries the tag. The reader forwards the data to the backend database, which stores authentic tag data and links this with the record collected by the reader. The reader, after being authorised, can access in-depth data on specific products on which the tags are mounted to identify.

2.2 RFID SYSTEM OVERVIEW

An RFID system is made up of very important component parts each of which plays a vital role for the successful operation of the overall system. Each of the component parts work simultaneously, seamlessly relaying information from the tags to the reader and to the middle ware where these information is decoded and displayed in readable format on a display screen. These component parts of the RFID system are discussed in this section.

- **Tag or transceiver**: This is the antenna that carries the unique identification information on a chip. It is made up of a conducting layer of antenna geometry formed by the etching process; this thin sheet of conducting layer carries a chip usually at the source of the antenna. This antenna is printed on a substrate of a certain permittivity. The battery (for active tags) forms a part of the complete tag package. This entire unit is called the RFID tag, and it performs a central operation in the RFID system.

- **RFID Reader**: This is also referred to as the interrogator. It queries the tags for their unique information and passes this information via a middle ware to a database for referencing. Usually typical readers are directly connected to a computer that has the middle ware installed. Latest improvements in RFID reader technology has seen the evolution of readers from fixed to mobile and wireless readers for remote and wireless transmission of information read from tags.

- **RFID Middleware**: this is a software based code that controls and interprets the series of actions between the tag, reader and computer application database. It forms a link for decoding and encoding information transfer between each of the entities. It also performs encryption and decryption functions where this is an additional functionality to improve security of the RFID system.

- **Application software:** The application is the final destination of data fetched from the tags. System application could be for monitoring purposes only, while

for some others it could be for monitoring and control where the data obtained from tags in the network are used to trigger other control processes.

The deployment of RFID technology has brought more efficiency, which translates into direct profit for companies, industries, retail outlets and the government. For the military, naval and air forces, it brings additional security and ease of operations. For the healthcare and pharmaceutical industry, it creates a better life and health service standard which has a direct impact on the life expectancy of the citizenry and the quality of service offered by health professionals. The advancement of this technology touches virtually every sphere of life.

Figure 2.2 presents a block diagram of an RFID system with the connection sequence between each of the component parts. Each of the communication steps depicted here plays a very sensitive role to the overall functionality of the entire set up.

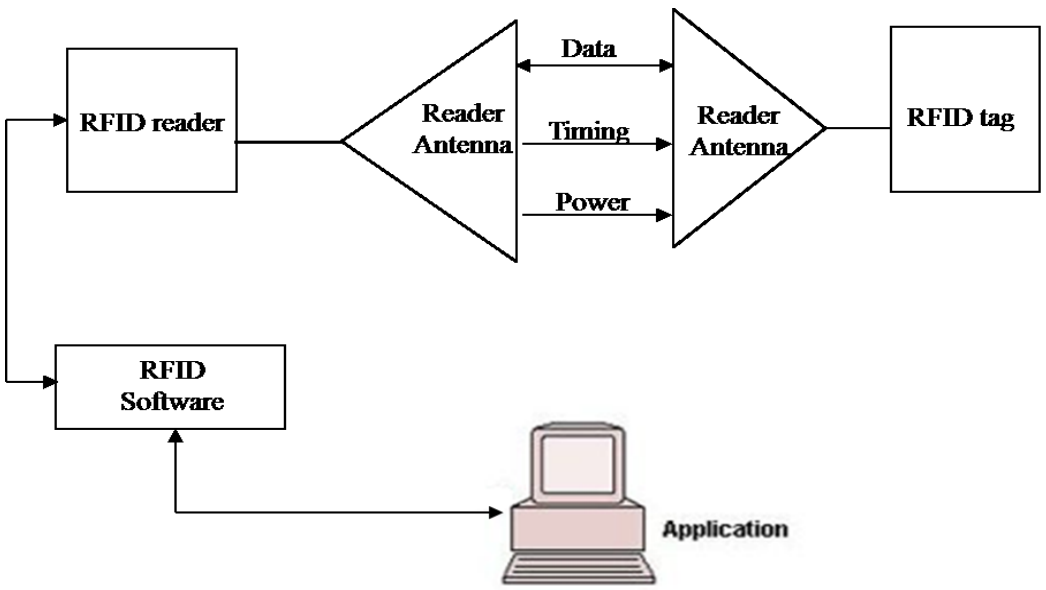

Figure 2.2: RFID system set up

2.3 RFID TAG

The tag is the basic component of an RFID system as it is the central component when information required to trigger other range of activities is sourced. There are different types of tags based on specification requirement of the application for which they are intended [29]. Some of these requirements are as enumerated below:

- Selected frequency of operation or bandwidth
- Size and geometry requirements
- Composition of the substrate material
- Production cost
- Gain
- Read/write range
- Polarization/orientation
- Casing or seal type etc.

The programmability and adaptability of a RFID tag make it very versatile and easily deployable as part of an existing sensor network; its quick response times in very unfavourable conditions makes it rugged and best suited for most applications [29]. The Electronic Product Code (EPC) global standards is used for RFID hardware and software coding as the standard numbering code for the unique chip ID. A unique ID is assigned for each tag; if this ID is rewritten it is done following the EPC standard [30]. The stored information ranges from a short ID code to a few bytes or kilobytes of data [31, 32]. The information stored in a unique ID number using EPC global standard are broken into different segments each of which represents a data set. This

is made up of the object class and serial bits, the EPC manager number, and the header. Each of these elements represents unique information about the tag, as follows:

- **The header**: holds information on the data string length, the type, structure and EPC generation.
- **The Electronic Product Code manager number**: updates and keeps records of each successive partition.
- **The object class**: represents a class of protocols as defined by the EPC Global.
- **The Serial number**: simply represents an identification of instances which is usually encoded in the tag in bits. Data retrieved from the chip on the tag antenna can be sent in wired or wireless form to a database that does the computer crunching calculations in split seconds and trigger other event and time driven control systems dependent on the tag data supplied.

Electronic Programmable Read Only Memory (EEPROM) is majorly used in active tags whilst passive tags store their unique ID using Static Random Access Memory (SRAM). The memory in EEPROM is not volatile; it also does not support online changes as compared to the SRAM where memory is volatile, supports online changes to the controller and produces a physical fingerprint on power up. The requirements for memory of a tag are affected by reader-tag transmission range and medium which is usually specified as a standard air interface in the ISO-8000 standard [33, 34]. Under the ISO 8000-6B standard, most readers readily operate in the read/write mode with the class 0 and 1 tags respectively. EPC classes are generally known as the GEN1 and GEN2 respectively. The frequency of operation

and the communication medium plays a major role in the success of transmission and reception of data between the tag reader and database. Every country has a frequency slot for each device application as assigned by the ITU standards.

The frequency range of 865-868 MHz is specified for UHF RFID operations in European countries. This research work takes this frequency allotment into consideration and aims to design tags that work efficiently within this range of frequency. The maximum distance between the tag and reader for effective transmission and reception of tag data is known as the detection range. This range is affected by a couple of factors such as the system frequency of operation, the gain and polarization of both reader and tag antenna and the nature and position of excitation, the coding technique for modulation and demodulation, the bits number and algorithm for detection, and then the nature of the propagating environment [35].

The physical measurement which is a reflection of the quality test suffers from some usual constraints such as the tag size and the ability of the reader antenna to withstand readings from multiple tags and the transmission environment [36]. Figure 2.3 shows a range of environmental factors which impairs the reader-tag operation. The quality of signals received from the tags in deployment depends on a couple of factors which have been identified earlier. However, the environment to which the tags are deployed affects the radiation properties of the tag. The tag jamming and related issues such as anti-collision techniques in populated RFID networks has been investigated and studied by Nikolas [37]. Tags mounted on metallic objects for example, have a major part of their signals reflected and degraded causing major difficulties for the reader to pick up the backscattered information from the chip IC

of the tag. Closeness or contact with any form of liquid affects the tag performance. These factors are taken into consideration and exploited to serve as the basis for tag sensor design and development presented in this thesis.

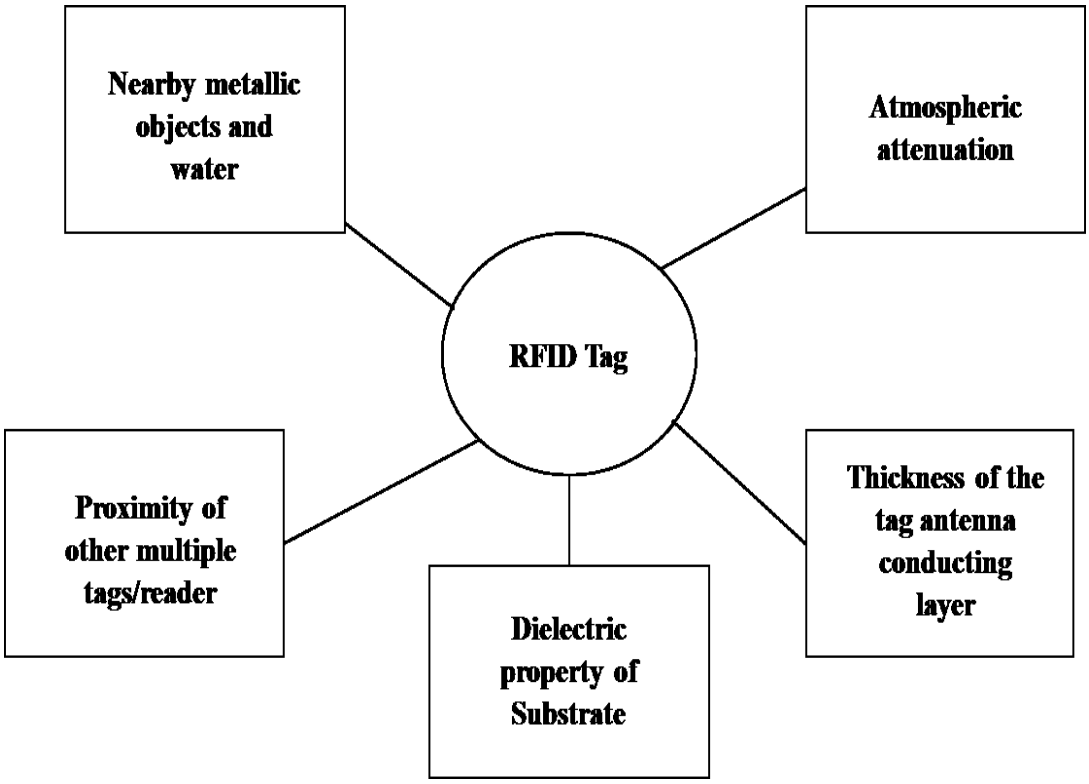

Figure 2.3: Factors affecting RFID tags in propagation environment

The RFID tag performs a central role in an RFID system and classified into three main types, these are:

- Active tags
- Passive tags and,
- Semi-active

Active tags employ a battery as a power source which forms an integral part of the tag making the tag a little bit chunkier in size compared to their passive counterparts. Passive tags do not use any on-board source to power the chip. They get their chip activated by the radio waves received when they come in proximity of a reader. This makes passive tags more energy efficient and portable in size. However, the active tags achieve longer read/write range compared to the passive tags. The semi active tags combine the features of the active and passive tags to transmit information and require more complex techniques to design.

2.4 PASSIVE RFID TAGS

Passive tags, out of all the tag types, are more power efficient as they do not require any on-board power for their operation. They are instead powered inductively by the power received from the reader antenna; they respond to this signal by backscattering the unique information held in their chip. These passive tags become most useful in terms of energy efficiency in scenarios where battery replacement for sensors will be almost an impossible or very expensive task to accomplish.

The indoor reflection and absorption of propagated signal along with the other forms of indoor and outdoor signal attenuation must be taken into consideration for compensation in the design of any RFID tag antenna, as its performance is adversely affected by these phenomena [37, 38]. For reasonable detection of tags, the reader distance should not be too far from the tags. The design range specifications should be adhered to in physical implementation terms. In a situation where the tags respond

simultaneously to a reader query, it leads to collisions which invalidate the data read and working efficiency of the whole system set up [39].

RFID applications, particularly those of the UHF band, have gained increased popularity due to flexibly in deployment to a wide range of applications. The RFID reader plays a central role in a wireless network system of tags and readers. It is designed to be compact, user friendly and versatile to various applications where tags within the designed frequency of operation are deployed. A reader usually comes with a transceiver which makes it transmit and/or a receive signal.

Propagation models in HFSS can be set up to observe signal reflections within an indoor or outdoor environment in order to adapt design properties of the tag and reader antenna to cope with real life environmental propagation factors earlier highlighted. Readers placed within a close range also suffer interruptions in signal and, hence, the separation distance between the reader antennas needs to be specified in real terms to avoid mutual coupling, which degrades their radiation characteristics consequently impairing performance of both readers and tags [24, 40]. Absorbers, whose shape and material must be carefully considered, may be used to reduce interference effects [41, 42].

The two major central processes fundamental to the success of an RFID network is the reader power for tag activation and the sensitivity of chip-tag in reacting to activation by effectively backscattering its unique data held in the chip or memory whether they are read only, read and write enabled, or Write-Once-Read-Many (WORM) [43].

The power requirements of a passive tag differ from an active tag. Figure 2.4 shows the difference in power transfer mechanism between passive and active tags. The passive tags are powered extrinsically while the active tags use an on-board battery. Passive RFID tags do not have a dedicated source of on-board power as a compact part of the tags; they depend largely on the electromagnetic waves sent from the RFID reader. Electrical fields are induced in the tag's antenna by the incident wave received from the reader in proximity; this gives rise to the generation of minute voltage across the tag antenna's region which is the input port of the chip. The power generated within this region of the tag is used to activate the chip IC and transmit the signal containing the unique data held in the IC memory. They can be said to go into a standby mode until they are re-activated by a reader in proximity and then it then starts to broadcast its encoded EPC. The range over which this is broadcasted depends on the chip IC excitation threshold, this is an important factor to consider [25].

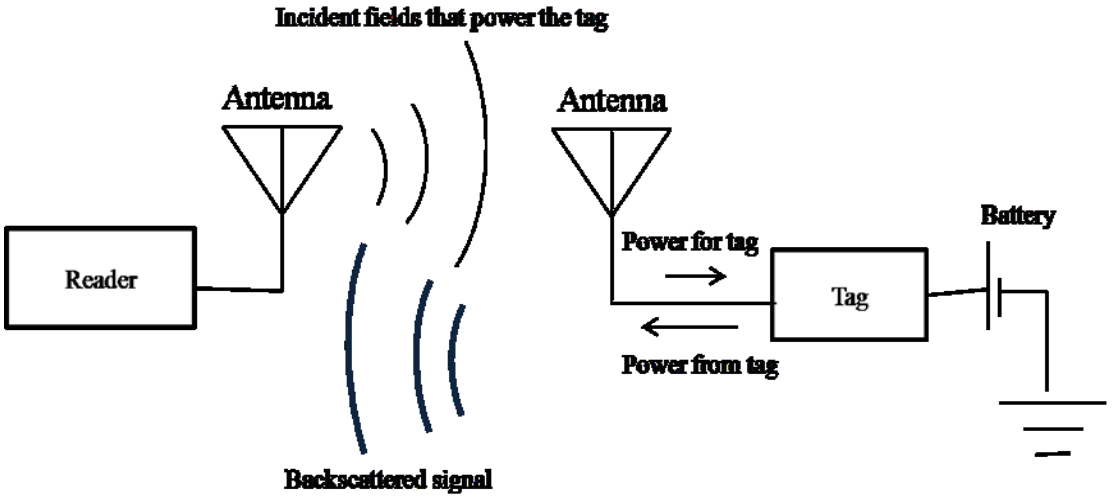

Figure 2.4: Backscattered signals from Passive and active tags

The reader-tag communication process is explained in two steps. The first communication phase is the power supplied to the tag from the reader's antenna,

which is the forward communication where the chip is activated by virtue of the electromagnetic field region of the reader antenna. The second phase of communication is the backward response from the tag to the reader where signal is sent backscattered to the receiving reader antenna. The active tags are usually internally powered by a small lightweight battery, which keeps them in a constant active state ready for communication at any given point in time. They also communicate over longer ranges compared to the passive tags for this obvious reason which is a major advantage. However, their functionality lifespan is limited due to the draining of battery power which is the main disadvantage of this type of tag. The third type of tag combines the advantages of the two types earlier mentioned above.

Figure 2.5 shows a complete RFID network with all the working component parts, the tags communicate their unique ID when queried by the reader antenna and this information is decoded by the reader software and compared with the database for referencing. The reader antenna comes in different shapes and sizes for increased portability and can be wired or wireless. Hand held RFID readers have now become more popular in RFID applications.

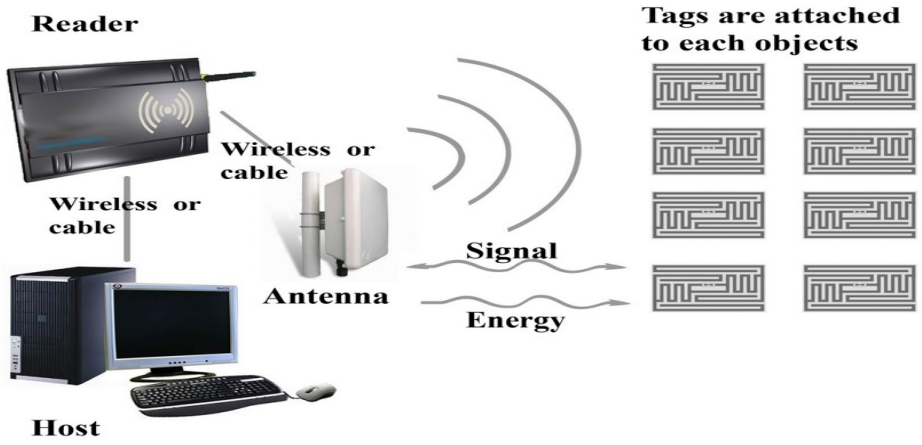

Figure 2.5: RFID network setup

This research focuses on the design of passive tags majorly due to the energy saving capabilities of this type of tag when deployed as part of a wireless communication/monitoring network. The other tags design complexity and the cost of batteries are a major disadvantage. In addition, the uncertainties involved with the inaccurate prediction of the performance of batteries become another challenge. Therefore, passive tags are proven to be more effective and suitable for deployment as liquid level sensors.

Table 2, summarises the differences between the various tag types in terms of their energy saving capacity, detection range, size and complexity of design, durability and cost effectiveness. For liquid level applications, the passive tag with a combination of novel deployment techniques proves to be most energy efficient and cost effective solution.

Table 2.0: Distinction between Passive, Active and, semi-active tags

PASSIVE TAGS	**SEMI-ACTIVE/PASSIVE TAGS**	**ACTIVE TAGS**
Reader powered	Battery powered	Battery powered
Minimum detection range (< 1m)	Shorter detection range compared to active tag (< 10m)	Improved and better read range (> 10 m)
Longer lifespan	Lifespan limited but greater than active tags	Shortest lifespan of the lot
Smallest and light weight	Moderately sized	Bigger than the other types
Cost effective	More expensive to produce	Most expensive to produce and maintain

The longer lifespan, simplicity, and cost effectiveness of passive tags makes them preferable for use as energy efficient sensors in this research work. Each type of tag serves its own purpose based on the application for which they are deployed. In a design application where the communication range is a principal pivotal factor, active tags would become more suitable. Passive tags are most suited for communication ranges within a few feet for auto identification and tracking. Identifying and working within the most appropriate frequency for design application is an important factor to consider when designing any transceiver.

The communication distance is affected by frequency selection of the design. For example, for high frequency operation, the communication distance will be shorter compared to lower frequencies. The reader deployed during physical measurement of the designed tag read range has two dedicated antennas, each with the function of transmitting and receiving respectively. The reading range can simply be measured between the tag and transmitting antenna. The Alien RFID reader AlR-8800 has been used throughout this research work, it operates between 865.6-867.6 MHz with 5.5 dBi gain [26].

The maximum range of detection r is expressed in Friis transmission equation as expressed below:

$$r = \frac{\lambda}{4\pi}\sqrt{\frac{P_t G_t G_r (1-|S|^2)}{P_{th}}} \qquad (1)$$

Here, λ is the wavelength, P_t is power transmitted from reader antenna, G_t the reader antenna gain, the Effective Isotropic Radiation Power (EIRP) of the reader is represented as P_tG_t, G_r represents the gain of the receiving antenna, P_{th} is threshold

activation power for the tag chip, and the power reflection coefficient is presented as $|s|^2$.

The return loss of the input signal is given as a coefficient, this is calculated as follows:

$$|S|^2 = \left|\frac{Z_c - Z_a}{Z_c + Z_a}\right|^2 \text{ for } 0 \le |S|^2 \le 1^2 \quad (2)$$

$$Z_c = R_c + jX_c; \;\; Z_a = R_a + jX_a \quad (3)$$

Where Z_c and Z_a are the chip and tag antenna impedances respectively.

The component parts of the Alien RFID reader is as illustrated in Figure 2.6, is composed of two reader antennas dedicated for transmitting and receiving, software tools, a power pack (240V) and passive tags. The software tool set is installed on computer that runs the software demo (Alien demo software) and links the information received from the reader to the computer database.

The communication line between the reader and middleware can be achieved by cabled or wireless network. An alternative wireless connection can be configured by assigning dynamic IP addresses for autonomous connection. The cabled antennas are six metres long, this makes it convenient for placement at various selected distances for tag detection, and range measurement. The Alien RFID reader was deployed for use all this research work. The Alien reader come with its own software which is installed to on a PC and then the ports of the reader connected to the serial port of the computer to physically link the systems. The reader antenna is then attached to a selected port and then the software is run on the system on a selected reader mode. This software has been used to read and write information to the chip IC of the tag.

Figure 2.6: Alien RFID technology kit

The frequency operations of the proposed tags are usually in the LF and UHF band with both near and far field coupling operations respectively [33]. The reader-tag communication in the near field is usually established using the electric or magnetic fields and electromagnetic radiation in the far field.

2.5 NEAR AND FAR-FIELD PROPAGATION

The propagation process involved with RFID systems is of two types, these are: near-field and the far-field systems. Communication in the near-field is a short range mode of communication process for tags deployed in Low and High frequency bands. Far-field propagation is adopted for a wider range of communication particularly in the UHF and Microwave frequencies. The primary magnetic field is generated at reader antenna regions in proximity to the tag; this magnetic field then induces an electric field (in the near field) at tag antenna region which activates the

chip IC and creates an impulse of electric waves in the near field region. During the far field transmission, the electromagnetic field created in the region of the tag antenna detaches itself from the surface and radiates into space (usually during backward communication from tag to reader). The ratio 120 π or 377 Ω relates the E and H fields particularly in the far field region. The operating distance between the near and far fields is expressed as:

$$r = \lambda / 2\pi \quad (4)$$

This is very true particularly for miniature antennas where the dimensions of their structure is much smaller than the wavelength ($D<<\lambda$). D represents the optimum size or structure of the tag antenna while *r* is a representation of the radius of the radiating structure. Distances in the far-field holds when $D>\lambda$, and this is denoted in equation (5):

$$r = 2D^2/\lambda \quad (5)$$

The radiating near-field is the region where the antenna radiation pattern not fully formed but taking shape, equations (4) and (5) is combined to get an expression for the near-field region:

$$\lambda / 2\pi < r < 2D^2/\lambda \quad (6)$$

The powers of range $1/r$, $1/r^2$ and $1/r^3$ usually represents the fields across the region of an antenna as denoted in Maxwell's equations. The higher order powers show up more frequently in the near-field solution, in the far field zones the first order power dominates.

2.5.1 FAR-FIELD PROPAGATION AND BACKSCATTER PRINCIPLE

RFID tags have an important feature fundamental to their success of operation. This is the backscatter property, where power is from the Reader antenna is absorbed to activate the chip and reflect the encoded signal held in the IC back to the reader. This mode of communication occurs at a longer range of field from the radiating structure (far field). The frequency phase of the reflected waves is shifted to encode information, this process is called modulation. For complete and successful full phase operation of tag-reader communication, the forward and backward power transfer must occur without any form of interference.

2.5.2 FORWARD POWER TRANSFER

The power at the region of the tag transmitted by the reader antenna must meet the threshold power activation requirements of the tag in order to successfully 'wake' the tag and trigger it into communication. The tag reacts by adjusting its input impedance and reflecting the signal back to the interrogator. The terms 'reader' and 'interrogator' are used intermittently all through this write up to connote the same meaning.

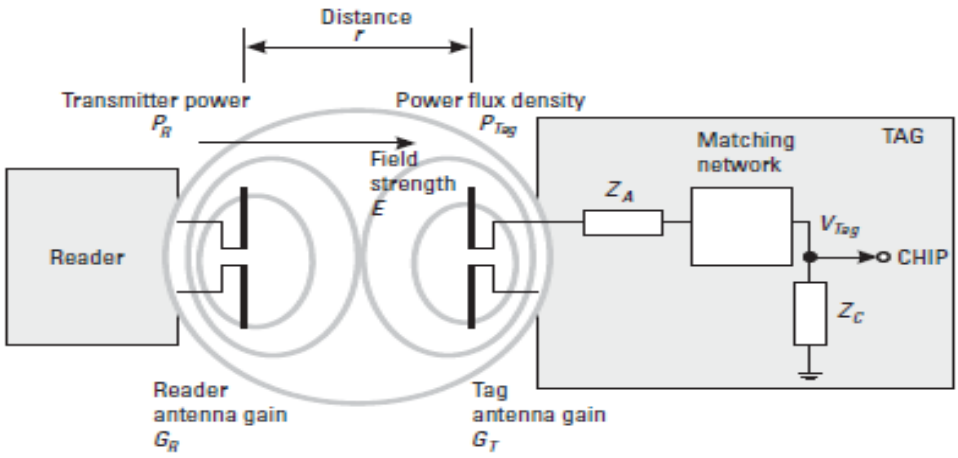

Figure 2.7: Forward power transfer principle for a chip based tag.

In the figure 2.7, as depicted, $Z_A = R_a + jX_a$ is the complex antenna impedance and $Z_C = R_c + jX_c$ is the chip impedance; Z_C may vary with the frequency and input power to the chip.

Passive tags are power efficient; however they have their own associated challenges as earlier mentioned. This should be taken into consideration in designing tags for specific applications as ignoring any of these challenges could invalidate the whole aim and concept of the design [23].

RFID tags are also classified into chipped and chipless tags based on techniques implored for data storage [46, 47]. Chipless tags do not carry the IC on board but have unique patterns which are encoded unto their surface. Chipped tags carry an IC which is used to store their unique identification. Each of these types of tags has been studied from an application perspective, undoubtedly each have its own advantages and weaknesses based on suitability for certain applications, and the cost implications involved. Generally, chipped tags have gained more popularity for use as liquid sensors because of the liquid level memory requirement of this type of application. Tremendous success in chipped RFID tag technology deployment has been made possible by the cost effective production and miniaturization of semiconductor components used in the development of IC's of the tags. This calls for a thorough and more detailed understanding of antenna performance measurement parameters. Some of these parameters are discussed in the subsequent sections of this chapter.

2.6 REVIEW OF LIQUID LEVEL MEASUREMENT TECHNIQUES

Previous approaches to both manual and automated methods applied to liquid level measurement have always had limitations. There have been various attempts at addressing the liquid level monitoring and control problem. Several technologies ranging from simple mechanical float switches to more complicated ultrasonic sensors have been deployed in a bid to provide more accurate, reliable and efficient liquid level information. Many of these technologies are complex, difficult to deploy, and generally not cost effective for multiple deployment over a large scale.

A sight glass used for manual measurement suffers from material failure and poses serious fire and explosion hazard to personnel. The seals easily develop leaks spots, and sludge build up obscures visibility making them less suitable for sensitive liquid monitoring operations. Some liquid level monitoring systems are based on specific gravity, which is the most commonly used physical property for liquid level detection. A float with a differential gravity between the process fluid and the container headspace vapour correctly and effectively follows fluid level fluctuations. A hydrostatic head measurement is also commonly used for level detection. Computers associated with other sensor technologies are deployed when more complex processes for level detection and control are needed. Transducers with various signal output formats like current loops, analogue voltages and digital signals are also deployed for automatic level detection. Analogue signals, because of their variable nature, come with a lot of interference and noise issues which are usually simple to deal with. Computer crunching calculations are often required for effective liquid level measurement especially for the more advanced measurement techniques

(e.g. laser, radar and ultrasonic). New wireless capabilities enabling signals to be sent over a longer range with little or no degradation is explored with passive RFID tags deployed for level sensing. Extensive literature reveals the previous approaches to liquid level monitoring [48-52].

RFID technology is used to automatically identify users and objects and in recent cases, the location of these objects can also be tracked. RFID has been employed in many applications specifically to exploit the energy efficient and saving capabilities achieved specifically when the passive tags are deployed. RFID tags communicate by radio waves through antenna attached to objects so that they can be identified, located and tracked. RFID as a dynamically emerging technology for product identification is widely accepted by many industries [53].

The application areas are also rapidly increasing most especially in commercial applications. It is used to track work in process, inventory, containers and finished products as they move from one section of the production process to the other. In transportation, it is deployed for logistics, fleet management, pallet, container, cargo track and improving asset utilization [54]. In the healthcare and Pharmaceutical Industry it is used to track patient's mobility and keep track of drug stock to reduce errors, in the Military and aerospace it is used to track hazardous materials to improve safety and reduce counterfeiting of parts. Ford's popular F-150 pickup trucks now come with on board RFID reader for monitoring cargo. The army has also deployed RFID systems to monitor and control the utility pattern of cannons on M1 Abrams tanks. The statistical data obtained will help the army engage in effective forcasting and precision planning ahead of operations, for example RFID

technology can be used to obtain informtion about the end–of–life of barrels and other artillery in order to expediate their replacement before full engagement in the battle field.

The most recent advances in the application areas has been in smart parking, remote moisture sensing, contactless payments, real time location systems. These applications have deployed existent technology and implemented them in creative ways that previously never existed. Some achievement has been made in the area of deployment of passive RFID tags for liquid level sensing. Some of these works are as discussed below:

- Effective moisture sensing was achieved using RFID tags [55]. The work presented showed the effect of humidity on ordinary tag operational performance. This behaviour of tags in presence of moisture is used as a basis for infering moisture level.

- In [56] long range interrogation of small liquid samples is achieved using a passive harmonic generator based wireless sensor. Two sensor designs were tested for their interrogation capabilities by loading them with liquid samples which induced changes in the power reflected from the tag. The liquid samples under test were mixtures of methanol-water, isopropyl alcohol-water, and glucose-water. This provided a range of dielectric properties for the evaluation of the long range sensor. The sensor presented an effective performance and recommended for potential application in food safety, bio sensing and hazardous chemicals monitoring and detection.

- RFID tags were deployed for wireless liquid sensing for restaurant applications [57]. In this work, fluid levels were successfully detected via a high resolution capacitance measurement with the prototype using a standard microprocessor and a number of passive components.

- The work done in [58] shows the characterisation of the liquids using cavity-perturbation-technique, producing good sensitivity at 4GHz. RFID dielectric permittivity sensing of liquids is achieved using two planar sensors.

- Humidity threshold monitoring is achieved in the work presented in [59]. The sensing principle adopted is based on the deliquiscence property of substances like salt. When the set humidity threshold for such substances are exceeded, it results in a situation of over exposure of the tags to moisture which degrades the tags performance, resulting into a permanent change in the electric resistance of the tag. The tags designed in this case are therefore suited for single use, as the damage done to the tags become irreversible.

- An RFID based sensing in volatile environment for underground oil well communications is analysed in the work presented by J.Zhu [60]. An optimum design for an RFID reader and tag is presented in this work with detailed consideration given to the environmental and tag deployment factors. Factors like proximity to liquid and metal pipes which has an effect on tag performance is fully considered for compensation in the optimised design.

- In [61] a method for measuring the freezing state of liquid Nitrogen is presented. This is achieved by monitoring the dielectric permittivity all through the freezing process. The tags deployed as sensors are powered by an external electromagnetic field, the values obtained from measurement is transmitted to a reader coil located on the exterior of the cooling container. Unlike the previous wired methods of measurement, this method achieves wireless and effective measurement and transmission of results. The precondition that needs to be met for the proper function of the sensor is that the sample liquid needs to show significant permittivity change as a result of lowering its temperature.

- RFID tags has been deployed to detect the volume of liquid in beverage glass cups [62]. This was achieved by mapping a change in Received Signal Strength Indicator (RSSI) power measurements from RFID tags to the level of liquid in the glass. Accuracy predicions of about 80% was achieved when the set up was tested in real restaurant –like setting.

- A chipless tag was used in designing a high-resolution RFID sensor [63]. The sensor designed, is a passive resonant LC circuit tag with a regenerative loop in the reader, to compensate losses and increase the quality factor of the system. Deep field penetration is achieved due to the high quality factor resulting in high resolution sensing. The tag quality factor is increased from 135 to 20 000 in air by the regenerative loop. The quality factor can also be adjusted by varying the applied dc voltage.

- An experimental test bed for the measurement of RFID tag antennas, inside pipes filled with liquids, was presented in [64]. Fixed and mobile tags were placed in distribution pipes to monitor the condition of these pipes. The test bed set up measured tag performance with fluctuating pipe pressure. Results obtained in terms of the received signal strength was was used to estimate and predict the state and condition of effluxes in the pipes.

A lot of these instances of RFID deployment has focused more on the possibility of tag deployment without giving adequate attention to the areas of cost, size, flexibility and energy cost savings of RFID deployment. These previous study has also shown the effectiveness of the WORM type of chips for adoption as humidity sensors at room temperature due to its sensitivity at higher temperatures [65]. The power requirements of the chip on the tag as well as the impedance matching with the antenna input impedance, has an important effect on certain radiation properties such as, the gain and reading range. The nature of the dielectric material used affects certain radiation characteristics of the tag, the chip IC and the antenna material are attached to this dielectric substrate which is usually made of material of different electrical conductivity and relative permittivity. Studies have shown that the rate of power utilization by the chip is inversely proportional to the range of communication [66]. For optimum performance particularly in the area of the antenna's gain; the antenna's input impedance should properly match the chip impedance.

The major aim of most research study on RFID tags is in a view to improve the gain, sensitivity and the read/write range of both reader and tag antenna. This research work extends the study beyond this to explore new application areas of passive tag deployment as liquid level sensors.

The UK sewerage network, at 302,000 km in length, is one of the largest infrastructures within the water industry. These assets are aging and are also subject to increasing capacity demands because of increased urbanization, more stringent environmental regulation and the projected consequences of climate change. Currently, the water industry is investing in excess of £200 M per annum in sewer replacement and rehabilitation [67-69]. To proactively reduce their risk of failure and become more operationally efficient, water companies have developed strategic partnerships with a range of organizations, including academia and instrumentation manufacturers, to help find solutions for improving the efficiency of responses to failure of key elements of critical infrastructure resulting from degradation, overload, or disasters due to natural or man-made causes. In recent years, wireless sensor network (WSN) research [70] has received substantial attention due to its low cost, ease of deployment and successful implementation in many applications in business, transportation, government, defense and healthcare. To further explore other potential applications, significant efforts have gone into the development of Wireless Underground Sensor Networks (WUSN) [71-73]. These can be an optimal practical solution allowing water companies to change radically the existing methods of data collection and monitoring of sewers.

Underground environments are obviously lossy since they contain soil, rocks and water, and are relatively complex compared with the surface environments. To achieve a better transmission range, lower operating frequencies are necessary. This results in larger antennas being deployed underground, which is theoretically desirable but less practical because of limited space. For these reasons, it is desirable, if challenging, to establish reliable wireless Sensor to Sensor (STS) communications

underground, and a Sensor to Base Station (STB) communication from underground to the surface [74-75].

To gain better understanding of the RF propagation below ground, extensive measurements and associated simulation modeling for horizontally, vertically, and cross-polarized signals in underground assets, i.e. mines and tunnels [76], manholes [77-78], and a gully pot [79], have been undertaken and reported in the literature. Interestingly, all the above research findings show the importance of operating frequency, antenna polarization, and electrical properties of the underground asset walls, for the signal propagation characteristics. This further confirms that the antenna element in a wireless system plays a pivotal role in enhancing the transmission and reception in such a harsh environment. For this reason, many antenna design concepts have been proposed and implemented for underground applications.

For STS underground communication, a zig-zag shaped monopole designed for 915 MHz operation [73], and an inverse triangular monopole antenna intended to operate from 900 to 1500 MHz [80], have been suggested and explored. For STB underground to above-ground communication, it is noticeable that many antenna design techniques have been developed to establish a reliable and longer distance wireless link through an above-ground base station [81-91]. In some published works [81-84], the authors attempted to convert the conventional manhole cover to operate as an antenna. In [81], a thick slot has been cut in a metal manhole cover to form a slot antenna, while in [82] a slot antenna was embedded in a shallow cavity inside a cast-iron manhole cover.

As this antenna is located on the surface of the ground, it increases the chances of communication with the base station. However, the technique suffers from difficulties of machining, and is rather impractical for widespread implementation, since covers of different sizes, shapes and materials are available. To solve this problem, a composite manhole cover slot antenna with a sandwich structure was suggested in [83], while in [84] an electronically steerable linearly spaced parasitic slot array was integrated with a composite manhole cover. Again, using a composite cover is still an expensive solution as all existing metal covers would have to be replaced if large-scale implementation were required. Apart from modifying the manhole cover, other underground antenna designs requiring less disturbance of the infrastructure also have been investigated [85-90]. These include a two-arm conical spiral [85] and normal mode helix antenna [86]. Both works [85-86] show that stronger signal reception above the ground can be achieved via radiation of a directed beam. A three-element wire-based inverted-F antenna array which offers high gain, a unidirectional pattern and polarization diversity was recommended in [87]. In order to reduce scattering, a novel antenna system combined with a carpet cloak and a cavity which possesses steerable radiation patterns was proposed for operation over 8-12 GHz [88]. In addition, a composite right-left handed (CRLH) microstrip patch antenna [89], and a single layer and stacked microstrip antenna [90], were used for UWSN.

Among all the designs proposed, it was found that they are mostly only capable of offering narrow single band operation [81-87, 89-90]; only very few such as in [80, 88] can handle wideband operation and no design demonstrates dual-band operation. This research work explores in practical terms, a novel dual band planar folded loop

antenna for wireless sewer monitoring, with a view to extending the communication capabilities with terresial networks for global reporing of underground sewer liquid levels for early warning, reporting and conrol purpose for multiple liquid level applications.

2.7 REVIEW OF PREVIOUS ANTENNA DESIGNS AND APPLICATIONS USING GENETIC ALGORITHM

A new approach incorporating GA with the electromagnetic simulator has been adopted recently with increasing popularity specifically for antenna designs. The GA has been applied in designing wire and micro strip antennas. GA has also been deployed for solutions in other applications in wideband antenna designs particularly in imaging tools used for detection of breast cancer. Successful beam steering for a set of array antennas has also been optimised using GA. Improvements in MIMO systems have also been explored with GA, this was found to tremendously enhance the capacity of the channel generally. MIMO transceiver systems designed and optimised with GA come with tremendous reduction in size, power consumption and making them more cost effective.

The basic benefit derived from the application of GA is the creation of fast, efficient and optimised solutions with best performances for antennas irrespective of the selected operating frequency. GA in combination with FORTRAN was used to analyse a series of randomly selected antenna types. A series of different antenna design derivation via GA has clearly shown the strength of this tool as an efficient optimiser for searching and finding fast and effective resolutions particularly for complicated antenna geometries.

A new subroutine in the form of an adaptive computational program coded in FORTRAN was added to the GA driver by some authors in order to simulate various geometries for the micro strip patch antenna. A surface patch model was combined with the GA driver which was capable of supporting 3D antenna structures with moderate dielectrics.

A series of previous work carried out exploring various application areas of GA is discussed below:

- One of the popularly known GA generated antennas is the Crooked Wire antenna known for its unique geometry [91]. The antenna geometry suggested was mainly in order to optimise both the radiation and polarisation patterns. His technique was to achieve a RHCP antenna radiating in a particular dominant direction. The result of his experimentation on this antenna with GA applied had no similarity with existing antenna designs but matched their functionalities with improved results.

- In [91], GA was applied to the yagi-uda with the main aim of improving the radiation characteristic (gain and VSWR) for four M-length specifications (M = 15, 16, 17 and 21) for the Yagi-Uda antenna, their quest was mainly motivated by the slow improvement of the yagi-uda radiation characteristics. The usual Yagi-Uda design is composed of a selection of elements in array with a dipole element carrying the feed input, a reflector, and parasitic elements. It is majorly deployed for applications requiring a high gain operating in the narrow band. Its physical realisation comes with a light weight which is very cost effective and makes this type of antenna suited for most

applications where its radiation parameters perfectly serves the best purpose. The gene, chromosome/Individual, Cost function, Population, Crossover mutation and generations parameters were set in the GA software.

The GA computation of the optimised dimensions for the elements of the Yagi-uda was very different from the conventional structural sizes but with much improved performance. Conventionally Yagi antennas are built with decreasing element lengths and increasing spacing between the subsequent elements along the array. In GA this conventional Yagi-uda spacing was not adhered to, the spacing in GA showed no symmetry in pattern and element spacing was rather random. The GA yagi-uda antenna results achieved a higher gain at a design frequency of 432 MHz. The other parameters like gain, side lobe level, back lobe level, VSWR, and polarization were controlled with a separate element of the GA. One of the realisations over a specific region in space had low side lobes while the other created a yagi-uda with circular polarization. The design results achieved here was a novel and new solution for the yagi-uda derivative.

- In [92], GA was used in achieving new designs for the broadband patch antenna. A metallic patch, represented by ones (metals) or zeros (non-metals) for the sub patches was generated with the main aim of widening the bandwidth of operation of this micro strip around a centre frequency of 2GHz by exploring different geometries of the patch for optimum result. The final result showed a fourfold bandwidth of ~8 % on simulation and physical measurement basis compared to the regular 1.98% bandwidth of the micro strip patch of dimensions (36 x 36 mm).

- In [93] the research was aimed at achieving an antenna for the 1.9 and 2.4GHz frequencies respectively by adopting the patch antenna working in dual band mode. The results of the optimised design in GA showed a 6.2 and 6.9 percent bandwidth of operation at 1.9GHz and 2.4GHz respectively.

- As presented in [94] the study compared the results of GA-optimised designs to other software optimised design in order to ascertain which of the optimisation platforms yielded a better bandwidth performance. The bow tie and reverse bow tie antenna was analysed. Results obtained revealed an excellent performance of the RBT over the BT, as the RBT achieved lesser bandwidth of up to 80% and a drastically reduced size compared to the BT.

- A circular micro strip antenna considered for optimisation with the GA was studied in [95]. A new approach of adopting GA for the optimisation process was presented [96]. The optimal parameters for the geometry size of the micro strip with radiant circular element and fed with a coaxial cable was determined using the GA optimisation technique. The major aim was to determine the optimum values of three parameters regarding the design, these are: radius 'a', substrate thickness 'H' and relative permittivity 'ε_r'. This was in order that the antenna achieves the resonant frequency constraint of 5 GHz. The results obtained for the three parameters are: a = 1.25 cm, H = 0.35 cm and ε_r = 1.36. This results showed global optimum solutions without a long set of parametric study as usually done with other software.

- The GA based on fuzzy decision making was used to optimise the bandwidth of the E-shaped micro strip antenna in [97]. The Fuzzy inference system (FIS) was used to manipulate and effectively control the parameter settings of the GA program [98]. The results established a 33% wide bandwidth for the E-shaped antenna with applicability to the 1.9 and 2.4GHz frequencies respectively. The GA solution showed faster convergence in simulation terms as compared to other simulation platforms.

- A comparative analysis is made of the techniques employed for Multi Objective Genetic Algorithm (MOGA), Multi Objective Simulated Annealing (MOSA) and Divided Range Multi Objective Particle Swarm Optimisation (DRMPSO) applied to LC filter tuning in [99]. The results showed a tremendous improvement in terms of the execution time of the algorithm and also demonstrate the fact that the applied DRMPSO technique produces a similar level of optimisation performance in comparison to the other methods. It therefore becomes very useful particularly for the miniaturisation of previous antenna designs with improved performance. Documented literature on the significant results obtained in improvement in antenna filter tuning over previous methods is presented in [100-101].

- GA optimisation was used to obtain optimisation results for a dual band planar monopole antenna, operating in both narrow and UWB frequencies respectively. The results showed a tremendous performance particularly in the notch-band for the monopole realisation [102-112]. It was demonstrated that the pattern symmetry in notch band can be improved by simultaneous optimisation of

impedance match and radiation pattern characteristics of the antenna. Effective and higher attenuation bandwidth levels were achieved while maintaining the same desirable bandwidth characteristics with the GA optimized band-notched antenna, which showed a better performance as compared to the traditional band-notched planar monopole.

- The miniaturization of antennas is explored by effective processing and optimisation of the chromosome length in GA as presented in [113-114]. The proposed design of the miniaturization process considered geometries fundamental to the operational efficiency of the antenna and removed the undesirable conductors in the design geometry hence lowering the cost of production in the process. The findings form a strong base for the miniaturization and design strategy of current and future antennas.

- Another study was focused towards the optimisation of the bandwidth and the gain of a rectangular shaped patch antenna using GA as presented in [115-116]. The thicknesses of the substrate and geometry dimensions were altered and the results examined. The results show improved performances in gain and bandwidth for the specified design using GA. It was observed and deducted that the greater the thickness of the substrate the higher the bandwidth improvements; also a change in the material of the substrate to those of higher permittivity values improves the gain performance of the antenna.

- In [117-118] the input impedance of a Koch triangular quasi-fractal antenna is optimised using GA. An in-set feed is used to match the impedance. A micro

strip line is used as the excitation of this structure. The onset geometry of the antenna is designed in the HFSS software and then fed into GA for optimisation after which the simulated and measured results are compared with those of the HFSS. The dimension of the inset feed is obtained by previous guidelines of samples explored in documentations [119-120]. The reflection coefficient obtained when GA is deployed, reflects a better result of -40 dB.

- The work presented in [121] is a dual band micro strip antenna based on the second iteration of modified Koch fractal configuration. A series of fractal element antenna structures which has been modified by GA was explored and results obtained was cross analysed with the previous modifications obtained. The Real Coded Genetic Algorithm (RCGA) is used in combination with electromagnetic simulation. Parametric definition of conventional Koch shape generates new geometries of antenna structure, which suggest wide space design [122]. The GA optimisation technique applied here efficiently obtained the workable combinations of parameters and the best structural specification for the antennas operation at the selected design frequency of 5.8 GHz and 2.4 GHz.

The reader antenna for the RFID tag obtained in this research write up is then proposed to be designed with the GA platform in order to obtain the best geometry sizes and specification within the shortest possible time. The reader antenna radiates in a with a circular polarization in order to avoid any signal loss issues during detection of tags since the tags will be linearly polarised in some design instances. It

is therefore necessary to create a reader polarisation that will match and effectively work with a large selection of tags to avoid polarisation mismatch [123]. For passive RFID systems, it is required that reader antenna performance shows minimal correlation coefficient compared to other normal communication scheme. The backscattered signals from the tags are often weak and this makes them prone to various types of interference like collision with other reflected signals from the reader [124].

2.8 ANTENNA PERFORMANCE PARAMETERS

An antenna is a vital part of a communication system and is in fact central to the operations of any communication system. It couples RF signals into space in the form of an electromagnetic wave and vice versa. These two processes are referred to as transmission and reception. Usually some antennas are dedicated to transmission or reception of signals only. But in most cases especially in telecommunications antennas are designed to function both as signal transmitters and receptors. It is therefore very important to understand the working elements of an antenna system in order to design them to meet certain application requirements.

1. **Antenna Power Gain**: is the magnitude of the energy emitted from a radiating antenna in a specified direction in comparison to the electromagnetic radiation of an isotropic antenna in similar direction with similar input power. The EIRP, is the product of the input power and maximum gain of the antenna. The tag antenna radiates at certain frequency; the size and geometry of the tag antenna is carefully tailored to match the operating wavelength.

2. **Directivity**: defines the capacity of an antenna to focus its radiated power in a defined direction achieving a greater transmission distance culminating in longer detection range particularly for RFID systems.

3. **Reciprocity**: is the ability of an antenna to transmit and receive power in both directions without degrading other parameters associated with its performance.

4. **Polarisation**: is the orientation or position of the electric field component in a radiated waveform. It comes in a circular (right or left) or linear pattern. In order to avoid a mismatch in polarisation which often results in signal loss, antennas communicating with each other must be designed to operate in similar polarization for optimum link coupling. Polarization concept in tag antenna design is crucial and fundamental to the performance of the tag and adversely affects the detection range if not properly matched with the polarisation of the reader antenna. Linearly polarised RFID systems require the two parts of the system, tag and reader to be in the same linear direction. Circular polarisation (CP) on the other hand radiates energy equally in all direction and eliminates the need for devices to be configured to radiate in the same orientation; this type of polarisation wastes a lot of energy because it radiates it evenly even to directions not needed. Radiation patterns in antenna analysis are usually represented in elevation and azimuthal patterns. The polarisation state shows the orientation of the electric and magnetic fields in the waveform. Figure 2.8 illustrates the polarisation types. It is very important to understand and decide from onset on a particular type of polarisation that

will guarantee successful performance of the antenna for the intended application.

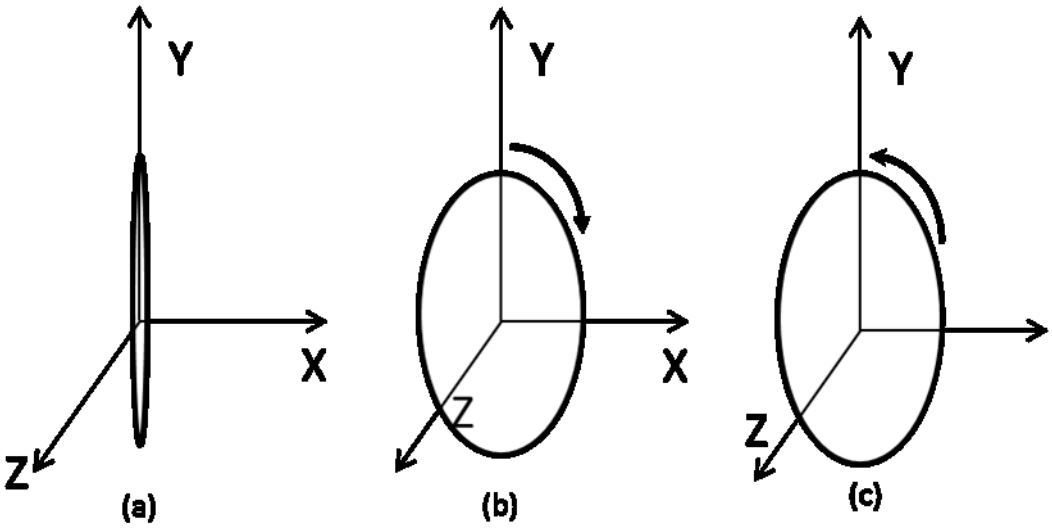

Figure 2.8: Antenna Polarisation Types; (a) LP, (b) RCP and (c) LCP

The radiation characteristic of an antenna is represented in the E-plane and the H-plane respectively. CP is produced or formed by combining two orthogonal linearly polarised antennas of same amplitude with their time signals phase shifted by 90 degrees. The type of circular polarization (right or left handed) is defined by the phase shift polarity [125]. In theory, the isotropic antenna emits equal radiation in all directions with a similar radiation pattern which does not exist physically.

5. **Impedance matching**: the nominal value for the input impedance of most antennas is specified at 50Ω impedance. This is in order for maximum energy transfer operation during communication. For RFID tags, the chip IC

impedance must closely match the tag antenna impedance for successful transmission of tag-reader signals.

6. **Return loss:** is a ratio between the incident and the reflected signals from the antenna, usually expressed in (dB); it is also referred to as the reflection coefficient.

7. **Bandwidth:** is the selection of a range of valid frequencies of operation of an antenna. It is usually expressed as shown in (7):

$$BW[\%] = \frac{f_H - f_L}{f_c} \times 100 \qquad (7)$$

where f_H represents the upper frequency, f_L symbolises the lower frequency while f_C represents the centre frequency.

8. **Radiation Pattern:** is a representation of the geometry of the radio waves coupled into space in the far region of the antenna. The peak radiation intensity is found and then half power beam width (-3 dB) points on either side are located. These points represent half the power of the peak intensity. The peak radiation will form a pattern known mostly as the main lobe and the power radiated to other directions will form the side lobes. Radiation patterns have nulls in them; these are points in which the effective radiated power is at minimum.

9. **Efficiency:** the efficiency of an antenna is defined in terms of the amount of energy received at its input which it is able to radiate away with minimal energy loss.

2.9 TARGET APPLICATIONS

The design realisations obtained from this research work is majorly intended for deployment in liquid sensing applications. Passive tags are designed, modelled and deployed to operate in different environments and applications. The design realisations discussed in this work have produced expected simulation and measurement results based on each application scenario to which they have been deployed. Some of the major applications to which the designed tags can be deployed are:

Water companies: for monitoring underground drainage systems to provide early warning against flooding thereby minimizing wastage and flooding occurrences across the globe. The tags also find application for domestic use in monitoring well or borehole water levels and give an insight for planning in times of famine or dry season. This is particularly important for irrigation farmers who rely solely on water available to maximise produce and profit especially in dry season particularly for areas with less than average rainfall compared to other parts of the world. This deployed tags also become a very important tool for geologist investigating the water levels across the globe.

Oil & gas: deployed for monitoring of surface and underground oil effluxes. The demand for efficient oil pipeline monitoring tools particularly in oil producing countries is on the rise. Passive tags networked with temperature and pressure sensors provide this all vital information for monitoring, automation and control of oil instrument data.

Power sector: An RFID tag deployed for smart remote metering of domestic power consumption helps cut down the cost of bill administration and improves the efficiency of service delivery of power company operations. Power companies are continuously seeking for better ways to provide services and conserve energy in the process by contributing as less as possible to the global carbon print indices. Competition perspective among companies now tends towards the going 'green' culture for which passive RFID tags play a major role.

Construction industry: The designed tags can be deployed as moisture or leak sensors in buildings which can give builders a perfect directional clue for resolving such issues especially in concealed areas. Typically, smart houses deploy a range of networked tags to achieve autonomous functions.

Mobility monitoring: in an organisation, employers can use these tags (if embedded on staff identification cards) to monitor staff movement, set access criteria and attendance and be able to study and assess the workflow of any department within the organisation. In times of emergency the specific location of staff can be communicated effectively. This is also applicable to hospitals and schools. Asset tracking is also an interesting application area for this tag design.

Transport Industry: Intelligent transportation Systems has deployed RFID tags to set and automate several functions within an automobile. This increasingly makes driving experience better and safer for the ever increasing commuter globally. Smart parking applications have also deployed RFID tags. The design realisations of this research work can be modified to work perfectly for these numerous applications.

This thesis is particularly focused on the improvement of the size, quality, polarisation, detection range, and deployment of passive RFID tags and reader for liquid level monitoring. RFID deployment for use as liquid level sensors is a novel application area in which this research work has recorded a lot of success. Various tag geometries are designed and deployed and their performances have been analysed and tested.

2.10 CONCLUSION

The history and application areas of RFID technology has been vividly explored in details in this chapter. RFID systems architecture and modes of operation has been explicitly discussed. Previous identification systems are studied and mentioned within the perspective of the subject matter. The advantages of RFID identification system over the previous methods are explained. The types of RFID tags and their differences are explored in the literature. A justification for the selection of tag type based on intended application for research is presented. A study of the various liquid level measurement methods and challenges are extrapolated and appreciated as a motivation towards the proposed work. A justification for adoption of passive UHF RFID tags has been made based on their simplicity, energy and cost saving capabilities. An expository illustration is given on RFID tag and overall system communication strategy. The advantages and disadvantages of RFID technology as well as their various classifications are discussed. A critical review of previous reader antenna design with GA has been presented. A review of an in-manhole chamber antenna with the associated challenges has been discussed as a premise to the development of a novel dual band in-manhole reader antenna. Typical Antenna

performance parameters are identified and briefly discussed. The tools and kits employed for physical measurement of the performance of tags have also been highlighted and component parts explained. The target application areas for the proposed tag design are highlighted. The background study has given the researcher an in-depth understanding of RFID design principles that would be a basis for the conceptualization of proposed design for the intended application. The subsequent chapters, presents the development of the working knowledge of RFID tags into practical concepts for liquid level sensing applications.

CHAPTER 3

GULLY POT MONITORING SYSTEM USING RFID

3.1 DESIGN AND DEPLOYMENT OF RFID TAGS FOR LIQUID SENSING

The research findings presented here is an energy efficient gully pot monitoring system using RFID Technology. It is aimed to demonstrate that water level data can be effectively collected using energy efficient and less expensive RFID network to monitor, report and efficiently prevent sewer and gully pot flooding. Residential and road network sewer and drainage flooding across the globe are mainly caused by blockages within the paths of the drainage network installation [67].

This chapter presents an alternative low cost, and energy efficient approach, to gully pot monitoring system, using passive UHF RFID tags. The tags were designed with ground plane for mounting on metallic surfaces and the other on polyethylene, for mounting on non metallic surface. The effects of conducting surfaces and water in particular on the realised tag radiation characteristics are explored as a basis for establishment of this a novel technique for monitoring liquid levels in a gully pot .

The increasing demand for remote and independent monitoring and control of water facilities and installations beyond the barcode capabilities has fuelled research into the design and production of cost effective RFID tags [68]. It is therefore necessary to implement a remote monitoring system for these installations in order to prevent

the disruption and inconvenience these blockages cause. Extensive investment into research has been made by Government organizations seeking a more advanced and cost effective way of monitoring the underground storage and drainage infrastructure with a view to drastically reduce or totally eliminate the inconveniences caused by persistent flooding experienced most especially in the residential areas mainly due to gully/sewer blockages. UK water industry alone is currently investing an excess of £200 M per annum [126]. As a result of these a more cost effective and Pro-active approach is sought by water companies across the globe. Manual and telemetry systems have been previously deployed for data collection of water levels for the gully pots, due to extensive cabling and power demands of these systems, they are not cost effective for deployment over a wide area of gully pot networks.

RFID tags are a cheaper alternative solution compared to other wireless sensors or cabled CCTV deployed to monitor water levels in gully pots. Passive tags are more power efficient in the sense that they only transmit in proximity of a reader.Research and development in producing low cost RFID tags is fuelled by the need to remotely identify and monitor objects and phenomenon beyond the limitations of traditional bar codes. Commercially low cost passive RFID chip with an analogue or digital input for sensor data is currently nonexistent. For example, resistance over the sensor port can be measured by an analogue version by incorporating simple passive sensor based components that adjusts its resistance in proportion to the physical quantity of interest.

One interesting application where this would be useful is for underground gully pot or sewer waste water level monitoring. It is in view of this that a cost effective gully

pot monitoring system is proposed using RFID technology. Remote independent and effective monitoring of gully pot water levels in real time is achieved for data collection and transmission for distant operator station monitoring to prevent and effectively reduce sewer flooding.

3.2 GULLY POT CHARACTERISATION

The system initial set up is as illustrated in Figure 3.1, highlighting the various observations with changing liquid levels. The tags are laminated and attached to the inner part of the cylindrical vaccum representing the gully pot. The various levels within the gully pot were marked on the basis of different levels; these are LL-Lower level, M-Mid level, H-High level and HH-Highest level. The tags were re-programmed for effective Identification on the graphical monitoring station based on the assigned levels within the gully pot. Tags AB65 – LL (Deep blue color), ABA4-M (light blue), AB08-H (Yellow) and AC08-HH (Pink) for easy identification. The RFID reader operating at 865-868MHz was connected to the computer and the antenna connected to a port on the Alien RFID reader.

The antenna was put at various distances from the gully point with the passive tags affixed to the respective levels intended for monitoring. The Alien RFID software was used and various levels of the gully pot was effectively indicated and transmitted for efficient monitoring. When the passive RFID tags come in contact with water ohmic losses occur in the antennas near-field. It has been previously shown how this property can be used to measure the amount of water concentration

in soil and water by connecting a transmission line to a buried monopole antenna [127].

A separation distance of 1.2 inches was maintained between the tags at different levels in the gully pot so that the near fields of their antennas do not interfere. The radiation characteristics of a passive RFID tag is impaired by environmental factors and particularly water [128-130].

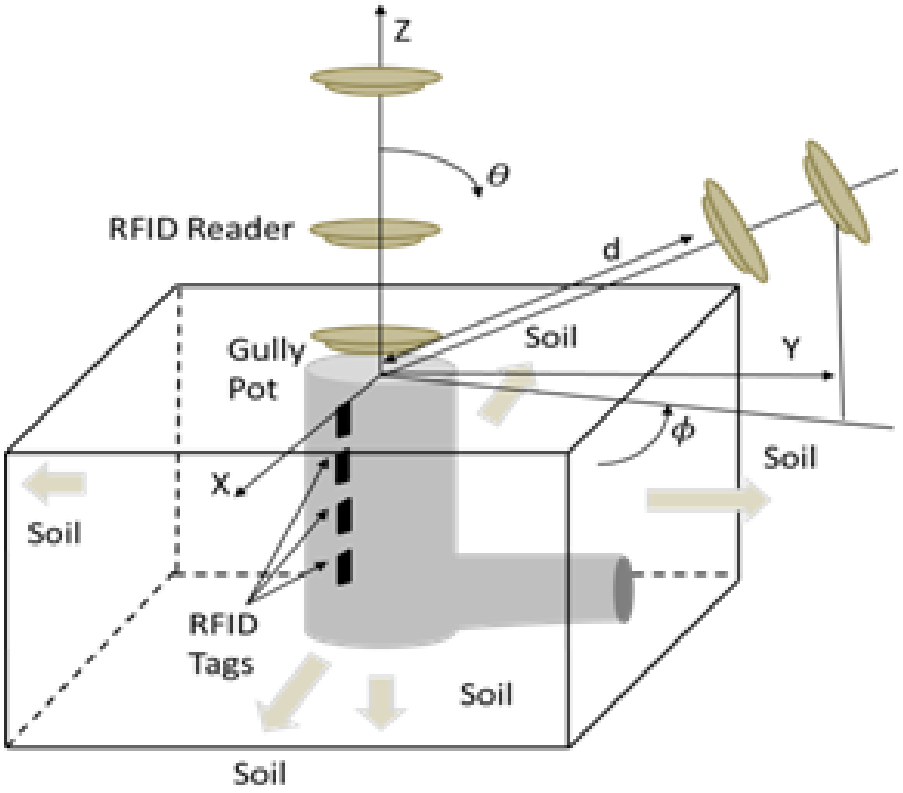

Figure 3.1:Gully pot experimental set up

Some soil was filled in around a cylindrical inner vessel inserted in a clay pot to replicate a real life scenario. The RFID reader was placed at varous distances away from the tags and the link coupling was observed from three different angulations (i.e., d, θ and ϕ as presented in Figure 3.1). The material composition of the gully pot wall was modelled to replicate ceramic, Aluminium and plastic. This was in

order to validate the tags operational efficiency when mounted on multiple surfaces with different electrical conducting properties. The performance of the tags showed consistent results in terms of the reflection coefficient and read range.

3.3 THE S-SHAPED AND MEANDER LINE TAG ANTENNA

This section presents the design of an S-shaped and the meander line antenna. The S-shaped tag has been designed with a ground plane for mounting on metallic surfaces while the meander line tag has been printed on polyethylene for mounting on non-metallic surfaces. RFID tag operation is affected by proximity to metallic surfaces, which distorts the signal received from the tag. One of the aim of developing a tag with a ground plane is to mitigate the effect on the radiation properties of the tag when mounted on surfaces with different electrical conducting properties. The main difference between the two tags presented is the existence of ground plane in the S-shaped tag, this is in order to avoid the maximum coupling with the wall of the gully pot. Both designs deliver improved results in terms the radiation performances and the required RFID chip impedance matching for the intended application requirement. A full parametric study was performed using HFSS; the results obtained were exported to MATLAB for further analysis. The dimension specifications of the two passive antennas are shown in Figure 3.2. The size descriptions are depicted in Table 3.1 and 3.2. The chip input impedance was specified at (15 + j140) which follows the EPC global class-1 Gen 2 specification.

Figure 3.2a is the realisation of a meander structure from a double twisted parallel line formation with operating frequency at 867 MHz and bandwidth of 3 MHz. The

structure adopted here is targeted at achieving the most minimal size with maximum radiation performance that matches the application requirement. The antenna performance has been studied in a semi-empirical fashion by tuning the parameter set (e, f and g) in controlled step size. It was observed that the parameter g and f had the most effect on the reflection coefficient of the meander line tag. The parametric analysis was carried out with each parameter set to increase in step sizes of 0.2 mm. The meander structure of the tag was maximised to obtain an overall miniature prototype for deployment as level sensors within the gully.

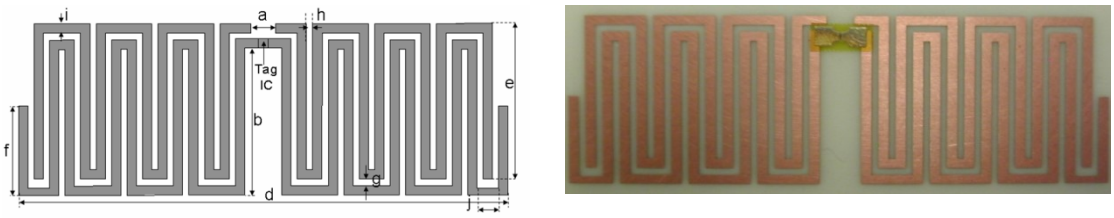

(a) Tag 1; (left) antenna model; (right) prototype.

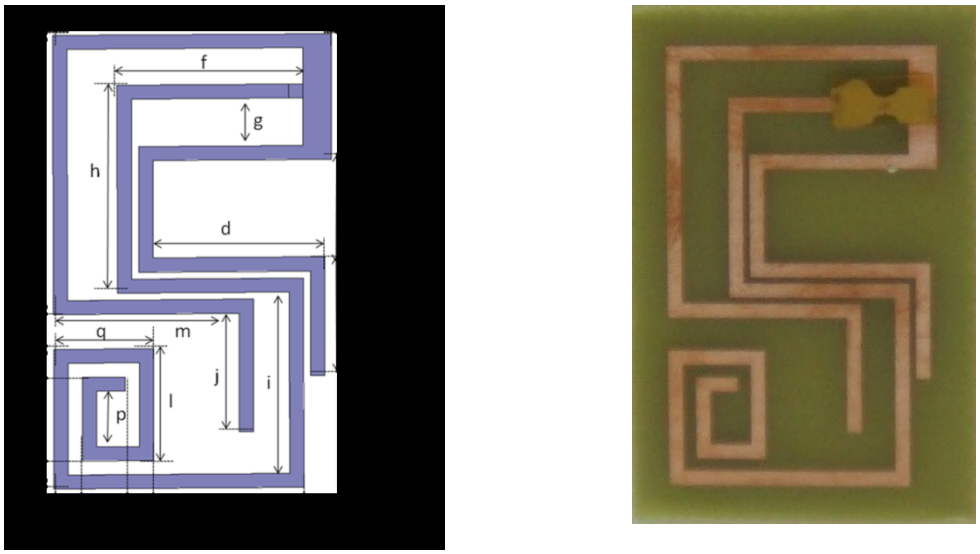

(b) Tag 2; (left) antenna model; (right) prototype.

Figure 3.2: RFID tag antennas; (a) tag 1 without ground plane; (b) tag 2 with ground plane.

Figure 3.2b shows the design for the S-shaped tag, which has been designed with similar approach. It has been formed from two rectangular parallel folded lines. The tag design has been printed with a ground plane to avoid coupling with conductive surfaces when mounted. This novel tag design consists of a double S-matching network, an inner spiral line, and an outer bent line. It operates in the European UHF RFID band with centre frequency of 900 MHz and a bandwidth of 3 MHz. The optimum dimensions has been obtained from parametric on HFSS; resulting in a prototype structure presented in figure 3.2b. Four parameters were observed to have the most effect on the working performance of the tag. These are the p, j and b slot sizes. It was also observed that the height of the substrate had an effect on the bandwidth performance of both tags; particularly for the S-shaped tag. The substrate height was kept at a constant value while the other parameters were incremented in step sizes of 0.1 mm.

The geometry specifications of the two tags are presented in table 3.1 and 3.2. Both tags was printed using the etching process. Tag 1 was printed on polyethylene substrate without ground while tag 2 was printed on epoxy with thickness of 1.6 mm and relative permittivity of 4.5 and loss tangent of 0.017

Table 3.1: Geometry specification of the proposed tag 1.

Parameter	Value (mm)	**Parameter**	Value (mm)
A	3.2	**F**	10.9
B	18.9	**G**	0.9
C	4.8	**H**	0.7
D	63.2	**I**	1.1
E	18.8	**J**	2.7

Table 3.2: Geometry specification of the proposed tag 2 with ground plane.

Parameter	Value (mm)	**Parameter**	Value (mm)
A	19.4	**F**	12.9
B	8.9	**G**	0.4
C	0.4	**H**	14.8
D	11.5	**I**	12.9
E	8.4	**J**	8.4
K	17.4	**P**	3.9
L	7.9	**Q**	6.9
M	12.5	**R**	4.9
N	19.9	**S**	5.9
O	9.9	**T**	1.9

The reflection coefficient, gain, and radiation patterns have been observed and optimised using HFSS software and the results show satisfactory performance. Figure 3.3 shows the measured and simulated reflection coefficient result which is the major focus of this tag sensor design. The reflection coefficient over bandwidth centred at 867 MHz is approximately between -18 to 35 dBs for both antennas. The geometry of the tags were explored and analysed for optimum performance and the stable geometries were presented as the optimised result.

The parametric studies have shown that a variation in some of the identified slot sizes affect the antenna performance more than the others. The major size alterations with optimum impact on the operational efficiency of the tags have been tuned and optimised in the final result presented. The gain values were quite satisfactory between (-2.1 to -0.5) dBs and (-3.2 to -1.1) dBs respectively for tag 1 and tag 2 antennas. It should be noted these gain values have quite an impact on the performance of these tags when they placed on the gully pot.

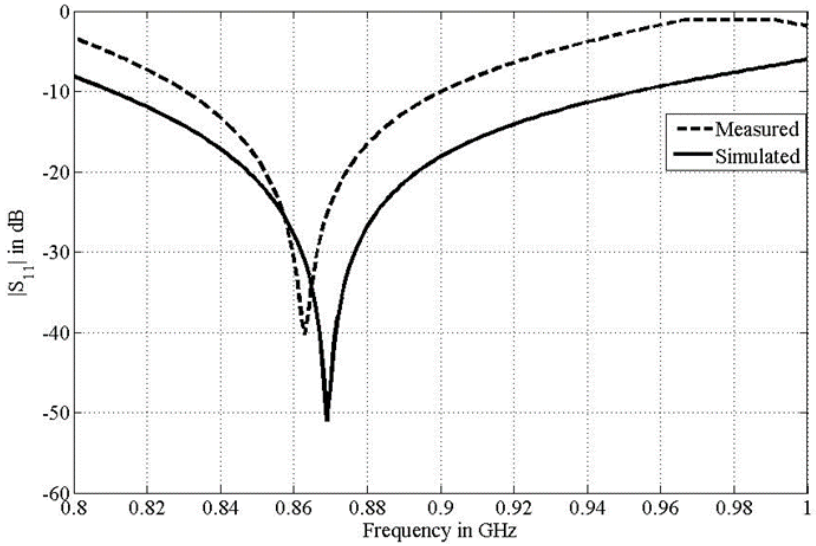

(a)

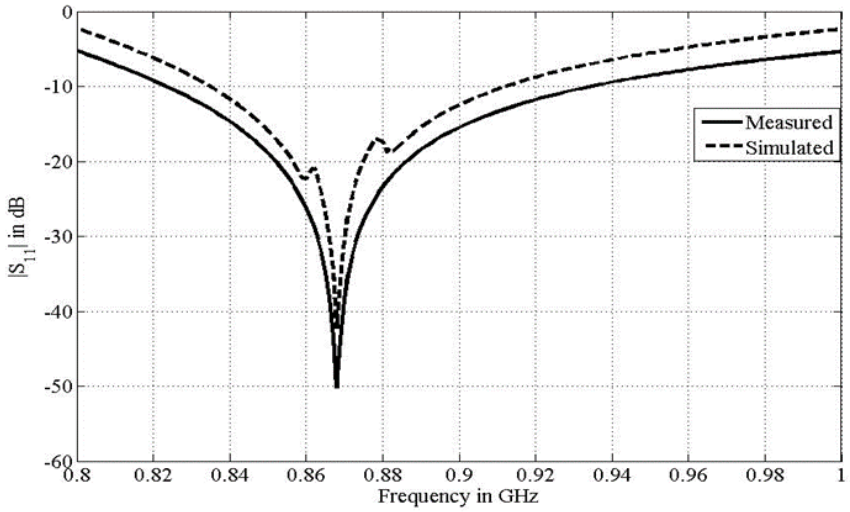

Figure 3.3:Refection coefficient |S11| in dB; (a) tag 1, (b) tag 2.

The antenna impedance was then measured and found to be (14.3-j140) Ω which closely matches the chip impedance. The preliminary test was carried to determine the detection range of both tags. The tags were mounted with the chip IC, a conducting epoxy was used to achieve this both for tag 1 and tag 2 respectively. The Alien RFID reader with 6.2 dBs gain was used for the preliminary measurements. They were observed to have a maximum detection range of about 0.8 m, which is

satisfactory for the application requirement. The total communication distance between the tag and reader for effective and consistent detection for application deployment is 0.5 m. Figure 3.3 shows the measured versus simulated reflection coefficient for both tags. This measured results shows close correlation with the simulated results. A second test was carried out to see the operational efficiency of the tags in terms of their read range when mounted on surfaces with different electrical conducting properties. The first test was with aluminium surface. It was observed that tag 2 performed better in terms of sensitivity measurements. The other surfaces on which the tags were mounted was ceramic and plastic. The performance of the tags were found to be consistent on both materials with tag 1 outperforming tag 2 in terms of the read range and orientation sensitivity. The series of performance tests carried out was to determine the best suited tags for deployment as level sensors in the gully pot. The tests confirmed that both tags can effectively serve as level sensors depending on the nature of surface to which they are deployed.

3.4 GULLY POT PRACTICAL SET UP

A workable prototype model for the Figure 3.1 was implemented for test as shown in Figure 3.4. The gully pot was fit inside the soil, for two wall thicknesses 18 and 22 mm. The conductivity and relative permittivity of the soil was repeatedly measured over the RFID band centred at 867 MHz for dry and wet conditions, on the range of (0.2 – 3) S/m conductivity and (1.2 – 22) relative permittivity.

Tap water was used to fill the gully pot on different stages in which the measurements were taken over a wide range of distances and angles; for which the

reader was placed between 2 cm and 75 cm distances over 360° azimuth angle (in 20° steps) and 60° zenith angle (in steps of 15°). The Alien RFID reader used for this test is circularly-polarized antenna with 6.2 dBs gain. The maximum dimensions of the RFID reader was kept at 8 × 8 × 1.9 cm^3.

Figure 3.4:Lower level-LL submerged in water.

A graphical reflection of the current status of the 4 tags placed at different levels in the gully was presented for all readings considered. As example from the Figure 3.4 that the tag AB65 at the LL-Level cannot be read because it has been submerged in the rising water level. The radiation efficiency of the RFID tags was totally degraded when the water covers them. However, it should be noted that the tags become unreadable as soon as the water level rises to touch the tag even midway before they are fully submerged.

The linear relationship between the level of water in the gully pot and the communication achieved at each level is shown in Figure 3.5. Previous techniques for remote liquid level detection has been based on microwave technologies [131-

132]. It has also been shown from previous study that the intensity of the backscattered signal from the tag has a linear relationship with the amount of water the tags are submerged in [7,130,133,134].

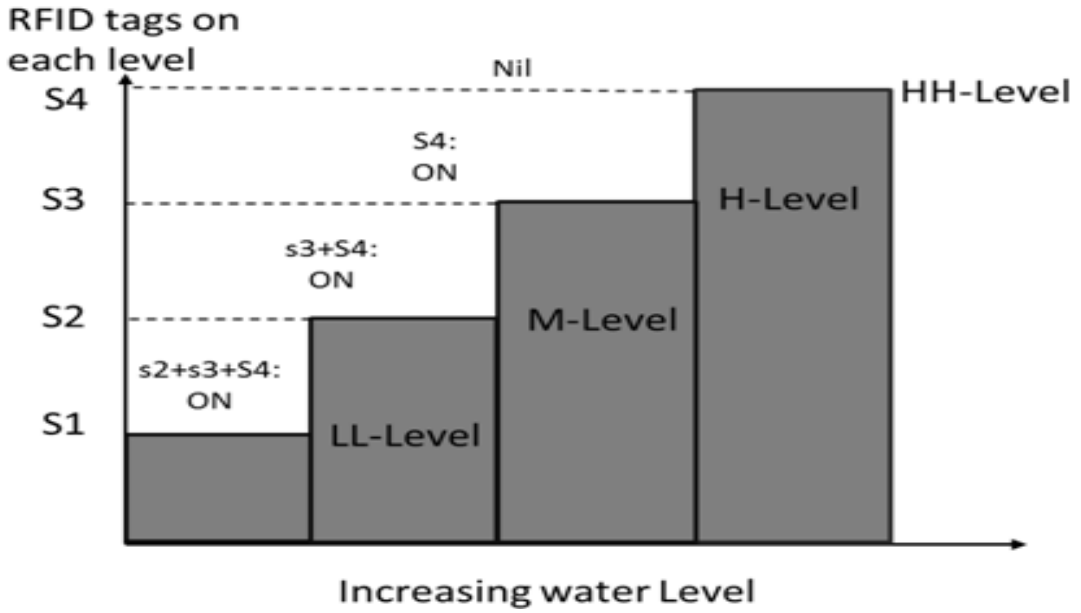

Figure 3.5: Sensors status by the reader versus water level

S1-S4 represents each of the tags deployed to sense respective threshold levels. When the liquid level is at level LL-level, the tag S1 at that level is submerged in liquid and shuts off communication with the reader. At this stage only three tags at level M, H and HH can be seen displayed on the screen by the reader. This information is interpreted to infer low level information. This sequence is followed till all the tags are submerged in water. Consequently at M-level only sensors S3 and S4 become visible to the reader and this is interpreted as Mid-level information. The number of sensors visible to the reader at each point in time form the basic information used to infer the level of the liquid in the gully pot. RFID readers can then be deployed to cover a network of gully pots and the information can be routed through a central server for collation and referencing.

3.5 CONCLUSION

Sewer flooding associated issues both at the consumer and water company perspective has posed a lot of problems. The design of the power efficient system for gully pot monitoring offers an effective solution to this tremendous challenge. This chapter has given a detailed presentation of the practical implementation of a cost effective gully pot monitoring system using RFID technology. The theoretical results obtained has been in agreement with the practical measurements. The radiation behaviour of the sensor tags when submerged in water has been used to calculate, interprete and effectively communicate liquid level information. Remote independent and effective monitoring of gully pot water levels in real time is achieved for data collection and transmission for distant operator station monitoring to prevent and effectively reduce sewer flooding. The designed passive tags are low cost and easy to deploy. The realised tags has been optimised to operate efficiently irrespective of the nature of the surface on which they are mounted. The results obtained from the practical experimental set up has enabled the researcher develop better understanding on the working elements and the problems associated with the deployment of RFID tags as liquid level sensors. The tag designs achieved in this chapter has been optimised and creatively deployed to sense liquid level in a gully pot. The other areas that can be explored for creative improvement it terms additional functionality with the level sensors is presented in the next chapter.

CHAPTER 4

PASSIVE UHF SENSOR TAG DESIGN

4.1 RECTANGULAR SHAPED TAG

This chapter presents the design, modelling, optimization and deployment of a rectangular and a mirrored P-shaped tag for liquid level detection and control application . The behaviour of the tags in proximity of metallic surfaces and water had been highlighted from the previous chapter. The two tag designs presented in this chapter shows improved performance. Detailed parametric analysis of a simple rectangular tag was carried out. This was in order to illustrate the potentials of the simple tag for use over a wider range of bandwiths. The geometry attributes with the most impact on the behaviour of the tag has been identified and presented. The mirrored P-shaped tag shows better performance in terms of the gain values. An automatic liquid level indicator and control system is presented. Most liquid monitoring systems comes with some mechanism which communicates with other complex circuits for control purposes. The tags serve as the sensors communicating with the level indicator circuit which relays information back to the pump control circuit. The circuits have not been designed but proposed as a way of extending the functions of the liquid monitoring system beyond simple indication of liquid levels.

The tag design set up in HFSS is in the 3D mode where the dimensions are carefully specified in the design software selection for any antenna design is very critical to the overall output and performance of the tag. HFSS is adopted to give the best

modelling for the tag antenna. This gives a complete view of the electromagnetic field distributions and radiations, which if unknown before the physical implementation of the design can greatly affect the system performance.

4.2 RECTANGULAR TAG DESIGN APPROACH

A three wire folded dipole for a passive tag working at frequency of 867 MHz is proposed. The frequency of operation is specified at 867 MHz (European standard) based on the Alien reader ALR 8800 which operates at the frequencies 865-867.6 MHz The HFSS software is used to design and model the proposed tag .The realised tag performance parameters such as efficiency, directivity, gain, radiation pattern, calculated read range and return loss are analysed.

Based on the Alien Higgs 2 standard, the IC input impedance for a passive tag at 867 MHz is (15 - j140). The tag antenna impedance should therefore be (15 + j140) in order to achieve conjugate matching. The proposed tag design is presented in 2D and 3D views respectively in Figure 4.1. The tag is printed with a thin sheet of copper on a dielectric substrate FR4-epoxy (with $\epsilon_r = 4.6$ and $\delta_\epsilon = 0.017$) and a substrate height of 1.6mm. The network analyser is used to obtain physical measurements of the reflection coefficient and impedance. The tag structure has no inductive or radiating stubs. Figure 4.1 shows the 2D and 3D dimensions of the rectangular tag.

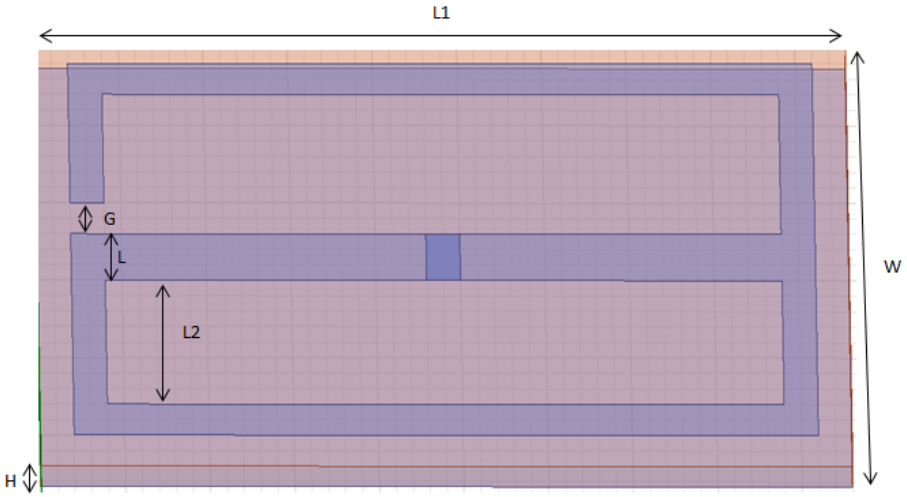

(a)

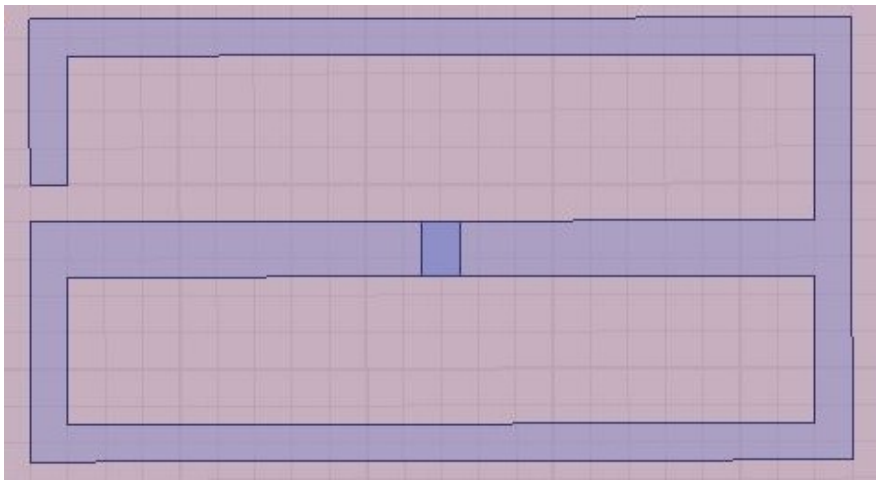

(b)

Figure 4.1: (a) The rectangular tag 3D view; (b) 2D view

G=2 mm, H=1.6 mm,

L=3 mm, L1= 48 mm, W = 27.7 mm, L2 = 9 mm,

4.3 SIMULATION ANALYSIS OF THE RECTANGULAR TAG

HFSS tool is used to run the simulation; the results obtained from this were then fed into the MATLAB software for full analysis of the results. The reflection coefficient as obtained on HFSS is as presented in the following figures. Figure 4.2 shows an excellent return loss at the selected frequency of operation which is an indication the desired reflection coefficient at -42 dB Most RFID tag antennas usually have a minimal gain of around 2 dBi and there is not much flexibility around improving this gain figure without affecting the omnidirectional property of the tag antenna. Consequently, a good tag design focuses on improvement of the reflection coefficient which is achieved by proper matching of the antenna to chip impedance.

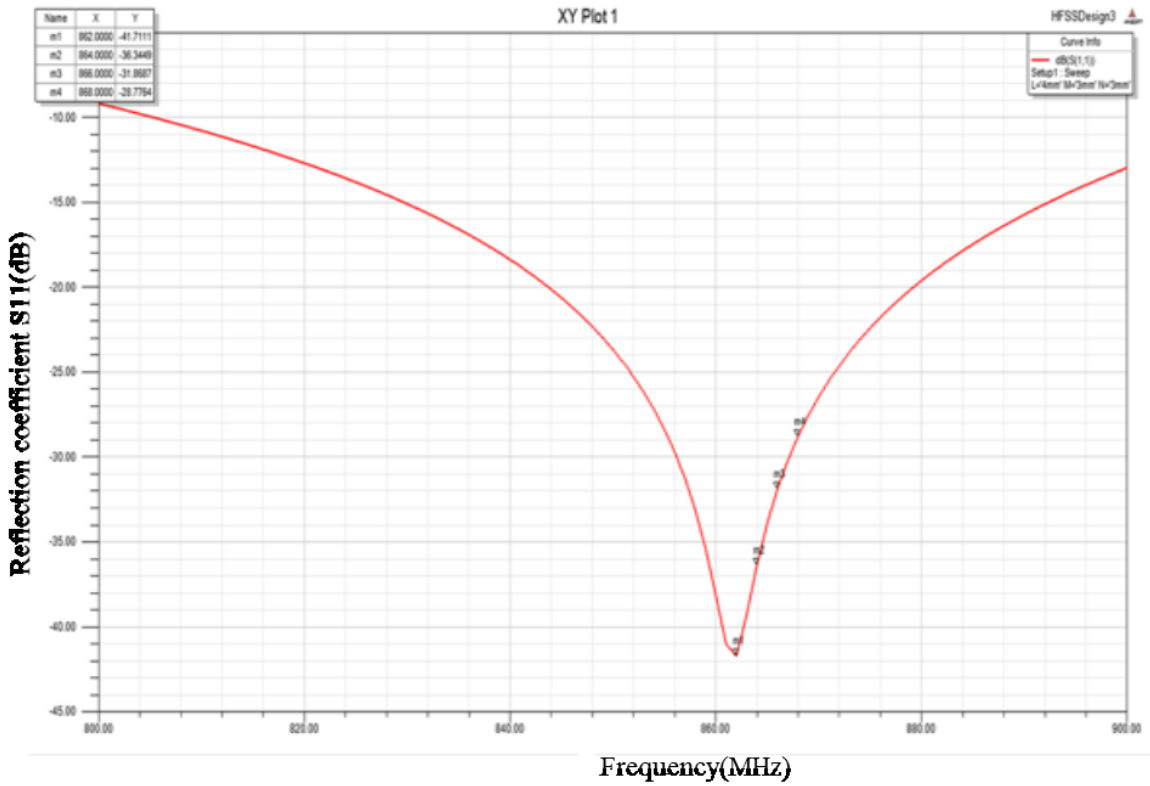

Figure 4.2: Frequency vs. Return loss of the rectangular shaped antenna when L=4mm

This is achieved as almost perfectly on the rectangular tag as simulated. Figure 4.3 shows the impedance plot of the chip and the tag antenna. An almost complete conjugate match is achieved.

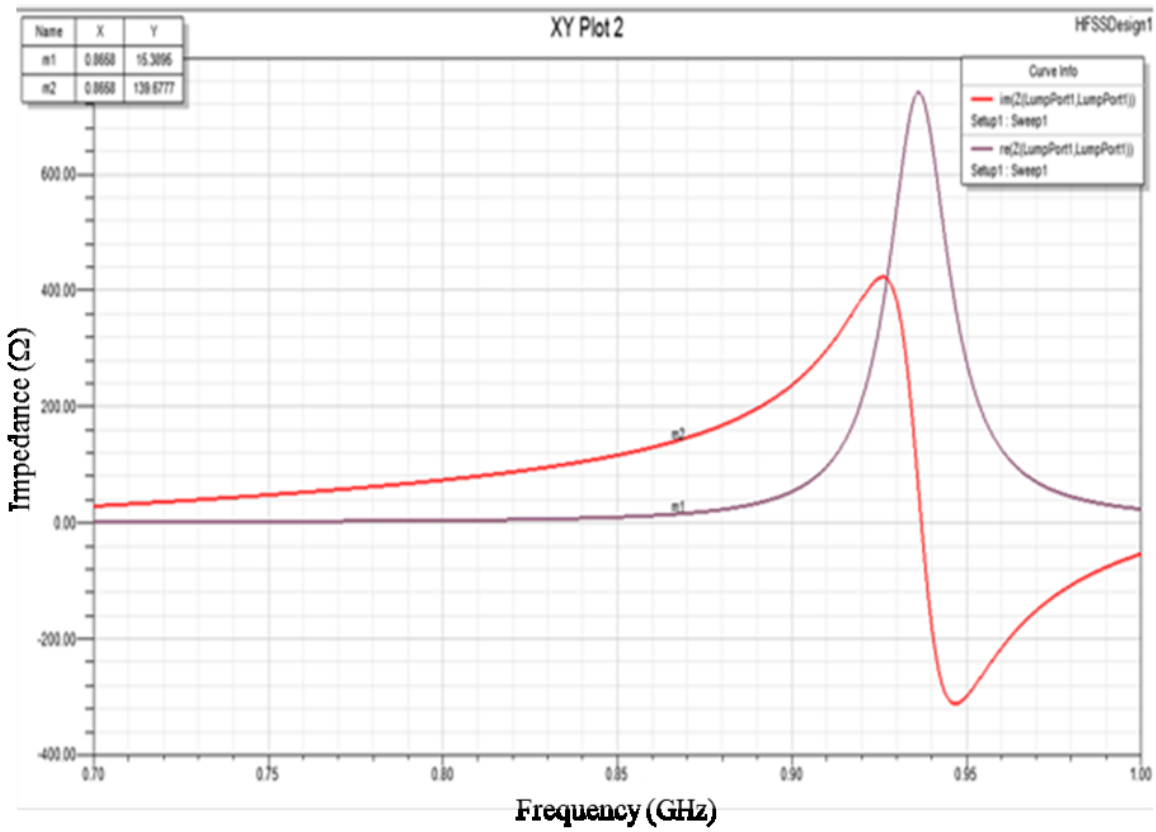

Figure 4.3: Matched Rectangular tag and chip impedance plot.

Figure. 4.3 depicts the matched antenna and chip input impedances at (15.39 + j139.58). The conjugate matching of the input impedances of the both chip and antenna is critical to the performance of the tag. This is very important for maximum power transfer in order for the RFID tag to backscatter the information held on the chip successfully across an acceptable range.

Figure 4.4 and 4.5 shows the simulated 2-D and 3-D radiation pattern for the 867 MHz UHF antenna design.

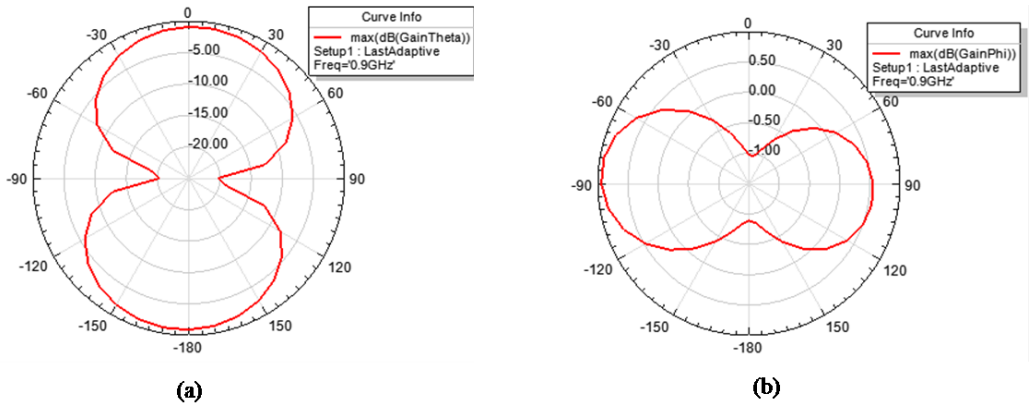

Figure 4.4: Normalised far field radiation pattern (a) X-Z plane (b) Y-Z plane

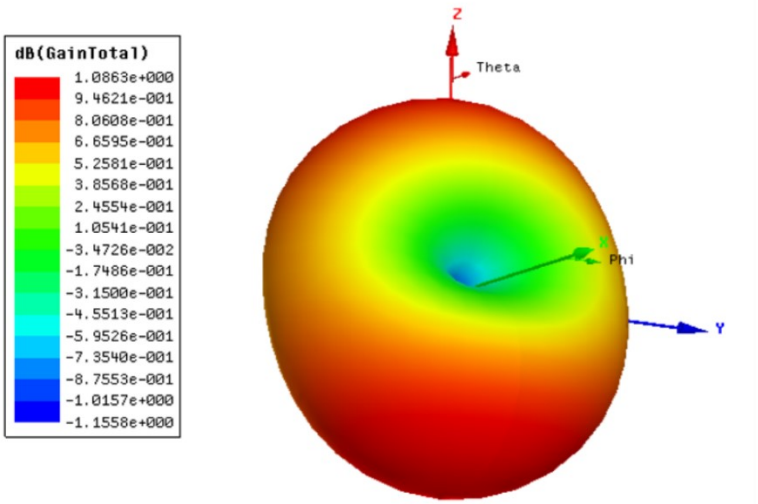

Figure 4.5:3D radiation pattern of the rectangular tag

The radiation pattern is Omni-directional as expected. The resistive factor of this antenna design is the creation of nulls in the X-Y (horizontal) plane. Maximum radiation should be achieved when the tag is read in the X-Z or Y-Z plane i.e. perpendicular to the reader antenna. The tag has this functionality to avoid orientation sensitivity and thus can be read from all angles irrespective of the reader antenna or tag positioning. Table 4.1 shows a summary of the Antenna radiation parameters obtained.

Table 4.1: Antenna Radiation Parameters

Tag Input Impedance (Ω)	Reflection Coefficient (dB)	Antenna Gain (dB)	Directivity of Antenna (dBi)	Efficiency of Antenna (%)
15.4 + j140	-42	1.09	1.26	78

4.4 PARAMETRIC ANALYSIS OF THE RECTANGULAR TAG

This section presents the results obtained from a full parametric analysis of the rectangular tag. Four properties of the tag geometry were observed to have tremendous impact on the reflection co-efficient of the tag. These properties are the: L, L1, L2 and G widths. The symbols M and N has been used interchangeably for L_1, and L2 all through the parametric analysis presented. The 'M' dimension represents L1 as shown in Figure 4.1a, while 'N' represents L2. The radiation characteristic of the rectangular tag is observed closely during this analysis in a bid to identify which particular geometric modification yields the best results in terms of the gain and reflection coefficient values.

The width of the L-slot was steadily increased from 1-4 mm while the other slot sizes were kept at their nominal values, the plot as shown in figure 4.6 was obtained with the best results when L=4 mm, reflection co-efficient as observed to be at -42 dB and shows very good performance. It was also observed from this analysis that increasing 'L' step sizes gradually improves the reflection co-efficient at higher frequencies which makes it a very important property to use to switch applicability of the tag for higher frequency operations making this design very flexible to modify

to adapt to various application requirements. Figure 4.7 below shows the effects varying the 'M' slot size on the reflection co-efficient.

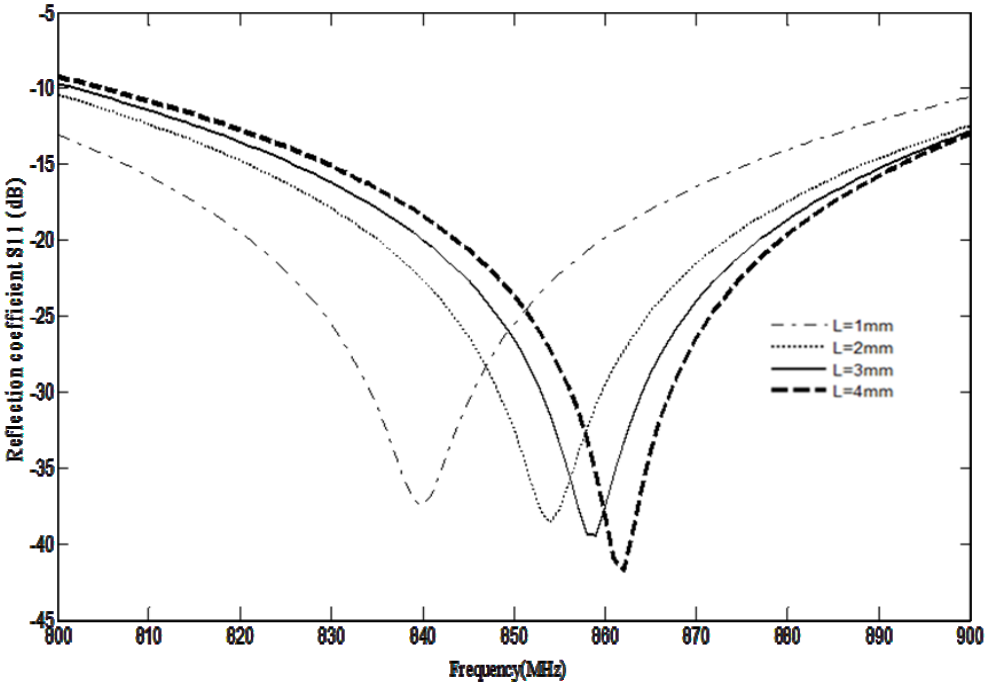

Figure 4.6: Reflection co-efficient vs. Frequency of the rectangular tag for L=1-4mm

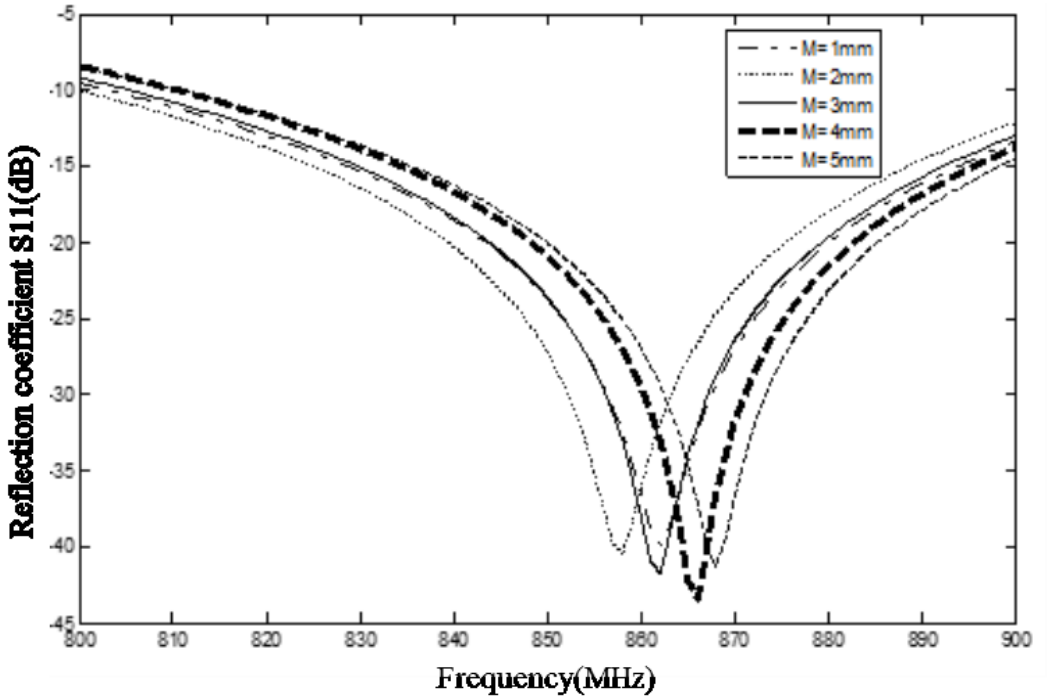

Figure 4.7: Reflection co-efficient vs. Frequency of the rectangular tag for M=1-5 mm

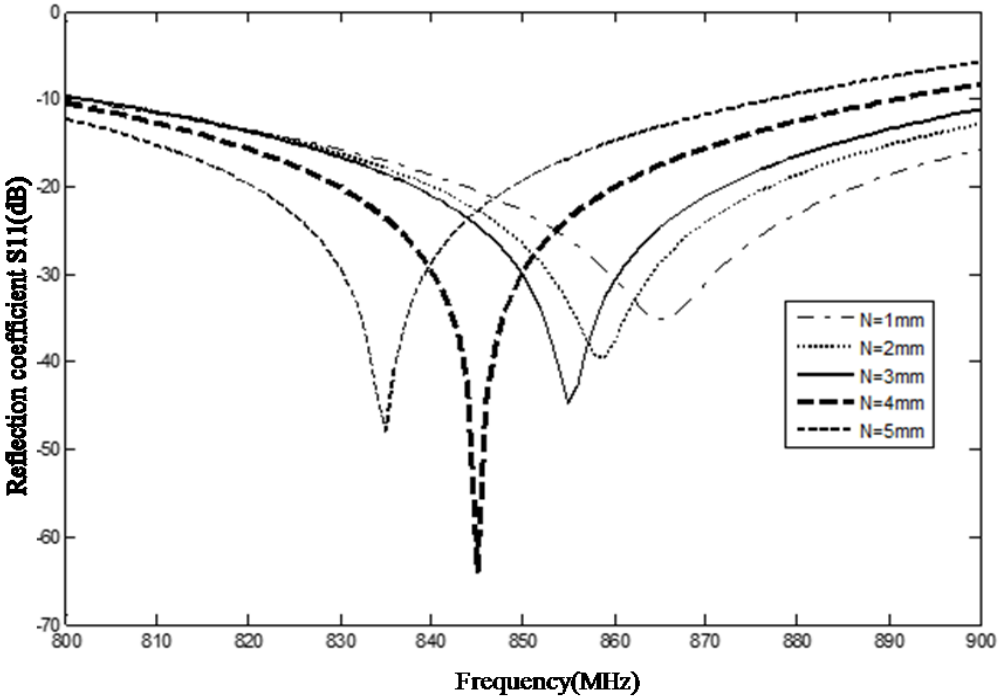

Figure 4.8 :(a) Reflection co-efficient vs. Frequency of the rectangular tag for N=1-5mm (L=3 mm)

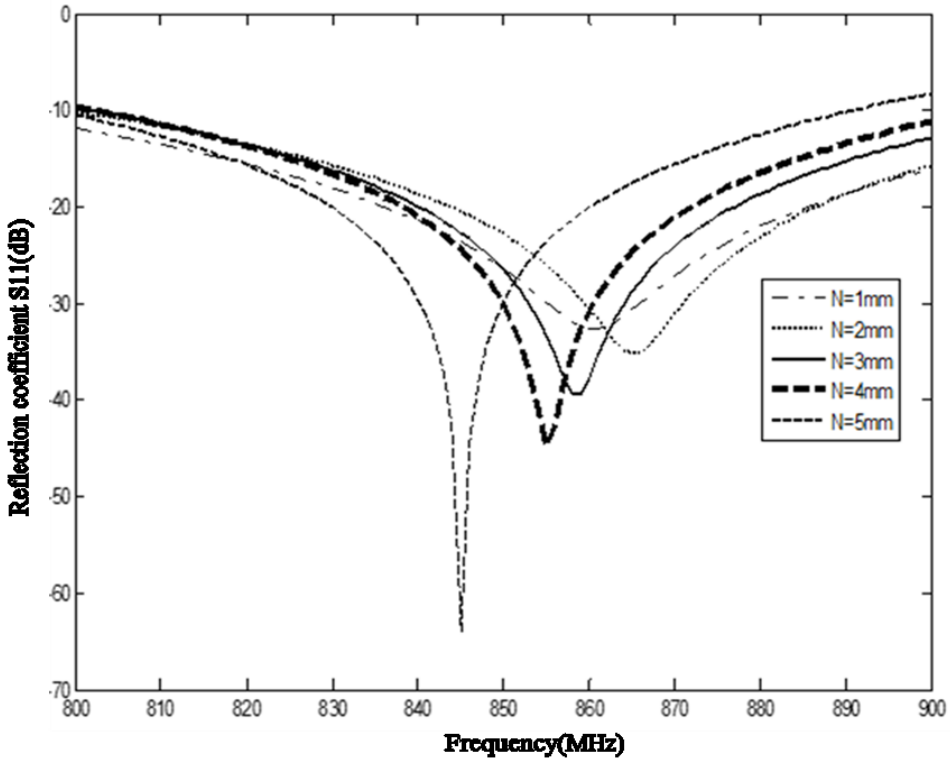

Figure 4.8: (b) Reflection co-efficient vs. Frequency of the rectangular tag for N=1-5mm (L=4 mm).

As observed from figure 4.7 the best results for the selected frequency of operation (860-868 MHz) is when M=3-4 mm respectively. This shows satisfactory performances as the reflection co-efficient is at a maximum of -44 dB when M=4 mm. Figure 4.8 shows the impact of varying the 'N' slot on the reflection co-efficient. As observed from this analysis, interestingly the tag shows good performance in terms of the reflection co-efficient when the 'N' slot width is steadily increased, but this is mostly so for frequencies below 860 MHz

This in essence means this interesting behaviour of the tag could be exploited to switch the tag's best operation at frequencies below 860 MHz. This is mostly so when 'L' is kept at 3 mm. The maximum reflection co-efficient is realised when N=4 which is -68 dB However the best performance at 860-868 MHz is realised when N=3. An interesting twist in the effects of this parameter on the entire tag performance is shown in figure 4.8b where L is at 4 mm. The reflection coefficient is greater at 845 MHz, which again makes this simple tag design very flexible in tuning to cover a wide range of frequencies even outside the allocated RFID band.

The 'G' dimension was then explored in step sizes of 0.25 mm and the effects on the tag's radiation characteristics was observed to show very promising results. Figure 4.9, shows the tag's operation is best at G = 3.25 mm.

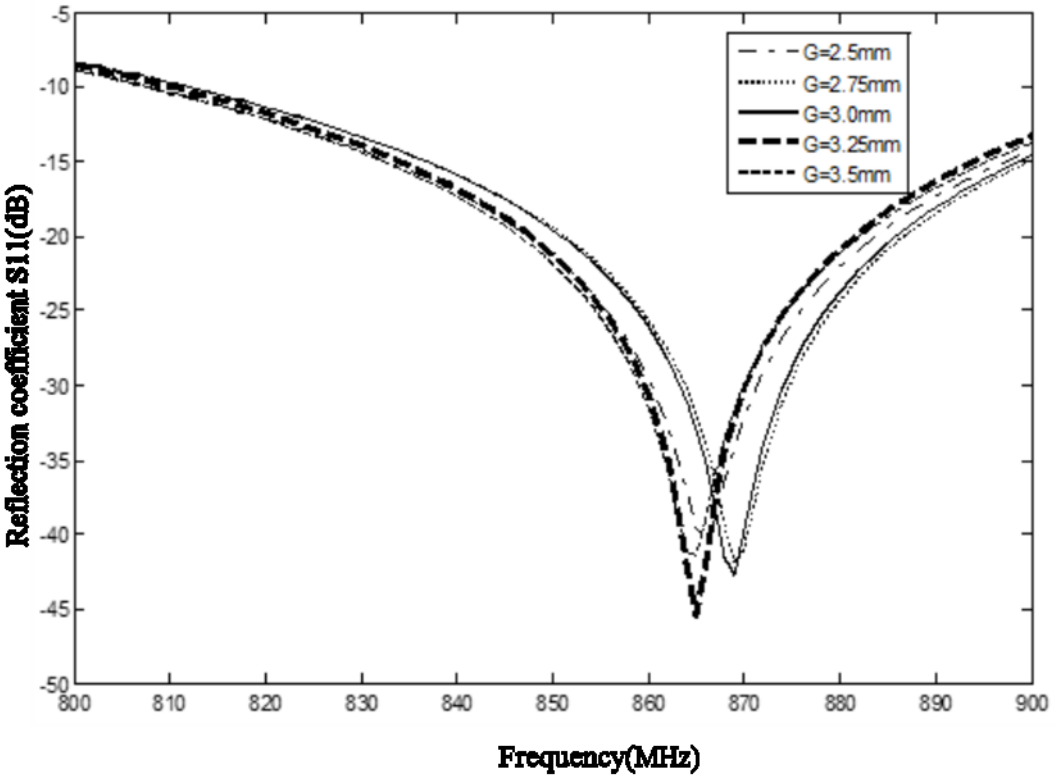

Figure 4.9: Reflection co-efficient vs. Frequency of the rectangular tag for G=2.5-3.5 mm.

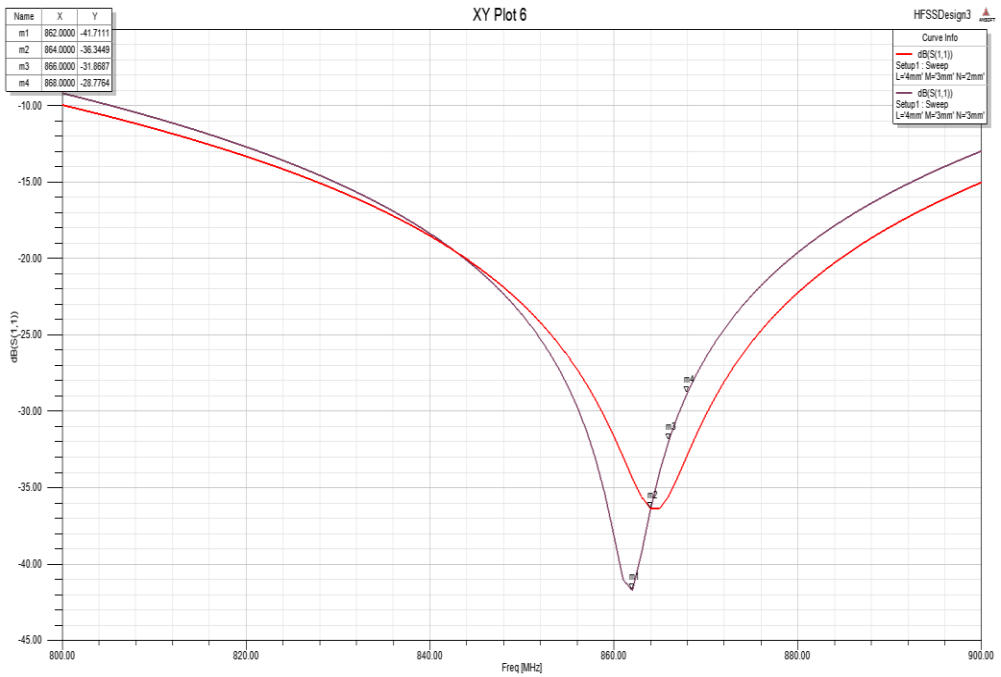

Figure 4.10: Reflection co-efficient the optimized rectangular tag (HFSS plots)

The optimised design plot shown in Figure 4.10 presents the best results from parametrics, particularly on the reflection coefficient which was at -41.7dB, The best geometry sizes obtained for L,M and N parts was 4mm,3mm and 3mm respectively with the G parameter kept at 3.5mm.

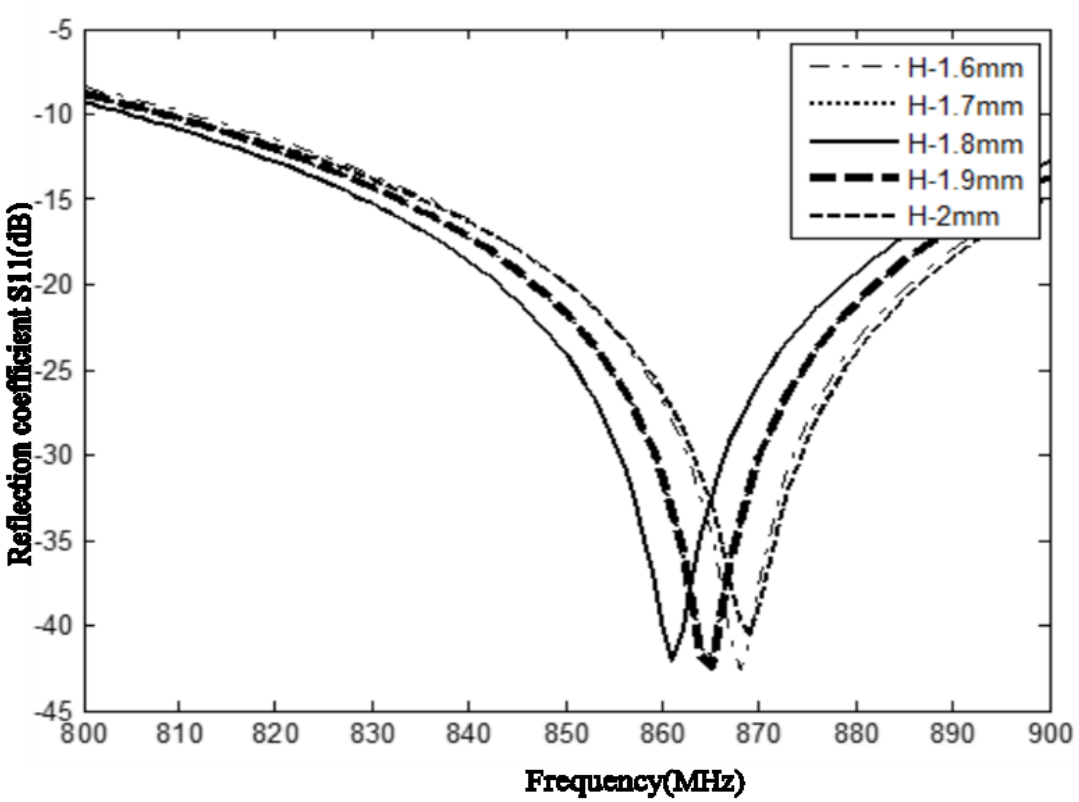

Figure 4.11: Reflection co-efficient vs. Frequency of the rectangular tag for H = 1.6-2.0 mm

Figure 4.11 depicts the radiation behaviour of the tag when the substrate height is observed in step sizes of 0.1 mm from 1.6 – 2.0 mm. As seen from the results, the tags reflection coefficient across the intended frequency of operation remains fairly at the same level and so a change in the substrate height applied does not have any significant impact on the reflection coefficient of this tag design. The optimised prototype design is as shown in figure 4.12. This prototype design has been printed on both epoxy and Polyethylene substrates for multi surface mounting. The realised tag was mounted on ceramic, metal and plastic and the results obtained showed

consistent performance in terms of the reflection coefficient and read range figures obtained.

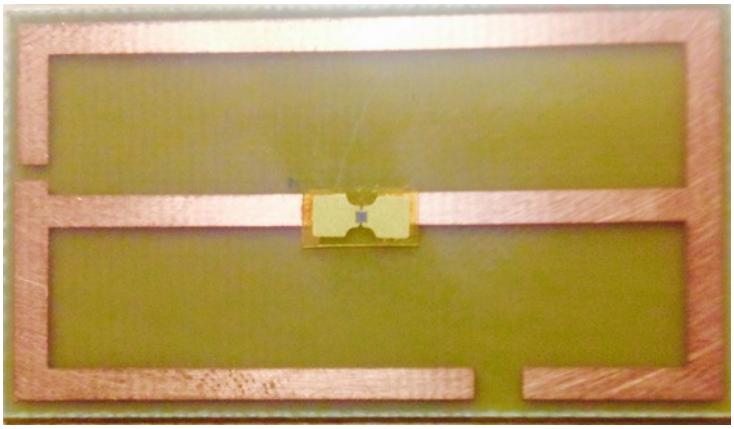

Figure 4.12: Prototype design of the rectangular tag

This optimised design, showed improved and better performance in terms of the reflection coefficient as reflected in the parametric report presented. For the intended application, an effective read range of 0.5 m (19.68 inches) was required since the absolute height of the gully used was 300 mm (11.8 inches). The read range achieved with this tag was 0.8 m (31.5 inches) and this was sufficient for the intended application. The tags were sealed and made water tight in order to prevent the chip IC from permanent damage during physical deployment. Run off test were conducted with off the shelf alien tags in characterisation to see the anticipated response in comparison to the rectangular tag. Results obtained with the rectangular tag showed consistency in information relayed back to the database.

4.5 TAG SENSOR MODELLING IN HFSS

The rectangular tag design obtained is subjected to application test using HFSS to model various environment scenarios to replicate a real life liquid level monitoring system. A total of five tags were deployed for this model in HFSS, four of which serve as the respective level sensors and the fifth tag as the reader antenna. The model set up developed in HFSS is as presented in Figure 4.13. Identical tags with similar radiation properties were used as both level sensors and reader antenna. The separation distance between the sensors tags were maintained at 1.2 inches, at alternate positions across the liquid tank set up. The fifth tag was placed in perpendicular position (z-axis) above the sensor tags. This distance was varied and the effective results observed.

The measurements consideration for the gully modelling is as shown in Figure 4.13a, these size measurements were strictly adhered to for accurate modelling in HFSS to replicate a real life scenario. The chip on the tags were rewritable and so level information were written to each of the tags deployed to each level using the Alien RFID middleware. A replica of such set up was achieved for a liquid tank with inlet for liquid control as shown in Figure 4.13b, the tags deployed has been designed for mounting on metallic and non-metallic surfaces to minimize the surface coupling effects, a set of the tags to be mounted on metallic surface has a ground plane, while those for other surfaces do not have the ground plane.

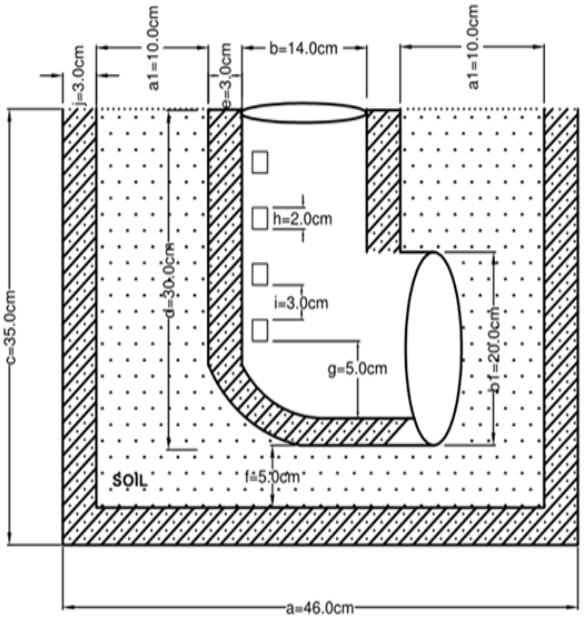

(a)

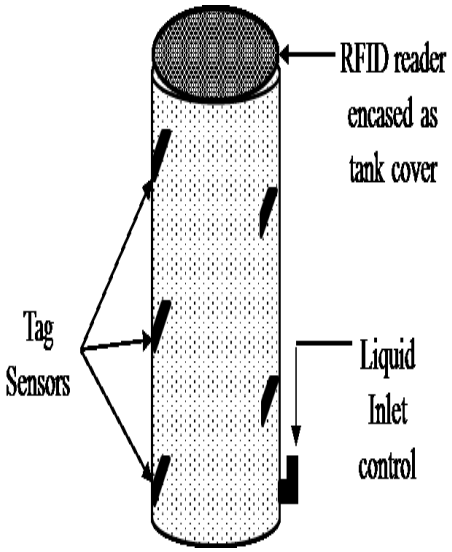

(b)

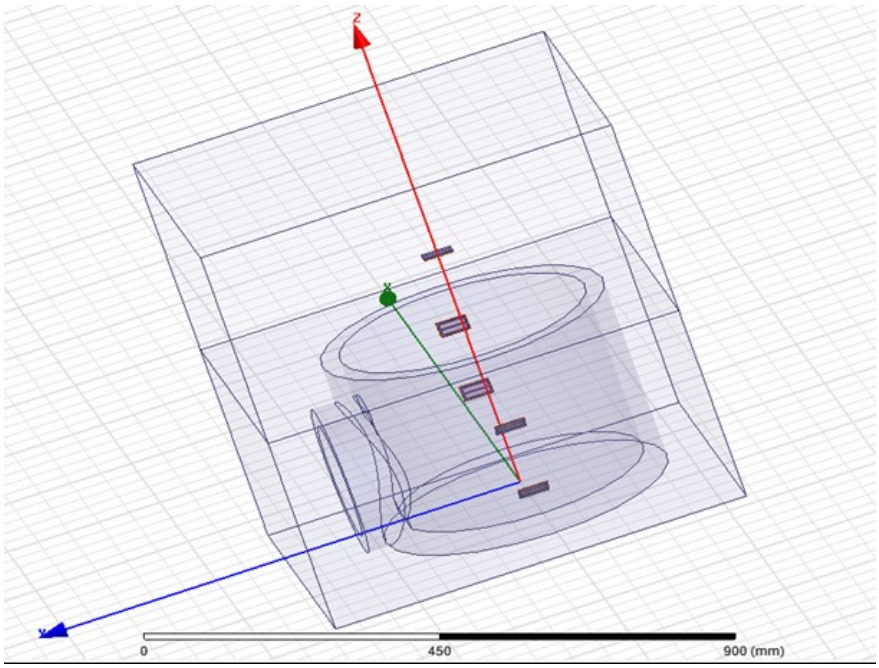

(c)

Figure 4.13: (a) Practical sensor tag deployment measurements for the mirrored P-shaped tag, (b) Sensor tag tank deployment for measurement, (c) HFSS sensor tag characterisation.

4.6 TAG SENSOR SIMULATION RESULTS

The link coupling between the tags is as shown in Figure 4.14. As can be seen, the reflection results are consistent across all the levels. This shows optimum performance for the intended application of liquid level sensing. The results obtained here were at the initial set up stage where liquid was not channelled into the gully and so the reflections from all the sensors at the various levels is observed. The overall gain and total directivity is as shown in Figures 4.15 and 4.16 respectively.

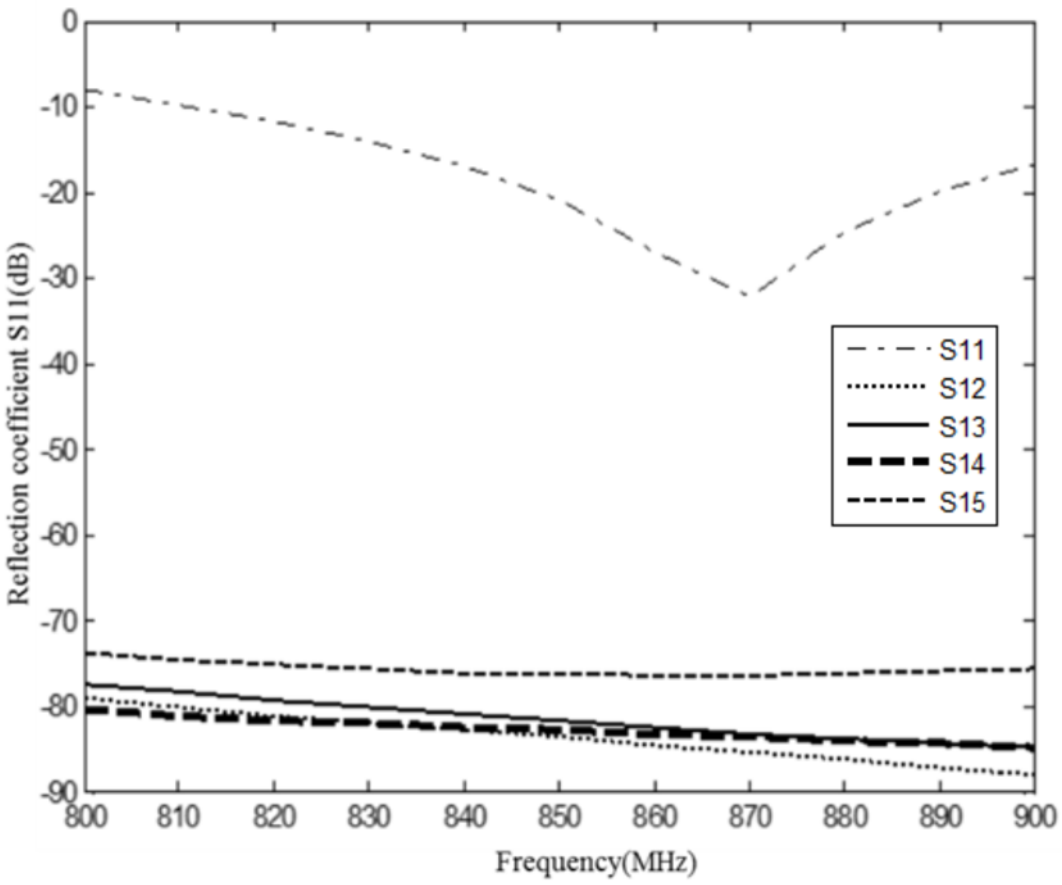

Figure 4.14: Frequency vs Reflection Coefficient of the HFSS gully set up.

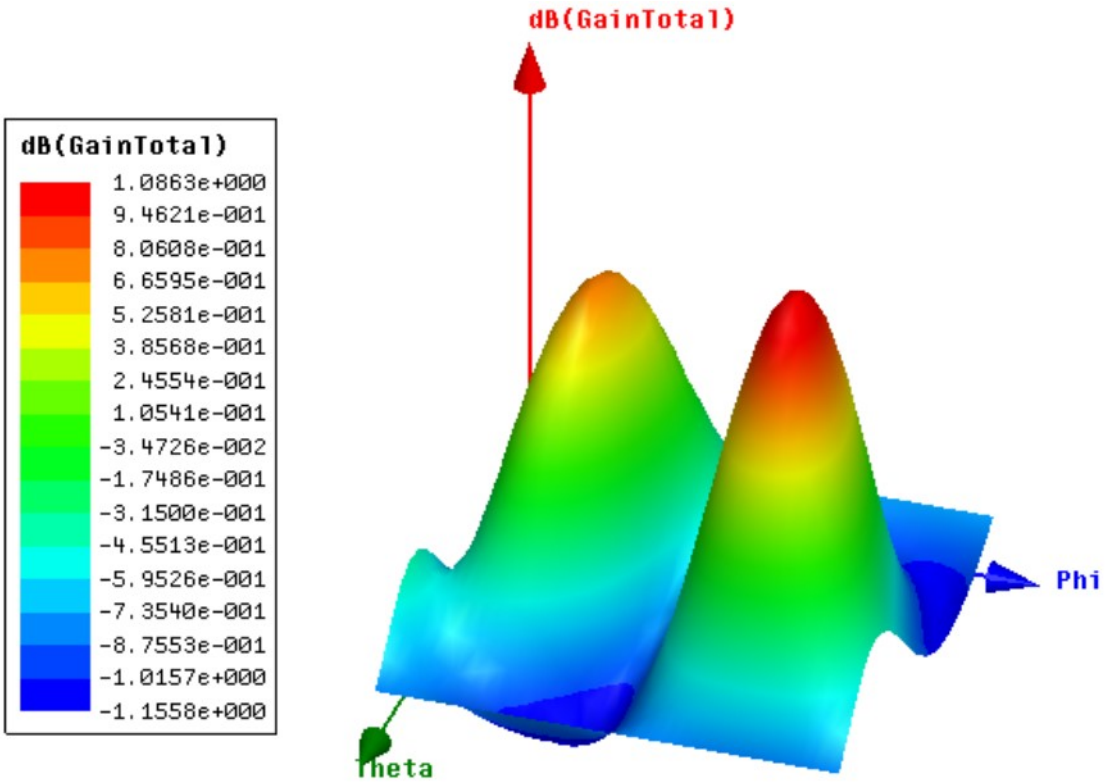

Figure 4.15: Overall gain of the RFID liquid level sensor.

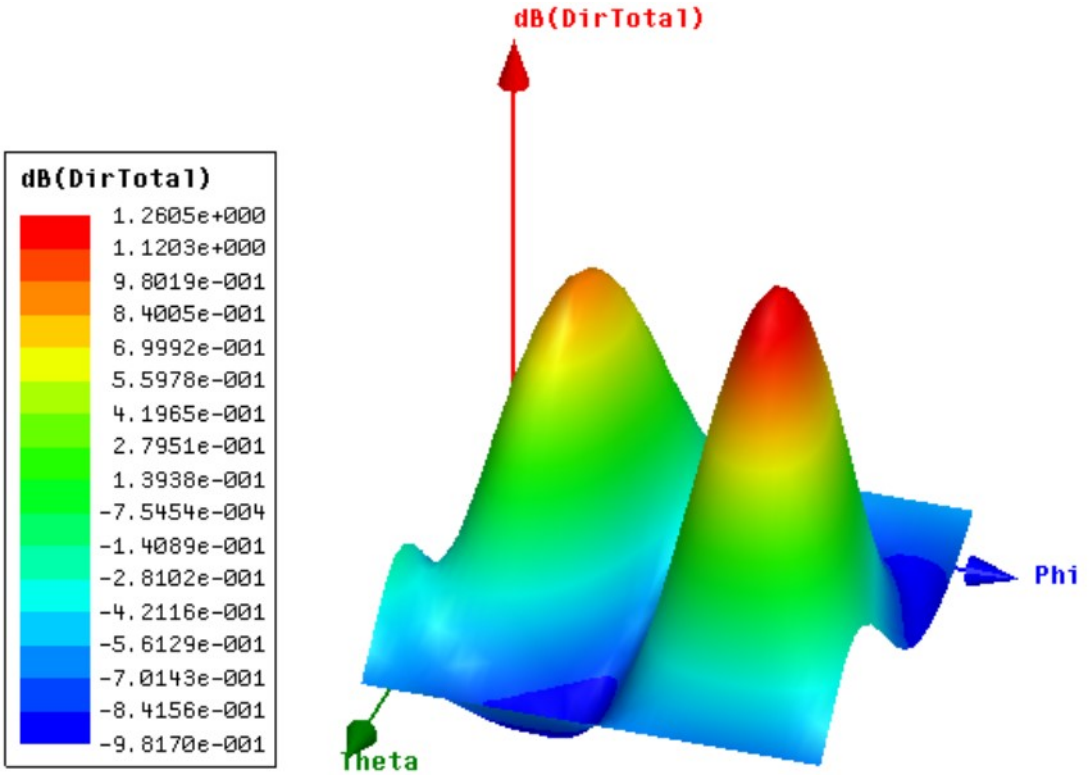

Figure 4.16: Total directivity of the gully pot HFSS set up.

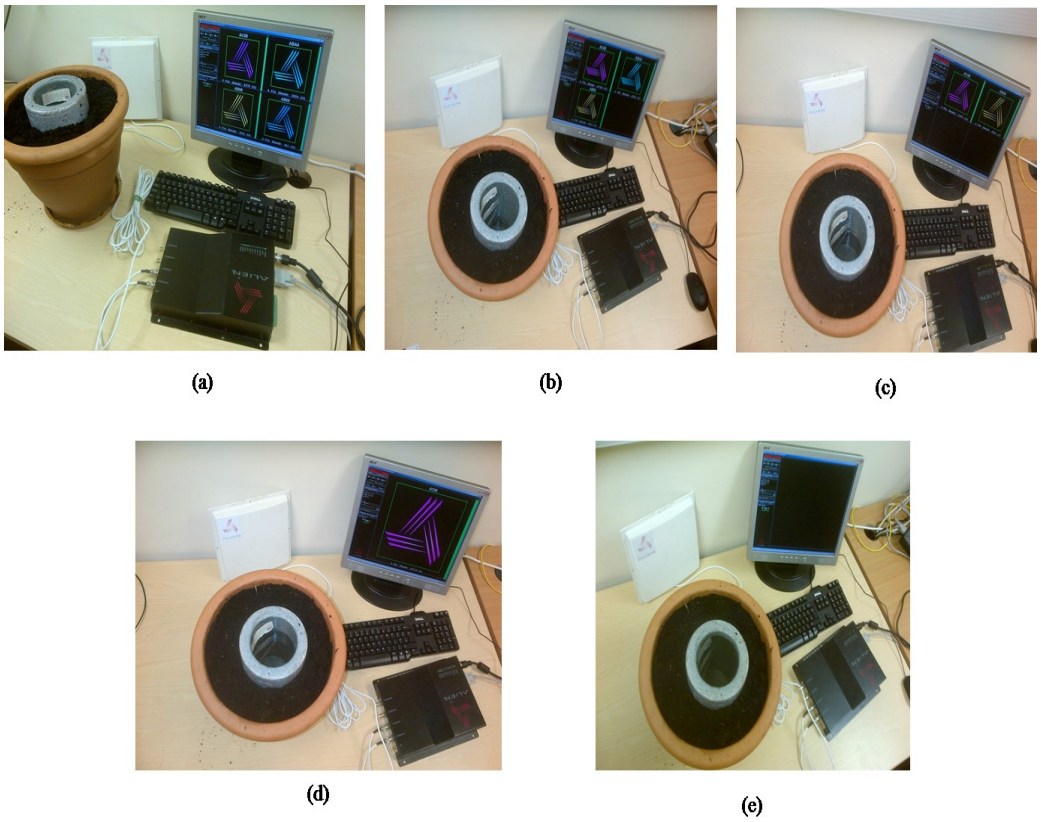

Figure 4.17: Practical gully pot measurement results (a) No liquid, (b) level 1 tag submeged, (c) level 2 tag submerged,(d) level 3 tag submerged,(e) level4 tag submerged.

The simulation shows projected performance. The environment properties are tested in HFSS to reflect an ideal situation. The nature of material of the gully pot is also explored and the effect of this on the radiation characteristic also observed. Figure 4.17 (a-e) shows consistency with the liquid level information obtained as reflected on the screen using the Alien RFID reader software. At stage 1 (reflected in 4.17a) ,the gully is empty and no liquid is introduced. As we proceed with introduction of liquid content to submerge the tag at the lower threshold level in Figure 4.17b it is clearly seen that only information from three tag levels is displayed, and this is consistent thoughout each of the stages with effective level information reflected respectively.

4.7 AUTOMATIC LIQUID LEVEL INDICATION AND CONTROL USING PASSIVE UHF RFID TAGS

This section presents a new perspective to the liquid level monitoring and control technique by deploying energy efficient passive UHF RFID tags as liquid level indication and control sensors. The level signals received from the sensors trigger a pump control circuit based on specified liquid level thresholds. The system proposed consists of the pump, storage tank, level sensors (passive tags), RFID tag reader, pump control circuit, alarm circuit, and an indicator circuit. The tags are sealed (air and water tight), programmed with unique level labels using the Alien Reader software(860-868 MHZ) and deployed to various levels of a storage tank for level monitoring and control. The mirrored P-shaped tag is designed modelled and deployed for use as the liquid level sensors. The RFID reader is disguised to form a part of the tank cover literarily few inches away from the tags. A variation of the tag readings received is used to infer level information which is communicated via the reader middleware to a computer database for monitoring.

Liquid level indication and control is enormously useful particularly in places where spillage or wastage of a particular sort of liquid poses a lot of danger to human life and to the ecosystem. An effective mechanism is needed to monitor and effectively control the level of liquid pumped through and into any surface or underground storage tank. In any liquid monitoring technique, the intended threshold levels are set to be monitored and controlled. In this work, five levels are marked for indication in the tank, these are: (UL-ultra Low), (L-Low) (M-Mid), (H-High), and (UH-Ultra high). The lower and upper level limits are set as the threshold levels which triggers

a pump control circuit and the alarm circuit. Level sensing information from the tags are fed directly to the level indicator circuit, the threshold level information triggers the pump control circuit to engage the liquid pump to commence pumping or to terminate pumping.

A safety mechanism is built into the circuit to escalate pump circuitry malfunction, this sends panic information to the alarm circuit if the pump fails to function when needed. When these threshold levels are exceeded, a set of feedback systems escalates this unusual activity which then triggers a range of other event driven control systems to automatically curtail the situation by taking prompt and appropriate action. Energy efficiency and improved accuracy in liquid level measurement has led to a tremendous reduction in chemical-process variability, resulting in higher product quality, reduced cost, and less waste. Newer level measurement technologies have helped in meeting requirements for accuracy reliability and electronic reporting.

Previous approaches both manual and automated methods applied to liquid level measurement have always had limitations [135-144]. Various liquid level monitoring techniques are explored extensively in literature [49] [145-148]. When more complex principles are involved computers and emerging sensor technologies are deployed to crunch the calculations. The transducer output signal formats for automation are current loops, analogue voltages and digital signals. The analogue signals are simple to deal with, but often comes with serious noise and interference issues. The more advanced measurement technologies (e.g., ultrasonic, radar and laser) require digital computer intelligence to format the codes. Combining this

requirement with the need for advanced communication capabilities and digital calibration schemes explains the trend toward embedding microprocessor-based computer in virtually all level measurement products. New wireless capabilities enabling signals to be sent over tremendous distances with virtually no degradation is explored with passive RFID tags deployed for level sensing.

Power efficient passive UHF RFID tags are deployed because of their flexibility in deployment, simplicity, cost effectiveness, user friendliness and less complexity as compared to other systems which have been previously deployed [148-156]. The block diagram of the proposed system is as shown in Figure 4.18.

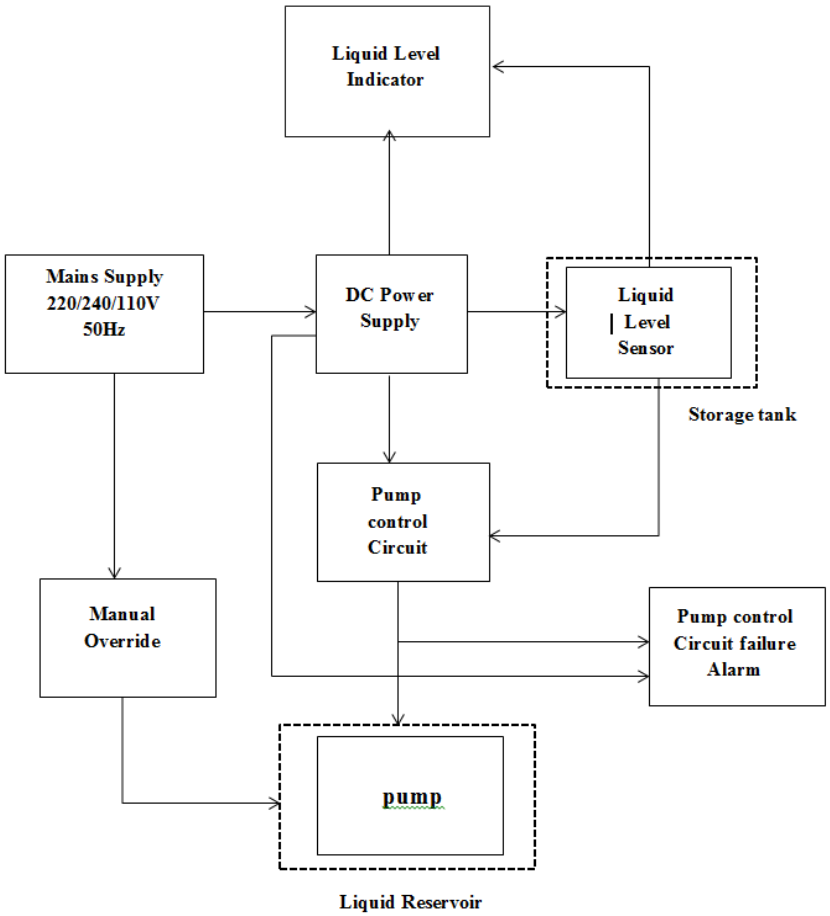

Figure 4.18: Block diagram of proposed automatic liquid level indicator and controller.

The liquid level indicator is a simple circuit which indicates on a display panel or computer screen as each successive level is submerged in liquid. This circuits receives information from the level sensors and feeds this back mainly for indication purposes. The level sensors send this information to the RFID reader which then displays the information on a graphical screen. The operation of the sensor tags in terms of radiation characteristics when immersed in different liquids (water, petrol, and transmission oil) of varying viscosity and conductivity is investigated. The behaviour of the sensor tags in terms of the effects on mutual coupling when mounted on storage tanks with different electrical properties (metal, plastic, and ceramic) is also observed and analysed to show consistent performance and has met application requirement. Two identical tags are assigned to each level for measurement, one of the tags will serve as a backup sensor; this is to allow smooth operation of the system, especially in a situation where any of main level sensors fail.

The liquid level sensors are the realised tags that are deployed to sense the respective levels, as soon as each level is sensed, the liquid level indicator displays the level sensed on the appropriate screen, the pump control circuit performs the central control operation based on information gathered from the level sensors. The basic two states proposed is ‘start pump’ and ‘off pump’. These two states are triggered by the level information embedded on the sensors at two threshold levels. In the ‘start pump’ state the level sensors at the low level threshold sends information to the pump control circuit when critical liquid level is sensed in order for the pump to commence pumping activity to the desired destination. The same process is followed to stop pumping action once the high threshold level is reached. The pump control

circuit failure alarm escalates unusual activity, especially when the set threshold levels are reached and no appropriate action is triggered by the pump control circuit.

4.8 RFID MIRRORED P-SHAPED TAG DESIGN

The design and modelling of a mirrored P-shaped tag is presented in this section. The tag geometry is optimised to achieve better bandwidth performance compared to the rectangular tag. This makes the tag more suitable for mounting on multiple surfaces as coupling with nearby objects will affect the reflection coefficient. The 3-D and 2-D view of the proposed tag is as presented in Figure 4.19.

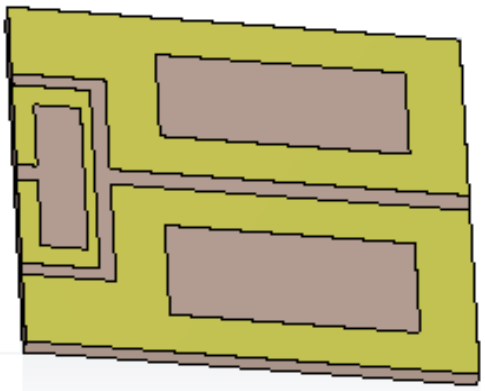

(a)

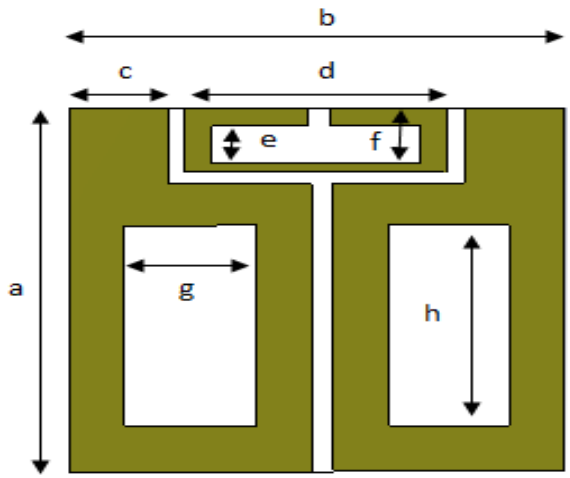

(b)

Figure 4.19: Geometry specification of the Mirrored P-shape tag
(a) 3-D view (b) 2-D view

Therefore, this tag has been designed to cover a slightly wider bandwidth. The tag is printed with a thin sheet of copper on a dielectric substrate FR4-epoxy (with $\epsilon_r = 4.6$ and $\delta_\epsilon = 0.017$) and a substrate height of 1.6mm. The ideal structure is printed on a single layer substrate with ground plane.

Table 4.2 presents the dimension description of the geometry realised. A 43.5mm by 45mm in dimension is realised. This has been printed on epoxy with the ground plane for mounting on metallic surfaces.

Table 4.2: Design parameters of the Mirrored P-shaped tag

a	43.5mm	f	7.5mm
b	45mm	g	12mm
c	5mm	h	24mm
d	24mm	i	1.5mm
e	4.5mm	j	2mm

This design delivers better bandwidth performance and has shown consistent reflection coefficient result. The geometry comprises of two mirrored symmetrical 'P' conducting sheet with a rectangular inset between them. The gap on this rectangular strip is where the chip is mounted. The dimensions of the antenna is commensurate to the intended resonant frequency. The feed point has been generated with (15 - j140) Ω normalised at 50 Ω. This feed point is usually where the IC chip is mounted. Various excitation types and position has been explored in a bid to observe the effects on the radiation behaviour of the tag. A consistent separation gap between the sensor tags were maintained during deployment in order to avoid tag jamming during measurements.

4.9 DESIGN SOLUTION OF THE MIRRORED P-SHAPED TAG

The simulation was set in HFSS. The dimensions were specified and boundaries of the various element of the design was stipulated. The radiation characteristics of the tag as observed, is as presented in this simulation results

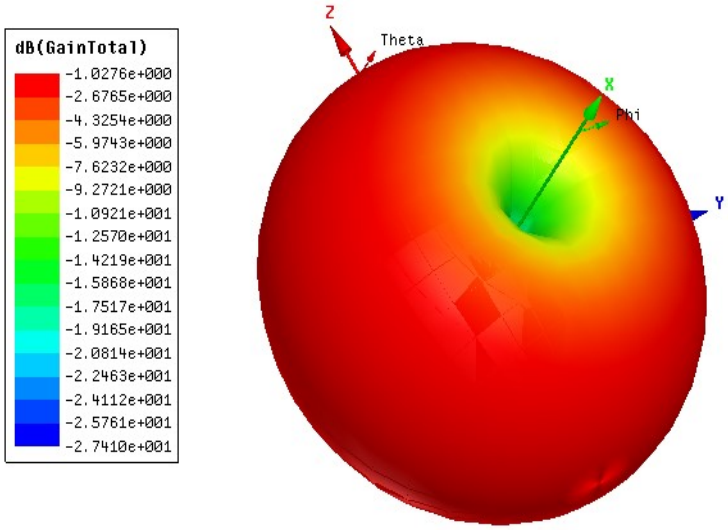

Figure 4.20: 3D radiation pattern of the Mirrored P-shaped tag

This shows a doughnut shape pattern which is desirable for the intended application (liquid sensors) for which this tag is to be deployed as this radiation pattern makes is less orientationally sensitive. The simulated gain obtained is -1dB. The chip impedance has been properly matched with the antenna impedance. Figure 4.21 presents the normalised far- field radiation pattern of the normalised tag antenna in the vertical and horizontal planes. This is very significant and fundamental to the performance of the tag antenna in terms of sensitivity to the reader antenna fields. The read/write range is also affected by the exact type of polarisation set for the tag

antenna. The results obtained from simulation shows promising performance for the proposed tag.

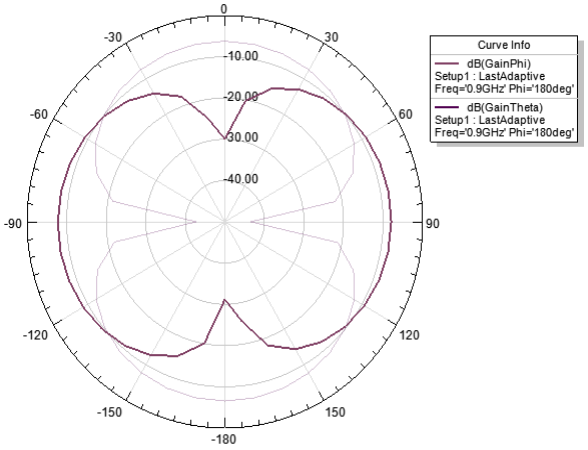

(a)

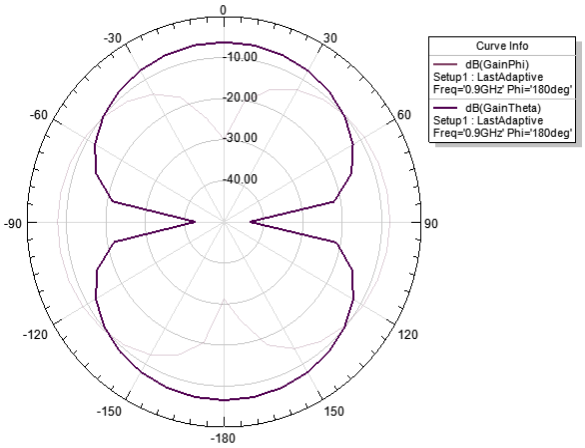

(b)

Figure 4.21: Normalised far field radiation patterns; (a) x-z plane and (b) y-z plane, for the mirrored P-shaped tag.

The reflection coefficient obtained was from -23 to -25.8 dB which shows a good return loss for the proposed tag as presented in Figure 4.22

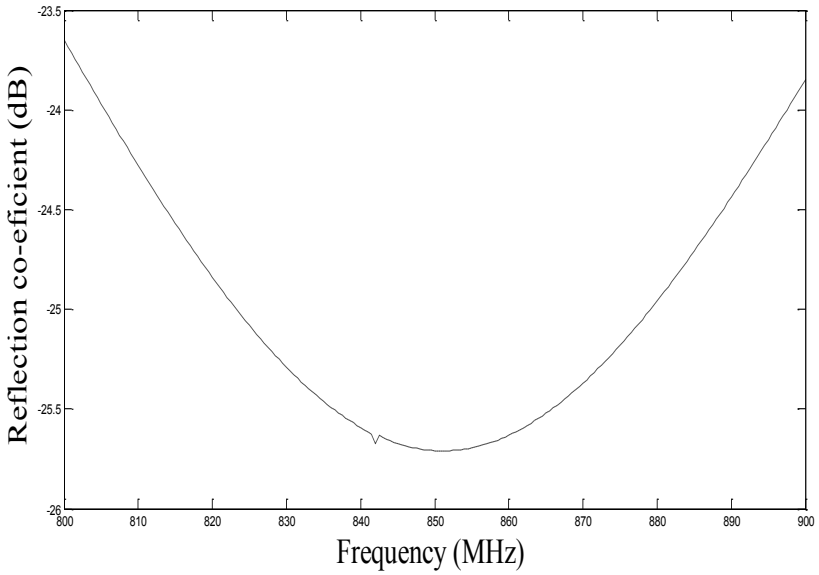

Figure 4.22: Reflection coefficient of the Mirrored P-shaped tag

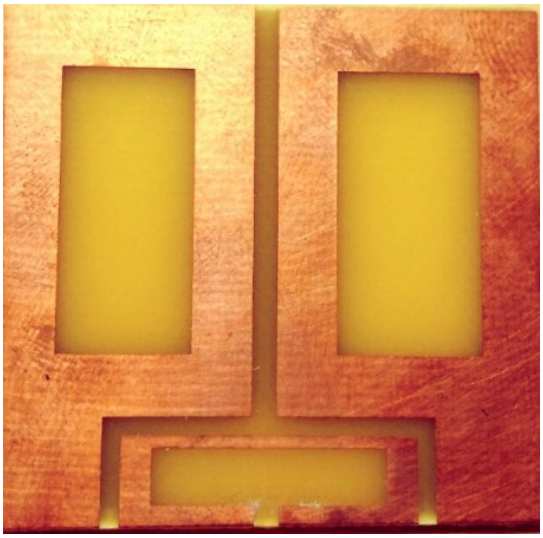

Figure 4.23: prototype design of the mirrored P-shaped tag

The realised tag is mounted with the Alien chip that can be read or write enabled. The tag antenna is highly inductive and less resistive. This is important to ensure maximum power transfer. For maximum power transfer, the source impedance should match the load impedance. The tag is sealed and made water tight and deployed to the intended levels for sensing and level indication.

The liquid tank is of plastic material with thickness of 15 mm. Tap water was used to fill the liquid tank to achieve different levels stipulated within the tank measurements were taken at each stage over a wide range of distances and angles; for which the reader was placed between 2 cm and 75 cm distances over 360° azimuth angle (in 20° steps) and 60° zenith angle (in 15° steps). The RFID reader used for this test is circularly-polarized antenna with 6.2 dBs gain. The maximum dimensions of the RFID reader was kept at $8 \times 8 \times 1.9$ cm^3. A graphical reflection of the current status of the 4 tags placed at different levels in the tank was presented for all readings considered.

The Alien RFID reader has been used for this practical application. The signals received from the liquid sensors are processed and displayed on a computer screen or a display panel for monitoring and referencing. The RFID reader is mounted as part of the liquid tank cover to achieve a compact design. The signals received from the sensors at the UL- level and UH-Levels are fed into the pump control circuit to take the necessary action of initiating liquid pump or turning off the liquid pumping activity. The sensors at the other levels are merely for level indication purpose and are fed into the level indicator circuit which can be displayed on a graphical computer screen interface. It was observed that the tags submerged in liquid became immediately readable when the liquid level fell below them. This was observed for the following liquids (water, waste water, diesel and petrol) and the results were consistent as depicted earlier in figure 4.14.

4.10 CONCLUSION

The rectangular tag antenna for this design is shown to exhibit an efficiency of 78%; the measured read range obtained was 50.5 cm. The tag antenna and chip IC impedances have been successfully matched at (15.39 + j139.58) Ω. The reflection coefficient of -43 dB is obtained which shows a good performance for the intended application. The parametric study carried out shows the most influential part of the geometry which affects the radiation properties. This also explored the suitability of the design for multiple frequencies. Optimisation of the tag parameters was effectively carried out on HFSS with the prototype of the optimised result presented. The parametric analysis has shown that increasing 'L' and 'N' step sizes gradually improves the reflection co-efficient at higher frequencies and lower frequencies respectively which makes it a very important property to use to switch applicability of the tag for various frequency operations; making this design very flexible to modify to adapt to various application requirements.

The HFSS simulation set was for observance of the performance within the (860-868) MHz operation. The geometry realised has been a result of several modifications in order to obtain a stable radiation characteristic. The best performance of tags obtained from repeated simulation and analysis has been obtained and presented. The tag was printed on epoxy (FR4) and polyethylene and the other with metallic ground to see the effect this would have when the tag is close to metallic surfaces and water. The tags deployed as level sensors were sealed and made water tight to prevent permanent damage to the tag IC. The reader distance from the sensors were varied and the maximum detection range observed. The

performance of the entire system as simulated in HFSS yielded satisfactory results in terms of the reflection coefficient. Remote, independent and effective monitoring of liquid levels in real time is achieved for data collection and transmission for distant operator station monitoring to prevent and effectively reduce flooding.

The importance of liquid level monitoring in both domestic and commercial sectors cannot be overemphasised. Previous approaches has paved way for a cheaper robust, compact, efficient and cost effective technologies as shown with the deployment of passive RFID tags in this piece of work. The tag has been modelled with the HFSS software and deployed for use as liquid sensors. These sensors do not contaminate the liquid medium in any way as they are sealed with a non-reacting casing based on the medium to which they are deployed. The radiation characteristics of the proposed tag meets the application demands.

The design presented here is highly efficient for adoption as a novel system for liquid monitoring. The tag behaviour varies based on the type of surface they are mounted. The variation of the signals received from the liquid sensors happens close to real-time. The concept proposed here clearly shows how flexible RFID tags are in terms of deployment to any existing system. The RFID reader mountable on the tank cover is most convenient for this type of application, the reader antenna was protected from direct contact with liquid. For a more compact and robust set up, a wireless reader with terrestrial communication capabilities will be best suited for this type of application majorly for remote global monitoring of liquid infrastructure. This has instigated the design and development of a dual band antenna for terrestrial communications from the manhole chamber presented in the next chapter.

CHAPTER 5

CHARACTERISATION OF A MANHOLE CHAMBER READER ANTENNA

5.1 DESIGN AND ANALYSIS OF A U-SHAPED IN-MANHOLE CHAMBER ANTENNA FOR UNDERGROUND COMMUNICATION SYSTEMS

This chapter presents an in-manhole chamber antenna for an underground mobile communications system. The design presented here is to serve as an RFID reader antenna;in order to extend the communication capabilities of the liquid monitoring system with terrestial networks. For this reason it has been designed to operate over the GSM850/900 and GSM1800/1900 and UMTS bands. The proposed antenna is a 3-dimensional folded loop antenna and has an envelope size of 47 × 43.5 × 60.5 mm, which is small enough to fit inside a manhole chamber**.** The performance of the antenna in terms of return loss, radiation patterns and gain was simulated and measured in both free space and in a real manhole chamber. To validate the simulated results, an experimental test bed was created to determine the antenna stability in terms of its achieved levels of return loss and received signal strength in different positions below the access cover of manhole chamber. Both numerical and experimental results suggested the best position of the antenna inside the manhole for the best received signal strength and confirmed that this antenna has adequate characteristics for incorporation in a mobile-band transceiver designed to communicate with mobile base stations from underground.

The lower operating mode is excited by the full length of the folded loop, while the higher resonant mode is generated by the inverted L-shaped part of the loop. Figure 5.1 a-c shows the geometry of the proposed antenna which is constructed as a folded planar loop.

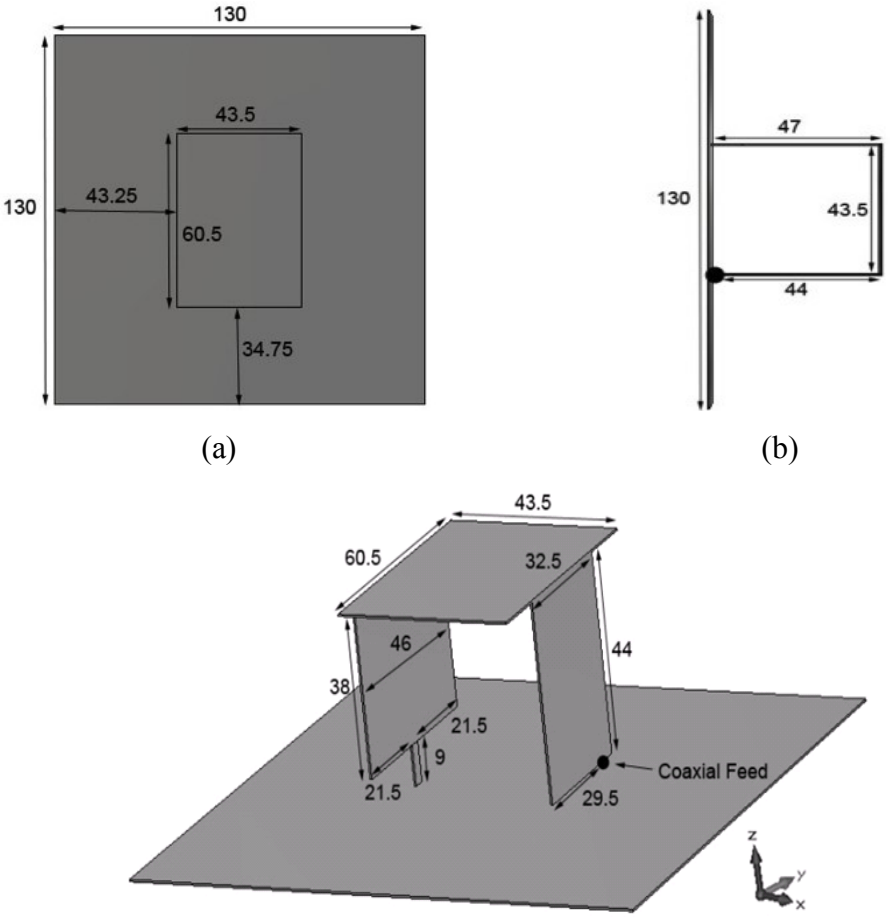

Figure 5.1:Geometry of the proposed U-shaped antenna. (a) Top view, (b) Side view, (c) Auxiliary view

The proposed antenna is designed to operate underneath the metal cover of the manhole chamber and it serves as the antenna for a data concentrator in a UWSN system to communicate with an existing long range above-ground mobile communication base station. Allowing for realistic constraints on acceptable size for

incorporation in a manhole chamber, the antenna dimensions and structure were chosen based on previous experience [49]. All the geometric parameters were then optimized through parametric studies. To enable its dual-band operating characteristic, a suspended rectangular feeding plate [159] with an optimized feed gap of 3 mm is used to excite this antenna assembly. As shown in Figure 5.1, the optimized dimensions of the antenna are 60.5 × 43.5 × 47 mm, equivalent to electrical dimensions of $0.18\lambda_o \times 0.13\lambda_o \times 0.14\lambda_o$, where λ_o is defined at the center frequency of the lower operating band, taken as 900 MHz. It is larger than a conventional mobile antenna, which is, however, acceptable in this application. For better performance and ease of integration within a manhole chamber, the antenna is designed to operate externally to a wireless transceiver and is mounted on the center of a 130 x 130 mm finite ground plane.

The basic operational principle of this antenna can be explained by separating the four differently sized rectangular metal plates which form the antenna assembly. This will aid understanding of the contribution of each metal plate to the antenna in term of matching and impedance bandwidth over the desired operating frequency bands, i.e. the lower band (824-960 MHz) and upper band (1710 – 2170 MHz). Figure 5.1 shows the detailed design evolution of the structure from a planar monopole to a folded loop planar antenna, i.e. Stage 1 to 4, while Figures.5.2 and 5.3 show the performance of the respective antenna geometries, in terms of return loss and input impedance.

As can be seen in Figure 5.2, this analysis divides into four stages and the whole structure is centered on the ground plane (not shown in Figure 5.2). It begins by

considering a 44 × 32.5 mm rectangular metal plate fed by an off-centre probe with a feed gap of 3 mm. This section constitutes a traditional planar monopole, depicted as Stage 1 of Figure 5.2. In this stage, the length of 44 mm, which corresponds to about 0.25λ, was selected to ensure that the antenna operates at the required centre operating frequency (COF) of the higher band, 1.9 GHz.

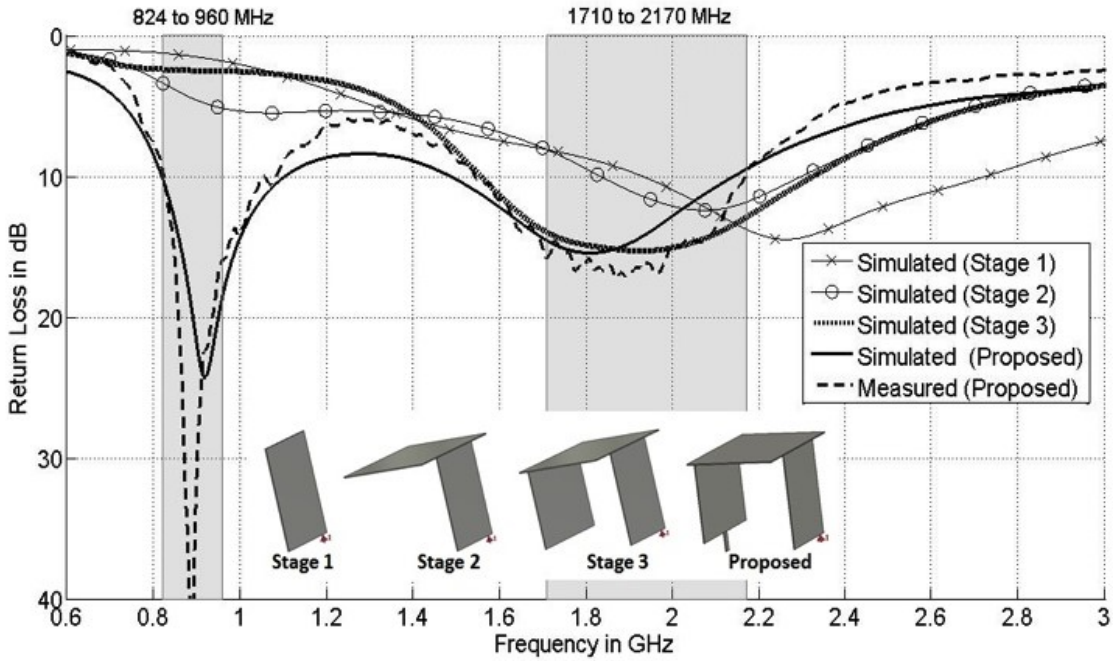

Figure 5.2: Simulated and measured return losses of the proposed antenna

By optimizing the width and the feed gap of the structure, acceptable impedance matching (better than 8 dB) in the higher operating band was achieved, as shown in Figure 5.3. Examining the relevant impedance plot in Figure 5.3b, it exhibits a typical monopole impedance response with a parallel resonance occurring at around 1.9 GHz.

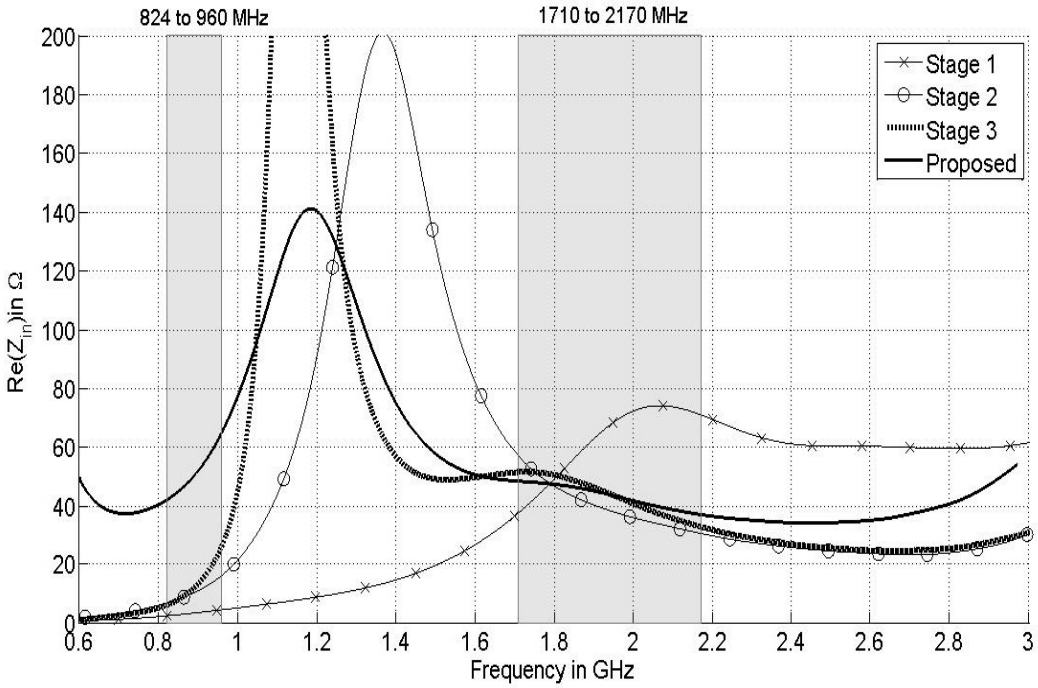

(a)

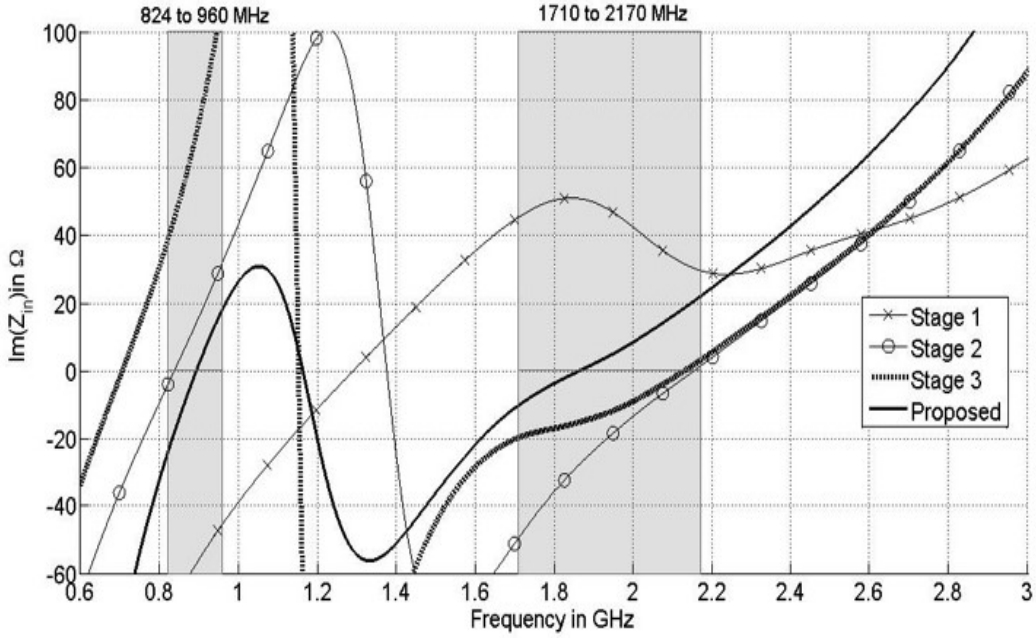

(b)

Figure 5.3: Simulated input impedance of proposed u-shaped antenna in the design evolution process from stages 1-3 (a) Real input impedance (b) Imaginary input impedance

To improve the impedance matching in the upper operating band without extending the height of the monopole component, the next course of action is to top-load the monopole with a 43.5 × 60.5 mm rectangular capacitive plate to construct an inverted L-shaped antenna structure, as shown in Stage 2, of Figure 5.2. The return loss plot shows a small improvement over the higher operating band, due to the top-loading effect, which shifts the parallel resonance down from 1.9 GHz to 1.35 GHz with associated resistances of 70 Ω and 200 Ω. This results in a small variation of the resistance, i.e. 30 to 58 Ω and changes the inductive reactance to capacitive in the higher operating band, as illustrated in Figure 5.3.

To further enhance the impedance matching in the higher operating band, a metal plate with dimensions of 38 × 46 mm is added at the edge of the top plate and parallel to the feeding plate: this is shown as Stage 3 in Figure 5.2. With this modification, this antenna partially resembles a loop antenna with an impedance bandwidth further improved to cover 1710 to 2170 MHz for a return loss better than -10 dB, as plotted in Figure 5.3. Examining the input impedance of this antenna, it is evident that this parallel plate further lowers the parallel resonance to 1000 MHz, with an increased impedance of 430 Ω, and results in good matching characteristics, i.e. resistance and reactance vary between 35 to 50 and -20 to 0 Ω, respectively. Finally, to achieve good matching at the lower operating frequency band, i.e. 824 to 960 MHz, this antenna is further modified by partially shorting the parallel plate to the ground plane using a 9 × 3 mm metal plate, as shown in Stage 4, Figure 5.2. After this step, the impedance response shows that the parallel resonance frequency of the antenna remains, but the impedance reduces from 430 Ω to 140 Ω, as plotted in Figure 5.3a. It was found, interestingly, that this change increases the resistance of

the antenna without altering reactance variation in the lower operating band, in comparison with the earlier form. Because of this, the whole antenna exhibits good impedance matching over the desired lower operating band. The simulated and measured results show excellent agreement as can be observed from Figure 5.3, two adjacent resonant frequencies in the range of return loss better than 10 dB occur at 900 MHz and 1900 MHz. The lower and upper modes offer 15.24% and 23.71% relative bandwidth from 824 to 960 MHz and 1710 to 2170 MHz, at a return loss of 10 dB or more. This is completely satisfactory for the desired GSM850, GSM900, GSM1800, GSM1900 and UMTS bands for mobile communication. In order to have more insight into the contributions of the individual parts of this antenna, vector plots of the surface current distributions at the center frequencies of the two required bands, i.e. 900MHz and 1900MHz, can be studied in Figure 5.4.

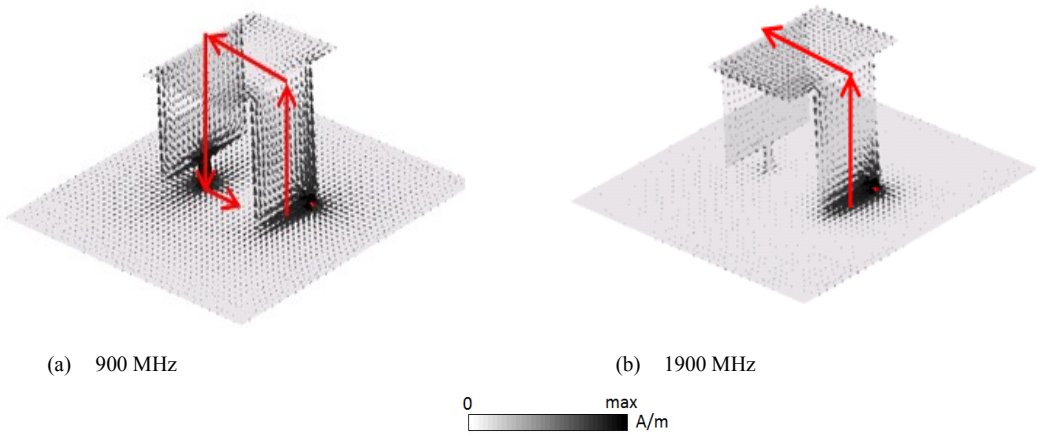

(a) 900 MHz (b) 1900 MHz

Figure 5.4: Current distributions of the proposed U-shaped antenna (a) Current distribution at 900 MHz and (b) current distribution at 1900 MHz

At 900 MHz, the total length of the continuous current path is 156 mm or about 0.47λ. As can be noted in Figure 5.4(a), the current flows from the feeding plate to

part of the top plate, then to the parallel and shorting plates, and finally to part of the ground plane to excite this mode. Therefore, the major dimensions of the geometry, including the height of the antenna, coupling distance between the feeding plate and parallel plate, and the width of the shorting plate, can be used to manipulate the lower operating mode. At 1900 MHz, the current path can be found from the feeding plate to the part of the top plate which connects the parallel and shorting plates with the feeding plate. This current path forms an inverted-L structure, as shown in Figure 5.4(b).

The length of this path is about 87.5 mm, corresponding to about 0.5 λ at this frequency. Figure 5.5 shows the physical prototype of the antenna which was fabricated from 0.5 mm thick copper plate It appears that the geometric parameters controlling the lower band also determine the higher band, except for the shorting plate which seems to have little influence at the higher frequency.

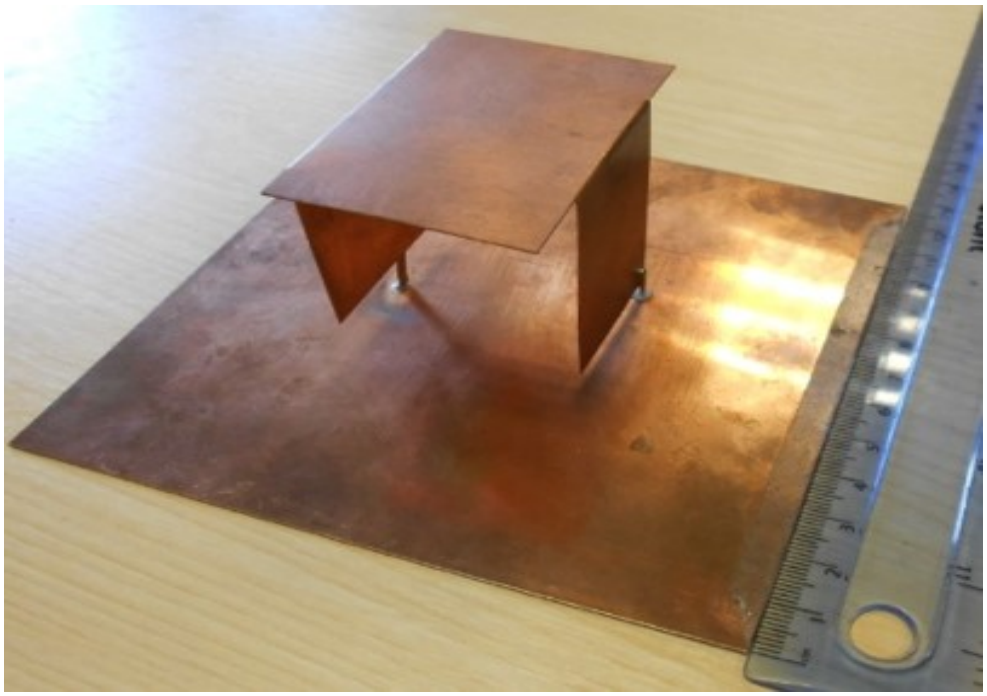

Figure 5.5: Prototype of the proposed U-shaped antenna

Figure 5.11 shows the physical prototype of the antenna which was fabricated from 0.5 mm thick copper plate. To verify the computed performance in terms of impedance bandwidth, the return loss of the prototype was measured using a HP8510C vector network analyzer. Figure 5.6 illustrates the simulated and measured peak gain and radiation efficiency of the designed antenna over the frequency ranges 824 to 960 MHz and 1710 MHz to 2170 MHz respectively.

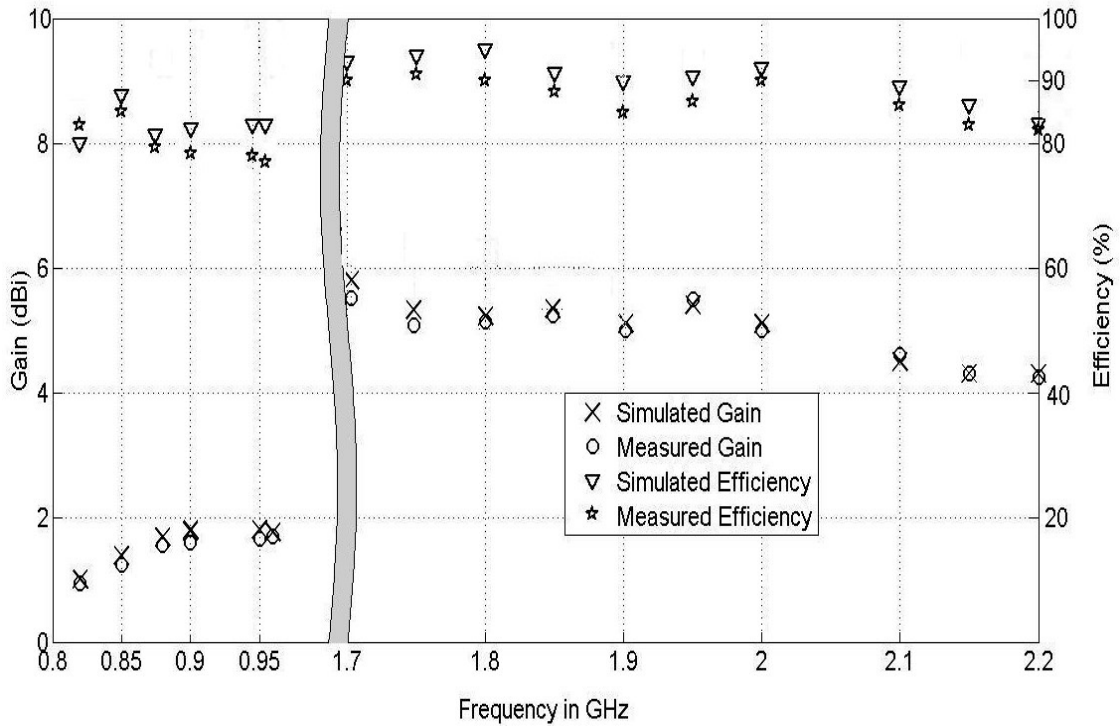

Figure 5.6: Simulated and measured radiation efficiency and gain of the U-shaped antenna.

In the lower band, a stable measured gain can be observed from 1 to 1.9 dBi, with 0.9 dBi gain variations. For the upper band, the measured gain ranges from about 4.2 to 5.8 dBi with corresponding 1.6 dBi gain variations. The computed and experimental gain results are essentially indistinguishable. In the lower frequency band, the simulated and measured radiation efficiencies vary from 80% to 88% and

76% to 85% respectively, corresponding to averages of 84% and 80.5% over the operating frequency range. At the upper frequency band, radiation efficiencies of 88.5% and 86% are achieved with ±13% and ±8% fluctuations for the computed and measured results respectively.

The far field radiation patterns of the prototype antenna were measured in a 6.75 × 4.5 × 3 m^3 anechoic chamber and the results are presented in Figure 5.7. In the far field measurement setup, a calibrated broadband horn (EMCO type 3115) was used as the reference antenna and held at a spacing of 4 m from the antenna under test (AUT).

An elevation-over-azimuth positioner was used, with the elevation axis coincident with the polar axis ($\theta = 0°$) in the AUT coordinate system The azimuth drive generates cuts at constant ϕ. The elevation positioner was rotated over $\theta \in [-180°, 180°]$ in 5° increments.

The prototype's radiation patterns were measured at the six frequencies representing the lower and upper operating bands, i.e. 825 MHz, 900 MHz, 960 MHz, 1750 MHz, 1950 MHz and 2150 MHz, and the corresponding results, cross-validated with the simulation data, are plotted in Figure 5.7

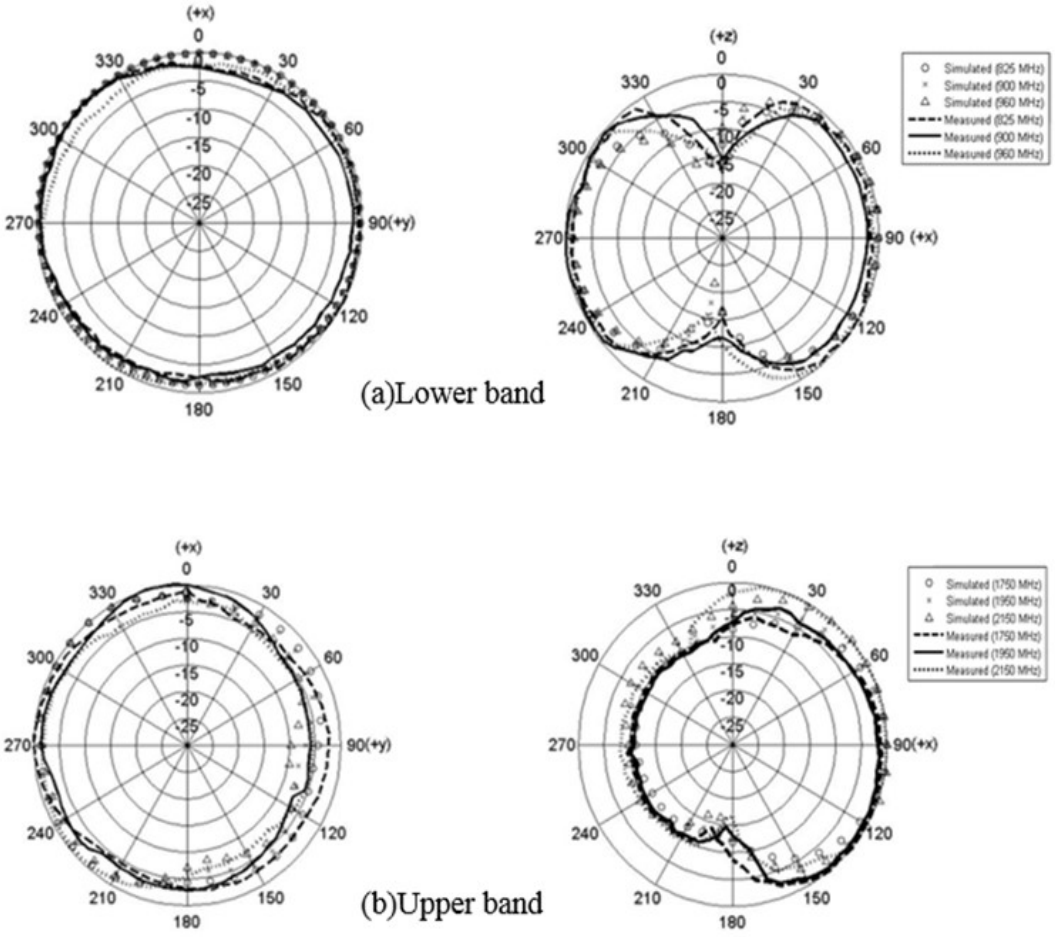

Figure 5.7: Simulated and measured normalized radiation patterns of the proposed antenna.

. In the measurement, two pattern cuts (H-plane and E-plane) were recorded at these selected operating frequencies covering the whole of the designated bandwidth in this study. The total power for both polarizations, i.e. vertical and horizontal components, of the antenna patterns was used. As illustrated in Figure 5.7, the radiation patterns are stable, consistent and nearly omnidirectional at all of the targeted operating bands.

5.2 ANTENNA IN MANHOLE CHAMBER - DESIGN AND ANALYSIS

In this section, the coupling effects of this antenna with the manhole chamber model will be investigated. Thus, a realistic manhole simulation model similar to that in [77-79] has been implemented and configured as shown in Figure 5.8. As can be seen, it consists of asphalt, a metal cover, concrete, PVC sewer pipes, a neck and chamber.

The manhole cover and its pedestal are constructed of cast iron with dimensions of approximately 0.75 x 0.6 x 0.1 m and they are buried in the asphalt layer ($\varepsilon_r = 3.15$, $\sigma = 0.026$) of the ground with dimensions of approximately 1.7 x 1.7 x 0.1 m. The neck and the chamber of the manhole are hollow cuboids surrounded by walls constructed of approximately 0.55 m and 0.3 m thicknesses of concrete ($\varepsilon_r = 7$, $\sigma = 0.12$), respectively. The corresponding dimensions of the neck and chamber are 0.6 x 0.6 x 0.5 m and 1.1 x 1.1 x 1.1 m. At 1.2 m below the asphalt layer, two orthogonal 0.425 m diameter PVC rectangular blocks ($\varepsilon_r = 2.1$, $\sigma = 0.0$) were modeled to mimic the drain pipes. The overall envelope size of the model is around 1.7 x 1.7 x 6.8 m including the height of the air region above ground, which is 5.0 m. To ensure affordable computational time, this model was truncated by Perfectly Matched Layer (PML) absorbing boundary conditions.

A preliminary analysis was carried out by investigating four orientations (0°, 90°, 180°, 270°) of the antenna, considering it to be placed at various heights (in the -z direction) and various positions in the x and y directions below ground, as shown in Figure 5.8.

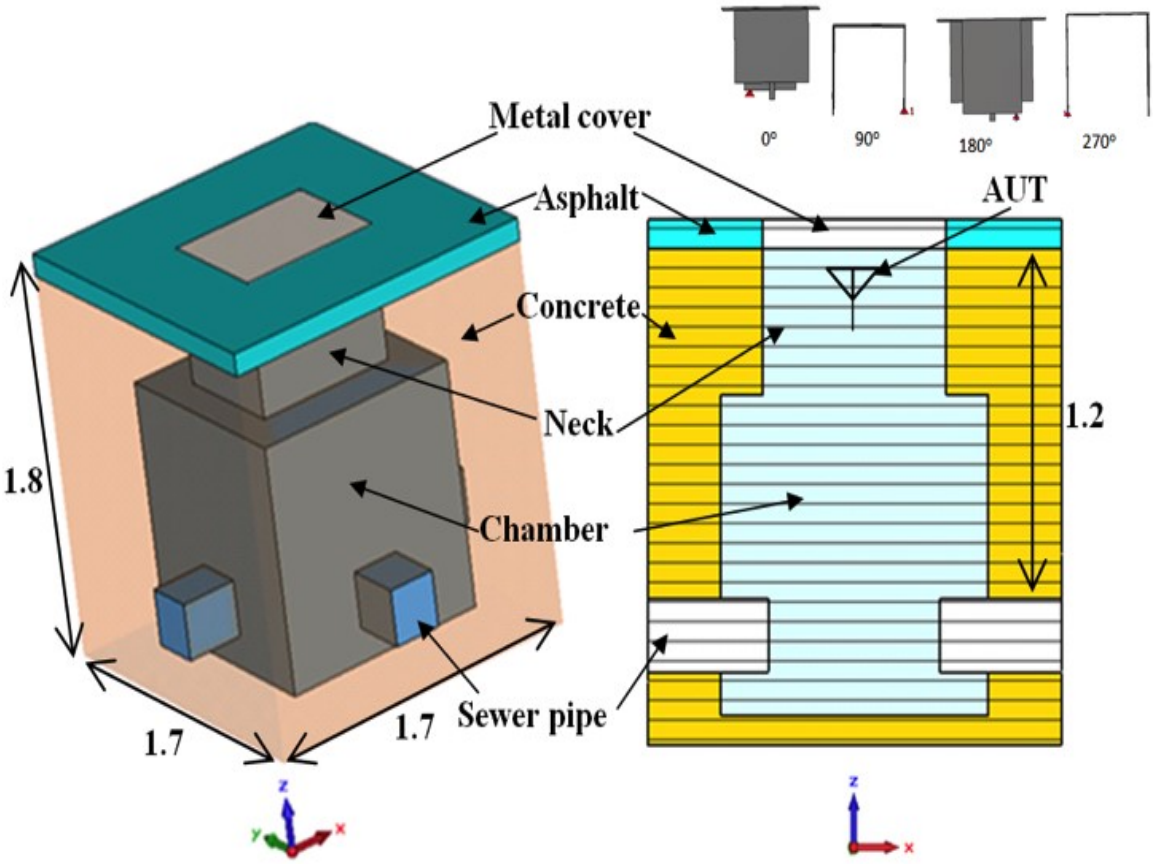

(a) Auxillary view (b) Side view

Figure 5.8 : Antenna in manhole chamber model (Unit: meters)

To better understand the importance of the antenna's position when it is fitted in the manhole, electric field intensity plots of the model at 900 MHz and 1900 MHz are shown in figures 5.9 and 5.10 respectively. These figures show the interface plane (xy-plane) between the open air and the manhole model. This provides a good indication of how much electric field can penetrate through the manhole.

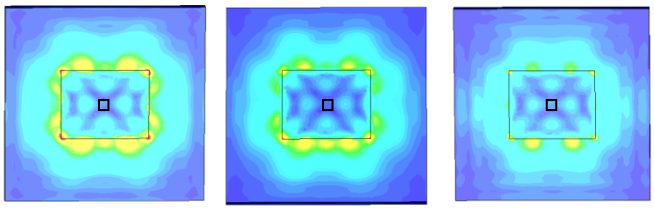

(a) AUT at centre of manhole cover

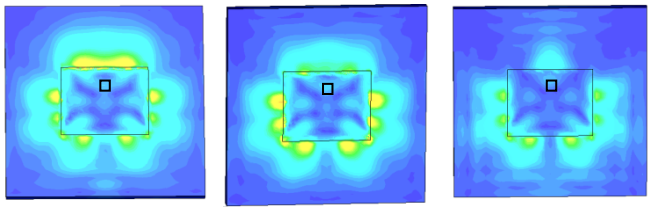

(b) AUT at a position between the centre and the edge of the manhole cover

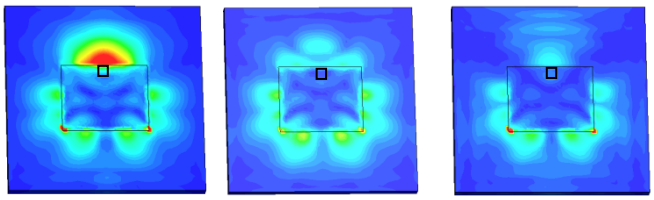

(c) AUT at the edge of the manhole cover

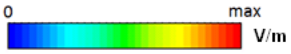

Figure 5.9: Total Electric Field over the surface of the manhole chamber at various position of the antenna under test (AUT) at 900 MHz.Left column: 50 cm depth, Middle column: 120 cm depth, Right column: 240 cm depth.

Small square represents the location of the antenna.It should be noted that the 0° and 180° orientations are where the feeding plate of the antenna is nearest to and farthest from the edge, respectively. Interestingly it was found that the antenna provides better electric field penetration to the surface of the ground at 0° orientation than for the other orientations. For the sake of brevity, other cases will not be shown here, and 0° orientation will be kept as a fixed parameter in the study. As can be observed in Figures 5.9 and 5.10, three antenna heights (from left to right), i.e. 50 cm, 120 cm and 240 cm, and three positions along the y-axis, i.e. (a) center, (b) between center

and edge, and (c) edge, were selected to cover possible scenarios for this investigation.

Examining the total electric field plots at 900 MHz, as in Figure 5.9, the fields are gradually attenuated when the depth of the antenna is increased from 50 cm to 240 cm, for all of the positions, i.e. Figures 5.9 (a) to 5.9 (c). When the antenna is placed underneath the center of the manhole cover, the fields exhibit nearly even distribution over the surface of the model, as shown in Figure 5.9 (a). This demonstrates that the power distribution in the center of the chamber is more favourable than close to any of the four walls. However, mounting the antenna centrally may obstruct the operator access to the manhole for any planned maintenance. Due to this, the antenna is generally mounted near the wall even though this incurs some additional power loss from a radio-propagation perspective. By moving the antenna between the edge and the center positions, reduced field strengths can be seen at three depth positions when they are compared to the center position. Further moving the antenna to the wall of the chamber and at 50 cm depth, the maximum field strength occurs near to the edge of the metal cover.

Figure 5.10 shows the total electric field distribution at 1900 MHz of the antenna and manhole model. In general, it is noticeable that the field intensity is also progressively reduced as the depth is increased, in agreement with the field distribution at 900 MHz. However, in contrast to the 900 MHz field plots, when the antenna is located in the center of the cover, the field intensity is lower than when it is placed at or near the edge of the cover. These results suggest that the antenna

should be placed near the edge of the cover or near the wall of the chamber for best performance in the upper operating frequency band.

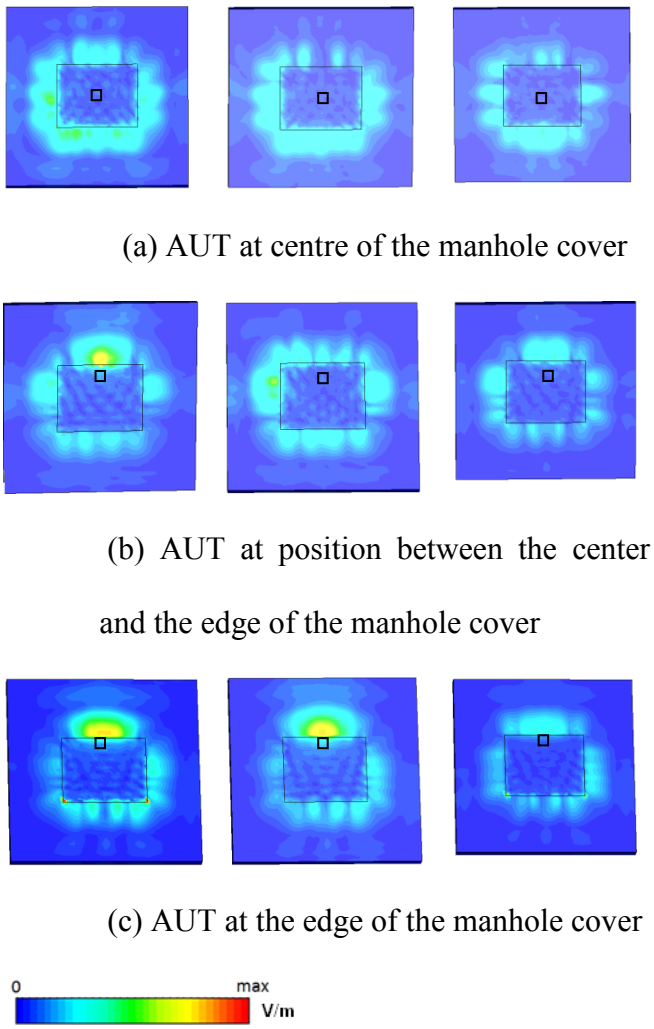

(a) AUT at centre of the manhole cover

(b) AUT at position between the center and the edge of the manhole cover

(c) AUT at the edge of the manhole cover

Figure 5.10: Total Electric Field over the surface of the manhole chamber for various positions of the (AUT) at 1900 MHz.

Left column: 50 cm depth, Middle column: 120 cm depth, Right column: 240 cm depth. Small square represents the location of the antenna. To understand the coupling properties of this antenna when it is installed in the manhole, the S-parameters of the antenna, including return loss and transmission coefficient, have been studied. Return loss here indicates whether the antenna operates in the desired

operating bands without being detuned, particularly when it is next to the metal cover,while the transmission coefficient measures the strength of the electromagnetic wave coupled through from the ground to air. To enable the transmission coefficient to be calculated in the model, eight broadband ridged pyramidal horn antennas were added to the model, as depicted in Figure 5.11. This will ensure that an average transmission coefficient can be obtained. The complete structures of the horns were included in the model. It should be noted that two geometric parameters, i.e. D (horn distance from the center of the manhole model) and H (height above from the manhole), were used in this study, where D was set to 2 m and H to 1.85 m. This ensures that the measurement was conducted within the far-field region.

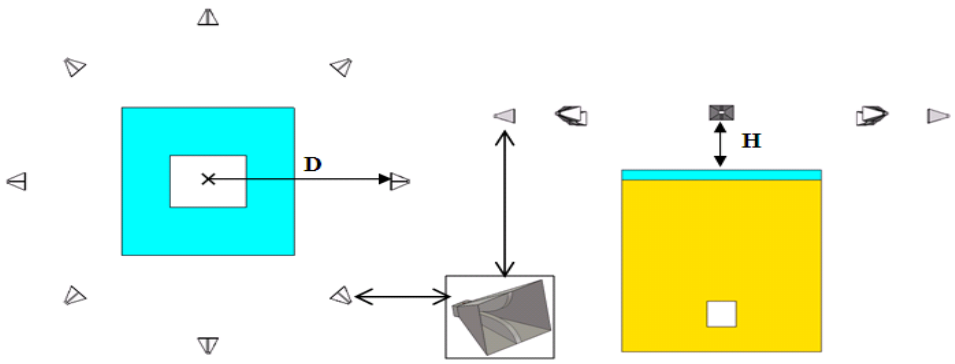

(a) Top view (b) Side view

Figure 5.11: Manhole chamber model surrounded by eight ridged pyramidal horn antenna locations, where D is 2 m and H is 1.85 m.

In order to verify the simulated variations of the return loss of the antenna under test (AUT), and assess the transmission coefficient, an in-situ measurement was also set up in a manhole chamber, as illustrated in Figure 5.12.

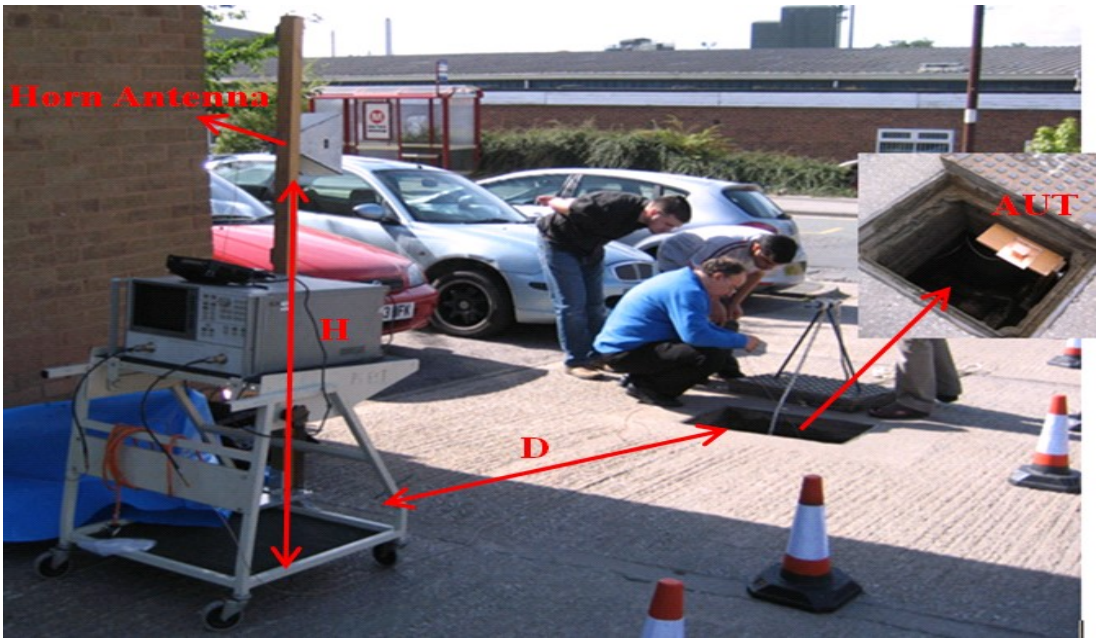

Figure 5.12: On-site practical measurement set up

The experimental equipment consisted of a reference horn antenna, positioned at height H=1.85m, Vector Network Analyser (model: Agilent 8720C), and a data acquisition unit (Panasonic Toughbook Tablet, Model: CF-U1). Transmission measurements were taken with the horn antenna at a constant distance of 2 m from the centre of the manhole cover. The horn and all measuring equipment were moved on a trolley between the eight positions surrounding the manhole metal cover, for recording the transmission coefficient. For all the measurements, the AUT was mounted on a height-adjustable L-shaped support structure. For the transmission coefficient measurement, the AUT acted as a transmitter, while the horn antenna played the role of a receiver. The two antennas were operating in a non-line of sight (NLOS) communication condition, but pointing towards each other. All the measured data were recorded five times and then further processed in MATLAB for a better interpretation of the measured data sets. Since mobile base stations are operated with vertical polarization, the antenna in vertical polarization orientation

was the primary target for this measurement, however, the two polarizations were considered in the measurements. Figure 5.13 shows the simulated and measured return losses and transmission coefficients of the antenna in the manhole chamber. It is noticeable that the antenna preserves good impedance matching (better than 10 dB) over the desired frequency bands, as plotted in Figure 5.13 (a). The computed and experimental results are in excellent agreement.

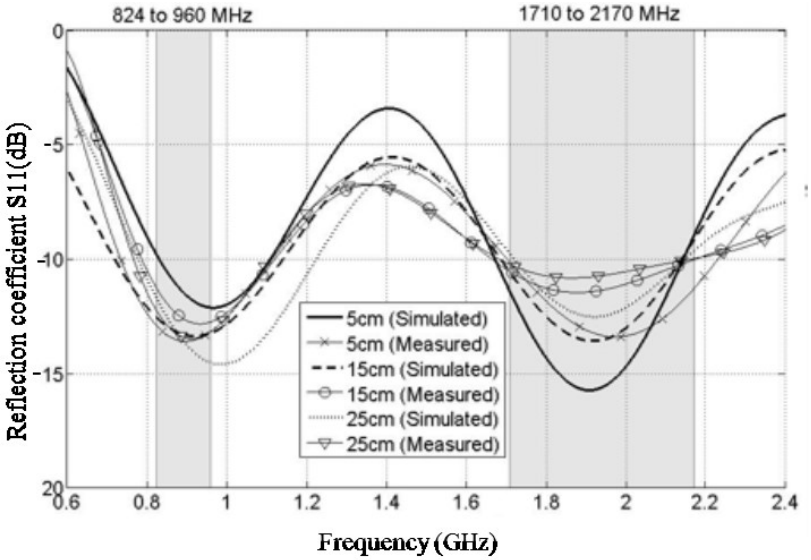

(a)

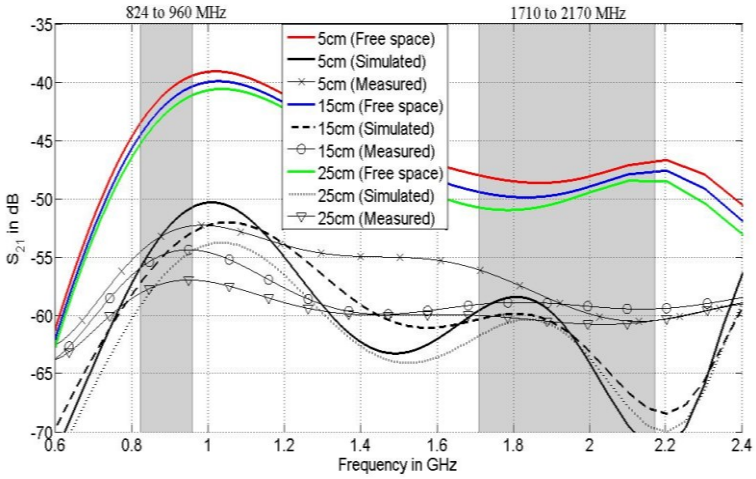

(b)

Figure 5.13: S-parameters between the horn antenna and the antenna under test (AUT) at different depths in the manhole chamber. (a) Return loss; (b) Transmission coefficient

Figure 5.13 (b) is the simulated coupling level when all material obstructions, including the chamber walls, the asphalt and the manhole cover, are removed. This is the meaning of the free space curves in the plot. As noted, in practical conditions there is no clear line of sight between the antennas, and the direct ray path traverses the asphalt and the chamber walls. The average loss of signal due to non-LOS conditions is around 10 to 15 dB in the lower band and 8 to 13 dB in the higher band.

For practical reasons, depths of 5, 15 and 25 cm. had to be used in these tests. For the transmission coefficient at a depth of 5 cm, the measured results show around -52.5 dB to -55 dB at the lower operating band, while at the higher band -56 to -61 dB is observed. Further increasing the depth to 15 cm, the results are further reduced by -2 dB to reach the range of -54.5 dB to -56.5 dB at the lower band and around -58 to -59 dB at the higher band. When the depth reaches 25 cm, the results drop by another 1.5 to 3 dB in the lower band and 2 to 3 dB in the higher band. This has resulted in a range of -57.5 to -58 and -60 to -62 dB over the lower and upper band respectively. Slight discrepancies between both simulated and measured results can be attributed to uncertainties in the electrical properties of the materials used in the simulation model, and the simplifications in the simulated structure. Some variation with the weather conditions would also be expected due to their effect on the water content of materials and on the water level in the gully.

5.3 CONCLUSION

A dual-band folded planar loop antenna for a partiall-underground utility sensing application has been presented and examined theoretically and experimentally. By combining impedance matching techniques, including off-centre rectangular plate feeding, top-loading and a shorting strip, the required dual-band impedance bandwidths, i.e. 824 to 960 MHz, and 1710 to 2170 MHz, have been achieved. To confirm the suitability of this antenna to operate inside a typical utility manhole chamber, a manhole-and-antenna model has been simulated and tested experimentally. The results show that the antenna prototype exhibits sufficient impedance bandwidth, suitable radiation characteristics, and adequate gains for the required underground wireless sensor applications. The reduction of signal strength due to N-LOS transmission is small enough to permit a viable communications system. The dual frequency band of operation makes the antenna very significant for use as an RFID reader. This is in order to extend the communication capabilities of of the liquid level monitoring system presented in chapters 3 and 4. The challenges faced during the practical set up has shed light to more areas of improvement of this design. The LSQHA presented in the next chapter represents an improvement in terms of the directivity of the reader antenna. The GA optimisation tool has been employed to achieve novel geometry for the LSQHA intended to be adopted as a highly directive reader antenna for future applications requiring longer range detection of tags for multiple applications.

CHAPTER 6

DESIGN AND ANALYSIS OF ANTENNAS WITH THE GENETIC ALGORITHM COMPUTATIONAL TOOL

6.1 ANTENNA DESIGN USING GENETIC ALGORITHM

This chapter presents the design and modelling of a LSQHA. The results obtained in this new reader antenna design shows improved performance (in terms of gain and directivity) and recommended for applications requiring a longer range detection of tags for multiple applications. The results from simulation shows very promising performance. Genetic Algorithm (GA) is a computational tool for modelling various antenna structures. The search and design procedure in GA is hinged on the theory of genetics, evolution and natural selection. This makes GA very effective in fast convergence to optimum design in optimisation. It was first introduced in the 1960's by J. Holland, and has evolved into a powerful optimisation and search tool [160]. Before the GA era, similar ideas was generated but applied mainly in games for entertainment and majorly for pattern recognition. GA has gained popularity over time as an important tool for design optimisation and control applications. This evolutionary computation method is not only effective in design optimisation but also in the creation of highly effective new antenna types with high flexibility in design process. It has made the design of antennas easier with increasing efficiency and less time spent on producing optimal design results. This is because in GA the desired design specification or expectations in terms of radiation characteristics is

pre-specified and then the computational analysis within the GA algorithm specifies the exact parameters to guarantee the specified performance metrics.

This makes design delivery faster and straightforward as compared to other soft wares where the geometry parameters needs to be repeatedly altered during optimisation or parametric analysis in order to obtain the optimum result.
GAs as adopted and applied by many researches is documented in [161-180]. GAs has created a niche as very effective computational tool for the generation and analysis of antennas of various types and kinds. GA's are particularly helpful for the following reasons:

- Since search spaces are highly multimodal and resistant to other forms of hands-on and numerical optimisation,
- Generally antenna principles based on the equations of Maxwell's are quite complicated and hard to fully grasp and apply.
- GA is naturally robust in optimisation and do not require any sort of initial guesswork to converge to exact design specifications, the amount of design information the engineer must supply to get a good result is minimal, this becomes very vital especially when there is a specified time frame for delivery of design specification.

GA has the ability to find new solutions to complex antenna configuration design problem which other known conventional antenna design tools cannot provide finite solutions to, it comes in as a very important tool especially when proposed design in other software's is expensive or difficult to manufacture. GA resolves and presents

the optimal parameters for a design based on the specified conventional characteristics. Different antenna types can be optimized for specific performance desired. The yagi-uda with inherently high-directivity can be optimised for maximum gain. This method of optimisation is very useful as it identifies the parameters that affect the performance of a design and goes straight to optimise those parameters to yield favourable results, this is most helpful since most conventional antenna design problems are difficult to handle in terms of optimisation.

The traditional methods of antenna solutions are too limited and have not been able to cope with the increasing demands. As the number of antenna problems grows yearly without good solutions, the GA solution is a perfect basis for a new era of optimisation platform more so that it provides increasing avenue for exploring previous areas of antenna design which was unsearchable and apply appropriate solutions without any form of restriction.

The communication process within the near field also needs to be taken into full consideration as this affects the read field strength more so that reader-tag communication within this zone is based on inductive coupling [124, 181]. Some existing types of antenna with high gain (Spiral and Helical) are examined based on their radiation characteristics for adoption and optimisation with GA for use as a compact size reader antenna for the tags realised. Some of these antennas are described in the next page.

6.2 TYPES OF READER ANTENNA

6.2.1 SPIRAL ANTENNA

The spiral antenna as the name implies is geometrically spiral and defines surfaces by angles. They function as low gain transceivers over a wide range of frequencies and are most often times classified as versatile antennas operating across multiple range of frequencies. The spiral antenna operates in circular polarization with usually low gain which can be effectively improved with a combination of a stack or an array of other spiral elements. In achieving optimal spiral geometry various spiral derivatives such as square spiral, Archimedean spiral and star spiral can be selected for optimisation [124, 182]. The number of spiral turns can be altered with a view to achieving the optimum geometry, and the spacing can also be adjusted to achieve better performance. The dielectric thickness and material permittivity could be altered to fine tune performance and obtain a light weight outcome. A compromise needs to be reached on material availability, cost and acceptable operational performance. The success of any spiral antenna design hinges on the geometry specifications and the nature of material selected [124, 183].

The three approaches to spiral antennas are: rapid wave, roving wave and leaky or spongy wave respectively. The wave which builds up on the arms of the spiral is the roving wave, the rapid or fast wave is created as a result of mutual coupling along the arms, and the leaky wave is created by the power leaks that occur along the arms during propagation The region where the spiral antenna emits most radiation is

referred to as the active region and is usually a part of the circumference of the spiral structure [124].

6.2.2 HELICAL ANTENNA

This type of antenna is made up of a conducting wire which has been woven in a helical shape and built on a specific ground plane which carries the power source usually situated in the middle. To modes of operation are employed in the Helix antenna, these are: the broadside helix or the axial style (end-fire helix) [124]. The broadside mode is characterised by significantly smaller structural parameters in comparison to the wavelength of operation. Signal radiation in the helical antenna is likened to the monopole or short dipole with an omnidirectional radiation pattern with higher radiation intensity at right angle to the helix axis. A linear polarised radiation pattern parallel to the helix axis is usually formed [124, 183].In the axial technique the helix dimensions are similar and corresponds to the wavelength. The end-fire helix antenna type radiates in a directional pattern along the axis of the helix emitting beam in a circular polarised nature. This type of antenna is therefore best suited for use as an RFID reader. The next chapter gives a detailed account of the proposed reader antenna design using GA.

6.3 DESIGN AND COMPUTATIONAL ANALYSIS OF A LINEARLY-SHIFTED QUADRIFILAR HELICAL ANTENNA USING GA

GA is deployed as an effective computational and design analyser for several antenna types. Antenna parameters are specified for a certain frequency of operation and the codes within the GA randomizes these size specification to fit a specific set

of radiation characteristics; several iterations are performed with the electromagnetic solver within the GA until an optimum solution is realised [184]. GA application in combination with the electromagnetic simulator has been adopted to generate new evolution of antennas [185-186]. GA has also gained increasing popularity and has been deployed for micro strip antenna solutions for fast, efficient, reliable and accurate computations for the generation of optimum sized antennas with highly efficient performance [187-190].

In this design realisation, the GA with FORTRAN code in combination with NEC 2 FORTRAN source code has been used to design and optimise the LSQHA. A series of randomly selected antenna structures was evaluated and analysed to yield an optimum design selected for the RFID reader antenna. The basic parameters considered for improvement in the optimisation are the axial ratio and the VSWR. The GA procedure applied firstly adopts the initial specified population randomly and computes the structure specifications to a format readable in the NEC 2 software platform. This NEC 2 software runs the computation and feeds this back into the GA to obtain an optimum solution.

The overall results presented during the course of this chapter generally shows excellent performance in terms of size reduction of the LSQHA where the axial length has been reduced by about 30%. The spiral surface area is also tremendously improved without affecting the major radiation characteristics of gain and directivity. Antennas constitute a very important part of Radio Frequency Identification (RFID) systems. Coming in various forms and types, they are designed with specifications to

ensure maximum effective and efficient communication links between tags or transponders and their associated readers or interrogators.

One of the primary challenges in the design and development of antennas in RFID applications as it is in other wireless applications is having an antenna with optimised parametric features that are desirable and in consonance with laid down specifications and functional requirements [191-192]. These parametric features include but are not limited to: profile, gain, directivity, bandwidth and polarisation.

Radio Frequency Identification (RFID) systems which represents the physical interaction between a tag and a reader for automatic identification operate within the global bandwidth of (860 – 960) MHz [193]. The orientation of the tags and associated readers must be fully established through the polarisation characteristics of their corresponding antennas in order to ensure optimum performance by avoiding polarisation mismatch.

The Quadrifilar Helical Antenna (QHA) has been identified by previous works as a suitable antenna for omnidirectional tag reading in RFID and other wireless applications, due to its circular polarisation radiation over a wide angular area [194-195]. Another excellent property of QHAs in terms of the symmetry of their geometry is their cardioid-shaped radiation pattern irrespective of the diameter and the axial length [196]. It has also been established that the inherent cardioid-shaped radiation patterns of QHAs can be made conical by extending the resonant fractional turns of the QHA to an integral number for improved characteristics [197].

The QHA (Figure 6.1a) is capable of providing an excellent beam width pattern with desirable circular polarisation, making it a good choice in RFID applications [198]. However, optimum caution is advised in the synthesis of QHAs in a bid to achieve the specified front to back power ratio as well as the axial ratio. A major notable pitfall in the design and development of QHAs is the overall axial length of antenna, which is often too bulky for many practical installations and applications.

To address this problem, a global optimisation technique was adopted to constrain the geometrical parameters of the conventional QHA. The selected global optimisation technique, genetic algorithm (GA) has been exemplified as a reliable tool for electromagnetic computation solutions. Broadly defined to be robust and offering better solutions, GA has been used in previous works to achieve low profile, compact designs for QHAs in other wireless communications applications. Figure 6.1 shows the geometry of the proposed antenna.

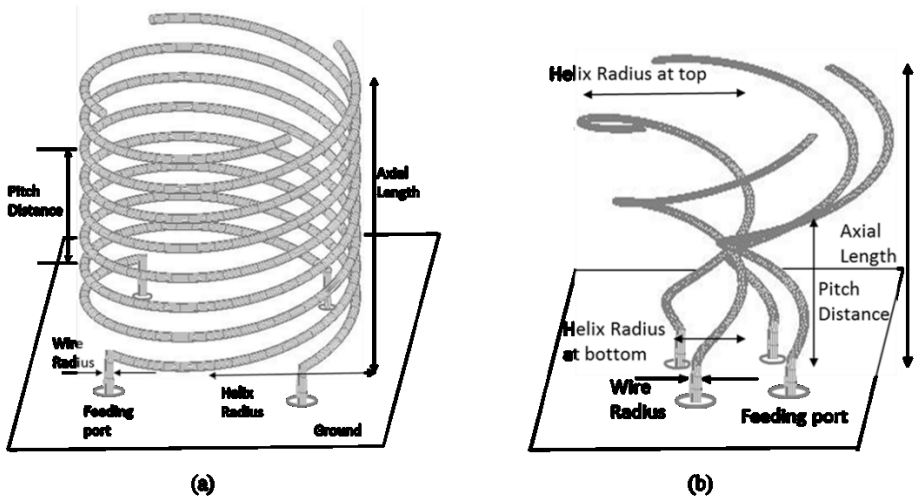

Figure 6.1: GA generated antenna configurations: (a) Basic geometry of the QHA; (b) Geometry of the LSQHA

A novel compact QHA has been generated to operate in the RFID global specified bandwidth (800-900 MHz). A novel QHA antenna is named Linearly-Shifted Quadrifilar Helical Antenna (LSQHA) because its elements are linearly-shifted and made compact as revealed in Figure 6.1b. With reference to its helical elements and as can be observed, the proposed LSQHA design does not take the form of the conventional QHA. Specifying a finite ground and feeding of the LSQHA via an integrated feed network is proposed, to avoid the intricacy and losses associated with multiple feed points of a centre feed. At the risk of repetition, the novel antenna structure is achieved by linearly-shifting the helical elements of the conventional QHA by 90° using a defined phase quadrature distance. The new structure generated is targeted at tremendously reducing the axial dimensions and overall volumetric equivalent of the LSQHA, while retaining good axial ratio, high power gain and wide beam width coverage.

6.4 RFID READER ANTENNA (LSQHA) DESIGN AND OPTIMISATION USING GA

The LSQHA design and optimisation using GA in combination with the Numerical Electromagnetic Code (NEC-2) is presented and adopted as an RFID reader antenna for use in combination with the rectangular tag discussed earlier as a complete RFID liquid level sensing system. This technique of combining the GA driver and electromagnetic Compiler has been previously applied in the optimisation of a series of antenna structures. The optimisation technique employed, GA which is based on the principles of genetics and natural selection provides optimum solutions for so many different antenna geometry.

The GA program is initialised by a set of initial solutions or parameters defined for the proposed LSQHA. Parametric iterations are then executed in GA in combination with NEC-2 program. In the work presented here, the source codes for the GA driver runs simultaneously with the NEC-2 codes written in FORTRAN. The codes were intuitively modified to randomly generate and evaluate antenna samples.

To achieve optimum results, the initial geometrical and parametric solution of the proposed LSQHA was defined for optimisation with GA based on established findings. Real-valued GA chromosomes were defined in this process.

Antenna parameters like the VSWR, axial ratio (AR) and total forward gain (G_T) were optimised at an operating frequency of 900MHz in consonance with the EPC Global RFID Tag/Reader specifications [195-197]. Individual antenna samples were generated using the industry-standard NEC-2 source code and corresponding results were juxtaposed with the desired fitness using the cost function 'F' stated as follows:

$$F = W_1 \times (1/VSWR) + W_2 \times AR + 0.5 \times 1/\left|\left(G_T - 14.5\right) + 1\right| \tag{6.1}$$

Where: $W_1 = 0.5$

$W_2 = 0.75$

$$VSWR = \left(1 + |\Gamma|\right)/\left(1 - |\Gamma|\right) \tag{6.2}$$

$$\Gamma = \left|\left(Z_{in} - 50\right)/\left(Z_{in} + 50\right)\right| \tag{6.3}$$

'VSWR' represents the Voltage Standing Wave Ratio, 'AR' defines the Axial Ratio, 'Z_{in}' is the impedance of the input, 'Γ' stands for the reflection coefficient, G_T

connotes the total gain usually denoted in dB, the weighing coefficients are denoted by 'W_1' and 'W_2' respectively. The goal of the optimisation process was to maximise '*F'* by using the threshold values of 'AR' and 'G_T'. To achieve this, GA driver is initialised by the random selection of a population or antenna configuration. Each and every structure specification of the antenna is converted into a series of codes stores in a file accessible to the NEC-2 software. Running concurrently, the NEC-2 program feeds its results to the GA driver for evaluation. This process is repeated by several computational iterations till a fully optimised solution is realised by the GA.

The LSQHA was designed to provide a very high forward gain and circular polarisation operating within (860 - 960) MHz. The structure of the LSQHA and its volumetric equivalent were ensured to conform to a very low profile. As evident, the proposed design differs from the conventional QHA in Figure 6.1a in that its helical elements were configured to be linearly-shifted at 90° from each other using a defined phase quadrature distance. This was deemed necessary in an effort to achieve a very compact design and lower the overall profile of the proposed antenna. In the study undertaken, the LSQHA offered a better performance with its helical elements shifted.

The aim in the design of a Linearly-Shifted Quadrifilar Helical Antenna (LSQHA) was to realise a very compact geometry and low-profile alongside the good radiation characteristics of the generic QHA. The simulation logic and GA optimisation model were structured in such a way that an optimum linear distance between the four helical elements of the LSQHA was sought while shifting them by 90° in phase-

quadrature. The performance of LSQHA has been analysed and verified using freeware antenna modeller and simulation software [198-200]. Figure 6.2 depicts the simulation logic and design architecture with the GA driver and the NEC-2 program.

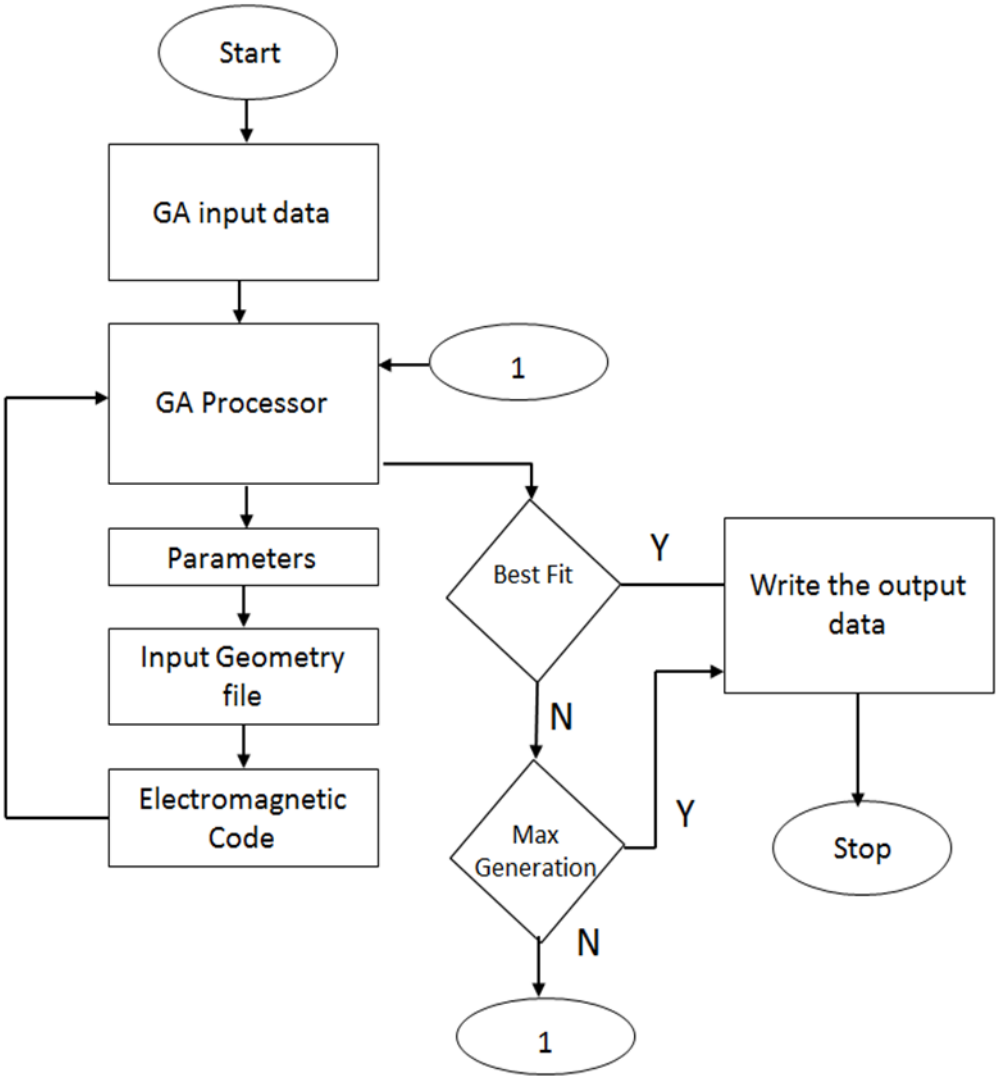

Figure 6.2: Simulation Logic and Design Architecture of the GA.

A table of the optimised parameter specification for the proposed antenna based on figures obtained from the GA solver for the LSQHA is as presented in Table 6.1

Table 6.1: Optimized GA design parameters LSQHA.

GA specified Parameters		**LSQHA optimised parameters (m)**			
	Initialisation inputs		**Lower threshold**	**Upper threshold**	**Best fit**
Sample size	15	Distance of pitch	0.00033	0.00721	0.00558
Parent count	5	Axial dimension	0.0045	0.010	0.00885
Probability of mutation	0.02	Helix radius (Top)	0.001	0.0035	0.0035
Maximum species	250	Helix radius (underside)	0.001	0.0035	0.00342
Probability of crossover	0.48	Linear separation between elements	0.0035	0.007	0.00501
Creep probability	0.004	Wire radius	0.0048	0.0048	0.0048
Number of occurrences	32768	Distance above ground	0.001	0.001	0.001

6.5 LSQHA SIMULATION RESULTS AND DISCUSSION

Evidently, the overall profile of the optimal design of LSQHA shows the effectiveness of the compactness achieved by employing the logic and architecture illustrated in Figure 6.2. In contrast to the conventional QHA design (See Figure 6.1a); the LSQHA was configured to have its helical elements more closely fitted together in volume and space. The LSQHA offers a robust solution particularly in the dimensions of its surface area, while retaining optimal axial ratio and beam width. Critical analysis of the performance of the optimal LSQHA was conducted to cross analyse the bandwidth, axial ratio coverage and gain performances of the realised design. From results obtained, LSQHA is found to have an optimum axial length of 8.85cm. The VSWR of the LSQHA at the input port was computed using an electromagnetic modelling software package [174] and evaluated to be 1.39 at the EPC Global RFID Tag/Reader frequency of 900 MHz. Other associated outcomes are given in Figure 6.3a. As observed, the optimised design clearly exhibits proper matching of impedances covering a considerable range of frequencies. A slight shift in the resonant frequency from 900 MHz to 890 MHz was observed as evident in the return loss characterisation detailed in Figure 6.3b. The nature of the ground plane adopted in this study is suggested to be largely responsible for this trait.

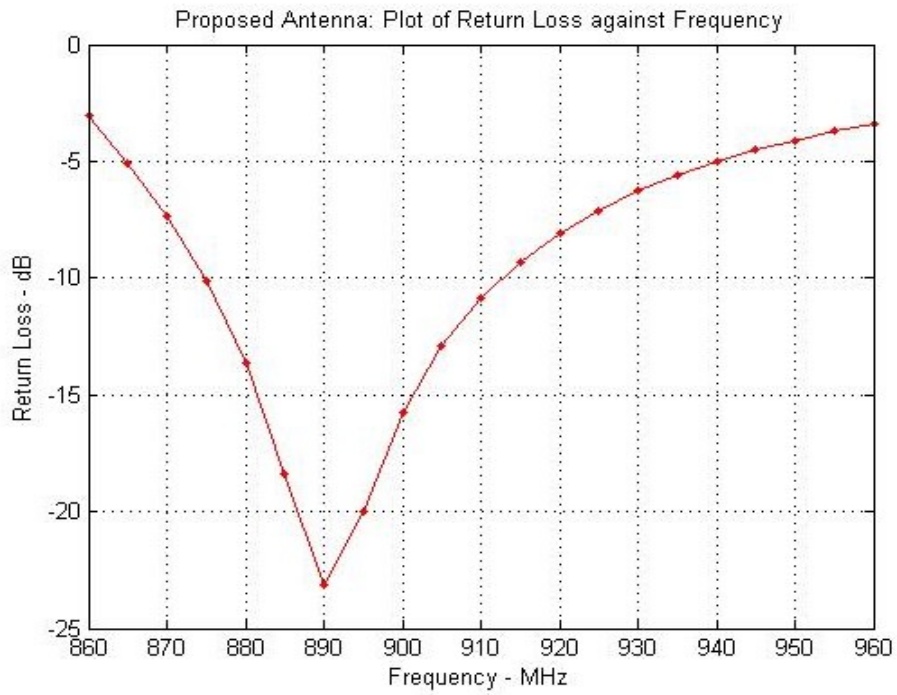

(a)

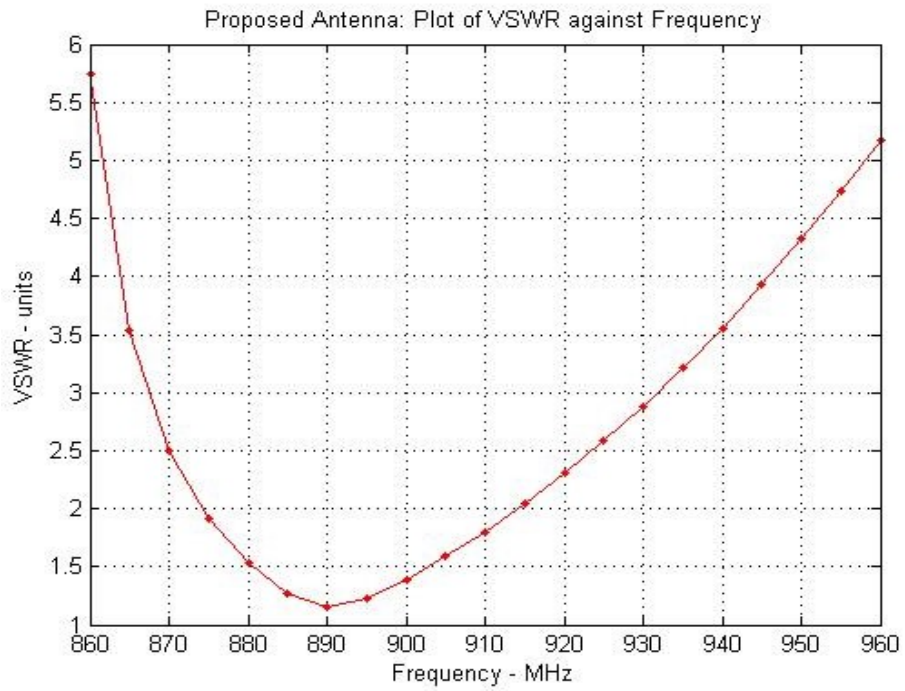

(b)

Figure 6.3: (a) Computed VSWR for the proposed LSQHA; (b) Computed Return Loss for the proposed LSQHA

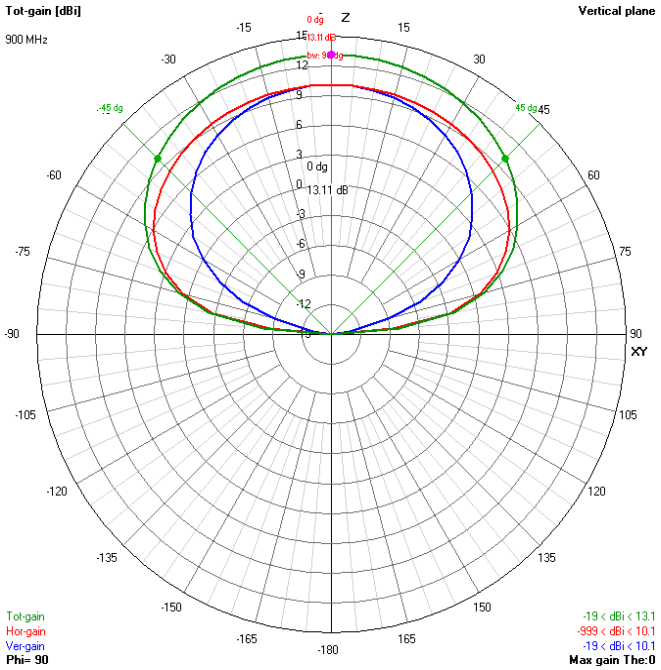

(a)

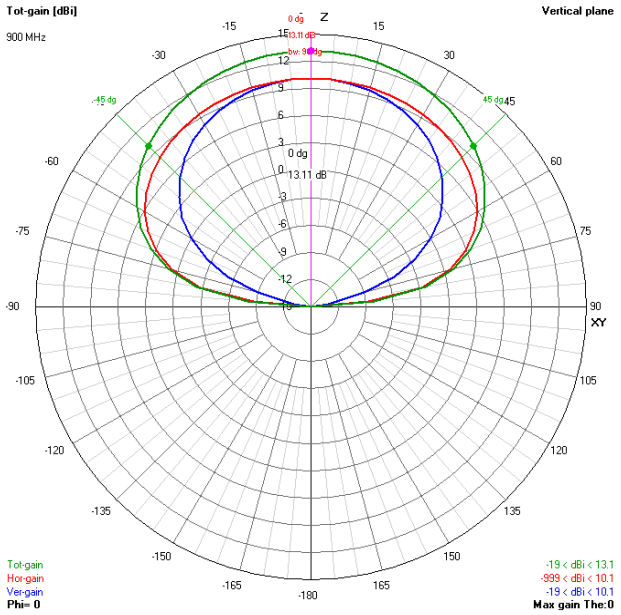

(b)

Figure 6.4: LSQHA Radiation Patterns from two perspectives

(a) Φ=0° and (b) Φ=90°

As depicted in Figure 6.3b, the return loss performance at the deployed frequency of application is less than -20 dB which is acceptable for the intended application.

Figure 6.4a and Figure 6.4b depict the measured power gain radiation characteristics of LSQHA at an operating frequency of 900 MHz. The results clearly show an elevation angle range of approximately ± 45° with an axial ratio of less than 3dB.

Also, the proposed LQHSA revealed a total forward isotropic gain of 13.1 dBi. Figure 6.5 depicts the circular radiation pattern obtained from simulation results of the LSQHA which perfectly meets the requirements for its use as an RFID reader antenna.

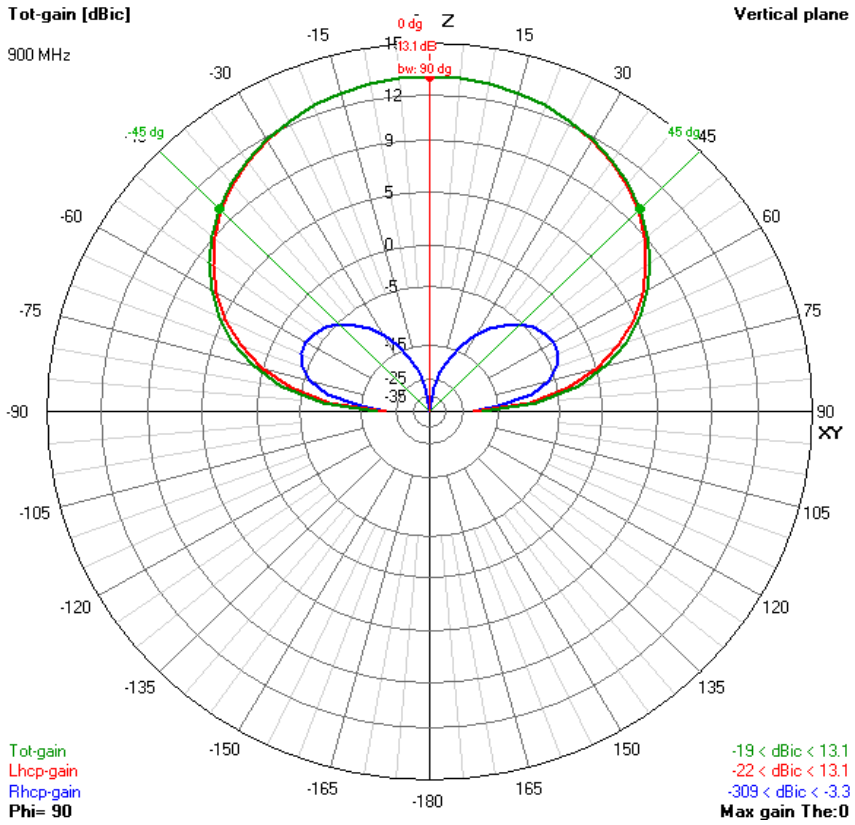

Figure 6.5: Computed circular polarisation patterns (left hand and right hand) for the proposed antenna

6.6 CONCLUSION

A comprehensive analysis and studies of previous approaches to RFID readers and various antenna designs using genetic algorithm was explored and presented earlier in the literature. The work presented here focuses on the optimum size, quality, polarisation of reader and various other types of antenna realisation and the effectiveness of GA at optimizing and selection of best geometry for each of the proposed designs. The GA tool was also explored as the one of the best tools for optimisation of antenna geometry for any range of intended frequency of application, as shown from the various extensive studies presented. The GA converges faster compared to the time other simulation platforms take to obtain results. The results of optimisation of parameters in GA give rise to more compact geometries which form an important basis for the miniaturisation of previous antenna solutions. The impact GA brings to the RF and electromagnetic antenna solutions cannot be over emphasised as this tool has been employed by leading manufacturers in the industry for more efficient and cost effective mass production of realised antenna designs. The working principles of the spiral and helical antenna were presented and a justification was given on their suitability for adoption for reader antenna design based on their radiation characteristic, design simplicity and cost effectiveness.

A novel circularly polarized LSQHA with a high forward isotropic gain and VSWR specifications desirable in RFID applications has been proposed and presented. The proposed antenna is intended for deployment in RFID systems, as the reader or interrogator antenna, where the orientation and polarisation of the associated tag antennas cannot be precisely predicted. The novel antenna has been named the

'Linearly-Shifted Quadrifilar Helical Antenna' (LSQHA). The antenna realisation presented was achieved using Genetic Algorithm method which has been well appreciated and showcased, the specified objective being deployment for liquid level sensing applications within the RFID global bandwidth of (860 - 960) MHz. The radiation characteristic of the optimal structure obtained was cross analysed using 4NEC-2. The results confirm the proposed antenna has a 3 dB beam width of 90° with a resonant frequency at about 890 MHz and an acceptable gain of 13.1dBi at 900 MHz. The optimal design reached was found to be compact and of an excellent profile. These results show that the proposed antenna can easily be configured to sample commercial RFID readers or interrogators. On the whole, Genetic Algorithm global optimisation method has also proved its strength and ingenuity in fast and optimal solutions to electromagnetic design problems.

The practical implementation of the design is recommended for future work and improvement in terms of developing it into a dual band antenna with terrestrial and satellite communication capabilities for global tracking of tagged objects.

CHAPTER 7

CONCLUSION AND FUTURE WORK

7.1 CONCLUSION

This research main focus is hinged on the design, modelling, analysis and characterisation of passive UHF RFID tags deployed for liquid level sensing applications. The liquid level measurement challenge and previous technologies deployed in an attempt to resolve these challenges has been identified and discussed. This forms a basis for the presentation of a novel RFID based sensing technique for various liquid level sensing applications. RFID system achitecture, history and tag types are discussed and presented. A justification for the selection of passive tags considered for this research work is also presented.

Four passive tag geometries are realised, with a comprehensive parametric analysis of the rectangular tag presented; the basic geometry attributes influencing the general performance of the tag was identifed and explored for optimum parameter setting in a view to obtaining an optimized design. Particular emphasis is laid on the improvement of the basic radiation characteristics of both reader and tag antennas taking the impacts of environmental factors into consideration. The realised tags geometries were explored to see what effects different types of surfaces had on their radiation characteristic when mounted. Metallic ground and non metalic mounting were adopted for tag practical realisation and characterisation.

The prototype print out of the tags were tested in laboratory with the network analyser to obtain details for comparison of theoretical results. The tags were mounted with the Alien chip and physical detection range measurements were made. The RFID tag and reader antennas have been designed to operate in circular polarization. They have also been deployed for energy efficient gully pot monitoring, and automatic liquid level detection applications. The Alien RFID system set up was used to observe the results of the liquid sensing for which the designed antennas were deployed.

The entire system set up was successfully modeled in HFSS and the signal coupling between the sensor tags and reader was observed. The results show a satisfactory reflection coefficient that will guarantee a successful operation when deployed as liquid level sensors. The observed reflection coefficient for all the tag realisation was less than -20dB in the UHF band (800 - 900) MHz.

Different types of subtrates was analysed to see the effects the would have on the optimum tag radiation characteristics. Epoxy (fr4) based substrate was used all through all the design process, it was found that subtrate materials with a higher relative permitivity had significant effects on the gain of the tag.

A dual-band folded planar loop antenna for a partiall-underground utility sensing application has been presented and examined theoretically and experimentally. The results show that the antenna prototype exhibits sufficient impedance bandwidth, suitable radiation characteristics, and adequate gains for the required underground wireless sensor applications.

The reader counterpart has been obtained using GA in combination with the NEC-2 software with FORTAN compiler. The physical measurements were compared to match the theoretical simulation results. The design and optimisation of a LSQHA reader's antenna using GA has also been presented. A detailed account of previous works on GA and new ground breaking areas of applicability was also discussed. This research work has opened wider perspectives to help understand and appreciate the full design elements and considerations for RFID systems particularly when deployed for liquid level sensing applications. The work presented here has clearly demonstrated that liquid level information can be effectively and reliably communicated in a cost effective and energy efficient way using RFID technology.

7.2 RECOMMENDATION FOR FUTURE WORK

RFID systems have found increasing popularity across a lot of applications. Great potentials lay ahead for RFID focused research applications, particularly in the areas of remote automation and control. A lot of applications are increasingly deploying RFID technology because of its flexibility of deployment as a part of an existing network. Future research studies will therefore be geared towards the deployment of RFID technology to IT infrastructure for automated control and monitoring purpose.

The research work presented, has been able to identify the signal attenuation issues which impair the performance of RFID tags as they are deployed for liquid level sensing applications. In a view to build upon the findings of the current work, the future work recommendations are as enumerated below:

- Further simulation can consider the modeling of tags and reader antenna with the aim of achieving improved radiation characteristics.
- Tags with better memory chip capacity can be deployed to analyze their energy saving capabilities in comparison to chipless tags.
- Design and modeling of reader antenna with improved directivity for better (1 meter and above) read distance.
- The effect of different substrate types on the performance of the tags can be critically analysed with the aim of developing hybrid substrate for improved tag performance over a wider range of frequencies.
- Parametric studies on the survivability of tags in different changing environmental conditions can be studied and fully analysed as a basis for a novel quality test technique for Passive RFID tags.
- The design optimisation results can be compared and subjected to a performance analysis studies with results of other optimisation algorithms to see the rate of convergence and establish which of the combination of the software platform produces the best design optimisation.
- Building a prototype for oil pipeline monitoring system with the integration of a solar powered RFID reader with hybrid networking (Satellite-4GLTE-WiMax-WiFi) capabilities.
- Novel tag deployment for patient mobility monitoring, indoor localization and intelligent transportation applications.

REFERENCES

1. A. Kalayci, “Design of a Radio Frequency Identification (RFID) Antenna,” MSc thesis, Department of Electrical and Electronic Engineering, Middle East Technical University, 2009.
2. Y. Zuo, “Survivable RFID Systems: Issues, Challenges and Techniques”, *IEEE Trans. on Systems, Man, and Cybernetics*—Part C: Applications and Reviews, vol.40, no.4, pp. 406-418, July 2010.
3. K. Fyhn, R. M. Jacobsen, P. Popovski, A. Scaglione, and T. Larsen, "Multipacket reception of passive UHF RFID tags: A communication theoretic approach," *IEEE Transactions on Signal Processing,* vol. 59, pp. 4225-4237, 2011.
4. P. D’Arcy and A. De Santi’s, "On ultra-lightweight RFID authentication protocols," *IEEE Transactions on Dependable and Secure Computing,* vol. 8, pp. 548-563, 2011.
5. S. Garfunkel and B. Rosenberg, RFID: applications, security, and privacy. Addison Wesley, 2006.
6. C. R. Medeiros, J. R. Costa, and C. A. Fernandes, "RFID reader antennas for tag detection in self-confined volumes at UHF," *IEEE Antennas and Propagation Magazine*, vol. 53, pp. 39-50, 2011.
7. E.Vahedi, V. Shah-Mansouri, V. W. S. Wong, I. F. Blake, and R. K. Ward, "Probabilistic analysis of blocking attack in RFID systems," *IEEE Transactions on Information Forensics and Security,* vol. 6, pp. 803-817, 2011.

8. V.Antti, Raisanen and A. Lehto, Radio Engineering for Wireless Communication and Sensor Application. Artech House, Boston, London, 2003.
9. I. Bahl, Lumped Elements for RF and Microwave Circuits. Artech House, INC, Boston, London, 2003.
10. W. A. Davis and K. K. Agarwal, Radio Frequency Circuit Design, John Wiley & Sons, INC., 2nd ed. New York, Chichester, 2001.
11. B.-S. Choi, J.-W. Lee, J.-J. Lee and K.-T. Park, "A hierarchical algorithm for indoor mobile robot localization using RFID sensor fusion," *IEEE Transactions on Industrial Electronics*, vol. 58, pp. 2226-2235, 2011.
12. Engheta, N., et al. (2005). "Circuit elements at optical frequencies: nano inductors, nano capacitors, and nano resistors." Physical Review Letters **95**(9): 095504.
13. L. Sang-Do, M. Shin and K. Hyoung-Jun, "EPC vs IPv6 mapping mechanism", presented at *ICACT2007, ICACT, Korea*, Feb. 2007, pp.1243-1245.
14. Y. Tikhov and J. H. Won, "Impedance-matching arrangement for microwave transponder operating over plurality of bent installations of antenna," Electronics Letters, vol. 40, pp. 574-575, 2004.
15. J. D. Krarus and R. J. Marhefka, Antennas for all applications. McGraw-Hill Higher Education, New York, 3rd ed., 2002.
16. W. C. Gibson, the Method of Moments in Electromagnetics. Taylor & Francis Group, LLC, the United States of America, 2008.
17. T. M. Millington and N. J. Cassidy, "Improving the accuracy of FDTD approximations to tangential components of the coupled electric and magnetic

fields at a material interface," *IEEE Transactions on Antennas and Propagation,* vol. 59, pp. 2924-2932, 2011.

18. Hambrice, K. (2004). "A dozen ways to measure fluid level and how they work." Sensors **21**(12): 14-20.
19. Ibeh, S. U., and S. E. Nnakaihe. "Challenges and Prospects of the Use of Horizontal Directional Drilling Techniques for Laying Oil and Gas Pipelines in Nigeria." *SPE Nigeria Annual International Conference and Exhibition*. Society of Petroleum Engineers, 2016.
20. E. Vahedi, V. Shah-Mansouri, V. W. S. Wong, I. F. Blake, and R. K. Ward, "Probabilistic analysis of blocking attack in RFID systems," *IEEE Transactions on Information Forensics and Security*, vol. 6, pp. 803-817, 2011.
21. V.Antti, and A. Lehto, Radio Engineering for Wireless Communication and Sensor Application, Artech House, Boston, London, 2003.
22. R. J. Marhefka and D. D. Kraus, Antennas for all applications, 3rd Ed. New York, McGraw-Hill, 2002.
23. L. Harvey, RFID Design Principles. USA: Artech House, Inc., 2008.
24. B. Glover and H. Bhatt, RFID Essentials. Beijing, Farnham, CA: O'Reilly, Jan. 2006.
25. J. Landt, "The history of RFID," IEEE Potentials, vol. 24, pp. 8-11, 2005.
26. L.O. Gorman and T. Pavlidis, "Auto ID technology: from barcodes to biometrics", *IEEE Robotics & Automation Magazine*, vol. 6, no. 1, pp. 4-6, March 1999.
27. J. Swartz, "The growing 'magic' of automatic identification", *IEEE Robotics & Automation Magazine*, vol. 6, no. 1, pp. 20-23, 56, March 1999.

28. K. Finkenzeller, RFID handbook: fundamentals and Applications in Contact less Smart Cards and identification. Chichester, England, Hobbken, N.J. Wiley, 2003.

29. S. Garfinkel and B. Rosenberg, RFID: applications, security, and privacy. Addison-Wesley, 2006.

30. H. M. Sun and W. C. Ting, "A Gen2-based RFID authentication protocol for security and privacy," *IEEE Transactions on Mobile Computing*, vol. 8, pp. 1052-1062, 2009.

31. Y. Tikhon and J. H. Won, "Impedance-matching arrangement for microwave transponder operating over plurality of bent installations of antenna," Electronics Letters, vol. 40, pp. 574-575, 2004.

32. J. A. Rodriguez-Rodriguez, M. Delgado-Restituto, J. Masuch, A. Rodriguez-Perez, E. Alarcon, and A. Rodriguez-Vazquez, "An ultralow-power mixed-signal back end for passive sensor UHF RFID transponders," *IEEE Transactions on Industrial Electronics*, vol. 59, pp. 1310-1322, 2012.

33. P. Wei, W. Che, Z. Bi, C. Wei, Y. Na, L. Qiang, and M. Hao, "High-efficiency differential RF front-end for a Gen2 RFID tag," *IEEE Transactions on Circuits and Systems II: Express Briefs*, vol. 58, pp. 189-194, 2011.

34. R. A. Abd-Alhameed, D. Zhou, Y. Ma, M. S. Alkhambashi, C. H. See, M. M. Abusitta, and P. S. Excell, "Equal-spaced rectangular meander-line antenna RFID tag design for UHF band," in *3rd International Conference on Internet Technologies and Applications*, ITA 09, September 8, 2009 - September 11, 2009, Wrexham, Wales, United Kingdom, 2009, pp. 426-430.

35. J. W. Lee and B. Lee, "Design of high-Q UHF radio-frequency identification tag antennas for an increased read range," *IET Microwaves, Antennas and Propagation,* vol. 2, pp. 711-717, 2008.

36. J. Ryoo, J. Choo, and H. Choo, "Novel UHF RFID tag antenna for metallic foil packages," *IEEE Transactions on Antennas and Propagation*, vol. 60, pp. 377-379, 2012.

37. N. Konstantinou, "Expowave: An RFID Anti-Collision Algorithm for Dense and Lively Environments", *IEEE Trans. on Communications*, vol.60, no.2, pp.352-356, Feb. 2012.

38. Y. Zuo, "Survivability experiment and attack characterisation for RFID" *IEEE Transactions on Dependable and Secure Computing,* vol. 9, pp. 289-302, 2012.

39. H. B. Chung, H. Mo, N. Kim, and C. Pyo, "An advanced RFID system to avoid collision Of RFID reader, using channel holder and dual sensitivities," Microwave and Optical Technology Letters, vol. 49, pp. 2643-2647, 2007.

40. L. Kang, K. Wu, J. Zhang, H. Tan, and L. M. Ni, "DDC: A novel scheme to directly decode the collisions in UHF RFID systems," *IEEE Transactions on Parallel and Distributed Systems*, vol. 23, pp. 263-270, 2012.

41. A. Khambashi, M. Salim, A. Raed and R.S.Haileselasi "Analysis and solutions for RFID tag and RFID reader deployment in wireless communications applications. Simulation and measurement of linear and circular polarized RFID tag and reader antennas and analyzing the tags radiation efficiency when operated close to the human body", University of Bradford, 2014.

42. X. Qing and Z. N. Chen, "Proximity effects of metallic environments on high frequency RFID reader antenna: Study and applications" *IEEE Transactions on Antennas and Propagation,* vol. 55, pp. 3105-3111, 2007.

43. J. Gao, J. Siden and H. Nilsson, “Printed Electromagnetic Coupler with an Embedded Moisture Sensor for Ordinary Passive RFID Tags” *IEEE Electron Device Letters*, vol.32, no.12, pp. 1767-1769, Dec. 2011.

44. S.-L. Chen, K.-H. Lin, and R. Mittra, "A measurement technique for verifying the match condition of assembled RFID tags," *IEEE Transactions on Instrumentation and Measurement,* vol. 59, pp. 2123-2133, 2010.

45. Alien Technology Corp., Morgan Hill CA, USA. Available: http://www.alientechnology.com, 2008.

46. B.S. Choi, J.-W. Lee, J.-J. Lee, and K.-T. Park, "A hierarchical algorithm for indoor mobile robot localization using RFID sensor fusion″ *IEEE Transactions on Industrial Electronics*, vol. 58, pp. 2226-2235, 2011.

47. R. Suwalak, C. Phongcharoenpanich, and D. Torrungrueng, "Chipped and chipless RFID sensors for quality monitoring of light weight concrete using the radar equation," in *Electrical Engineering/Electronics, Computer, Telecommunications and Information Technology (ECTI-CON), 2016 13th International Conference on*, 2016, pp. 1-4.

48. K. Belsey, A. Parry, C. Rumens, M. Ziai, S. Yeates, J. C. Batchelor*, et al.*, "Switchable disposable passive RFID vapour sensors from inkjet printed electronic components integrated with PDMS as a stimulus responsive material," *Journal of Materials Chemistry C,* vol. 5, pp. 3167-3175, 2017.

49. C.H. See, K.V. Horoshenkov, R.A. Abd-Alhameed, Y.F. Hu and S.J. Tait, A Low Power Wireless Sensor Network for gully Pot Monitoring in Urban Catchments, *IEEE Sensors Journal*, vol.12, no. 5, pp.1545-1553, May 2012.

50. Fabre, Arthur, et al. "Deploying a 6LoWPAN, CoAP, low power, wireless sensor network." (2016).

51. Nesbitt, Pamela A., Jake Palmer, and Donnie Smith. "Combined sewer overflow warning and prevention system." U.S. Patent No. 9,631,356. 25 Apr. 2017.

52. A. Darehshoorzadeh and A. Boukerche, "Underwater sensor networks: A new challenge for opportunistic routing protocols," *IEEE Communications Magazine,* vol. 53, pp. 98-107, 2015.

53. N. Nasri Kachouri, A. Andrieux, Communications, Computing and Control Applications (CCCA), International Conference "New approach for wireless underwater identification: Acoustic Frequency Identification (AFID)", Page(s): 1 – 6, 2011.

54. R. Imura, "Driving ubiquitous Network-How can RFID solutions meet the customer's expectations", *10th International Conference on emerging technologies and factory automation Italy*, Page(s) 4-6, 2005.

55. Y. Z. Zhao; O. P. Gan, "Distributed design of RFID network for large-scale RFID deployment", *4th IEEE International conference on industrial informatics*, 2006.

56. J. Siden et al. (2007). Remote moisture sensing utilizing ordinary RFID tags. Sensors, 2007 IEEE.

57. S. Karuppuswami, et al. (2016). RFID Compatible Sensor Tags for Remote Liquid Sample Interrogation. Electronic Components and Technology Conference (ECTC), 2016 IEEE 66th, IEEE.

58. D. H. Paul, D. Leigh, and S. William Yerazunis. "Wireless liquid level sensing for restaurant applications." *Sensors, 2002. Proceedings of IEEE*. Vol. 1. IEEE, 2002.

59. Lobato-Morales, Humberto, Alonso Corona-Chavez, and Jose L. Olvera-Cervantes. "Planar sensors for RFID wireless complex-dielectric-permittivity sensing of liquids." Microwave Symposium Digest (IMS), 2013 IEEE MTT-S International. IEEE, 2013.

60. Sauer, Sebastian, and Wolf-Joachim Fischer. "An Irreversible Single-Use Humidity-Threshold Monitoring Sensor Principle for Wireless Passive Sensor Solutions." *IEEE Sensors Journal* 16.18 (2016): 6920-6930.

61. Zhu, Jixuan, Bo Tao, and Zhouping Yin. "A Customized RFID-Based Sensor System for Intelligent Oilwell." *IEEE Sensors Journal* 16.13 (2016): 5426-5432.

62. Holler, Gert, Michael J. Moser, and Hubert Zangl. "Monitoring of freezing processes in liquid nitrogen by means of passive RFID through container walls." *Instrumentation and Measurement Technology Conference* (I2MTC), IEEE, 2011.

63. Bhattacharyya, Rahul, C. Floerkemeier, and S. Sarma. "RFID tag antenna based sensing: Does your beverage glass need a refill?" RFID, 2010 *IEEE International Conference on. IEEE, 2010.*

64. Zarifi, M. Hossein, and M. Daneshmand."High-Resolution RFID Liquid Sensing Using a Chipless Tag." IEEE Microwave and Wireless Components Letters 27.3 (2017): 311-313.

65. R. Stefanelli and D. Trinchero, "Customized experimental test set for characterization and calibration of RFID tags in liquids," in *RFID-Technologies and Applications (RFID-TA), 2011 IEEE International Conference on*, 2011, pp. 148-151.

66. Zhao, Hongran, et al. "Organic-inorganic hybrid materials based on mesoporous silica derivatives for humidity sensing." Sensors and Actuators B: Chemical 248 (2017): 803-811.

67. Yu, Bo, et al. "Microstrip line based sub-THz interconnect for high energy-efficiency chip-to-chip communications." Radio-Frequency Integration Technology (RFIT), 2016 *IEEE International Symposium on. IEEE, 2016.*

68. OFWAT, "The Development of the Water Industry in England and Wales," 2015 [Online]. Available: http://www.ofwat.gov.uk/wp-content/uploads/2015/11/rpt_com_devwatindust270106.pdf.

69. J.P. Davies, B.A. Clarke, et al, "A statistical investigation of structurally unsound sewers," Underground Infrastructure Research Industrial and Environmental Applications, pp. 125-131, 2001.

70. E. Ana, W. Bauwens, M. Pessemier, et al., "An investigation of the factors influencing sewer structural deterioration," Urban Water, vol.6, no.4, pp. 303-312, 2009.

71. S. Zhang and H. Zhang, "A Review of Wireless Sensor Networks and its Applications," IEEE international conference on Automation and Logistics (ICAL), pp.386-389, 2012.

72. X. Tan, Z. Sun and I.F. Akyildiz, “Wireless Underground Sensor Network: MI-based communication systems for underground applications,” IEEE Antennas & Propagation Magazine, vol.57, no.4, pp.74-87, 2015.

73. Ram, Kondamudi Siva Sai, and A. N. P. S. Gupta. "IoT based Data Logger System for weather monitoring using Wireless sensor networks." International Journal of Engineering Trends and Technology (IJETT)–Volume 32 (2016). D.

74. Trinchero and R. Stefanelli, “Microwave Architectures for Wireless Mobile Monitoring Networks inside Water Distribution Conduits,” IEEE Trans Microwave Theory and Techniques, vol.57, no.12, pp.3298-3306, 2009.

75. M.D. Bedford and G.A. Kennedy, “Evaluation of ZigBee (IEEE 802.15.4) Time-of-Flight-Based Distance Measurement for Application in Emergency Underground Navigation”, IEEE Trans. Antennas and Propagation, vol.50, no.5, pp.2502-2510, April 2012.

76. C.H. See, R.A. Abd-Alhameed, D. Zhou, Y.F Hu and K.V Horoshenkov “Measure the Range of Sensor Network”, Microwaves & RF, vol. 54, no.10, pp.69-76, Oct. 2008.

77. C. Zhou, T. Plass, R. Jacksha and J. A. Waynert, “RF Propagation in Mines and Tunnels,” IEEE Antennas & Propagation Magazine, vol.57, no.4, pp.88-102, 2015.

78. A. Ando, T. Ito, H. Tsuboi and H. Yoshioka, “Propagation Loss, XPR and Height Pattern Characteristics on Road from Antenna Set in Manhole,” IEEE Antennas and Propagation Society International Symposium (APSURSI), pp.1-4, 2010.

79. A. Ando, T. Ito, H. Yoshioka, H. Tsuboi and H. Nakamura, “Effects of Receiver Antenna Height and Polarization on Received Signal Levels at Road

Level from Transmitter Antennas Set in Manhole," IEEE International Symposium on Antennas and Propagation (APSURSI) , pp.2399-2402, 2011.

80. S. Mizushina, A. Adachi and T. Watanabe, "Radiation from an antenna in manhole," Asia-Pacific Microwave Conference (APMC), 2052-2055, 2006.
81. A.S. Kesar and E. Weiss, "Wave Propagation between buried Antennas", *IEEE Trans. Antennas and Propagation,* vol.61, no.12, pp.6153-6156, April 2013.
82. J.F. Mastarone and W.J. Chappell, "Urban Sensor Networking Using Thick slots in Manhole covers," IEEE Antennas and Propagation Society International Symposium, pp.779-782, 2006.
83. S. Jeong, D. Ha, M.M. Tentzeris, "A Cavity-backed Slot Antenna with High Upper Hemisphere Efficiency for Sewer Sensor Network," IEEE Antennas and Propagation Society International Symposium (APSURSI), pp.49-50, 2013.
84. S.Jeong, C-L. Yang, J.R. Courter, S. Kim, R.B. Pipes and W.J. Chappell, "Multilayer Composite for Below Ground Embedded Sensor Networking," IEEE Antennas and Propagation Society International Symposium, pp.1-4, 2008.
85. S.Jeong and W.J. Chappell, "Adaptive composite antennas for a city-wide sensor network," IET Microwaves. Antennas and Propagation, vol.4, no.11 pp-1916-1926, 2010.
86. T.W. Hertel and G.S. Smith, "The Conical Spiral Antenna over the Ground", IEEE Trans. Antennas and Propagation, vol.50, no.12, pp.1668-1675, December 2002.
87. D.Ghosh, H. Moon and T.K. Sarkar, "Design of through-the-earth mine communication system using helical antennas," IEEE Antennas and Propagation Society International Symposium, pp.1-4, 2008.

88. R.Y. Chao and K.S. Chung, “A Low Profile Antenna Array for Underground Mine Communication,” *Singapore ICCS '94. Conference Proceedings,* vol.2, pp.702-709, 1994.

89. W. Tang, Y. Hao, “Cloak on Underground Antenna Using Transformation Electromagnetics,” IEEE International Symposium on Antennas and Propagation (APS/URSI), pp.2865-2868, 2011.

90. G. Pandey, R. Kumar and R.J. Weber, “A low profile, low-RF band, small antenna for underground, in-situ sensing and wireless energy-efficient transmission, IEEE 11th International Conference on Networking, Sensing and Control (ICNSC), pp.179-184, 2014.

91. P. Soontornpipit, C.M. Furse, Y.C. Chung and B.M. Lin, “Optimisation of a Buried Microstrip Antenna for Simultaneous Communication and Sensing of Soil Moisture”, IEEE Trans. Antennas and Propagation, vol.54, no.3, pp.797-800, 2006.

92. D. S. Linden, “Automated design and optimisation of wire antennas using genetic algorithms,” PhD thesis, MIT, Cambridge, MA, Sept. 1997.

93. H. Choo, A. Hutani, L. C. Trintinalia, and H. Ling, “Shape optimisation of broadband micro strip antennas using genetic algorithm,” Electron. Lett, vol. 36, no. 25, pp. 2057–2058, Dec. 2000.

94. F. Villegas, T. Cwik, Y. Rahmat-Samii, M. Manteghi, “A parallel electromagnetic genetic-algorithm optimisation (EGO) application for patch antenna design*,” IEEE Trans. Antennas Propagation*., vol. 52, no. 9, September 2004.

95. A. Kerkhoff, R. Rogers, and H. Ling, “The use of the genetic algorithm approach in the design of ultra-wideband antennas,” in Proc. IEEE Radio and Wireless Conf., Aug. 2001, pp. 93–96.

96. L. Merad, F. T. Bendimerad and S. M. Meriah, “Genetic algorithm optimisation for circular micro strip antenna,” ITG, INCA, Berlin on September 17-18-19, 2003.

97. Goldberg, D. E.: Genetic algorithm search, optimisation and machine learning: Addison-Wesley, 1994.

98. A. A. Lofti Neyestanak, F. H. Kashani, and K, Barkeshli, “E-shaped patch antenna design based on genetic algorithm using decision fuzzy rules*,” Iranian Journal of Electrical and Computer Engineering*, vol. 4, no. 1, 2005.

99. R. Matouek, Realization of Fuzzy-Adaptive Genetic Algorithms in a Matlab Environment, Institute of Automation and Computer Science, Brno University of Technology, 2001.

100. Y. Zhang, W. Q. Malik, “Analogue filter tuning for antenna matching with multiple objective particle swarm optimisation,” *IEEE Symposium on Advances in Wires and Wireless Communication,* pp. 196-198, 2005.

101. M. Thompson, J.K. Fidler, “A Novel Approach for Fast Antenna Tuning using Transporter based Simulated Annealing”, Electronic Letters, Vol. 36 No. 7, 2000.

102. M. Thompson, Application of Multi Objective Evolutionary Algorithms to Analogue Filter Tuning. EMO 2001, pp. 546-559.

103. A. J. Kerkhoff and H. Ling, “Design of a band-notched planar monopole antenna using genetic algorithm optimisation,” *IEEE Transaction on Antennas and Propagation,* vol. 55, no. 3, pp. 604-610, March 2007.

104. A. Kerkhoff and H. Ling, “Design of a planar monopole antenna for use with ultra-wideband (UWB) has a band-notched characteristic,” in IEEE AP/S Int. Symp. Dig., Columbus, OH, Jun. 2003, vol. 1, pp. 830–833.

105. H. Schantz, G. Wolenec, and E. Myszka, “Frequency notched UWB antennas,” in Proc. IEEE Conf. Ultra-Wideband Syst. Technology., Nov. 2003, pp. 214–218.

106. A. Kerkhoff and H. Ling, “A parametric study of band-notched UWB planar monopole antennas,” in IEEE AP/S Int. Symp. Dig., Monterey, CA, Jun. 2004, vol. 2, pp. 1768–1771.

107. Y. Kim and D. Kwon, “CPW-fed planar ultra-wideband antenna having a frequency band notch function,” Elect. Lett, vol. 40, no. 7, pp. 403–405, 2004.

108. J. Qiu, Z. Du, J. Lu, and K. Gong, “A band-notched UWB antenna,” Microw. Opt. Tech. Lett., vol. 45, no. 2, pp. 152–154, 2005.

109. W. Lee, W. Lim, and J. Yu, “Multiple band-notched planar monopole antenna for multiband wireless system,” IEEE Microw. Wireless Compon. Lett, vol. 15, pp. 576–578, Sep. 2005.

110. S. Rogers, C. Butler, and A. Martin, “Design and realization of GA-optimized wire monopoles and matching network with 20:1 bandwidth,” IEEE Trans. Antennas Propagation., vol. 51, pp. 493–502, Mar. 2003.

111. Y. Noh, Y. Kim, and H. Ling, “A broadband on-glass antenna with a mesh-grid structure for automobiles,” Elect. Lett, vol. 41, pp. 1148–1149, Oct. 2005.

112. A. Kerkhoff, R. Rogers, and H. Ling, “Design and analysis of planar monopole antennas using a genetic algorithm approach,” IEEE Trans. Antennas Propagation., vol. 52, pp. 2709–2718, Oct. 2004.

113. J. Kim, T. Yoon, J. Kim, and J. Choi, “Design of an ultra-wide-band printed monopole antenna using FDTD and genetic algorithm,” IEEE Microw. Wireless Compon. Lett, vol. 15, pp. 395–397, Jun. 2005.

114. D. Zou, R. A. Abd-Alhameed, and P. S. Excel, “Design of antenna for wide harmonic suppression using adaptive meshing and genetic algorithm,” IET 7th International Conference on Computation in Electromagnetics, pp. 187–188, 2008.

115. T. Yamamoto, K. Fujimuri, M. Sanagi, S. Nogi, and T. Tsukagoshi, “Efficient antenna miniaturization technique by cut chromosome-length in genetic algorithm,” Asia Pacific Microwave Conference, pp. 1837–1840, 2009.

116. Z. Lukes, J. Lacik, and Z. Raida, “Novel ultra-wideband slot-line antenna designed by adaptive real coded genetic algorithm,” International Conference on Electromagnetics in Advanced Applications, pp. 682–685, 2009.

117. J. M. J. W. Jayasinghe, D. N. Uduwawala, “Design of broadband patch antennas using genetic algorithm optimisation,” International Conference on Industrial and Information Systems, pp. 60–65, 2010.

118. J. Chakraborty, U. Mukherjee, “Microstrip antenna optimisation using genetic algorithm optimisation,” International Conference on Computer and Communication Technology, pp. 635–640, 2010.

119. E. Eldervitch C. de Oliveira, A.G. D'Assunção and C.R.M. da Silva, “Optimisation of the input impedance of Koach triangular quasi-fractal antennas using genetic algorithm,” IEEE Conference on Electromagnetic Field Computation, pp. 1, 2010.

120. M. Ramesh and Y. KB, “Design Formula for Inset Fed Microstrip Patch Antenna”, *Journal of Microwaves and Optoelectronics*, Vol. 3, 2003.

121. C. Balanis, Antenna Theory: Analysis and Design, 2nd ed., Vol. 2. New York: Wiley, 1997.

122. Z. Adelpour, F. Mohajeri, and M. Sadeghi, "Dual-frequency micro strip patch antenna with modified koch fractal geometry based on genetic algorithm," Loughborough Antennas and Propagation Conference, pp. 401-404, 2010.

123. C. Borja and J. Romeu, "on the behaviour of Koch island fractal boundary micro strip patch antenna," IEEE Trans. on Antennas and Propagation, vol. 15, no. 6. June 2003.

124. F. Paredes, G. Zamora, J. Bonache, and F. Martin, "Dual-band impedance-matching networks based on split-ring resonators for applications in RF identification (RFID)", IEEE Trans. Microw. Theory Tech., vol.58, no.4, pp. 1159–1166, Apr. 2011.

125. S. Ahson and M. Ilyas, RFID Handbook, Applications, Technology, Security and privacy. Taylor &Francis Group LCC, 2008.

126. Y.K. Jung and B. Lee, "Dual-Band Circularly Polarised Microstrip RFID Reader Antenna Using Metamaterial Branch-Line Couple", IEEE Trans. on Antennas and Propagation, vol. 60, no. 2, pp. 786-791, Feb. 2012.

127. Hayward P., Sewerage: fairy tale spending, water and waste treatment 35(8), 30-31, 2002.

128. A. Denote, "The monopole-antenna: a practical snow and soil Wetness sensor", IEEE Trans. Geoscience and Remote Sensing,Vol. 35, Issue 5, pp. 1371 – 1375, Sept. 1997.

129. J. D. Griffin, G. D. Durgin, A. Haldi and B. Kippelen, "RF tag Antenna performance on various materials using radio link budgets", Antennas and Wireless Propagation Letters, Vol. 5, pp. 247 – 250, 2006.

130. D. M. Dobkin and S. M. Weigand, “Environmental effects on RFID tag antennas”, IEEE Int. Microwave Symp. 2005, pp. 135-138.

131. J. Sidén, H.-E. Nilsson, “Adaption to Background Material for Printed RFID Antennas”, In Proc. Antenn-06, Sweden, 2006.

132. F. Menke, R. Knochel, T. Boltze, C. Hauenschild, and W. Leschnik, “Moisture measurement in walls using microwaves”, IEEE Int.Microwave Symp. 1995, Vol. 3, pp. 1147 – 1150, 1995.

133. J. Sidén, Xuezhi Zeng, T.Unander, Andrey Koptyug, Hans-Erik Nilsson, “Remote Moisture sensing using ordinary RFID tags” IEEE sensors conference, 2007.

134. T. Hauschild, and F. Menke, “Moisture measurement in masonrywalls using a non-invasive reflectometer”, Electronics Letters, Vol.34, Issue 25, pp. 2413 – 2414, 1998.

135. Zhang; K.Yemelyanov; Xin Li; Moeness G. Amin “Effect of metallic objects and liquid supplies on RFID links” IEEE Antennas and Propagation Society International Symposium, 2009.

136. L. Chen, X. Dong, J. Han and P. Ye “Development of a ultrasonic instrument for the sealed container's liquid level measurement”, Proceedings of the Sixth World Congress on Intelligent Control and Automation (WCICA 2006), vol. 1, pp. 4972-4976, 2006.

137. C.W. Lai, Y.-L. Lo, J.-P. Yur and C.-H. Chuang, “Application of fiber Bragg grating level sensor and Fabry-Pérot pressure sensor to simultaneous measurement of liquid level and specific gravity”, vol. 12, no. 4, pp. 827-831, April, 2012.

137. H. Singh, S. Chakroborty, H. Talukdar, N. Singh and T. Bezboruah “A new nonintrusive optical technique to measure transparent liquid level and volume” vol. 11, no. 2, pp. 391-398, Feb., 2011.

138. H. Canbolat “A novel level measurement technique using three capacitive sensors for liquids” vol. 58, no. 10, pp. 3762-3768, Oct., 2009.

139. W. Liu, G. Xie and L. Yang “Research on high-precision real-time online measurement of liquid level changes “Proceeding of the WASE International Conference on Information Engineering (ICIE), vol. 1, page(s) 107-110, 2010.

140. C. P. Nemarich “Time domain reflectometry liquid levels sensors”vol. 4, no. 4, pp. 40-44, 2001.

141. M. Gerding, T. Musch and B. Schiek,“A novel approach for a high-precision multi-target-level measurement system based on time-domain reflectometry” vol. 54, no. 6, pp. 2768-2773, June, 2006.

142. E.Piuzzi, A. Cataldo and L. Catarinucci, “Enhanced reflectometry measurements of permittivity and levels in layered petrochemical liquids using an ‘in-situ’ coaxial probe” Measurement, vol. 42, no. 5, pp. 685-696, 2009.

143. A. Cataldo, G. Cannazza, N. Giaquinto, A. Trotta and G. Andria “Microwave TDR for real-time control of intravenous drip infusions” vol. 61, no. 7, pp. 1866-1873, July, 2012.

144. A.Cataldo, G. Cannazza, E. De Benedetto, N. Giaquinto and A. Trotta “Reproducibility analysis of a TDR-based monitoring system for intravenous drip Infusions: Validation of a novel method for flow-rate measurement in IV infusion”pp. 1-5, 2013.

145. S.D. Nawale; N.P. Sarawade, "RFID vapour sensor: Beyond identification sensing Technology (ICST), 2012 Sixth International Conference on Digital Object Identifier, Page(s): 248-253,2012

146. A. Nasir; S. Boon-Hee "Pipe Sense: A framework architecture for in-pipe water monitoring system" Communications (MICC), 2009 IEEE 9th Malaysia International Conference, Page(s): 703-708, 2009

147. G. Benelli; A. Pozzebon; D. Bertoni; G.Sarti; "An Analysis of the Performances of Low Frequency Cylinder Glass Tags for the Underwater Tracking of Pebbles on a Natural Beach" RFID Technology (EURASIP RFID), 2012 Fourth International EURASIP Workshop, Page(s): 72-77, 2012

148. N.Nasri, Kachouri, A. Andrieux, L. Samet, M. Communications, Computing and Control Applications (CCCA), 2011 International Conference " New approach for wireless underwater identification: Acoustic Frequency Identification (AFID)" Page(s): 1-6, 2011.

149. N.Skeie, S. Mylvaganam, and B. Lie. Using multi sensor data fusion for level estimation in a separator. 16th European Symposium on Computer Aided Process Engineering and 9th International Symposium on Process System Engineering W. Marquardt, C. Pantelides (Editors). Elsevier B.V, 2006.

150. K. Svehara. Development of an Air-oil and Oil-Water Interface Detector Using Plastic Optical Fiber and Its Application for Measurement of Oil Layer Thickness of Industrial Kitchen Wastewater in a Grease Trap. Journal of Chemical Engineering of Japan, pages 670-677, 2006.

151. R.Casanella; O. Casas and R. Pallas-Aren. Oil-water interface level sensor based on an electrode array. IEEE instrumentation and measurement technology conference proceedings, pages: 710-713, 2006.

152. S.Punan. Development and application of YSJ-1 type oil-water interface level gauge. Nuclear technology, page(s):641-644, 2003

153. M. Meribout, M. Habli, A. AI-Naamany and K. AI-Busaidi. A new ultrasonic-based device for accurate measurement of oil, emulsion, and water levels in oil tank. In Proc. of the 21th IEEE Instrumentation and Measurement Technology Conference, 2004.

154. L.Hua-yi and F. Shi-yu. Segmentation type capacitance sensor and its application. Chinese journal of sensors and actuators, page(s):196-198, 2006.

155. L.Chongxiang Research on measurement of Na level using inductive sensor. Nuclear Industry Automation, 1989 (4):19-23.

156. G.Ming, Z. Xuezhi. Eddy-current type molten steel level detection system for mold and its application. Metallurgical Industry Automation, 1994(4): 26-29.

157. L.Jian, D. Tianhuai, X. Yuzheng, Fu Zhibin. Modification of Differential Eddy Current Level Sensor and Its Application. Instrument Technique and Sensor, 2003(2): 12-14.

158. A.B.M. Ismail, K. Shida. Measurement of very low concentration of electrolytic solution by a novel contactless eddy-current sensor, IEEE transaction 1998.

159. R. Feick, H. Carrasco, M. Olmos, and H. D. Hristov, "PIFA input bandwidth enhancement by changing feed plate silhouette," Electron. Lett, vol. 40, pp. 921–922, Jul. 2004.

160. J. H. Holland, "Genetic algorithms," *Scientific American,* vol. 267, pp. 66-72, 1992.

161. J. M. Johnson and Y. Rahmat-Samii, “Genetic algorithm optimisation for aerospace electromagnetic design and analysis,” in Proc. IEEE Aerospace Applications Conf., Feb. 1996, pp. 87–102.

162. J. M. Johnson. Rahmat-Samii, “Genetic algorithms and method of moments (GA/MOM) for the design of integrated antennas,” IEEE Trans. Antennas Propagation., vol. 47, pp. 1606–1614, Oct. 1999.

163. D. P. Jones, K. F. Sabet, J. Cheng, L. P. B. Katehi, K. Sarabandi, and J. F. Harvey, “An accelerated hybrid genetic algorithm for optimisation of electromagnetic structures,” in Proc. IEEE Antennas and Propagation Soc. Int. Symp. Dig., July 1999, pp. 426–429.

164. L. Alatan, M. I. Aksun, K. Leblebicioglu, and M. T. Birand, “Use of computationally efficient method of moments in the optimisation of printed antennas,” IEEE Trans. Antennas Propagation., vol. 47, pp. 725–732, Apr. 1999.

165. R. M. Edwards and G. G. Cook, “Design of printed spiral antennas using a moment method running under a genetic algorithm optimisation routine,” in Proc. IEEE Seminar Practical Electromagnetic Design Synthesis, Feb. 1999, pp. 61–65.

166. R. Zentner, Z. Sipus, and J. Bartolic, “Optimum synthesis of broadband circularly polarized micro strip antennas by hybrid genetic algorithm,” Microwave and Optical Technol. Lett., vol. 31, no. 3, pp. 197–201, Nov. 2001.

167. R. L. Haupt and S. E. Haupt, “Optimum population size and mutation rate for a simple real genetic algorithm that optimizes array factors,” Applied Computational Electromagnetics. Society Journal, vol. 15, no. 2, pp. 94–102, July 2000.

168. B. Aljibouri, E. G. Lim, H. Evans, and A. Sambell, “Multi objective genetic algorithm approach for a dual-feed circular polarized patch antenna design,” Electronic Letters., vol. 36, no. 12, pp. 1005–1006, June 2000.

169. C. Zuffada, T. Cwik, and C. Ditchman, “Synthesis of novel all-dielectric grating filters using genetic algorithms,” IEEE Trans. Antennas Propagation., vol. 46, pp. 657–663, May 1998.

170. Y. Rahmat-Samii and H. Mosallaei, “GA optimized Luneberg lens antennas; characterisations and measurements,” in Proc. Int. Symp. Antennas and Propagation, Aug. 2000, pp. 979–982.

171. H. Mosallaei and Y. Rahmat-Samii, “Non-uniform Luneburg lens antennas: a design approach based on genetic algorithms,” in IEEE Antennas and Propagation Soc. Int. Symp. Dig., July 1999, pp. 434–437.

172. H. Sun, C. Gu, X. Chen, Z. Li, L. Liu, B. Xu*, et al.*, "Broadband and Broad-angle Polarization-independent Metasurface for Radar Cross Section Reduction," *Scientific reports,* vol. 7, p. 40782, 2017

173. D. Simmons, K. Cools, and P. Sewell, "A hybrid Boundary Element Unstructured Transmission-line (BEUT) method for accurate 2D electromagnetic simulation," *Journal of Computational Physics,* vol. 324, pp. 275-288, 2016.

174. A. F. Muscat and C. G. Parini, “Novel compact handset antenna,” in Proc.11th Int. Conf. Antennas and Propagation, Apr. 2001, pp. 336–339.

175. J. Bartolic, Z. Sipus, N. Herscovici, D. Bonefacic, and R. Zentner, “Planar and cylindrical micro strip patch antennas and arrays for wireless communications,” in Proc. 11th Int. Conf. Antennas and Propagation, Apr. 2001, pp. 569–573.

176. J. C. Maloney, M. P. Kesler, L. M. Lust, L. N. Pringle, T. L. Fountain, P. H. Harms, and G. S. Smith, “Switched fragmented aperture antennas,” in IEEE Antennas and Propagation Soc. Int. Symp. Dig., July 2000, pp. 310–313.

177. D. Lee and S. Lee, “Design of a coaxially fed circularly polarized rectangular micro strip antenna using a genetic algorithm,” Microwave and Opt. Technol. Lett., vol. 26, no. 5, pp. 288–291, Sept. 2000.

178. E. E. Altshuler, “Design of a vehicular antenna for GPS/Iridium using a genetic algorithm,” *IEEE Trans. Antennas Propagation*., vol. 48, pp. 968–972, June 2000.

179. A. Lommi, A. Massa, E. Storti, and A. Trucco, “Side lobe reduction in sparse linear arrays by genetic algorithms,” Microwave and Opt. Technol. Lett., vol. 32, no. 3, pp. 194–196, Feb. 2002.

180. C. H. Chen and C. C. Chiu, “Novel radiation pattern by genetic algorithms, in wireless communication,” in Proc. *IEEE Vehicular Technology Conf.*, May 2001, pp. 8–12.

181. W.-I. Son, M.-Q. Lee, and J.-W. Yu, "Module integrated antenna with circular polarization for mobile UHF RFID reader", *IEEE Transactions on Microwave Theory and Techniques*, vol. 59, pp. 1157-1165, 2011.

182. F. Paredes, G. Zamora, F. J. Herraiz-Martinez, F. Martin, and J. Bonache, "Dual-band UHF-RFID tags based on meander-line antennas loaded with spiral resonators," *IEEE Antennas and Wireless Propagation Letters*, vol. 10, pp. 768-771, 2011.

183. A. M. Shire and F. C. Seman, "Parametric studies of Archimedean spiral antenna for UWB applications," in *Applied Electromagnetics (APACE), 2014 IEEE Asia-Pacific Conference on*, 2014, pp. 275-278.

184. D. E. Goldberg, Genetic Algorithms in Search, Optimisation and Machine Learning. Addison-Wesley, 1997.

185. H. Mohammed, F. Abdulsalam, A. Abdulla, R. Ali, R. Abd-Alhameed, J. Noras*, et al.*, "Evaluation of genetic algorithms, particle swarm optimisation, and firefly algorithms in antenna design," in *Synthesis, Modeling, Analysis and Simulation Methods and Applications to Circuit Design (SMACD), 2016 13th International Conference on*, 2016, pp. 1-4.

186. D. Zhou, S. Gao, R. A. Abd-Alhameed, C. Zhang, M. S. Alkhambashi, and J. D. Xu, "Design and optimisation of compact hybrid quadrifilar helical-spiral antenna in GPS applications using Genetic Algorithm," in 6th European Conference on Antennas and Propagation, EuCAP, Prague, Czech republic, 2012.

187. E.E.Altshuler and D. S. Linden, "Wire-antenna designs using genetic algorithms", IEEE Antennas and Propagation Magazine, vol. 39, pp. 33-43, 1997.

188. R. A. Abd-Alhameed, D. Zhou, and P. S. Excell, "A wire-grid adaptive-meshing program for microstrip-patch antenna designs using a genetic algorithm [EM Programmer's Notebook]", IEEE Antennas and Propagation Magazine, vol. 51, pp. 147-151, 2009.

189. Carroll, David L. "DL Carroll's FORTRAN Genetic Algorithm Driver." (1997).

190. G. L. Burke and A. J. Poggio, Numerical Electromagnetics Code (NEC)-Method of Moments. Lawrence Livermore Laboratory, Livermore, CA, 1981.

191. Z. N. Chen and X. Qing, "Antennas for RFID Applications" *Presented at International Workshop on Antenna Technology. 2010.*

192. Zo. Blazevic and M. Skiljio, “Helical Antennas in Satellite Radio Channel” in Advances in Satellite Communications, 2011.

193. ISO - International Organisation for Standardisation (2013) ISO/IEC 18000-6:2013 Information technology -RFID for item management -- Part 6: Parameters for air interface communications at 860 MHz to 960 MHz General [Online]Available:http://www.iso.org/iso/home/store/catalogue_tc/catalogue_detail.htm?csnumber=59644.

194. D. Zhou, R. A. Abd-Alhameed, C. H. See, P. S. Excell and E. A. Amushan, “Design of Quadrifilar Helical and Spiral Antennas in the Presence of Satellite-mobile Handsets Using Genetic Algorithms” 1st European Conference on Antennas and Propagation, 2006.

195. D. Zhou, S. Gao, R. A. Abd-Alhameed, C. Zhang, M. S. Alkhambashi and J. D. Xu, “Design and Optimisation of Compact Hybrid Quadrifilar Helical-Spiral Antenna in GPS Applications Using Genetic Algorithm” 6th European Conference on Antennas and Propagation. 2012.

196. Fan, Bizhou, et al. "Design of a dual (UHF/S) bands antenna handset." *Antennas, Propagation and EM Theory (ISAPE), 2016 11th International Symposium on*. IEEE, 2016.

197. Z. Blazevic and M. Skiljio (2011). “Helical Antennas in Satellite Radio Channel” in Advances in Satellite Communications, M. Karimi, Ed. [Online eBook]Available:http://cdn.intechopen.com/pdfs/16867/InTech-Helical_antennas_in_satellite_radio_channel.pdf.

198. J. M. Johnson and Y. Rahmat-Samii, “Genetic Algorithms in Engineering Electromagnetics”, *IEEE Antennas and Propagation Magazine* [Online]. vol. 38, no. 4, pp. 7 - 21, 1997.

199. B. R. Behera and P. Suraj, "Behaviour of metamaterial antenna under the influence of genetic algorithm: Design, modelling and modelling of microstrip antenna with EBG and GA," in *Communication and Electronics Systems (ICCES), International Conference on*, 2016, pp. 1-5.

200. M. Akinsolu, A. Ali, A. Atojok, E. Ibrahim, I. Elfergani, R. Abd-Alhameed*, et al.*, "Novel Quadrifilar Helical Antenna for RFID Applications Using Genetic Algorithms," *Session 1P0,* p. 585.

Author’s Publication Record

LIST OF PUBLICATIONS

REFERRED JOURNALS

1. **Link Budget Maximization for a Mobile-Band Subsurface Wireless Sensor in Challenging Water Utility Environments (Accepted)**

   Chan H. See, Raed A. Abd-Alhameed, **Achimugu A. Atojoko (***achieved design in HFSS environment on 900 MHz*)

   IEEE Transactions on industrial Electronics, 16-TIE-3390.

REFEREED CONFERENCES

1. **Design and analysis of a simple UHF passive RFID tag for liquid level monitoring applications**

   A. Atojoko; R. A. Abd-Alhameed; H. S. Rajamani; N. J. McEwan; C. H. See; P. S. Excell 2015 Internet Technologies and Applications (ITA)

   Year: 2015.Pages: 484 - 488, DOI: 10.1109/ITechA.2015.7317453

   IEEE Conference Publications

2. **Novel Quadrifilar Helical Antenna for RFID Applications Using Genetic Algorithms,**

   M. O. Akinsolu , A. Ali1 **, A. Atojoko** (*NEC2 FORTRAN source code for design generated*) , E. Ibrahim, , I. T. E. Elfergani , R. A. Abd-Alhameed , J. M. Noras ,PIERS Proceedings, Prague, Czech Republic, July 6–9, 2015

3. **Automatic liquid level indication and control using passive UHF RFID tags**

A. Atojoko; R. A. Abd-Alhameed; Y. Tu; F. Elmegri; C. H. See; M. B. Child

2014 Loughborough Antennas and Propagation Conference (LAPC)

Year: 2014, Pages: 136 - 140, DOI: 10.1109/LAPC.2014.6996339

IEEE Conference Publications

4. **"Compact MIMO/Diversity Antenna for Portable and Mobile UWB Terminals,"**

C.H.See, **A. A. Atojoko** *(contributed to literature review),* N.A. Jan, R. A. Abd-Alhameed, N.J. McEwan and E. Elkazmi In proceeding of 2014 Asia Pacific Microwave Conference (APMC), Sendai, Japan, 4-7 Nov. 2014, pp.1-3

5. **Energy efficient gully pot monitoring system using radio frequency identification (RFID)**

Atojoko, A. ; Jan, N.M. ; Elmgri, F. ; Abd-Alhameed, R.A. ; See, C.H. ; Noras, J.M. Antennas and Propagation Conference (LAPC), 2013 Loughborough

Digital Object Identifier: 10.1109/LAPC.2013.6711914

Publication Year: 2013 , Page(s): 333 – 336

IEEE Conference Publications

6. **Liquid level monitoring using passive RFID tags**

Atojoko, A. ; Bin-Melha, M. Elkazmi, E. ; Usman, M. ; Abd-Alhameed, R.A.; See, C.H. Design and Test Symposium (IDT), 2013 8th International

Digital Object Identifier: 10.1109/IDT.2013.6727088

Publication Year: 2013 , Page(s): 1 - 5

IEEE Conference Publications

7. **A Review of Location Based Services: Current Developments, Trends and Issues,** R.A. Abd-Alhameed, K.O.O. Anoh, I. Ahmad, H.S.O. Migdadi, R. Asif, N.A. Jan, T.S. Ghazaany, S. Zhu, F. Elmegri, M. Bin-Melha, **A. Atojoko** *(reviewed literature),* J.M. Noras, S.M.R. Jones, C.H. See, H. Alhassan and M.B. Child

Selected Author’s publications

ENERGY EFFICIENT GULLY POT MONITORING SYSTEM USING RADIO FREQUENCY IDENTIFICATION (RFID)

A. Atojoko[1], N. M Jan[1], F. Elmgri[1], R. A. Abd-Alhameed[1], C. H. See[2], J. M. Noras[1]
[1]Radio Frequency and Antenna Design Group, School of Engineering, Design and Technology,
University of Bradford, Bradford, BD7 1DP, UK
{a.a.atojok, r.a.a.abd}@bradford.ac.uk
[2]Bolton University, UK
c.see@bolton.ac.uk

***Abstract* - Sewer and gully flooding have become major causes of pollution particularly in the residential areas majorly caused by blockages in the water system and drainages. An effective way of avoiding this problem will be by deploying some mechanism to monitor gully pot water level at each point in time and escalating unusual liquid levels to the relevant authorities for prompt action to avoid a flooding occurrence. This paper presents a low cost power efficient gully pot liquid level monitoring technique. Passive RFID tags are deployed and signal variation from the Alien Reader Software are used to effectively estimate the level of liquid in the gully pot. The experimental set up is presented and an expository presentation is made of the passive tag design, modelled and simulated and adopted for same application.**

keywords-Sewer Blockages, Passive RFID tags, power efficient, gully pot liquid monitoring

I. INTRODUCTION

RFID technology is used to automatically identify users and objects and in recent cases, the location of these objects can also be tracked. RFID has been employed in many applications specifically to exploit the energy efficient and saving capabilities achieved specifically when the passive tags are deployed. RFID tags communicate by radio waves through antenna attached to objects so that they can be identified, located and tracked. An RFID system is made up of the RFID tag, reader, RFID software and a database. The reader scans the tags simultaneously and transmits the information to a database where it is stored for referencing. RFID as a dynamically emerging technology for product identification is widely accepted by many industries [1]. The application areas are also rapidly increasing most especially in commercial applications. It is used to track work in process, inventory, containers and finished products as they move from one section of the production process to the other. In transportation, it is deployed for logistics, fleet management, pallet, container, cargo track and improving asset utilization [2]. In the healthcare and Pharmaceutical Industry it is used to track patient's mobility and keep track of drug stock to reduce errors, in the Military and aerospace it is used to track hazardous materials to improve safety and reduce counterfeiting of parts. The most recent advances in the application areas has been in smart parking, remote moisture sensing, contactless payments and real time location systems. These applications do not necessarily use new technology; they have implemented existing technologies in innovative ways. Ford's popular F-150 pickup trucks are now available with an RFID reader integrated in the bed to monitor cargo. The Army is testing an RFID-based sensor system to record and store how often the cannons on M1 Abrams tanks are fired. The data will support proactive maintenance operations and help the Army determine when the barrels approach their end-of-life and should be replaced.

Engineers at Purdue University are creating a wireless implantable passive micro-dosimeter designed to be injected into tumors to tell physicians the precise dose of radiation received and locate the exact position of tumors during treatment.

The work presented here is an energy efficient gully pot monitoring system using RFID Technology. The aim of this research work is to demonstrate that water level data can be effectively collected using energy efficient and less expensive RFID network to monitor, report and efficiently prevent sewer and gully pot flooding.

Residential and road network sewer and drainage flooding across the globe are mainly caused by sewer, gully and drainage path blockages[3].Extensive investment into research has been made by Government organizations seeking a more advanced and cost effective way of monitoring the underground storage and drainage infrastructure with a view to drastically reduce or totally eliminate the inconveniences caused by persistent flooding experienced most especially in the residential areas. It is therefore necessary to implement a remote monitoring system for these installations in order to prevent the disruption and inconvenience these blockages cause.Sewer flooding occurs when sewage (wastewater) escapes through a manhole, drain or toilet.

Companies have repeatedly tried to remove the risk of sewer flooding to a property by upsizing the sewer, building greater sewage storage facilities, installing a pumping station to increase the flow of sewage, or even increasing the capacity

978-1-4799-0091-6/13/$31.00 ©2013 IEEE

of a sewage treatment works which may significantly reduce the risk of flooding, but not eliminate it altogether. As a result of the 2009 price review, around 6,300 properties in England and Wales will be subject to schemes delivered during 2010 to 2015 to reduce or remove the risk of sewer flooding

UK water industry alone is currently investing an excess of £200M per annum [4]. As a result of these a more cost effective and pro-active approach is sought by water companies across the globe. Manual and telemetry systems have been deployed for data collection of water levels for these systems.They are not cost effective over a wide area of gully pot networks. RFID tags are cheaper solution compared to other wireless sensors or cabled CCTV deployed to monitor water levels in gully pots. The desire to remotely monitor objects beyond the limitations of bar codes has driven research in producing RFID tags at extremely low cost[5] Passive tags are more power efficient in the sense that they only transmit in proximity of a reader.

Research and development in producing low cost RFID tags is fuelled by the need to remotely identify and monitor objects and phenomenon beyond the limitations of traditional bar codes. Commercially low cost passive RFID chip with an analogue or digital input for sensor data is currently nonexistent. For example, resistance over the sensor port can be measured by an analogue version by incorporating simple passive sensor elements that changes resistance proportional to the physical quantity of interest. One interesting application where this would be useful is for surface/underground gully pot or sewer liquid level monitoring

It is in view of this that a cost effective gully pot monitoring system is proposed using RFID technology. Remote independent and effective monitoring of gully pot water levels in real time is achieved for data collection and transmission for distant operator station monitoring to prevent and effectively reduce sewer flooding. This paper presents an alternative low cost approach to sewer or gully pot liquid level monitoring.

II. Experimental Setup

The system initial set up is as shown in Fig. 1 highlighting the various observations with changing water levels. The tags are laminated and attached to the inner part of the cylindrical vacuum representing the gully pot. The various levels within the gully pot were marked on the basis of different levels; these are LL-Lower level, M-Mid level ,H-High level and HH-Highest level. The tags were re-programmed for effective identification on the graphical monitoring station based on the assigned levels within the gully pot. Tags AB65 – LL (Deep blue color), ABA4-M (light blue), AB08-H (Yellow) and AC08-HH (Pink) for easy identification. The RFID reader operating at 865-868MHz was connected to the computer and the antenna connected to a port on the Alien RFID reader. The antenna was put at various distances from the gully point with the passive tags affixed to the respective levels intended for monitoring. The Alien RFID software was used and various levels of the gully pot was effectively indicated and transmitted for efficient monitoring. When the passive RFID tags come in contact with water,losses occur in the antennas'near-field. There is also a change in resonant frequency and degradation to the tag antennas due to a change in input impedance. It has been previously shown how this property can be used to measure the amount of water concentration in soil and water by connecting a transmission line to a buried monopole antenna [6]. A separation distance of two inches was maintained between the tags at different levels in the gully pot so that the near fields of their antennas do not interfere. The performance of low cost tags constructed with simple one-layered antennas is very sensitive to surrounding environment especially to nearby lossy surfaces and water [7-9]. The practical set up realised is illustrated below.

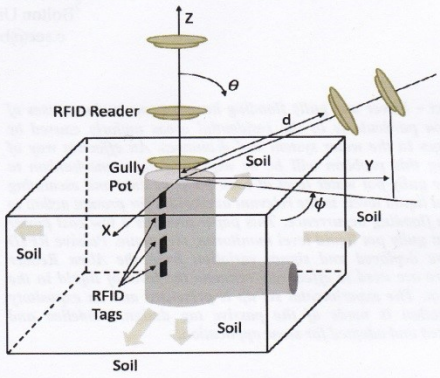

Fig. 1: Gully pot set up Illustration

Some soil was filled in around a cylindrical inner vessel inserted in a clay pot to replicate a real life scenario. The RFID reader was placed at varous distances from the tags and the link coupling was observed from three different angulations (i.e., d, θ and ϕ as presented in Figure 1).

III. RFID TAG ANTENNA

The design descriptions of two RFID passive tags to operate within the gully pot were considered in this present work. The main difference between them is the existence of ground plane in the second design to avoid the maximum coupling with the wall of the gully pot; however, the first tag was placed 2cm away from the wall of the gully pot. Both designs deliver improved results in terms of the radiation performances and the required RFID chip impedance matching. A full parametric study was performed using HFSS from which a candidate structures have been fabricated. The basic configurations of the two passive antennas are shown in Figure 2. The structure parameters are summarised in Table 1 and 2 for which the feed point (chip placement) has been generated with an (14-J130)Ω input impedance for matching purposes.

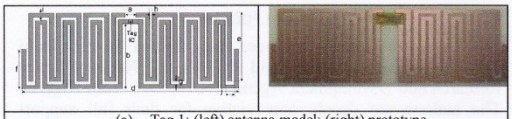

(a) Tag 1; (left) antenna model; (right) prototype.

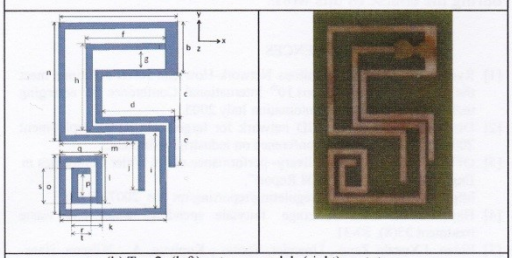

(b) Tag 2; (left) antenna model; (right) prototype.

Figure 2: RFID tag antennas; (a) tag 1 without ground plane; (b) tag 2 with ground plane.

Table 1: Parameters of the proposed RFID tag 1.

a	3.2	**e**	19.8	**h**	0.8
b	19	**f**	11.5	**i**	1.2
c	4.8	**g**	0.9	**j**	2.8
d	63.2				

Table 2: Parameters of the proposed RFID tag 2 with ground plane.

A	19.5	**k**	17.5
B	9	**l**	8
C	0.5	**m**	13
D	12	**n**	20
E	8.5	**o**	10
F	13	**p**	4
G	0.5	**q**	7
H	14.9	**r**	5
I	13	**s**	6
J	8.5	**t**	2

The return loss, coupling and radiation pattern of the radiator have been measured and the results have been verified to ensure adequate performance. As demonstrated in Figure 3 the return loss i.e. reflection coefficient over bandwidth centred at 867MHz is approximately between -18 to 35 dBs for both antennas. It is worth mentioning that the best geometry sizes with a highest reflection coefficient at the specified frequency were studied, analysed and tested before the optimum RFID tag antenna was implemented. Through the simulations, a few of the parameters' lengths have been found to be more influential to the antenna properties. From these parameters, the study analyses have been focused on their size and the remaining sizes have been kept constant. The gain values were quite satisfactory between (-2.1 to -0.5)dBs and (-3.2 to -1.1)dBs respectively for tag 1 and tag 2 antennas. It should be noted these gain values have quite impact on the performance of these tags when they placed on the gully pot even for expected strong coupling with the water and the wet wall of the gully pot.

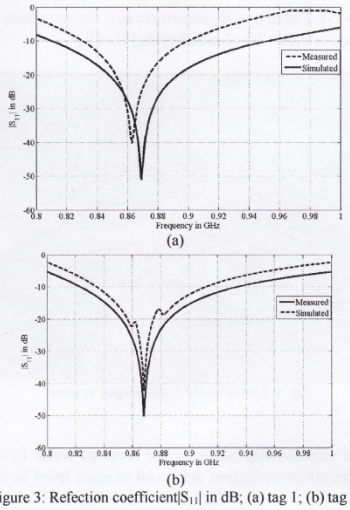

Figure 3: Refection coefficient$|S_{11}|$ in dB; (a) tag 1; (b) tag 2.

IV. GULLY POT PRACTICAL SETUP

A workable prototype model for the Figure 1 was implemented for test as shown in Figure 4. The gully pot was fit inside the soil, the soil round the gully had a thickness of 18mm. The conductivity and relative permittivity of the soil was repeatedly measured over the RFID band centred at 867MHz for dry and wet conditions, and these found on the range of 0.2 to 3S/m conductivity and relative permittivity ranging from 1.2 to 22. Tap water was used to fill the gully pot on different stages in which the measurements were taken over a wide range of distances and angles; for which the reader was placed between 2 cm and 75 cm distances over 360 ° azimuth angle (in 20°steps) and 60°zenith angle (in 15° steps). The RFID reader used for this test has a circularly- polarized antenna with 6.2 dB gain. The maximum dimensions of the RFID reader were kept at $8 \times 8 \times 1.9$ cm^3. A graphical reflection of the current status of the 4 tags placed at different levels in the gully was presented for all readings considered. As an example, in Fig.4 tag AB65 at the LL-Level cannot be read because it has been submerged in the rising water level. The radiation efficiency of the RFID tags was totally degraded when the water covers them. However, it should be noted that the tags become unreadable as soon as the water level rises to touch the tag even midway before they are fully submerged. Existing technologies for remote reading of water levels in hidden locations are based on microwave technologies[10-11] It has also been shown from previous study that the difference in minimum output power required from the RFID reader in order to read passive tags is almost linear to the amount of water the tags are submerged in[12]. It is well known that the performance of low cost tags, constructed with simple one-layer antennas, is very sensitive to the surrounding environment and especially to nearby metallic surfaces and

water[13-15]. Extensive literature reveals the previous approaches to water level monitoring[16-20]

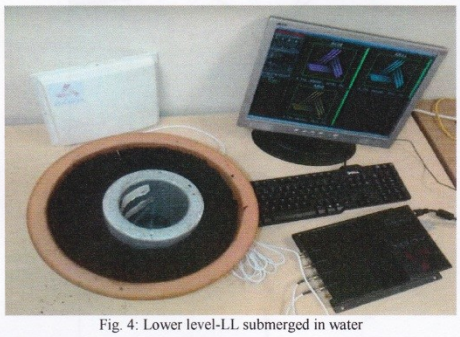

Fig. 4: Lower level-LL submerged in water

The linear relationship between the level of water in the gully pot and the communication achieved at each level is shown in Fig. 5.

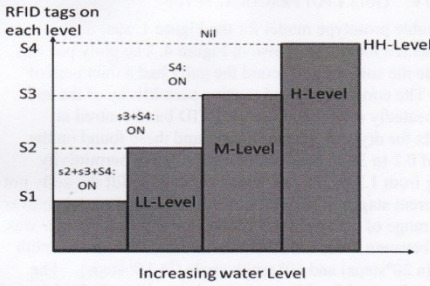

Fig. 5: Sensors status by the reader versus water level

V. Conclusion

Sewer flooding associated issues both at the consumer and water company perspective has posed a lot of problems. The design of the power efficient system for gully pot monitoring offers an effective solution to this tremendous challenge. This paper presents the practical implementation of a cost effective gully pot monitoring system using RFID technology. Remote independent and effective monitoring of gully pot water levels in real time is achieved for data collection and transmission for distant operator station monitoring to prevent and effectively reduce sewer flooding. The designed passive tags are low cost and easy to deploy. The results obtained from the practical experimental set up has enabled the researcher develop better understanding on the working elements and the problems associated with the power efficient gully pot monitoring system.

Acknowledgement

This research paper has been fully funded by Petroleum Technology Development Fund (PTDF) and National Space Research and Development Agency (NASRDA) from Nigeria. The authors are deeply appreciative for their full support during the course of this work.

References

[1] Ryo Imura, Driving ubiquitous Network-How can RFID solutions meet the customer's expectations.10th International Conference on emerging technologies and factory automation Italy 2005.

[2] Distributed design of RFID network for large-scale RFID deployment 2006 IEEE International conference on industrial informatics

[3] OFWAT, "Service and Delivery- performance of the Water Companies in England and Wales 2007-08 Report", http://www.ofwat.gov.uk/regulating/reporting/rpt_los_2007-08.pdf

[4] Hayward P. 2002 Sewerage: fairytale spending, water and waste treatment 35(8), 30-31.

[5] Siden, J.Xuezhi Zeng ; Unander, Tomas ; Koptyug, A. ; Nilsson, Hans-Erik Sensors, Remote Moisture Sensing utilizing Ordinary RFID Tags 2007 IEEE Digital Object , 2007 , Page(s): 308 - 311

[6] A. Denote, "The monopole-antenna: a practical snow and soil Wetness sensor", *IEEE Trans. Geoscience and Remote Sensing*,Vol. 35, Issue 5, pp. 1371 – 1375, Sept. 1997.

[7] J. D. Griffin, G. D. Durgin, A. Haldi and B. Kippelen, "RF tag Antenna performance on various materials using radio link budgets", *Antennas and Wireless Propagation Letters,* Vol. 5, pp. 247 – 250, 2006.

[8] D. M. Dobkin and S. M. Weigand, "Environmental effects onRFID tag antennas", *IEEE Int. Microwave Symp. 2005*, pp. 135-138.

[9] J. Sidén, H.-E. Nilsson, "Adaption to Background Material for Printed RFID Antennas", *In Proc. Antenn-06*, Sweden, 2006.

[10] F. Menke, R. Knochel, T. Boltze, C. Hauenschild, and W. Leschnik,"Moisture measurement in walls using microwaves", *IEEE Int.Microwave Symp.* 1995, Vol. 3, pp. 1147 – 1150, 1995.

[11] J. Sidén, Xuezhi Zeng, T.Unander, Andrey Koptyug, Hans-Erik NilssonRemote Moisture sensing using ordinary RFID tags IEEE sensors 2007 conference

[12] T. Hauschild, and F. Menke, "Moisture measurement in masonry walls using a non-invasive reflectometer", *Electronics Letters,* Vol.34, Issue 25, pp. 2413 – 2414, 1998

[13] J. D. Griffin, G. D. Durgin, A. Haldi and B. Kippelen, "RF tag antenna performance on various materials using radio link budgets", *Antennas and Wireless Propagation Letters,* Vol. 5, pp. 247 – 250,2006.

[14] D. M. Dobkin and S. M. Weigand, "Environmental effects on RFID tag antennas", *IEEE Int. Microwave Symp. 2005*, pp. 135-138.

[15] J. Sidén, H.-E. Nilsson, "Adaption to Background Material for Printed RFID Antennas", *In Proc. Antenn-06*, Sweden, 2006.

[16] Nawale, S.D. ; Sarawade, N.P. "RFID vapor sensor: Beyond identification Sensing Technology (ICST), 2012 Sixth International Conference on Digital Object Identifier, 2012 , Page(s): 248 - 253

[17] C.H. See, K.V. Horoshenkov, R.A. Abd-Alhameed, Y.F. Hu and S.J. Tait, A Low Power Wireless Sensor Network for Gully Pot Monitoring in Urban Catchments, IEEE Sensors Journal, vol.12, no. 5, pp.1545-1553, May 2012

[18] Nasir, A. ; Boon-Hee Soong "PipeSense: A framework architecture for in-pipewater monitoring system" Communications (MICC), 2009 IEEE 9th Malaysia International Conference , 2009 , Page(s): 703 – 708

[19] Benelli, G. ; Pozzebon, A. ; Bertoni, D. ; Sarti, G. ; Ciavola, P.; Grottoli, E. "An Analysis of the Performances of Low Frequency Cylinder Glass Tags for the Underwater Tracking of Pebbles on a Natural Beach" RFID Technology (EURASIP RFID), 2012 Fourth International EURASIP Workshop , 2012 , Page(s): 72 - 77

[20] Nasri, N. ; Kachouri, A. ; Andrieux, L. ; Samet, M. Communications, Computing and Control Applications (CCCA), 2011 International Conference " New approach for wireless underwater identification: Acoustic Frequency IDentification (AFID)" 2011 , Page(s): 1 - 6

LIQUID LEVEL MONITORING USING PASSIVE RFID TAGS

A. Atojoko[1], M Bin-Melha[1], E Elkazmi[2], M. Usman[3], R. A. Abd-Alhameed[1], C. H. See[4]
[1]Mobile and Satellite Communications Research Centre, University of Bradford UK, BD7 1DP
{a.a.atojok, r.a.a.abd}@bradford.ac.uk
[2]The higher institute of electronics, bani walid-libya
[3]Department of Electrical & Electronics Engineering, University of Hail, Saudi Arabia
[4]Bolton University, UK
{c.see@bolton.ac.uk}

Abstract* - *Tank flooding have become major causes of pollution both in residential and industrial areas majorly caused by overflows of water(mostly residential) and volatile poisonous industrial liquids from the storage tanks. An effective way of avoiding this problem will be by deploying some mechanism to monitor liquid level at each point in time and escalating unusual liquid levelsto a pump control circuit or to the relevant authorities for prompt action to avoid a flooding occurrence. This paper presents a low cost power efficient liquid level monitoring technique. Passive RFID tags are designed modelled and deployed,the signal variation from the Alien Reader Software are used to effectively estimate the level of liquid in any surface or underground tank. The experimental set up is presented and an expository presentation is made of the passive tag design, modelled and simulated and adopted for same application.

keywords-Tank flooding, Passive RFID tags, power efficient, liquid level monitoring

I. INTRODUCTION

Automatic Identification and location of objects is achieved using RFID technology. RFID has been employed in many applications specifically to exploit the energy efficient and saving capabilities achieved specifically when the passive tags are deployed. RFID tags communicate by radio waves, RFID transponders have its application in many major fields of industry. An RFID transponder stores and transmits data to the reader in a seamless fashion using the all-important radio waves. An RFID system is made up of the RFID tag, Reader, RFID software and a database. The reader scans the tags simultaneously and transmits the information retrieved from these tags to a database where it is stored for referencing. RFID as a dynamically emerging technology for product identification is widely accepted by many industries [1]. The application areas are also rapidly increasing most especially in commercial applications. It is used to track work in process, inventory, containers and finished products as they move from one section of the production process to the other. In transportation, it is deployed for logistics, fleet management, pallet, container, cargo track and improving asset utilization [2]. In the healthcare and Pharmaceutical Industry it is used to track patient's mobility and keep track of drug stock to reduce errors, in the Military and aerospace it is used to track hazardous materials to improve safety and reduce counterfeiting of parts. The most recent advances in the application areas has been in smart parking, remote moisture sensing, contactless payments, Real time location systems etc. These applications do not necessarily use new technology; they have implemented existing technologies in innovative ways. Liquid level indication and control can be achieved using RFID tags,this application area is yet to be exploited extensively.Volatile liquid spillage has in the past caused a lot of havoc in industrial and residential areas, resulting in accidental flares that has led to loss of life and property,for deep ocean spills,the resultant destruction to the coral reef can be visibly seen. Existing technologies in liquid level indication,sensing and control have explored other form of sensing technologies which are not as energy efficient as the system proposed in this paper.

The work presented here is a liquid level monitoring system using RFID Technology. The aim of this research work is to design and deploy the liquid level sensors and demonstrate that liquid level data can be remotely collected using energy efficient and less expensive RFID network to monitor, report and efficiently prevent surface or underground tanks from overflowing,thereby avoiding flooding and wastage in the process while saving energy.

Residential and road network sewer and drainage flooding across the globe are mainly caused by sewer, gully and drainage path blockages[3].The desire to remotely monitor objects beyond the limitations of bar codes has driven research in producing RFID tags at extremely low cost[4].Extensive investment into research has been made by Government organizations seeking a more advanced and cost effective way of monitoring the underground storage and drainage infrastructure with a view to drastically reduce or totally eliminate the inconveniences caused by persistent flooding experienced most especially in the residential areas. In the Industrial areas and most especially in refineries,efficient ways of communicating finished product(petrol ,diesel,kerosene etc) storage tanks liquid levels are continously beign sought.The resultant loss of life and destruction of the ecosystem due to pipeline oil spillages has been a recurring issue particularly in

978-1-4799-3525-3/13/$31.00 ©2013 IEEE

oil producing countries;effective remote pipeline monitoring technologies are sought after.

UK water industry alone is currently investing an excess of £200Million per annum [5]. As a result of these a more cost effective and Pro-active approach is sought by water companies across the globe. Manual and telemetry systems previously deployed by the water companies are not power efficient nor cost effective over a wide area of tank networks because of the heavy cabling involved. RFID tags are cheaper alternative sloution compared to other wireless sensors or cabled CCTV deployed to monitor water levels in storage or drainage tanks.Passive tags are more power efficient in the sense that they only transmit in proximity of a reader.

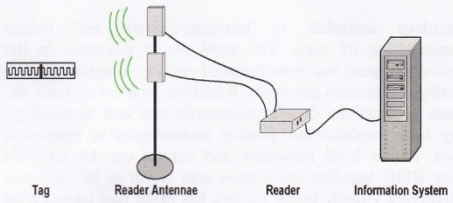

Fig1:RFID system

The need to remotely identify and monitor objects and phenomenon beyond the limitations of traditional bar codes has fuelled the research and development in producing low cost RFID tags. Commercially low cost passive RFID chip with an analogue or digital input for sensor data is currently nonexistent. For example, resistance over the sensor port can be measured by an analogue version by incorporating simple passive sensor elements that changes resistance proportional to the physical quantity of interest. One interesting application where this would be useful is for surface/underground storage tank liquid level monitoring and control.

It is in view of this that a cost effective liquid level monitoring system is proposed using RFID technology. Remote independent and effective monitoring of liquid levels in real time is achieved for data collection and transmission for distant operator station monitoring to prevent and effectively reduce flooding,wastage and spillages as the case may be for oil pipelines. This paper presents an alternative low cost approach to liquid level monitoring both for residential and industrial purpose.

II. SYSTEM MODELLING

The system model set up is achieved in the HFSS software,the initial set up is as shown in Fig.2. The tags are sealed and attached to the inner part of the cylindrical vaccum representing the gully pot or water tank. The various levels within the water tank were marked according to intended threshold levels; these are LL-Lower level, M- Mid level, H-Highlevel and HH-Highest level. The tags were re-programmed for effective Identification on the Graphical monitoring station based on the assigned levels within the water tank. Tags AB65 – LL (Deep blue color), ABA4-M (light blue), AB08-H (Yellow) and AC08-HH (Pink) for easy identification. The RFID reader operating at 865-868MHz was connected to the Computer and the Antenna connected to a port on the Alien RFID reader. The antenna was put at various distances from the gully with the passive tags affixed to the respective levels intended for monitoring. The Alien RFID software was used and various alternating water levels of the tank/Gully was effectively indicated and transmitted for efficient monitoring. Ohmic losses occur in the antennas near-field when the passive tags come in contact with water . It has been previously shown how this property can be used to measure the amount of water concentration in soil and water by connecting a transmission line to a buried monopole antenna [6]. A separation distance of two inches was maintained between the tags at different levels in the gully pot so that the near fields of their antennas do not interfere. The performance of low cost tags constructed with simple one-layered antennas is very sensitive to surrounding environment especially to nearby lossy surfaces and water [7-9]. The practical set up realised is illustrated below.

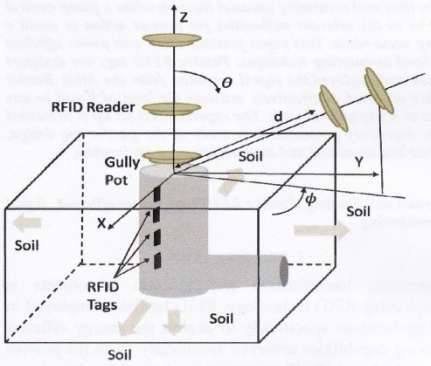

Fig. 2: Gully pot set up Illustration

Some soil was filled in around a cylindrical inner vessel inserted in a clay pot to replicate a real life gully pot/underground pipeline scenario,a seperate set up to replicate normal surface storage tanks was also achieved. The RFID reader was placed at varous distances from the tags and the link coupling was observed from three different dirctions (i.e., d, θ and ϕ as presented in Figure 2).

III. RFID TAG ANTENNA

The design descriptions of the RFID passive tags to operate within the Gully pot were considered in this present work. The main difference between them is the existence of ground plane in the second tag type to avoid the maximum coupling with the wall of the Gully pot. Both designs are more basic and deliver improved results in terms the radiation performances and the required RFID chip impedance matching. Candidate structures have been fabricated from a full parametric study performed using HFSS. The basic

configurations of the passive antennas is as shown in Figure 3 for which the feed point (chip placement) has been generated with an (15-J150)Ω input impedance for matching purposes.

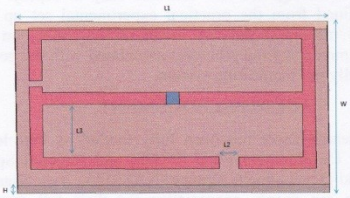

Fig3:Passive tag top view
L1= 48 mm, W = 27.7mm, L2 = 3mm, L3 = 9mm

The return loss, coupling and radiation pattern of the radiator have been measured and the results have been verified to ensure adequate performance.The best geometry sizes with the highest reflection coefficient at the specified frequency were studied, analysed and tested before the optimum RFID tag antenna was implemented. Through the simulations, few of the parameters lengths have been found to be more influential to the antenna properties. From these parameters, the study analyses have been focused on their size and the remaining sizes have been kept constant.The properties of the designed tag is summerised in Table 1 below

Impedance(ohm)	15.4+j140
Return loss(dB)	-54.9
Gain(dB)	-1.29
Directivity(dBi	0.65
Antenna efficiency(%)	78

Table1:Tag characteristics

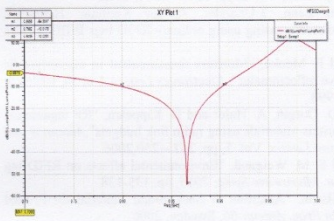

(a)

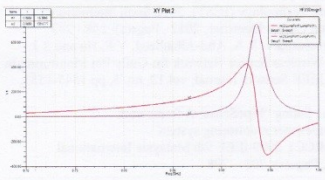

(b)

Figure 3: (a)frequency vs Return loss (b)Impedance vs frequency

(A)

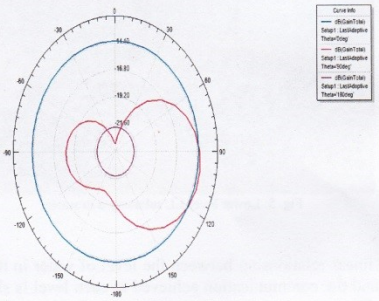

(B)

Fig 4:Antenna Radiation Pattern (a) 3D (b) 2D

IV. GULLY POT PRACTICAL SETUP

A workable prototype model for the Figure 3 was implemented for test as shown in Figure 5. The Gully pot was fit inside the soil, for two wall thicknesses 18 and 22 mm. The conductivity and relative permittivity of the soil was repeatedly measured over the RFID band centred at 867MHz for dry and wet conditions, and these found on the rang of (0.2 – 3) S/m conductivity and (1.2 – 22) relative permittivity. A tap water was used to fill the Gully pot on different stages in which the measurements were taken over a wide range of distances and angles; for which the reader was placed between 2 cm and 75 cm distances over 360°azimuth angle (in 20 steps) and 60° zenith angle (in 15° steps). The RFID reader used for this test is circularly- polarized antenna with 6.2 dBs gain. The maximum dimensions of the RFID reader was kept at 8 × 8 × 1.9 cm^3. A graphical reflection of the current status of the 4 tags placed at different levels in the gully was presented for all readings considered. As example from the Fig. 4 that the tag AB65 at the LL-Level cannot be read because it has been submerged in the rising water level. The radiation efficiency of the RFID tags was totally degraded when the water covers them. However, it should be noted that the tags become unreadable as soon as the water level rises to

touch the tag even midway before they are fully submerged. Existing technologies for remote reading of water levels in hidden locations are based on microwave technologies[10-11] It has also been shown from previous study that the difference in minimum output power required from the RFID reader in order to read passive tags is almost linear to the amount of water the tags are submerged in[12]. It is well known that the performance of low cost tags, constructed with simple one-layer antennas, is very sensitive to the surrounding environment and especially to nearby metallic surfaces and water[13-15].Extensive Literature reveals the previous approaches to water level monitoring[16-20]

Fig. 5: Lower level-LL submerged in water

The linear relationship between the level of water in the gully pot and the communication achieved at each level is shown in Fig. 5.

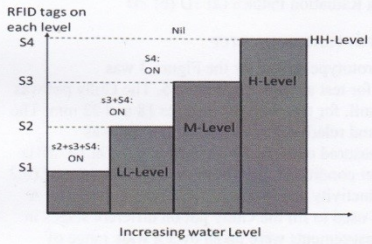

Fig. 6: Sensors status by the reader versus water level

V. Conclusion

Liquid level indication and monitoring techniques have helped prevent flooding issues both in residential and industrial applications.The design of a power efficient system for liquid level monitoring offers an effective solution to this tremendous challenge in water companies as well as oil and gas companies. This paper presents the practical implementation of a cost effective liquid level monitoring system using RFID technology. Remote independent and effective monitoring of Gully pot/surface tank/pipeline water levels in real time is achieved for data collection and transmission for distant operator station monitoring to prevent and effectively reduce water flooding and oil spillages. The designed passive tags are low cost and easy to deploy. The results obtained from the practical experimental set up has enabled the researcher develop better understanding on the working elements and the problems associated with the power efficient Gully pot monitoring system.

ACKNOWLEDGEMENT

This research paper has been fully funded by Petroleum Technology Development Fund (PTDF) and National Space Research and Development Agency (NASRDA) from Nigeria. The authors are deeply appreciative for their full support during the course of this work.

References

[1] Ryo Imura, Driving ubiquitous Network-How can RFID solutions meet the customer's expectations.10th International Conference on emerging technologies and factory automation Italy 2005.
[2] Distributed design of RFID network for large-scale RFID deployment 2006 IEEE International conference on industrial informatics
[3] OFWAT, "Service and Delivery- performance of the Water Companies in England and Wales 2007-08 Report", http://www.ofwat.gov.uk/regulating/reporting/rpt_los_2007-08.pdf
[4] Siden, J.Xuezhi Zeng ; Unander, Tomas ; Koptyug, A. ; Nilsson, Hans-Erik Sensors, Remote Moisture Sensing utilizing Ordinary RFID Tags 2007 IEEE Digital Object , 2007 , Page(s): 308 - 311
[5] Hayward P. 2002 Sewerage: fairytale spending, water and waste treatment 35(8), 30-31.
[6] A. Denote, "The monopole-antenna: a practical snow and soil Wetness sensor", *IEEE Trans. Geoscience and Remote Sensing*,Vol. 35, Issue 5, pp. 1371 – 1375, Sept. 1997.
[7] J. D. Griffin, G. D. Durgin, A. Haldi and B. Kippelen, "RF tag Antenna performance on various materials using radio link budgets",*Antennas and Wireless Propagation Letters,* Vol. 5, pp. 247 – 250, 2006.
[8] D. M. Dobkin and S. M. Weigand, "Environmental effects onRFID tag antennas", *IEEE Int. Microwave Symp. 2005*, pp. 135-138.
[9] J. Sidén, H.-E. Nilsson, "Adaption to Background Material for Printed RFID Antennas", *In Proc. Antenn-06*, Sweden, 2006.
[10] F. Menke, R. Knochel, T. Boltze, C. Hauenschild, and W. Leschnik,"Moisture measurement in walls using microwaves", *IEEE Int.Microwave Symp.* 1995, Vol. 3, pp. 1147 – 1150, 1995.
[11] J. Sidén, Xuezhi Zeng, T.Unander, Andrey Koptyug, Hans-Erik NilssonRemote Moisture sensing using ordinary RFID tags IEEE sensors 2007 conference
[12] T. Hauschild, and F. Menke, "Moisture measurement in masonrywalls using a non-invasive reflectometer", *Electronics Letters,* Vol.34, Issue 25, pp. 2413 – 2414, 1998
[13] J. D. Griffin, G. D. Durgin, A. Haldi and B. Kippelen, "RF tagantenna performance on various materials using radio link budgets",*Antennas and Wireless Propagation Letters,* Vol. 5, pp. 247 – 250,2006.
[14] D. M. Dobkin and S. M. Weigand, "Environmental effects on RFID tag antennas", *IEEE Int. Microwave Symp. 2005*, pp. 135-138.
[15] J. Sidén, H.-E. Nilsson, "Adaption to Background Material for Printed RFID Antennas", *In Proc. Antenn-06*, Sweden, 2006.
[16] Nawale, S.D. ; Sarawade, N.P. "RFID vapor sensor: Beyond identification Sensing Technology (ICST), 2012 Sixth International Conference on Digital Object Identifier, 2012 , Page(s): 248 - 253
[17] C.H. See, K.V. Horoshenkov, R.A. Abd-Alhameed, Y.F. Hu and S.J. Tait, A Low Power Wireless Sensor Network for Gully Pot Monitoring in Urban Catchments, IEEE Sensors Journal, vol.12, no. 5, pp.1545-1553, May 2012
[18] Nasir, A. ; Boon-Hee Soong "PipeSense: A framework architecture for in-pipewater monitoring system" Communications (MICC), 2009 IEEE 9th Malaysia International Conference , 2009 , Page(s): 703 – 708

Novel Quadrifilar Helical Antenna for RFID Applications Using Genetic Algorithms

M. O. Akinsolu[1], A. Ali[1], A. Atojok[1], E. Ibrahim[1,2], I. T. E. Elfergani[3], R. A. Abd-Alhameed[1], Abubakar Sadiq Hussaini[1,3,5], J. M. Noras[1], and Jonathan Rodriguez[3,4]

[1]University of Bradford, Bradford, West Yorkshire, BD7 1DP, UK
[2]College of Electronic Technology Bani Walid, Libya
[3]Instituto de Telecomunicacoes, Aveiro, Portugal
[4]Universidade de Aveiro, Portugal
[5]School of Information Technology & Communications, American University of Nigeria, Nigeria

Abstract— For excellent tag-read communication in RFID applications, an interrogator equipped with an antenna having a circularly polarised radiation pattern is required. The antenna must also maintain a low profile and be compact for ease of installation. A more compact QHA is developed by linearly-shifting its helical elements for minimal optimum quadrature-distance. As a result, a novel QHA design, a "linearly-shifted quadrifilar helical antenna" (LSQHA) is proposed to operate at 900 MHz RFID applications using Genetic Algorithm (GA) driver with the industry-standard NEC-2 computational analysis program. Performance of the GA-optimised antenna shows that it has a 3 dB beamwidth of 90 degrees and a total gain of 13.1 dBi at the design frequency of 900 MHz. The proposed antenna excellently meets VSWR and return loss requirements within the frequency boundary of (875–912.5) MHz. The performance also shows that the proposed LSQHA is circularly polarised.

1. INTRODUCTION

Antennas constitute a very important part of Radio Frequency Identification (RFID) systems [1]. Coming in various forms and types, they are usually designed and intended to ensure maximum effective and efficient communication links between tags or transponders and their associated readers or interrogators. One of the primary challenges in the design and development of antennas in RFID applications as it is in other wireless applications is having an antenna with optimised parametric features that are desirable and in consonance with laid down specifications and functional requirements [1, 2].

RFID systems which connote the physical interaction between a tag and a reader for automatic identification operate within the global bandwidth of (860–960) MHz as specified by the International Standards Organisation (ISO) [3]. RFID systems function by adopting a non-contact application of radio-frequency that does not require a line-of-sight channels [4]. In order to optimise an RFID system, the orientation of the tags and associated readers must be fully established through the polarisation characteristics of their corresponding antennas. RFID tags are often designed to have linearly polarised dipoles [5].

The quadrifilar helical antenna (QHA) (example see Figure 1) has been identified by previous works as a suitable antenna for omnidirectional tag reading in RFID and other wireless applications, due to its ability to give circular polarisation over a wide angular area [6, 7]. Another excellent property of QHAs in terms of the symmetry of their geometry is their ability to give a cardioid-shaped radiation pattern regardless of the axial length and diameter [8]. It has also been established that the inherent cardioid-shaped radiation patterns of QHAs can be made conical by extending the resonant fractional turns of the QHA to an integral number for improved characteristics [9].

The QHA (Figure 1) is capable of providing an excellent beamwidth pattern with desirable circular polarisation, making it a good choice in RFID applications [2]. However, optimum caution is needed in the design and development of QHAs to realise the specified axial ratio and front to back power ratio. One of the notable pitfalls in the design and development of QHAs is the overall axial length of antenna, which is often too bulky for many practical installations and applications To address this problem, a global optimisation technique was employed to constrain the geometrical parameters of the conventional QHA. The selected global optimisation technique, genetic algorithm (GA) has been exemplified as an effective and efficient tool in RF and EM engineering optimisation [10]. In addition GA has been used in previous works to achieve low profile, compact designs for QHAs in other wireless communications applications [6, 7].

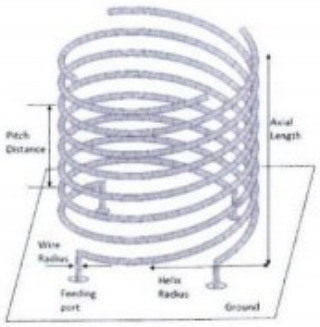

Figure 1: Basic geometry of the QHA.

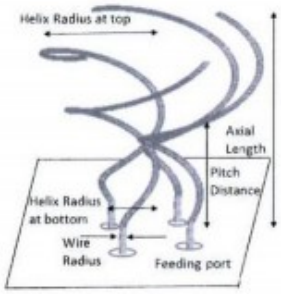

Figure 2: Geometry of the linearly-shifted quadrifilar helical antenna (LSQHA).

The novel QHA antenna is named linearly-shifted quadrifilar helical antenna (LSQHA) because its elements are linearly-shifted and made compact to cover the global BW 860–960 MHz as revealed in Figure 2. With reference to its helical elements and as can be observed, the proposed LSQHA design does not take the form of the conventional QHA. Specifying a finite ground and feeding of the LSQHA via an integrated feed network is proposed, to avoid the intricacy and losses associated with multiple feed points of a centre feed. At the risk of repetition, the novel antenna structure is achieved by linearly-shifting the helical elements of the conventional QHA by 90° using a defined phase quadrature distance. This design is expected to reduce the axial length and overall volumetric equivalent of the LSQHA, while retaining good axial ratio, high power gain and wide beamwidth coverage.

2. ANTENNA DESIGN STRUCTURE

The design and optimisation of the proposed linearly-shifted quadrifilar helical antenna in RFID applications was conducted using a GA driver synchronised with the industry-standard Numerical Electromagnetic Code (NEC-2). The GA driver is initialised by a set of initial solutions or parameters defined for the proposed LSQHA. Parametric iterations are then executed with the conjunctive running of the GA driver and the NEC-2 computational analysis program. As adopted in this work, the source codes for the GA driver synchronised with the industry-standard NEC-2 were written in FORTRAN [11, 12]. The codes were intuitively modified to randomly generate and evaluate antenna samples.

To achieve optimum results, the initial geometrical and parametric solution of the proposed LSQHA was defined for optimisation with GA based on established findings in [6, 7]. In this process, real-valued GA chromosomes were defined. Antenna parameters such as the, VSWR, axial ratio (AR) and total forward gain (G_T) were optimised at an operating frequency of 900 MHz in consonance with the EPC Global RFID Tag/Reader specifications [13]. Individual antenna samples were generated using the industry-standard NEC-2 source code and corresponding results were juxtaposed with the desired fitness function.

A summary of the GA input parameters, antenna variables and best solutions for the proposed LSQHA design is detailed in Table 1. The LSQHA was designed to provide a very high forward gain and circular polarisation within the RFID global bandwidth of (860–960) MHz. As evident, the proposed design differs from the conventional QHA in Figure 1 in that its helical elements were configured to be linearly-shifted at 90° from each other using a defined phase quadrature distance. This was deemed necessary in an effort to achieve a very compact design and lower the overall profile of the proposed antenna. In the study undertaken, the LSQHA offered a better performance with its helical elements shifted.

The simulation logic and GA optimisation model were structured in such a way that an optimum linear distance between the four helical elements of the LSQHA was sought while shifting them by 90° in phase-quadrature. Optimal parametric features for the proposed LSQHA antenna, with an excellent VSWR and AR, were found within the maximum number of GA generations specified (250): the antenna's parameters for the optimum design are detailed in Table 1. The performance of the proposed LSQHA has been analysed and verified using freeware antenna modeller

Table 1: Summary of GA input parameters and antenna variables.

GA PARAMETERS		QUADRIFILAR HELICAL ANTENNA DESIGN PARAMETERS			
	Input Values		Minimum Value (m)	Maximum Value (m)	Optimum Value (m)
Population Size	10	Pitch Distance	0.0033	0.0721	0.0558
Number of Parents	5	Axial Length	0.045	0.10	0.0885
Probability of mutation	0.02	Radius of Helix (Top)	0.01	0.035	0.035
Maximum Generation	250	Radius of Helix (Bottom)	0.01	0.035	0.0342
Probability of Crossover	0.5	Linear Quadrature Distance Between Helical Elements	0.035	0.07	0.0501
Probability of Creep	0.04	Fixed Radius of Wires	0.0005	0.0005	0.0005
Number of Possibilities	32768	Fixed Distance above ground	0.01	0.01	0.01

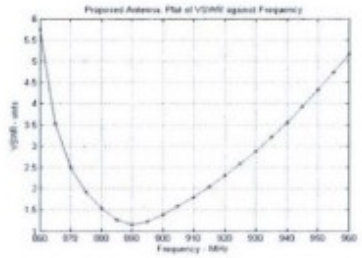

Figure 3: Computed VSWR for the proposed LSQHA.

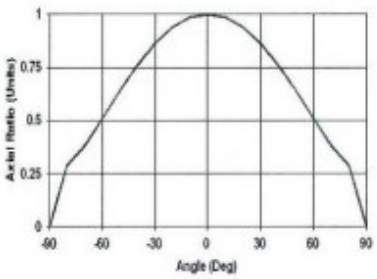

Figure 4: Axia ratio of the LSQHA.

and simulation software [14].

Evidently, the overall profile of the optimal design of LSQHA showcases the effectiveness of the compactness achieved by employing the logic and architecture illustrated in Figure 2. In contrast to the conventional QHA design (see Figure 1), the LSQHA was configured to have its helical elements more closely fitted together in volume and space. The LSQHA offers a more compact design in terms of its surface area, while retaining a good axial ratio and a very good beamwidth. Critical analysis of the performance of the optimal LSQHA was conducted to ascertain parametric features in terms of bandwidth, axial ratio coverage and antenna gain. The proposed LSQHA was found to have an optimum axial length of 8.85 cm as revealed in Figure 3.

The VSWR at the input ports of the optimised LSQHA antenna was calculated using an electromagnetic modelling software package and evaluated to be 1.39 at the EPC Global RFID Tag/Reader frequency of 900 MHz respectively as shown in Figure 3. As can be seen, the optimised antenna appears to have excellent impedance matching that covers most of the bandwidth specified for RFID communications (875–912.5) MHz.

Figure 4 confirms the excellent circularly-polarised characteristic of the proposed antenna over a good elevation angle mostly prominent in the counter-clockwise direction (left hand). Figure 5(a) and Figure 5(b) depict the measured power gain radiation patterns of the proposed LSQHA at an operating frequency of 900 MHz for two vertical cut planes at $\Phi = 0°$ and $\Phi = 90°$ respectively. The

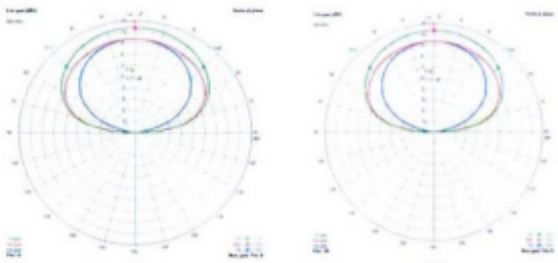

(a) (b)

Figure 5: Computed gain radiation patterns of the proposed antenna for two vertical cut planes; (a) $\Phi = 0°$ and (b) $\Phi = 90°$.

proposed antenna shows approximately $\pm 45°$ elevation angle range for an axial ratio less than 3 dB that is, a 3 dB beamwidth of 90°. Also, the proposed LQHSA revealed a total forward isotropic gain of 13.1 dBi.

3. CONCLUSIONS

A novel 'linearly-shifted quadrifilar helical antenna' (LSQHA) circularly polarized with a high forward isotropic gain and VSWR specifications desirable in RFID applications has been proposed. The proposed antenna is intended for deployment in RFID systems, as the reader or interrogator antenna, where the orientation and polarisation of the associated tag antennas cannot be precisely predicted. The design and optimisation of the proposed antenna using Genetic Algorithm method have been well appreciated and showcased, the specified objective being deployed for antenna design within the RFID global bandwidth of (860–960) MHz. The performance of the optimal selected antenna structure was validated using 4NEC-2. The results confirm the proposed antenna has a 3 dB beamwidth of 90° with a resonant frequency at about 890 MHz and an acceptable total forward gain of 13.1 dBi at the design frequency of 900 MHz. The optimal design reached was found to be compact and of an excellent profile. These results tell that the proposed antenna can easily be configured to sample commercial RFID readers or interrogators. On the whole, Genetic Algorithm global optimisation method has also proved its advantage in quickly finding optimal solutions for RF and EM designs.

ACKNOWLEDGMENT

This work is supported by the following projects: CATRENE-BENEFIC (CA505), co-financed by the European Funds for Regional Development (FEDER) by COMPETE — Programa Operacional do Centro (PO Centro BENEFIC-38887); and VALUE (PEst-OE/EEI/LA0008/2013-UID/EEA/50008/2013), funded by national funds through FCT/MEC.

REFERENCES

1. Chen, Z. N. and X. Qing, "Antennas for RFID applications," *2010 International Workshop on Antenna Technology (iWAT)*, 1–4, 2010, Online Available: IEEEXplore, Doi: 10.1109/IWAT.2010.5464865.
2. Blazevic, Z. and M. Skiljio, "Helical antennas in satellite radio channel," *Advances in Satellite Communications*, M. Karimi, Ed., 2011, Online eBook Available: http://cdn.intechopen.com/pdfs/16867/InTech-Helical_antennas_in_satellite_radio_channel.pdf.
3. ISO — International Organisation for Standardisation, "ISO/IEC 18000-6:2013 information technology — RFID for item management — Part 6: Parameters for air interface communications at 860 MHz to 960 MHz general," 2013, Online Available: http://www.iso.org/iso/home/store/catalogue_tc/catalogue_detail.htm?csnumber=59644.
4. Lee, B. and P. Xiang, "Review of RFID tag antenna issues at UHF band," *Asia-Pacific Microwave Conference, APMC 2008*, 1–4, 2008, Online Available: IEEEXplore, Doi: 10.1109/APMC.2008.4958401.
5. Rimbault, N., A. Sharaiha, and S. Collardey, "Low profile high gain helix antenna over a conical ground plane for UHF RFID applications," *15th International Symposium on Antenna*

Technology and Applied Electromagnetics, ANTEM, 1–3, 2012, Online Available: IEEEXplore, Doi: 10.1109/ANTEM.2012.6262424.

6. Zhou, D., R. A. Abd-Alhameed, C. H. See, P. S. Excell, and E. A. Amushan, "Design of quadrifilar helical and spiral antennas in the presence of satellite-mobile handsets using genetic algorithms," *1st European Conference on Antennas and Propagation, EuCAP 2006*, 1–5, 2006, Online Available: IEEEXplore, Doi: 10.1109/EUCAP.2006.4584999.
7. Zhou, D., S. Gao, R. A. Abd-Alhameed, C. Zhang, M. S. Alkhambashi, and J. D. Xu, "Design and optimisation of compact hybrid quadrifilar helical-spiral antenna in GPS applications using genetic algorithm," *6th European Conference on Antennas and Propagation, EuCAP 2012*, 1–4, 2012, Online Available: IEEEXplore, Doi: 10.1109/EuCAP.2012.6206315.
8. Kilgus, C., "Resonant quadrafilar helix," *IEEE Transactions on Antennas and Propagation*, Vol. 17, No. 3, 349–351, May 1969, Online Available: IEEEXplore, Doi: 10.1109/TAP.1969.1139459.
9. Kilgus, C. C., "Shaped-conical radiation pattern performance of the backfire quadrifilar helix," *IEEE Transactions on Antennas and Propagation*, Vol. 23, No. 3, 392–397, May 1975, Online Available: IEEEXplore, Doi: 10.1109/TAP.1975.1141084.
10. Johnson, J. M. and Y. Rahmat-Samii, "Genetic algorithms in engineering electromagnetics," *IEEE Antennas and Propagation Magazine*, Vol. 38, No. 4, 7–21, Aug. 1997, Online Available: IEEEXplore, DOI: 10.1109/74.632992.
11. Carroll, D. L., FORTRAN Genetic Algorithm Driver, Version 1.7, Dec. 11, 1998, Download from: http://www.staff.uiuc.edu/∼carroll/ga.html.
12. Burke, G. L. and A. J. Poggio, "Numerical electromagnetics code (NEC)-method of moments," Lawrence Livermore Laboratory, Livermore, CA, 1981.
13. GS-1 EPCglobal Inc., "Regulatory status for using RFID in the EPC Gen 2 band (860 to 960 MHz) of the UHF spectrum," May 31, 2013, Online Available: http://www.gs1.org/docs/epcglobal/UHF_Regulations.pdf.
14. Voors, A., "NEC based antenna modeler and optimizer," Mar. 2014, Online Availa

Design of an In-Manhole Chamber Antenna for Underground Communication Systems

Chan H. See, Raed A. Abd-Alhameed, Achimugu A. Atojoko, Yim F. Hu, Neil J. McEwan and Peter S. Excell

Abstract —**This paper presents an in-manhole chamber antenna for an underground mobile communications system. It operates over the GSM850/900 and GSM1800/1900 and UMTS bands. The proposed antenna is a 3-dimensional folded loop antenna and has an envelope size of 47 × 43.5 × 60.5 mm, which is small enough to fit inside a manhole chamber. The performance of the antenna in term of return loss, radiation patterns and gain was simulated and measured in both free space and in a real manhole chamber. To validate the simulated results, an experimental test bed was created to determine the antenna stability in term of its achieved levels of return loss and received signal strength in different positions below the manhole chamber access cover. Both numerical and experimental results suggested the best position of the antenna inside the manhole for the best received signal strength and confirmed that this antenna has adequate characteristics for incorporation in a mobile-band transceiver designed to communicate with mobile base stations from underground.**

Index Terms —folded loop antenna, GSM, return loss, received signal strength, underground utilities.

I. Introduction

The UK sewerage network, at 302,000km in length, is one of the largest infrastructures within the water industry. These assets are aging and are also subject to increasing capacity demands because of increased urbanization, more stringent environmental regulation and the projected consequences of climate change. Currently, the water industry is investing in excess of £200 million per annum in sewer replacement and rehabilitation [1-3]. To proactively reduce their risk of failure and become more operationally efficient, water companies have developed strategic partnerships with a range of organizations, including academia and instrumentation manufacturers, to help find solutions for improving the efficiency of responses to failures of key elements of critical infrastructure resulting from degradation, overload, or disasters due to natural or man-made causes.

In recent years, wireless sensor network (WSN) research [4] has received substantial attention due to its low cost, ease of deployment and successful implementation in a great many applications in business, transportation, government, defense and healthcare. To further explore other potential applications, significant efforts have gone into the development of wireless underground sensor networks (WUSN) [5-7]. These can be an optimal practical solution allowing water companies to change radically the existing methods of data collection and monitoring of sewers.

Underground environments are obviously lossy since they contain soil, rocks and water, and are relatively complex compared with the above-ground environments. To achieve a better transmission range, lower operating frequencies are necessary. This results in larger antennas being deployed underground, which is theoretically desirable but less practical because of limited space. For these reasons, it is desirable, if challenging, to establish reliable wireless Sensor to Sensor (STS) communications underground, and a Sensor to Base Station (STB) communication from underground to above ground [8-9].

To gain better understanding of the RF propagation below ground, extensive measurements and associated simulation modeling for horizontally, vertically, and cross-polarized signals in underground assets, i.e. mines and tunnels [10], manholes [11-12], and a gully pot [13], have been undertaken and reported in the literature. Interestingly, all the above research findings show the importance of operating frequency, antenna polarization, and electrical properties of the underground asset walls, for the signal propagation characteristics. This further confirms that the antenna element in a wireless system plays a pivotal role in enhancing the transmission and reception in such a harsh environment. For this reason, many antenna design concepts [14-25] have been proposed and implemented for underground applications. For STS underground communication, a zig-zag shaped monopole designed for 915 MHz operation [6], and an inverse triangular monopole antenna intended to operate from 900 to 1500 MHz [14], have been suggested and explored. For STB underground to above-ground communication, it is noticeable that many antenna design techniques have been developed to establish a reliable and longer distance wireless link through an above-ground base station [15-25]. In some published works [15-18], the authors attempted to convert the conventional manhole cover to operate as an antenna. In [15], a thick slot has been cut in a metal manhole cover to form a slot antenna, while in [16] a slot antenna was embedded in a shallow cavity inside a cast-iron manhole cover. As this antenna is located on the surface of the ground, it increases the chances of communication with the base station. However, the technique suffers from difficulties of machining and is rather impractical for widespread implementation since covers of different sizes, shapes and materials are available. To solve this problem, a composite manhole cover slot antenna with a sandwich structure was suggested in [17],

C.H. See, R.A. Abd-Alhameed, A.A. Atojoko ,Y.F.Hu and N.J. McEwan are with Antennas and Applied Electromagnetics Research Group, School of Engineering Design and Technology, University of Bradford, Bradford, BD7 1DP, UK (email: chsee2@bradford.ac.uk, r.a.a.abd@bradford.ac.uk)

P.S.Excell is with Glyndŵr University, Wrexham, LL11 2AW, UK (email: p.excell@ glyndwr.ac.uk)

C.H.See is also with School of Engineering, University of Bolton,

while in [18] an electronically steerable linearly spaced parasitic slot array was integrated with a composite manhole cover. Again, using a composite cover is still an expensive solution as all existing metal covers would have to be replaced if large-scale implementation were required. Apart from modifying the manhole cover, other underground antenna designs requiring less disturbance of the infrastructure also have been investigated [19-24]. These include a two-arm conical spiral [19] and normal mode helix antenna [20]. Both works [19-20] show that stronger signal reception above the ground can be achieved via radiation of a directed beam. A three-element wire-based inverted-F antenna array which offers high gain, a unidirectional pattern and polarization diversity was recommended in [21]. In order to reduce scattering, a novel antenna system combined with a carpet cloak and a cavity which possesses steerable radiation patterns was proposed for operation over 8-12 GHz [22]. In addition, a composite right-left handed (CRLH) microstrip patch antenna [23], and a single layer and stacked microstrip antenna [24], were used for UWSN.

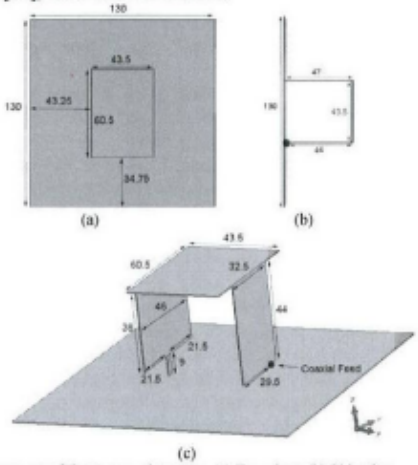

Fig. 1. Geometry of the proposed antenna. (a) Top view, (b) Side view, (c) Auxiliary view.

Among all the above designs [14-25], it was found that they are mostly only capable of offering narrow single band operation [15-21, 23-24]; only very few such as in [14, 22] can handle wideband operation and no design demonstrates dual-band operation. To fill this gap, this paper proposes a dual-band planar folded loop antenna for a wireless sewer condition monitoring system. The lower operating mode is excited by the full length of the folded loop, while the higher resonant mode is generated by the inverted L-shaped part of the loop. In section II, the antenna operating principles will be explained. Simulated and measured results will be discussed in section III. Section IV considers the antenna in a model of the manhole. Finally, conclusions are drawn in section V.

II. Antenna Design Concepts and Structure

The proposed antenna is designed to operate underneath the metal cover of the manhole chamber and it serves as the antenna for a data concentrator in a UWSN system to communicate with an existing long range above-ground mobile communication base station. Fig. 1 depicts the geometry of the proposed antenna, which is constructed as a folded planar loop. Allowing for realistic constraints on acceptable size for incorporation in a manhole chamber, the antenna dimensions and structure were chosen based on previous experience [25]. All the geometric parameters were then optimized through parametric studies. To enable its dual-band operating characteristic, a suspended rectangular feeding plate [26] with an optimized feed gap of 3 mm is used to excite this antenna assembly. As shown in Fig. 1, the optimized dimensions of the antenna are 60.5 × 43.5 × 47 mm, equivalent to electrical dimensions of $0.18\lambda_o \times 0.13\lambda_o \times 0.14\lambda_o$, where λ_o is defined at the center frequency of the lower operating band, taken as 900MHz. It is larger than a conventional mobile antenna, which is, however, acceptable in this application. For better performance and ease of integration within a manhole chamber, the antenna is designed to operate externally to a wireless transceiver and is mounted on the center of a 130 x 130 mm finite ground plane.

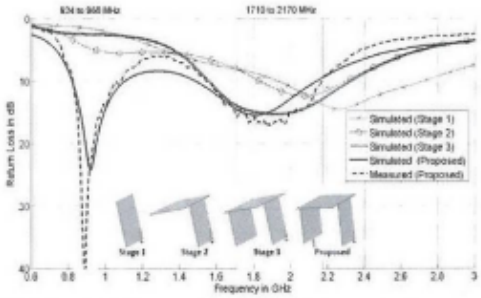

Fig. 2. Simulated and measured return losses of the proposed antenna.

The basic operational principle of this antenna can be explained by separating the four differently sized rectangular metal plates which form the antenna assembly. This will aid understanding of the contribution of each metal plate to the antenna in term of matching and impedance bandwidth over the desired operating frequency bands, i.e. the lower band (824-960 MHz) and upper band (1710 – 2170 MHz). Fig. 2 shows the detailed design evolution of the structure from a planar monopole to a folded loop planar antenna, i.e. Stage 1 to 4, while Figs. 2 and 3 show the performance of the respective antenna geometries, in terms of return loss and input impedance.

As can be seen in Fig. 2, this analysis divides into four stages and the whole structure is centered on the ground plane (not shown in Fig. 2). It begins by considering a 44 × 32.5 mm rectangular metal plate fed by an off-centre probe with a

feed gap of 3 mm. This section constitutes a traditional planar monopole, depicted as Stage 1 of Fig. 2. In this stage, the length of 44 mm, which corresponds to about 0.25λ, was selected to ensure that the antenna operates at the required centre operating frequency (COF) of the higher band, 1.9 GHz. By optimizing the width and the feed gap of the structure, acceptable impedance matching (better than 8 dB) in the higher operating band was achieved, as shown in Fig. 2. Examining the relevant impedance plot in Fig. 3, it exhibits a typical monopole impedance response with a parallel resonance occurring at around 1.9 GHz.

Without extending the height of the monopole component, but to improve the impedance matching in the upper operating band, the next course of action is to top-load the monopole with a 43.5 × 60.5 mm rectangular capacitive plate to construct an inverted L-shaped antenna structure, as shown in Stage 2, Fig. 2. The return loss plot shows a small improvement over the higher operating band, due to the top-loading effect, which shifts the parallel resonance down from 1.9 GHz to 1.35 GHz with associated resistances of 70 ohm and 200 ohm. This results in a small variation of the resistance, i.e. 30 to 58 ohm and changes the inductive reactance to capacitive in the higher operating band, as illustrated in Fig. 3.

To further enhance the impedance matching in the higher operating band, a metal plate with dimensions of 38 × 46 mm is added at the edge of the top plate and parallel to the feeding plate: this is shown as Stage 3 in Fig. 2. With this modification, this antenna partially resembles a loop antenna with an impedance bandwidth further improved to cover 1710 to 2170 MHz for a return loss better than 10 dB, as plotted in Fig. 2. Examining the input impedance of this antenna in Fig. 3, it is evident that this parallel plate further lowers the parallel resonance to 1.17 GHz, with an increased impedance of 430 ohm (not shown in Fig. 2) and results in good matching characteristics, i.e. resistance and reactance vary between 35 to 50 and -20 to 0 ohms, respectively.

Finally, to achieve good matching at the lower operating frequency band, i.e. 824 to 960 MHz, this antenna is further modified by partially shorting the parallel plate to the ground plane using a 9 × 3 mm metal plate, as shown in Stage 4, Fig. 2. After this step, the impedance response shows that the parallel resonance frequency of the antenna remains, but the impedance reduces from 430 ohms to 140 ohms, as plotted in Fig. 3. It was found, interestingly, that this change increases the resistance of the antenna without altering reactance variation in the lower operating band, in comparison with the earlier form. Because of this, the whole antenna exhibits good impedance matching over the desired lower operating band, as shown in Fig. 2.

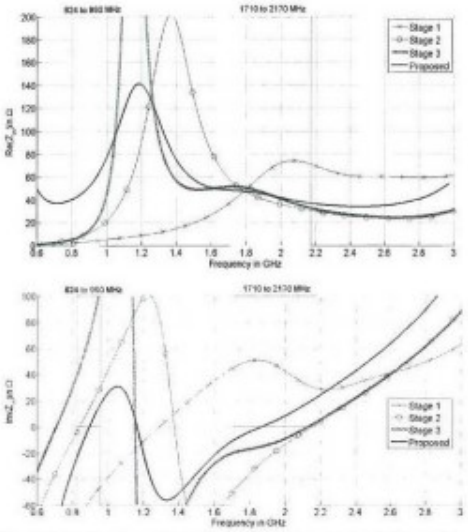

Fig. 3. Simulated input impedance of proposed antenna in the design evolution process from Fig. 2.

Fig. 4. Current distributions of the proposed antenna.

To have more insight into the contributions of the individual parts of this antenna, vector plots of the surface current distributions at the center frequencies of the two required bands, i.e. 900MHz and 1900MHz, can be studied in Fig. 4. At 900 MHz, the total length of the continuous current path is 156 mm or about 0.47λ. As can be noted in Fig. 4(a), the current flows from the feeding plate to part of the top plate, then to the parallel and shorting plates, and finally to part of the ground plane to excite this mode. Therefore, the major dimensions of the geometry, including the height of the antenna, coupling distance between the feeding plate and parallel plate, and the width of the shorting plate, can be used to manipulate the lower operating mode. At 1900 MHz, the current path can be found from the feeding plate to the part of the top plate which connects the parallel and shorting plates with the feeding plate. This current path forms an inverted-L structure, as shown in Fig. 4(b). The length of this path is about 87.5 mm, corresponding to about 0.5λ at this frequency. It appears that the geometric parameters controlling the lower band also determine the higher band, except for the shorting

plate which seems to have little influence at the higher frequency.

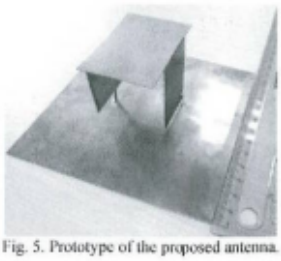

Fig. 5. Prototype of the proposed antenna.

III. Results for Antenna in Free Space

Fig. 5 shows the physical prototype of the antenna which was fabricated from 0.5 mm thick copper plate. To verify the computed performance in terms of impedance bandwidth, the return loss of the prototype was measured using a HP8510C vector network analyzer. The simulated and measured results show excellent agreement: see Fig. 2. As can be observed, two adjacent resonant frequencies in the range of return loss better than 10 dB occur at 900 MHz and 1900 MHz. The lower and upper modes offer 15.24% and 23.71% relative bandwidth from 824 to 960 MHz and 1710 to 2170 MHz, at a return loss of 10 dB or more. This is completely satisfactory for the desired GSM850, GSM900, GSM1800, GSM1900 and UMTS bands for mobile communication.

Fig. 6 illustrates the simulated and measured peak gain and radiation efficiency of the designed antenna over the frequency ranges 824 to 960 MHz and 1710 MHz to 2170 MHz respectively. In the lower band, a stable measured gain can be observed from 1 to 1.9 dBi, with 0.9 dBi gain variations. For the upper band, the measured gain ranges from about 4.2 to 5.8 dBi with corresponding 1.6 dBi gain variations. The computed and experimental gain results are essentially indistinguishable. In the lower frequency band, the simulated and measured radiation efficiencies vary from 80% to 88% and 76% to 85% respectively, corresponding to averages of 84% and 80.5% over the operating frequency range. At the upper frequency band, radiation efficiencies of 88.5% and 86% are achieved with ±13% and ±8% fluctuations for the computed and measured results respectively.

The far field radiation patterns of the prototype antenna were measured in a $6.75 \times 4.5 \times 3$ m^3 anechoic chamber and the results are presented in Fig. 7. In the far field measurement setup, a calibrated broadband horn (EMCO type 3115) was used as the reference antenna and held at a spacing of 4 m from the antenna under test (AUT).

An elevation-over-azimuth positioner was used, with the elevation axis coincident with the polar axis ($\theta = 0°$) in the AUT coordinate system The azimuth drive generates cuts at constant ϕ. The elevation positioner was rotated over $\theta \in [-180°, 180°]$ in 5° increments. The prototype's radiation patterns were measured at the six frequencies representing the lower and upper operating bands, i.e. 825 MHz, 900 MHz, 960 MHz, 1750 MHz, 1950 MHz and 2150 MHz, and the corresponding results, cross-validated with the simulation data, are plotted in Fig. 7. In the measurement, two pattern cuts (H-plane and E-plane) were recorded at these selected operating frequencies covering the whole of the designated bandwidth in this study. The total power for both polarizations, i.e. vertical and horizontal components, of the antenna patterns was used. As illustrated in Fig. 7, the radiation patterns are stable, consistent and nearly omnidirectional at all of the targeted operating bands.

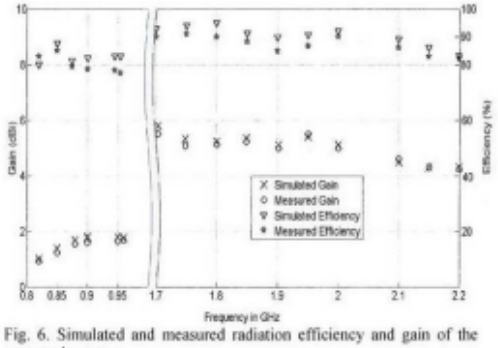

Fig. 6. Simulated and measured radiation efficiency and gain of the proposed antenna.

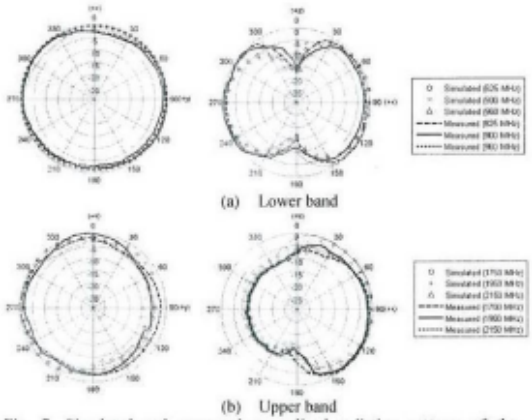

(a) Lower band

(b) Upper band

Fig. 7. Simulated and measured normalized radiation patterns of the proposed antenna.

IV. Antenna in Manhole Chamber - Design and Analysis

In this section, the coupling effects of this antenna with the manhole chamber model will be investigated. Thus, a realistic manhole simulation model similar to that in [11-13] has been implemented and configured as shown in Fig. 8. As can be seen, it consists of asphalt, a metal cover, concrete, PVC sewer pipes, a neck and chamber. The manhole cover and its pedestal are constructed of cast iron with dimensions of approximately 0.75 x 0.6 x 0.1 m and they are buried in the asphalt layer (ε_r = 3.15, σ = 0.026) of the ground with dimensions of approximately 1.7 x 1.7 x 0.1 m. The neck and the chamber of the manhole are hollow cuboids surrounded by walls constructed of approximately 0.55 m and 0.3 m thicknesses of concrete (ε_r = 7, σ = 0.12), respectively. The corresponding dimensions of the neck and chamber are 0.6 x 0.6 x 0.5 m and 1.1 x 1.1 x 1.1 m. At 1.2 m below the asphalt layer, two orthogonal 0.425 m diameter PVC rectangular blocks (ε_r = 2.1, σ = 0.0) were modeled to mimic the drain pipes. The overall envelope size of the model is around 1.7 x 1.7 x 6.8 m including the height of the air region above ground, which is 5.0 m. To ensure affordable computational time, this model was truncated by perfectly matched layer (PML) absorbing boundary conditions.

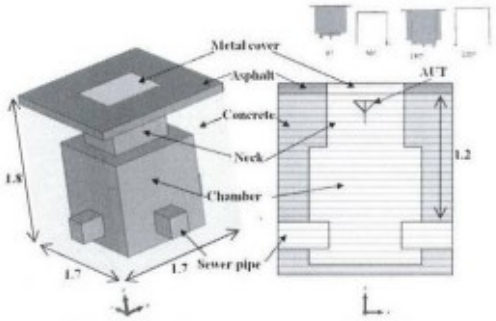

(a) Auxillary view (b) side view

Fig. 8. Antenna in manhole chamber model (Unit: meters).

To better understand the importance of the antenna's position when it is fitted in the manhole, electric field intensity plots of the model at 900 MHz and 1900 MHz are shown in Figs. 9 and 10 respectively. These figures show the interface plane (xy-plane) between the open air and the manhole model. This provides a good indication of how much electric field can penetrate through the manhole. A preliminary analysis was carried out by investigating four orientations (0°, 90°, 180°, 270°) of the antenna, considering it to be placed at various heights (in the -z direction) and various positions in the x and y directions below ground, as shown in Fig. 8. It should be noted that the 0° and 180° orientations are where the feeding plate of the antenna is nearest to and farthest from the edge, respectively. Interestingly it was found that the antenna provides better electric field penetration to the surface of the ground at 0° orientation than for the other orientations. For the sake of brevity, other cases will not be shown here, and 0° orientation will be kept as a fixed parameter in the study. As can be observed in Figs. 9 and 10, three antenna heights (from left to right), i.e. 50 cm, 120 cm and 240 cm, and three positions along the y-axis, i.e. (a) center, (b) between center and edge, and (c) edge, were selected to cover possible scenarios for this investigation.

Examining the total electric field plots at 900 MHz, as in Fig. 9, the fields are gradually attenuated when the depth of the antenna is increased from 50 cm to 240 cm, for all of the positions, i.e. Figs. 9(a) to 9(c). When the antenna is placed underneath the center of the manhole cover, the fields exhibit nearly even distribution over the surface of the model, as shown in Fig. 9(a). This demonstrates that the power distribution in the center of the chamber is more favourable than close to any of the four walls. However, mounting the antenna centrally may obstruct the operator access to the manhole for any planned maintenance. Due to this, the antenna is generally mounted near the wall even though this incurs some additional power loss from a radio-propagation perspective. By moving the antenna between the edge and the center positions, reduced field strengths can be seen at three depth positions when they are compared to the center position. Further moving the antenna to the wall of the chamber and at 50 cm depth, the maximum field strength occurs near to the edge of the metal cover.

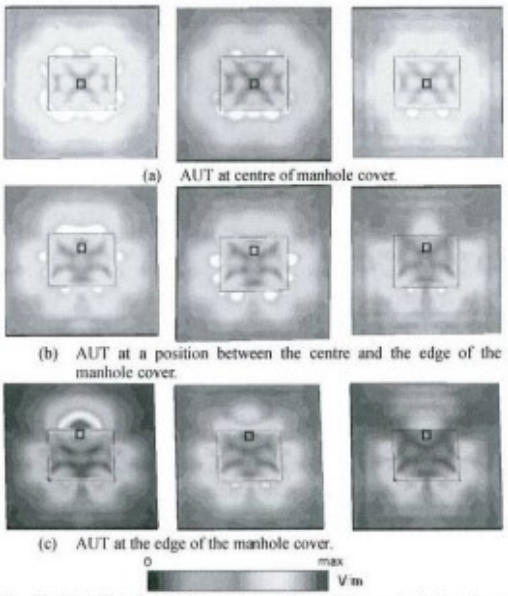

(a) AUT at centre of manhole cover.

(b) AUT at a position between the centre and the edge of the manhole cover.

(c) AUT at the edge of the manhole cover.

Fig. 9. Total Electric Field over the surface of the manhole chamber at various position of the antenna under test (AUT) at 900 MHz. Left column: 50 cm depth, Middle column: 120 cm depth, Right column: 240 cm depth. Small square represents the location of the antenna.

Fig. 10 shows the total electric field distribution at 1900 MHz of the antenna and manhole model. In general, it is noticeable that the field intensity is also progressively reduced as the depth is increased, in agreement with the field distribution at 900 MHz. However, in contrast to the 900 MHz field plots, when the antenna is located in the center of the cover, the field intensity is lower than when it is placed at or near the edge of the cover. These results suggest that the antenna should be placed near the edge of the cover or near the wall of the chamber for best performance in the upper operating frequency band.

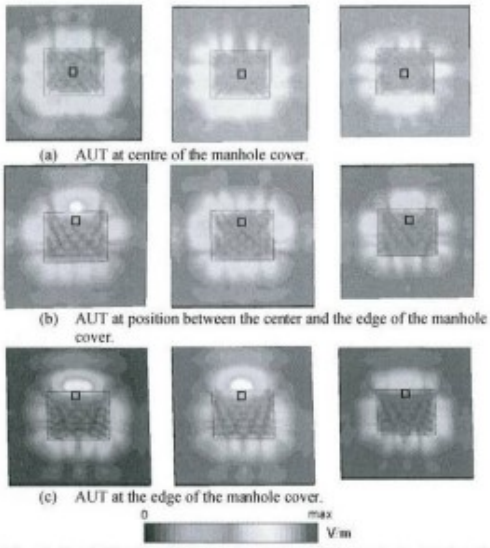

(a) AUT at centre of the manhole cover.

(b) AUT at position between the center and the edge of the manhole cover.

(c) AUT at the edge of the manhole cover.

Fig. 10. Total Electric Field over the surface of the manhole chamber for various positions of the antenna under test (AUT) at 1900 MHz. Left column: 50 cm depth, Middle column: 120 cm depth, Right column: 240 cm depth. Small square represents the location of the antenna.

To understand the coupling properties of this antenna when it is installed in the manhole, the S-parameters of the antenna, including return loss and transmission coefficient, have been studied. Return loss here indicates whether the antenna operates in the desired operating bands without being detuned, particularly when it is next to the metal cover, while the transmission coefficient measures the strength of the electromagnetic wave coupled through from the ground to air. To enable the transmission coefficient to be calculated in the model, eight broadband ridged pyramidal horn antennas were added to the model, as depicted in Fig. 11. This will ensure that an average transmission coefficient can be obtained. The complete structures of the horns were included in the model. It should be noted that two geometric parameters, i.e. D (horn distance from the center of the manhole model) and H (height above from the manhole), were used in this study, where D was set to 2 m and H to 1.85 m. This ensures that the measurement was conducted within the far-field region.

To verify the simulated variations of the return loss of the antenna under test (AUT), and assess the transmission coefficient, an in-situ measurement was also set up in a manhole chamber, as illustrated in Fig. 12. The experimental equipment consisted of a reference horn antenna, positioned at height H=1.85m, Vector Network Analyser (model: Agilent 8720C), and a data acquisition unit (Panasonic Toughbook Tablet, Model: CF-U1). Transmission measurements were taken with the horn antenna at a constant distance of 2 m from the centre of the manhole cover. The horn and all measuring equipment were moved on a trolley between the eight positions surrounding the manhole metal cover, for recording the transmission coefficient. For all the measurements, the AUT was mounted on a height-adjustable L-shaped support structure. For the transmission coefficient measurement, the AUT acted as a transmitter, while the horn antenna played the role of a receiver. The two antennas were operating in a non-line of sight (NLOS) communication condition, but pointing towards each other. All the measured data were recorded five times and then further processed in MATLAB for a better interpretation of the measured data sets. Since mobile base stations are operated with vertical polarization, the antenna in vertical polarization orientation was the primary target for this measurement, however, the two polarizations were considered in the measurements.

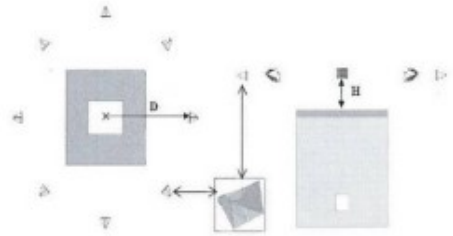

(a) Top view (b) Side view

Fig. 11. Manhole chamber model surrounded by eight ridged pyramidal horn antenna locations, where D is 2 m and H is 1.85 m.

Fig. 12. On-site measurement setup.

Fig. 13 shows the simulated and measured return losses and transmission coefficients of the antenna in the manhole chamber. It is noticeable that the antenna preserves good impedance matching (better than 10 dB) over the desired frequency bands, as plotted in Fig. 13(a). The computed and experimental results are in excellent agreement. For practical reasons, depths of 5, 15 and 25 cm. had to be used in these tests. For the transmission coefficient at a depth of 5 cm, the measured results show around -52.5 dB to -55 dB at the lower operating band, while at the higher band -56 to -61 dB is observed. Further increasing the depth to 15 cm, the results are further reduced by ~2 dB to reach the range of -54.5 dB to -56.5 dB at the lower band and around -58 to -59 dB at the higher band. When the depth reaches 25 cm, the results drop by another 1.5 to 3 dB in the lower band and 2 to 3 dB in the higher band. This has resulted in a range of -57.5 to -58 and -60 to -62 dB over the lower and upper band respectively. Slight discrepancies between both simulated and measured results can be attributed to uncertainties in the electrical properties of the materials used in the simulation model, and the simplifications in the simulated structure. Some variation with the weather conditions would also be expected due to their effect on the water content of materials and on the water level in the gully.

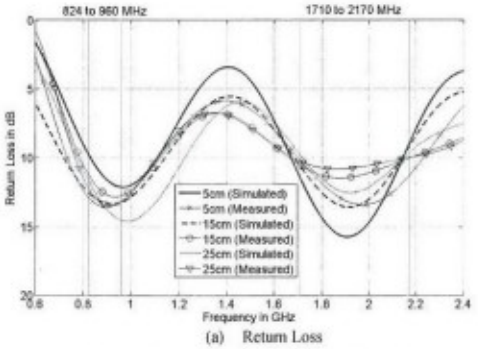

(a) Return Loss

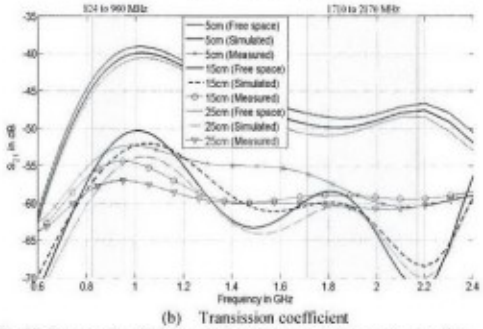

(b) Transission coefficient

Fig. 13. S-parameters between the horn antenna and the antenna under test (AUT) at different depths in the manhole chamber.

Also shown in Fig 13(b) is the simulated coupling level when all material obstructions, including the chamber walls, the asphalt and the manhole cover, are removed. This is the meaning of the free space curves in the plot. As noted, in practical conditions there is no clear line of sight between the antennas, and the direct ray path traverses the asphalt and the chamber walls. The average loss of signal due to non-LOS conditions is around 10 to 15 dB in the lower band and 8 to 13 dB in the higher band.

To further confirm whether this antenna works in the practical environment, it was integrated with a Telit HE910 cellular module [27] and installed in a manhole chamber over period of 3 months. This radio module has a receiver sensitivity of -109 dBm and -111 dBm for GSM900 and GSM1800 bands respectively and it was programmed to send a SMS message to report the received signal strength and water level in the chamber. It should be noted that the water level was measured by using the commercial ultrasonic sensor [28]. It was interesting found that the antenna shows a good RSS level over this field trial. A selected four days field trial results are shown in Fig.14. As can be seen, the RSS level is between 80 to 96 dBm even at the worst condition when it was raining (the water level of the chamber is high).

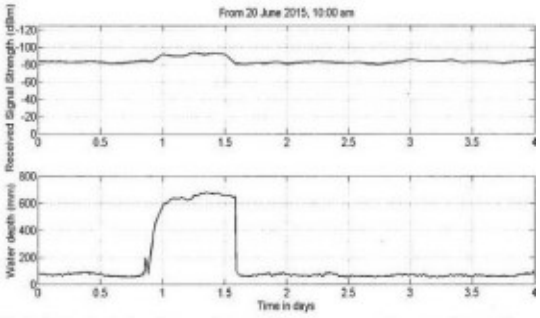

Fig. 14. Received signal strength level of antenna verse the water depth of manhole chamber in a practical site over time.

IV. Conclusion

A dual-band folded planar loop antenna for a partially-underground utility sensing application has been presented and examined theoretically and experimentally. By combining impedance matching techniques, including off-centre rectangular plate feeding, top-loading and a shorting strip, the required dual-band impedance bandwidths, i.e. 824 to 960 MHz, and 1710 to 2170 MHz, have been achieved. To confirm the suitability of this antenna to operate inside a typical utility manhole chamber, a manhole-and-antenna model has been simulated and tested experimentally. The results show that the antenna prototype exhibits sufficient impedance bandwidth, suitable radiation characteristics, and adequate gains for the required underground wireless sensor applications. The reduction of signal strength due to non-LOS transmission is small enough to permit a viable communications system.

REFERENCES

1. OFWAT, "The Development of the Water Industry in England and Wales," 2015 [Online]. Available: http://www.ofwat.gov.uk/wp-content/uploads/2015/11/rpt_com_devwatindust270106.pdf
2. J.P. Davies, B.A. Clarke, et al, "A statistical investigation of structurally unsound sewers," *Underground Infrastructure Research Industrial and Env Applications*, pp. 125-131, 2001
3. E. Ana, W. Bauwens, M. Pessemier, et al., "An investigation of the factors influencing sewer structural deterioration," *Urban Water*, vol.6, no.4, pp. 303-312, 2009.
4. S. Zhang and H. Zhang, "A Review of Wireless Sensor Networks and its Applications," IEEE international conference on Automation and Logistics (ICAL), pp.386-389, 2012.
5. X. Tan, Z. Sun and I.F. Akyildiz, "Wireless Underground Sensor Network: MI-based communication systems for underground applications," *IEEE Antennas & Propagation Magazine*, vol.57, no.4, pp.74-87, 2015
6. C.H. See, K.V. Horoshenkov, R.A. Abd-Alhameed, Y.F. Hu and S.J. Tait, "A Low Power Wireless Sensor Network for Gully Pot Monitoring in Urban Catchments", *IEEE Sensors Journal*, vol.12, no. 5, pp.1545-1553, May 2012.
7. D. Trinchero and R. Stefanelli, "Microwave Architectures for Wireless Mobile Monitoring Networks inside Water Distribution Conduits," *IEEE Trans Microwave Theory and Techniques*, vol.57, no.12, pp.3298-3306, 2009.
8. M.D. Bedford and G.A. Kennedy, "Evaluation of ZigBee (IEEE 802.15.4) Time-of-Flight-Based Distance Measurement for Application in Emergency Underground Navigation", *IEEE Trans. Antennas and Propagation*, vol.50, no.5, pp.2502-2510, April 2012.
9. C.H. See, R.A. Abd-Alhameed, D. Zhou, Y.F Hu and K.V Horoshenkov "Measure The Range of Sensor Network", *Microwaves & RF*, vol. 54, no.10, pp.69-76, Oct. 2008.
10. C. Zhou, T. Plass, R. Jacksha and J. A. Waynert, "RF Propagation in Mines and Tunnels," *IEEE Antennas & Propagation Magazine*, vol.57, no.4, pp.88-102, 2015.
11. A. Ando, T. Ito, H. Tsuboi and H. Yoshioka, "Propagation Loss, XPR and Height Pattern Characteristics on Road from Antenna Set in Manhole," *IEEE Antennas and Propagation Society International Symposium (APSURSI)*, pp.1-4, 2010.
12. A. Ando, T. Ito, H. Yoshioka, H. Tsuboi and H. Nakamura, "Effects of Receiver Antenna Height and Polarization on Received Signal Levels at Road Level from Transmitter Antennas Set in Manhole," *IEEE International Symposium on Antennas and Propagation (APSURSI)* , pp.2399-2402, 2011.
13. S. Mizushina, A. Adachi and T. Watanabe, "Radiation from an antenna in manhole," *Asia-Pacific Microwave Conference (APMC)*, pp.2052-2055, 2006
14. A.S. Kesar and E. Weiss, "Wave Propagation Between Buried Antennas", *IEEE Trans. Antennas and Propagation*, vol.61, no.12, pp.6153-6156, April 2013.
15. J.F. Mastarone and W.J. Chappell, "Urban Sensor Networking Using Thick slots in Manhole covers," *IEEE Antennas and Propagation Society International Symposium*, pp.779-782, 2006
16. S. Jeong, D. Ha, M.M. Tentzeris, "A Cavity-backed Slot Antenna with High Upper Hemisphere Efficiency for Sewer Sensor Network," IEEE Antennas and Propagation Society International Symposium (APSURSI), pp.49-50, 2013
17. S. Jeong, C-I.. Yang, J.R. Courter, S. Kim, R.B. Pipes and W.J. Chappell, "Multilayer Composite for Below Ground Embedded Sensor Networking," *IEEE Antennas and Propagation Society International Symposium*, pp.1-4,2008
18. S. Jeong and W.J. Chappell, "Adaptive composite antennas for a city-wide sensor network," *IET Microwaves. Antennas and Propagation*, vol.4, no.11, pp.1916-1926, 2010
19. T.W. Hertel and G.S. Smith, "The Conical Spiral Antenna over the Ground", *IEEE Trans. Antennas and Propagation*, vol.50, no.12, pp.1668-1675, December 2002.
20. D. Ghosh, H. Moon and T.K. Sarkar, "Design of through-the-earth mine communication system using helical antennas," *IEEE Antennas and Propagation Society International Symposium* , pp.1-4, 2008
21. R-Y. Chao and K-S. Chung, "A Low Profile Antenna Array for Underground Mine Communication," *Singapore ICCS '94. Conference Proceedings.*, vol.2, pp.702-709, 1994
22. W. Tang, Y. Hao, "Cloak on Underground Antenna Using Transformation Electromagnetics," *IEEE International Symposium on Antennas and Propagation (APS/URSI)*, pp.2865-2868, 2011.
23. G. Pandey, R. Kumar and R.J. Weber, "A low profile, low-RF band, small antenna for underground, in-situ sensing and wireless energy-efficient transmission, *IEEE 11th International Conference on Networking, Sensing and Control (ICNSC)*, pp.179-184, 2014.
24. P. Soontornpipit, C.M. Furse, Y.C. Chung and B.M. Lin, "Optimization of a Buried Microstrip Antenna for Simultaneous Communication and Sensing of Soil Moisture", *IEEE Trans. Antennas and Propagation*, vol.54, no.3, pp.797-800, 2006.
25. C.H. See, R.A. Abd-Alhameed, H.I. Hraga, N.J. McEwan, P.S. Excell, and J.M. Noras, "A Low-Profile Ultra-Wideband Modified Planar Inverted-F Antenna," *IEEE Trans. Antennas and Propagation*, vol.61, no. 1, pp.100-108, Jan. 2013
26. R. Feick, H. Carrasco, M. Olmos, and H. D. Hristov, "PIFA input bandwidth enhancement by changing feed plate silhouette," *Electron. Lett.*, vol. 40, pp. 921–922, Jul. 2004.
27. Telit HE910 Cellular radio module, available: http://www.telit.com/fileadmin/user_upload/products/Downloads/3G/xe910/Telit_HE910_Hardware_User_Guide_r27.pdf
28. Hawkeye Ultrasonic level sensor, aailable: http://www.isodaq.co.uk/clear_downloads/146_1393261032hawkeye2-2007_001.pdf